Università
Ca'Foscari
Venezia

Corso di Dottorato di ricerca

in Environmental Science

ciclo 32°

Tesi di Ricerca

Stabilized materials from contaminated waste recycling: characterization, immobilization, and leaching of contaminants

SSD: CHIM/12

Coordinatore del Dottorato
ch. prof. Enrico Bertuzzo

Supervisore
ch. prof. Antonio Marcomini

Co. Supervisore
ch. prof. Elena Badetti

Dottorando
Loris Calgaro
Matricola 834759

This page was intentionally left blank

Stabilized materials from contaminated waste recycling: characterization, immobilization, and leaching of contaminants

Index

I. List of publications

L. Calgaro, E. Badetti, A. Bonetto, S. Contessi, R. Pellay, G. Ferrari, G. Artioli, A. Marcomini. *Consecutive thermal and wet conditioning treatments of sedimentary stabilized cementitious materials from HPSS® technology: Effects on leaching and microstructure*. (2019)
Journal of Environmental Management, 250, art. No. 109503
https://doi.org/10.1016/J.JENVMAN.2019.109503

S. Contessi, L. Calgaro, M.C. Dalconi, A. Bonetto, M. Pietro Bellotto, G. Ferrari, A. Marcomini, G. Artioli; *Stabilization of lead contaminated soil with traditional and alternative binders*. (2020)
Journal of Hazardous Materials, 382, art. No. 120990
https://doi:10.1016/j.jhazmat.2019.120990

Manuscripts in preparation, submission expected by December 2019.

L. Calgaro, S. Contessi, A. Bonetto, E. Badetti, G. Ferrari, G. Artioli, A. Marcomini, *Calcium aluminate cement as an alternative to ordinary Portland cement for the remediation of a heavy metals contaminated soil: mechanisms and performance*

A. Bonetto, L. Calgaro, S. Contessi, E. Badetti, G. Artioli, A. Marcomini, *Past environmental pollution in an industrial site: using stable lead isotopic analysis to identify multiple contamination sources.*

II. Acronym list

Afm	Alumina, Ferric oxide, Mono-sulfate ($Ca_2(Al, Fe)(OH)_6)]\cdot X\cdot nH_2O$)
AFt	Alumina, Ferric oxide, Tri-sulfate ($Ca_3(Al, Fe)(OH)_6\cdot 12\ H_2O]_2\cdot X_3\cdot nH_2O$)
AH_3	Aluminium Hydroxide ($Al(OH_3)$)
C_2AH_8	diCalcium Aluminate hexaHydrate ($2CaO\cdot Al_2O_3\cdot 6H_2O$)
C_2S	diCalcium Silicate ($2CaO\cdot SiO_2$)
C_3A	triCalcium Aluminate ($3CaO\cdot Al_2O_3$)
C_3AH_6	triCalcium Aluminate hexaHydrate ($3CaO\cdot Al_2O_3\cdot 6H_2O$)
C_3S	triCalcium Silicate ($3CaO\cdot SiO_2$)
C_4AF	tetraCalcium AluminoFerrite ($4CaO\cdot Al_2O_3\cdot Fe_2O_3$)
CA	monoCalcium Aluminate ($CaO\cdot Al_2O_3$)
CA_2	monoCalcium diAluminate ($CaO\cdot 2Al_2O_3$)
CAC	Calcium Aluminate Cement
CAH_{10}	Calcium Aluminate decaHydrate ($CaO\cdot Al_2O_3\cdot 10H_2O$)
CDI	Chronic Daily Intake
CH	Calcium Hydroxide ($Ca(OH)_2$)
COD	Chemical Oxygen Demand
CSC	Concentrazioni Soglia di Contaminazione
C-S-H	Calcium Silicate Hydrate
CSR	Concentrazioni Soglia di Rischio
DRC	Dynamic Reaction Cell
DTPA	DiethyleneTriaminePentaacetic Acid
EDDS	EthyleneDiamine-N,N'-diSuccinic Acid
EDTA	EthyleneDiamineTetra-Acetic acid
EPC	Electronic Pressure Control
ESEM	Environmental Scanning Electron Microscope
EU	European Union
FESEM	Field Emission Scanning Electron Microscope
FID	Flame Ionizing Detector
GC	Gas Chromatography
GGBFS	Ground Granulated Blast Furnace Slag
H	Henry’s law constant
HDPE	High Density PolyEthylene

HEDTA	HydroxyEthylene Diamine Triacetic Acid
HHRA	Human Health Risk Assessment
HI	Hazard Index
HO·	Hydroxyl radicals
HPSS®	High Performance Solidification/Stabilization
HQ	Hazard Quotient
ICP-MS	Inductively Coupled Plasma Mass Spectrometry
ICP-OES	Inductively Coupled Plasma Optical Emission Spectrometry
In.T.Ec.	Ingegnerie Tecnologie Ecologiche
ISPRA	Istituto Superiore per la Protezione e la Ricerca Ambientale
K_{AW}	Air-water partition coefficient
KED	Kinetic Energy Discrimination
K_{OC}	Organic carbon referenced solids-water partition coefficient (L/kg)
KP	Partition coefficient
MF	MicroFiltration
MK	Metakaolin
MSW	Municipal Solid Waste
NF	NanoFiltration
NIH	National Institutes of Health
NIMBY	Not-In-My-Back-Yard
NIST	National Institute of Standards and Technology
NNE	North-North-East
NOAEL	No Observed Adverse Effect
NTA	Nitrilo Triacetic Acid
OPC	Ordinary Portland Cement
PAC	PolyAluminium Chloride
PAHs	Polycyclic Aromatic Hydrocarbons
PAM	PolyAcryl Amide
PBBs	PolyBrominated Biphenyls
PBDEs	PolyBrominated Diphenyl Ethers
PCBs	PolyChlorinated Biphenyls
PCDDs	PolyChlorinated Dibenzo-p-Dioxins
PCDFs	PolyChlorinated DibenzoFurans
PFS	PolyFerric Sulfate

POPs	Persistent Organic Pollutants
RBCA	Risk Based Corrective Action
RCRA	Resource Conservation and Recovery Act
R_{cum}	Cumulative Risk
RfD	Reference Dose
RO	Reverse Osmosis
RO·	Alkoxy radicals
RO_2·	Peroxy-radicals
S/S	Solidification/Stabilization
SEM	Scanning Electron Microscopy
SEM/EDX	Scanning Electron Microscopy/Energy Dispersive X-ray
SF	Slope Factor, referred to the dose-response curve for cancerogenic substances
SNI	Sites of National Interest
SSTLs	Site-Specific Target Levels
SSW	South-South-West
SW	South-West
TMP	TransMembrane Pressure
TSS	Total Suspended Solids
TT	Thermal Treatment
UF	UltraFiltration
UV	Ultraviolet
UV-Vis	Ultraviolet–Visible spectroscopy
VCR	Volumetric Concentration Ratio
VF_i	Uncertainty Factors
WC	Wet Conditioning
WDS	Wavelength Dispersive Spectrometer
WPs	Work Packages
XRD	X-Ray Diffraction
XRF	X-ray Fluorescence

III. Acknowledgments

"We must find time to stop and thank the people who make a difference in our lives."

John F. Kennedy

(1917 – 1963)

"Always remember people who have helped you along the way, and don't forget to lift someone up."

Roy T. Bennett

(1939 – 2014)

IV. Abstract

The contamination of soils, sediments and various industrial wastes from both heavy metals and organic pollutants is recognised as one of the most relevant environmental problems caused by past and present industrial activities, as well as by unsustainable waste disposal practices, highlighting the need to improve or develop effective remediation techniques to support sustainable management strategies. To this purpose, many technical solutions have been studied to reduce the toxicity, mobility and/or concentration of contaminants, depending on their nature and concentration level, as well as on the polluted solid matrix. Among the many processes developed and applied over the last decades, immobilization technologies based on the solidification/stabilization (S/S) of both organic and inorganic contaminants using various hydraulic binders showed interesting results. In particular, the High Performance Solidification/Stabilization (HPSS®) process is an *ex-situ* S/S treatment specifically addressed to granular material production, which is intended to facilitate the reuse of treated contaminated matrixes in environmental rehabilitation interventions, e.g. as filling material or for manufacturing of non-structural concrete items. It is therefore fundamental to understand the mechanisms involved in the retention and leaching of contaminants from the granular material produced, to both improving their performances and to develop new processes for the sustainable management of contaminated matrixes.

This Ph.D. thesis focuses on the characterization of several stabilized cementitious granular materials obtained from the application of the High Performance Solidification/Stabilization (HPSS®) process by a set of analytical techniques such as Inductively Coupled Plasma Mass and Optical Emission Spectrometry (ICP-MS and ICP-OES), Ultraviolet–Visible spectroscopy (UV-Vis), Gas Chromatography (GC), X-Ray Diffraction (XRD), and Scanning Electron Microscopy (SEM).

The obtained results obtained allowed to elucidate the mechanisms, mineralogical phases, and key parameters regulating the solidification/stabilization performances of different binders (i.e. calcium aluminate cement, alkali-activated metakaolin) involved in the treatment of different contaminated matrixes. Moreover, the established HPSS® was successfully integrated with alkaline soil washing, nanofiltration and heavy metals' chemical precipitation processes to recover heavy metals from stabilized matrixes. In addition, a bench scale prototype for this new process was developed and tested.

The overall experimental activity led to four manuscripts that are discussed in detail in this thesis.

V. Objectives and Thesis Structure

The main objective of this thesis work was to investigate the inertization of different matrices (soils, sediments and ashes deriving from the combustion of municipal solid waste) contaminated by organic and inorganic pollutants through the use of several cementitious binders (e.g. ordinary Portland cement and calcium aluminate cement) and various geopolymeric binders (e.g. alkali-activated metakaolin and GGBFS-based binders). In particular, the aim was to better elucidate the mechanisms involved in the immobilization and release of these contaminants, as well as to improve the performance of the materials obtained through the studied solidification/stabilization processes.
The main questions asked are:

1. What additional steps can be added to the High Performance Solidification/Stabilization process, in order to improve the performances of the cementitious granular materials produced from the treatment of materials contaminated by organic and inorganic pollutants? What are the effects of each step of the process on the leaching behaviour and microstructure of these materials?
2. Which other hydraulic binders be used as a better alternative to ordinary Portland cement for the solidification/stabilization of heavy metals contaminated matrixes? What are the key parameters and retention mechanisms controlling the retention of these contaminants?
3. Can conventional analytical techniques be used to establish the accurate extent of the contamination caused by the presence of heavy metals contaminated wastes in a dismissed site for the production of sulfuric acid?
4. Can the High Performance Solidification/Stabilization process be integrated with chemical extraction and membrane separation processes to produce re-usable materials while also recovering part of the heavy metals present?

The thesis is made up of six chapters, the first of which is an introduction to the topics covered, while the other chapters explore in detail the phenomena and mechanisms involved in the tested inertization and decontamination of materials polluted by both organic and inorganic substances. Specifically:

Chapter 1 briefly describes the main chemical pollutants present in the environment, their sources, equilibrium partitioning between phases, transport mechanisms, transformation mechanisms, and persistence in the environment. Then, the properties of soils and sediments i.e. morphology, texture, and chemical constituents, are reported. This general Introduction is concluded by an overview on the remediation of contaminated matrixes, focused on risk assessment and management, on the most

used remediation technologies and on the Italian regulatory framework regarding the reclamation of contaminated sites.

Chapter 2 reports the materials, instruments and methods common to the work discussed in this thesis.

Chapter 3 describes the investigation on the remediation of sediment dredged from the Mincio river (Italy) and contaminated by mercury and heavy hydrocarbons (C_{12-40}), carried out by applying the High Performance Solidification/Stabilization technology to produce reusable granulated materials. This study is focused on the effects on the leaching and microstructure of the stabilized granular material produced, caused by the consecutive thermal and wet conditioning treatments used.

Chapter 4 illustrates a study on the comparison between ordinary Portland cement, calcium aluminate cement and metakaolin for the remediation of Pb contaminated soil. The first part deals with the characterization of the contaminated soil, while the second part correlates the phase composition and internal microstructure of the stabilized products with the leaching of Pb, to better elucidate the mechanisms involved in the retention and leaching of this contaminant for each of the investigated binders.

Chapter 5 reports further research work aimed at implementing the findings on the application of calcium aluminate cement, ordinary Portland cement, and different binders prepared with different combinations of these two cements for the treatment of a polluted soil, focusing on the retention of several pollutants of environmental concern (e.g. Ba, As, Be, Cd, Co, Cr, Cu, Hg, Ni, Pb, Sb, Se, Sn, Tl, V, and Zn). Leaching and mechanical tests were carried out to evaluate the solidification/stabilization performance of the proposed binders, while XRD analysis and SEM/EDX imaging were used to investigate the phase composition and internal microstructure of the treated samples. The overall results are used to better elucidate the mechanisms involved.

Chapter 6 illustrates the application of several analytical techniques to ascertain the dispersion into the surrounding area of several heavy metals from a lead-contaminated industrial site in Bagnolo Mella (Italy). Specifically, stable Pb isotopes analysis and a two-source model were used to define the pollution sources responsible for the similar levels of contamination found both at the edge of the contaminated site and in the fields nearby.

Chapter 7 outlines the results of the HPSS-NANOEXTRA project (Veneto Region, POR FESR 2014-2020- ID 10052461), which aimed at the development of an innovative technology for the treatment of special/hazardous waste (i.e. contaminated soil and sediments, fly ash, bottom ash, sewage sludge from chemical-physical treatment of wastewater) that, coupled with the already established High

Performance Solidification/Stabilization process, allowed to produce re-usable materials and to recover heavy metals by extraction.

1. Chapter 1

Introduction

1.1. Chemical pollutants in the environment

The great industrialization that characterized the last two centuries has played a key role in our society's progress, so much that until around the 1950's only the positive effects of industrialization were considered: each country's economy grew together with its industrial capacity. However, after several accidents, people began to realize that most of those facilities were releasing great amounts of potentially harmful substances into the environment, posing serious hazards not only for the environment and the living organisms, but also for the human health of populations living close to emission sources [1,2].

Chemical pollution has therefore been defined as "the presence of an element or a substance in greater amounts than background concentrations, generally as a result of human activity, having a net detrimental effect on the environment and its components, principally affecting biological processes in living organisms (plants, animals, humans) [3].

Many substances have been found having negative effects on various environmental compartments, ranging from complex organic molecules to simple inorganic ions.

The inorganic contaminants include metals (e.g., Cd, Cr, Cu, Hg, Mn, Ni, Pb, V, and Zn), metalloids (e.g., As, B, and Sb), non-metals (e.g., Se), actinoids (e.g., U), and halogens (e.g., Br, I and F) [4]. Some of these elements, such as B, Cl, Cu, Fe, Mn, Mo, and Zn are fundamental for life in small quantities, but toxic when exceeding certain thresholds, while many others can cause toxic effects at all concentrations (Hg, As and Tl). Some of these elements tend also to form some lipophilic and highly toxic organometallic compounds, like methyl mercury and tributyl tin oxide [5]. Another important category of inorganic contaminants is that of radionuclides, unstable isotopes that may undergo radioactive decay (i.e. Cs, Sr, Eu, and Th), emitting radiation which may be harmful [6]. There are also some other inorganic pollutants which, although not particularly toxic, may cause problems to the environment if used in large quantities (i.e. nitrates and phosphates), resulting in eutrophication of lakes and rivers, and in acid rain [7].

The term organic pollutant refers to compounds that contain carbon in their structure (with or without functional groups) and includes several classes of compounds such as hydrocarbons, PAHs, polychlorinated dibenzo-p-dioxins (PCDDs), polychlorinated dibenzofurans (PCDF), polychlorinated biphenyls (PCBs), polybrominated biphenyls (PBBs), polybrominated diphenyl ethers (PBDEs), surfactants, pesticides, and pharmaceuticals.

These compounds are characterized by a great variability of their properties (i.e. polarity, solubility, volatility, persistence), even within the same class, resulting in different environmental behaviours and toxicity [8]. In particular, persistent organic pollutants (POPs) are probably considered the most

important group of organic contaminants, due to their toxicity, mobility, persistence, bioaccumulation potential, carcinogenic and/or mutagenic potential and their massive use or continued emission into the environment [9,10].

Moreover, the number of chemicals released into the environment is ever growing, coming from many different applications ranging from flame retardants, combustion by-products, pesticides, pharmaceuticals, personal care products, detergents, di-electric fluids and numerous other applications [11].

Generally, sources of environmental pollution can be divided into two categories, depending if the origin of the pollution can be traced to any discernible, confined and discrete point (source pollution) or if the pollutants are spread in the environment in a way that cannot be traced to a single source (diffuse pollution or non-point-source pollution) [12].

These emissions may be caused by both natural and anthropogenic sources. In particular, the most common natural processes resulting in pollutants' release are the weathering of bedrock and ore bodies (inorganic pollutants), volcanic eruptions, forest fires (inorganic and organic pollutants), sea-salt sprays, biogenic sources and wind-borne soil particles. In some cases, particularly high concentrations of some toxic elements may also be attributed to the local geochemistry [5,13].

Nevertheless, in most cases, pollution is a result of human activities, either deliberate or accidental. Deliberate pollution sources include mining, smelting, inappropriate disposal of wastes, fossil fuel combustion, gas works, sports shooting, military training, and application of agrochemicals or sewage and many others industrial activities. On the other hand, accidental pollution can be caused by leaks from landfills or storage tanks, flooding by rivers or seas, nuclear accidents, and accidental spills [14].

After entering the environment, chemical pollutants may be found in different environmental compartments, such as air, water, soils, sediments, and biota. These compartments are not static or self-contained, but chemically and physically dynamic, leading to a series of continuous interactions. For these reasons, environmental contamination migrates from one compartment to the other according to the physic-chemical conditions of each system. In addition, these chemicals may also be subjected to a multitude of processes resulting in their degradation or transformation [15–20].

The principles that govern the fate and transport of chemical pollutants are herein briefly discussed, considering both the transport and transformation phenomena involved.

1.1.1. Equilibrium partitioning between phases

Following the fundamental laws of thermodynamics, chemicals tend to spontaneously migrate from one phase (i.e. air, water or soil/sediments) to another if they are not in equilibrium.

Defining the equilibrium as the state in which each contaminant's chemical potential, activity and fugacity have the same value in the different phases, various mass balance models for the environmental fate of chemicals, known as "fugacity models" or "Mackay models", have been developed [21]. In these models, the equilibrium state can usually be expressed by stating that chemicals reach the equilibrium between two phases when the ratio of concentrations (C_1 and C_2) is equal to an intermedia equilibrium constant K, also known as partition coefficient (K_P):

$$K_P = \frac{C_1}{C_2} \qquad \text{(Eq. 1.1)}$$

1.1.1.1. Solids-Water equilibrium

The partitioning of chemicals pollutants between water and solids is the result of the adsorption and the desorption of these substances onto the surface of particles. For low concentrations of each chemical in water, K_P is usually constant and independent of both C_1 and C_2. In the case of high concentrations, it has been often observed experimentally that K_P depends on both C_1 and C_2, and the equilibrium relationship between the concentrations is given in such cases by a non-linear sorption isotherm (i.e. Freundlich-isotherm equation).

For many hydrophobic or non-ionic chemicals, ionizing organic acids and bases, the methods most commonly used to estimate water-solids partition coefficients K_P assume that there is a "hydrophobic sorption" mechanism involved. This mechanism is generally modelled based on the organic carbon content of the solid (f_{OC}) and the octanol-water partition coefficient of the chemical K_{OW}, using the following equation:

$$logK_P = log(K_{OC} \cdot f_{OC}) = a\ log\ K_{OW} + b + log\ f_{OC} \qquad (Eq.\ 1.2)$$

where:

K_{OC}: organic carbon referenced solids-water partition coefficient (L/kg)

a, b: constants, specific for chemical classes

From this expression it can be seen that, given a value of K_P, the extent to which partitioning from water to solids occurs depends on the amount of solids present. For this reason, the mass fraction of chemical dissolved in water ($\Phi_{dissolved}$) at equilibrium can be calculated as:

$$\Phi_{dissolved} = \frac{1}{1 + K_P \cdot TSS} \qquad (Eq.\ 1.3)$$

where

TSS = mass concentration of suspended solids in water (= ~ 10-5 kg/L)

However, for metals no generally applicable estimation methods are known, since K_P values strongly depend on the composition of both the solid and the aqueous phases between which the metal is distributed [22–24]. For this reason, the pH is an important parameter to be considered, and its decrease is usually proportional to K_P decrease.

1.1.1.2. Air-Water equilibrium

The equilibrium between air and water is described by Henry's law [25], which affirms that, in equilibrium, the partial pressure of a chemical in the gas phase is proportional to its concentration in water. The ratio of these is known as the Henry's law constant (H), and it can be obtained as the ratio of the saturated vapour pressure $P_{L,S}^{S}$ and the water solubility $S_{L,S}$ of the pure compound, assuming that they refer to the same temperature and to the same physical state (liquid or solid). The air-water partition coefficient K_{AW} can be derived from Henry's law constant as follows:

$$K_{AW} = \frac{C_{air}}{C_{water}} = \frac{H}{RT} = \frac{P_{L,S}^{S}}{S_{L,S} \cdot RT} \qquad (Eq.\ 1.4)$$

where:

R: gas constant (8.314 Pa·m^3/mol/K)

T: temperature at the air-water interface (K)

1.1.1.3. Air-Aerosol equilibrium

The extent of association of chemicals with the aerosol phase of air is known to be inversely related to the chemical's vapour pressure. The fraction associated with the aerosol phase $\Phi_{aereosol}$ has successfully been described by Junge [6]:

$$\Phi_{aereosol} = \frac{c\Theta}{P_L^S + c\Theta} \qquad (Eq.\ 1.5)$$

where

Θ: aerosol surface area per volume unit of air (m^2/m^3)

P_L^S: vapour pressure of the pure compound in the liquid state (Pa)

c = constant (Pa·m) depending on the heat of condensation and molecular weight for many organics

Since P_L^S is strongly temperature dependent, the fraction of a substance absorbed to particles will also be temperature dependent.

1.1.2. Transport mechanisms

The two main kinds of transport mechanisms for chemical pollutants in the environment are (1) intramedia transport, defined as the transport of a contaminant within the same environmental medium, and (2) intermedia transport, defined as the transport of a contaminant from one environmental medium to another. The first type of transport is mainly related to environmental media such as air, water and groundwater, while the second one principally involved the transport of chemicals to and from stationary media such as sediments and soils. Both these transports take place through the mechanisms of advection and dispersion. In the case of intramedia transport, advection causes a chemical to travel from one place to another as a result of the flow of the medium in which it occurs, while dispersion mechanism (molecular diffusion) make the chemical move down concentration gradients until the gradients have disappeared.

With intermedia transport (air-water, water-sediment, etc.) advective phenomena take place if a chemical is transported from one environmental compartment to another by a physical carrier (i.e. deposition of fog, raindrops and aerosol particles from air to water or soil, sedimentation and resuspension of particulate matter across the water-sediment interface, and percolation of water through soil). Advective transport is also a one-way phenomenon: the chemical is carried by the medium in which it resides in the direction of the medium flows. Intermedia dispersion is also diffusive in nature and follows concentration gradients, as in the case of volatilization and gas absorption (air-water and air-soil) or diffusive exchange of chemicals between sediment and water. Transport from one environmental medium to another is commonly described by using the box/compartment modelling approach [21,26–30]. The most important interfaces are briefly described below.

1.1.2.1. Air-Water and Air-Soil exchange

Atmospheric deposition and volatilization processes transport chemicals between air and the earth's surface. These phenomena are usually distinguished between dry deposition and wet (precipitation-mediated) deposition mechanisms, which are themselves further split into rain-out (in-cloud processes) and wash-out (below-cloud processes). Considering dry deposition as the sum of aerosol deposition and gas absorption, it is treated as a bi-directional exchange mechanism while rain-out, wash-out and aerosol deposition are considered as one-way advective transport processes. Transport of a chemical from water and soil into the gas phase of air and vice versa is commonly described by a two-resistance approach where the resistance to intermedia transfer is considered to be concentrated in two thin films on either side of the interface [31]. Transport through this interfacial double layer has to take place by molecular diffusion and is, therefore, slower than the transport to

and from the interface. The net diffusion depends on the concentrations in the two phases, going from the compartment with the highest fugacity to the compartment with the lowest fugacity.

1.1.2.2. Deposition with aerosol and rain

Chemical pollutants adsorbed to aerosol particles can be carried from the air compartment to the earth's surface by dry particle deposition, while the aerosol particles can also be scavenged by rain drops as wet particle deposition. In addition, raindrops absorb chemicals from the gas phase and carry chemicals to the earth's surface by rain-out and wash-out. The deposition rates depend from the physical parameters of the particle, of which the size is the most important. Small particles tend to behave like gases, while larger particles (> 2 μm) are efficiently removed from the atmosphere by deposition under the influence of gravity.

The efficiency of wet deposition varies greatly, depending on both meteorological factors such as the duration, intensity and type of precipitation (snow, rain, hail), the size and the number of droplets and the physic-chemical properties of each contaminant [32,33].

1.1.2.3. Soil run-off

With the runoff of rainwater to surface waters or sewerage systems, or during floods, soil and dust, the particles are eroded and washed away transporting the chemicals associated with the particulate into the water, causing both advective and diffusive transport.

Assuming the water which runs off to be in equilibrium with the soil, the resulting chemical pollutants' mass flow can be estimated, however, for most cases it is often more practical and accurate to conduct field measurements on contaminated sites than applying models. These phenomena are also very dependant from rainfall [34,35].

1.1.2.4. Deposition and resuspension of sediment particles

The transport of chemicals across the sediment-water interface can be treated in the same manner as air-water and air-soil exchanges. In this case there is an advective transport component (i.e., sedimentation and resuspension), and a diffusive transport component (i.e., direct adsorption onto and desorption from the sediment). To estimate the rate of advective transport from water to sediment by sedimentation of suspended particles, both the concentration of the chemical on the particles and the settling rate need to be known. In most cases it is sufficient to assume equilibrium between the suspended particles and water phase, following the equation already shown to describe solids-water equilibrium [36].

1.1.2.5. Exchange between water and sediment by direct adsorption and desorption

Diffusive transport between sediment and water, by direct adsorption and desorption across that interface, is analogous to diffusive transport across the air-water and air-soil interfaces and can be described with a two-film resistance mechanism.

The mass-transfer on the pore water side of the sediment-water interface can be treated as molecular diffusion in the aqueous phase of a porous solid material, however, additional processes that are typically of a non-equilibrium nature (i.e. bioturbation and shipping), may greatly affect the net mass-transfer of all kinds of chemicals [36].

1.1.3. Transformation processes

After their release into the environment, chemical pollutants may undergo various biotic and abiotic processes which modify their chemical structure. The degradation or transformation of a compound, defined as the disappearance of the parent compound from the environment by a change in its chemical structure, can be caused by both micro-organisms (biodegradation) or abiotic transformations (i.e. hydrolysis, oxidation, reduction and photo degradation).

When chemicals are converted entirely to simple molecules and ions, such as carbon dioxide, methane, water and chloride, the process is referred to as mineralization. The rate of degradation of a specific chemical depends on its intrinsic sensitivity to undergo chemical transformations, the presence of reactants and their availability, and environmental conditions like pH, temperature, light intensity and red-ox conditions [37].

1.1.3.1. Hydrolysis

Hydrolysis is the chemical breakdown of substances by water, in which a hydroxyl group typically replace another chemical group in a molecule. However, certain functional groups, including alkanes, alkenes, benzenes, biphenyls, (halogenated) polycyclic aromatics (e.g., PAHs, PCBs, PCDD, PCDFs), alcohols, esters and ketones, are often inert to this reaction. The importance of hydrolysis stems from the fact that the products obtained are more polar and, consequently, more water soluble and less lipophilic than the parent compounds. Since hydrolysis reactions are commonly catalysed by $[H^+]$ or $[OH^-]$ ions, their rate directly depends on the pH.

1.1.3.2. Oxidation

Oxidation is the chemical process in which an electron-deficient molecule (the oxidant) accepts electrons from the compound to be oxidized. Some of the most common oxidants present under environmental conditions in sufficiently high concentrations and that react rapidly with organic

compounds are: alkoxy radicals (RO·), peroxy-radicals (RO_2·), hydroxyl radicals (HO·), singlet oxygen ($^1O_2$) and ozone (O_3).

Most of these oxidants are directly or indirectly generated from chemicals that interact with solar radiation, forming an "excited state". Oxidations are the main transformation routes for most organic compounds in the troposphere and for various micro-pollutants in surface waters [38]. In general, the hydroxyl radical (HO·) is the only oxidant of importance in the atmospheric systems, while in aquatic systems its concentration is so low that its contribution is negligible compared with RO· or RO_2·.

1.1.3.3. Reduction

Reduction is the chemical process by which electrons are transferred from an electron donor (reductant) to the compound to be reduced. These reaction pathways can contribute significantly to the removal of several micro-pollutants, like nitro aromatics, azo compounds, halogenated aliphatic and some aromatic compounds (i.e. PCBs, PCDD and PCDF) [39].

Reduction can take place in a variety of non-oxic systems, including sewage sludge, anaerobic biological systems, saturated soil systems, anoxic sediments, as well as in the gastronomic tract of invertebrate species, depending on several environmental factors, such as the prevailing redox potential, temperature, pH and the physical and chemical properties of the pollutants to be reduced. As in hydrolytic transformations, more polar products are usually formed with respect to the parent compound, which makes them more susceptible to further chemical attack and less likely to accumulate.

1.1.3.4. Photochemical degradation

The primary requirement for photochemical processes is the penetration of radiation, in particular UV light, in aqueous and atmospheric environments, which can initiate a wide variety of photolytic processes. Following absorption of a photon by a compound, the photon's energy either needs to be transferred to the reactive site within the molecule or transferred to another molecule, which may subsequently undergo a photochemical transformation. In particular, three categories of photochemical conversions can be usually distinguished:

- Direct photoreaction, in which the reacting molecule itself directly absorbs light and reacts;
- Indirect or sensitized photolysis, in which a light-absorbing molecule transfers its excess energy to an acceptor molecule causing the acceptor to react;
- Photo oxidation, in which molecules react with photochemically formed oxidative species.

In the aquatic environment, a fundamental factor is the absorption of light by dissolved and particulate matter, that clearly reduces the rates of direct photo-transformations changing also the light spectrum reaching in deeper water layers. However, dissolved and particulate matter may also be capable of initiating indirect photo-conversions. Given the various direct and indirect transformations that can take place due to interaction with solar radiation, a variety of primary and secondary photoproducts is often observed. Since penetration of light is usually possible only in oxic systems, most photoproducts formed are in a more oxidized state, compared with the parent compound.

1.1.3.5. Biodegradation

For most xenobiotic organic chemicals, microbial degradation plays a key role in their environmental fate. Biodegradation in the oxygen-containing biosphere of many pollutants often ends to their mineralization into inorganic end-products, like carbon dioxide and water. In the anaerobic environment, microbial degradation processes are generally much slower and may not always result in complete mineralization [40].

Environmental factors affect both the population distribution and the biochemistry of the bacteria responsible for these processes. For example, aerobic bacteria use oxygen both as a reactant for the oxidation of organic compounds, and as a terminal electron acceptor, which is necessary for the conversion of organic compounds into carbon dioxide, while facultative anaerobic bacteria can use oxygen but have the capability to change to another electron acceptor (i.e. nitrate and sulphate) if their environment turns anaerobic. On the contrary, oxygen is very toxic to the obligate anaerobic bacteria like the methanogens, which can only use alternative electron acceptors to derive energy from the conversion of hydrogen and carbon dioxide into methane.

The biodegradation of chemicals pollutants does not always result in bacterial growth, such as when micro-organisms, while growing on another widely available substrates, also have the capacity to transform other compounds xenobiotics without deriving any benefit from that transformation (co-metabolism) [41].

1.1.4. Persistence in the environment

The persistence of the various chemical pollutants introduced into the environment can depend from many factors, going from their nature and chemical structure to the prevailing environmental conditions. As they persist in the environment, these substances are capable of long-range transportation, bioaccumulation in human and animals, and biomagnifications in food chain [42], with consequent negative effects on human, flora and fauna's health. In the case of organic contaminants, for example, the type, number and position of substituents on aliphatic or aromatic

structures may cause “violation of comparative biochemistry and enzyme specificity” [43]. Moreover, substitution in radicals may cause important changes on the major metabolic pathways of biochemical oxidation.

Temperature is also an important factor, since around and below 4°C microbial processes become very slow. The mean temperature of the oceans (15°C) is borderline between the optimal temperature for psychrophilic (cold-loving) bacteria (0-20 °C) and mesophilic (moderate temperature loving) bacteria (20-40 °C). The amount of inorganic nutrients also affects the biodegradation rate, sometime exceeding the temperature effect. Lack of some chemical pollutants’ biodegradation may also be attributed to the presence of other, more easily degradable compounds leading to diauxism [44]. The pH is also a fundamental variable for these processes, determining both the form in which some chemicals exist and influencing the distribution of microorganisms’ populations [33]. The concentration of oxygen is also a critical parameter, since in aerobic environments, microorganisms utilize molecular oxygen both as a terminal electron acceptor and as a reactant in the degradation of a number of organic compounds [43]. In particular, the concentration of dissolved oxygen in aquatic systems is dependent on the water temperature, salinity, biological activity, and reaeration rate. Biodegradation processes in soils and sediments are greatly influenced on the extent of the partitioning of contaminants to the solid phase, since degradation takes place entirely in the water phase [43]. The degradation of chemical pollutants may also be impeded by their encapsulation in micro sites (i.e. clay minerals or the organic matrix of soil or sediment) or strong chemical bonding to solids, which may could make interaction with bacteria physically impossible.

1.2. Composition and properties of soils and sediments

Soils can be generally defined as the unconsolidated top layer of the Earth's surface, consisting of mineral particles mixed with organic matter (humus), water and air formed by a combination of physical, chemical, and biological processes, called pedogenesis, which act upon the parent material, or bedrock, through a period of time and are driven by geological, biogeochemical, topological, climatic, chronological and, anthropogenic influences [45].

This can cause significant differences between soils and their parent materials regarding morphology, physico-chemical, mineralogical properties and biological characteristics. For these reasons soil types can vary widely from one region to another, mainly depending on the type of bedrock they overlie and the climate and topography in which they form [46,47].

Soils are fundamental environmental components for many reasons, since they are the substrate which provides support and food for primary producers and regulate both biological activity and molecular exchanges among solid, liquid and gaseous phases, consequently affecting nutrient cycling, plant

growth and decomposition of organic materials. Soils can also act as filters to protect water quality, influencing water runoff, infiltration, storage and deep drainage.

Sediment can be defined as "suspended or deposited solids, acting as a main component of a matrix which has been or is susceptible to being transported by water" [48] and it is an essential, integral and dynamic part of river basins, including estuaries and coastal zones. Sediment is also one of the fundamental components of the aquatic ecosystem, since it forms a variety of habitats and environments and is an important source of nutrients for a variety of organisms and, indirectly, for species higher in the food chain.

In general, sediment can either be produced from the weathering and erosion in upstream areas of minerals, organic material, and soils susceptible to being transported downstream by surface waters, from the erosion of riverbanks or it can be originated from biogenic processes.

Sedimentation is not restricted or limited to a specific area or part of a river basin, but as flow rates tend to decline in lowland areas, transported suspended solids settles along the riverbanks and on the bed of the river. This phenomenon occurs also on floodplains during flooding, in reservoirs and in lakes.

1.2.1. Morphology and texture

One of the main characteristics of soil is its constituents' organisation into layers related to present day surface. Each of these layers, normally referred to as horizons, can be usually identified through colour or texture and show subtle differences in chemical properties and composition, of which the most relevant are pH, organic matter content, mineral assemblages and metal concentrations [47]. They are usually classified according to their position in profile, which is also closely linked to their mineralogical constitution and grain size.

The first layer of the profile is the O horizon, composed of partially decomposed organic debris, derived from plants and animal litter. It is in this region that a large variety of microorganisms carry out humidification, one the most important processes in soil formation, changing these organic debris into soil organic matter. Underneath this layer there is the A horizon, characterized by the obliteration of all or much of the original rock structure and by the accumulation of organic components decomposed beyond recognition [49]. Underneath these layers, the transition to the base of the profile made of the parent material (R horizon) can be divided into three other horizons, composed mainly of sand, silt clay and other weathered by-products. The two following layers are identified on the basis of the main processes controlling the migration and redeposition of nutrients and inorganics that that take place within them. The E horizon is characterized by the leaching and transport of dissolved or suspended material by the percolation of water (eluviation), which causes the loss of silicate clay,

carbonates, gypsum, iron and aluminium and leaves a concentration of sand and silt particles [50]. The consequent deposition of these materials (illuviation) instead takes place in the B horizon.
The last layer before hard bedrock, referred to as C horizon, represents the stage nearest to the parent material and is made up of partially or poorly weathered material containing only very limited amounts of organic matter and clay [50].

Sediments, on the contrary, do not present such differentiated morphology, because their deposition essentially depends on the surface spread of the catchment area, the intensity of physical weathering of rocks, particles dimensions, and the hydrology, geology, topography of the water bodies involved [51]. Without considering stones and gravel, soil particles range in size over four orders of magnitude, going from 2.0 mm to less than 0.2 μm in diameter. Particles that are large enough (2.0–0.05 mm) to be seen by the naked eye and do not adhere to one another are classified as sand, while particles having particle diameter between 0.050 μm and 0.2 μm are classified as silt. The smallest mineral particles (<0.2 μm) are classified as clays, some of which (<0.1 μm) have colloidal properties [50]. Clay's particles are characterized by high surface area and exhibit net surface charge that attract positive or negative ions as well as water, making this fraction of the soil very chemically and physically reactive.

The percentage of clay, silt and sand (soil texture) of a particular soil deeply affects many of its physical and chemical properties, as well as its suitability for most uses. At the same time, the association of these primary soil particles to form secondary aggregates (soil structure) due to the presence of fungal hyphae, plant roots, microbial gums, polysaccharides, and other microbial metabolites is fundamental in controlling air and water movement through the soil [50,52].

1.2.2. Soil constituents

Soil can be considered as a three-dimensional system, made of a solid, a liquid and a gaseous phase, each in an amount depending both on the abundance of its constituents and the complex series of interactions leading to its formation. In the following section each of these components will be briefly described.

1.2.2.1. Minerals

Minerals are natural inorganic compounds having definite physical, chemical, and crystalline properties [53]. They can be classified into various categories depending on their formation (primary or secondary), silica content (silicates or non-silicates) crystallinity (crystalline or non-crystalline) or chemical composition. Those minerals that have not been substantially altered chemically since their crystallization within igneous or metamorphic rocks or their deposition in sedimentary rocks are

called primary minerals, while those that have been subjected to weathering (chemical breakdown and/or alteration of under ambient conditions) are called secondary minerals [53]. The separation of soil minerals in primary and secondary classes is not necessarily mutually exclusive since some of them, like quartz, carbonates and mica, can occur in both classes. Minerals composed of atoms arranged in a three-dimensional periodic pattern are classified as crystalline, while those lacking this structural periodicity are defined as non-crystalline. Based on their chemical composition and their dominant anion or anionic group, minerals are divided into eight classes including [53].

- Native elements;
- Sulphides;
- Oxides and hydroxides;
- Halides
- Carbonates, nitrates, and borates;
- Sulphates, chromates, and selenates;
- Phosphates, arsenates, molybdates and vanadates;
- Silicates.

These classes are subdivided further according to chemical and structural similarities [54]. Some of them, such as the native elements, nitrates, borates, chromates, molybdates, arsenates and vanadates are rarely found in soil environments and therefore will not be described further.

Sulphides

A class of minerals containing sulphide (S^{2-}) or persulfide (S_2^{2-}) as the major anion, which constitute the major source of world supplies of a very wide range of metals (i.e. Fe, Zn, Pb, Cu and Ag) and are the most important group of ore minerals [55]

Pyrite (FeS_2) is the most common mineral of this group, although it is found only in a few soils. It forms under prolonged anaerobic conditions characteristic of wetlands, which explains its common association with coal deposits. These minerals are sensitive to oxygen, water and microbial attack, readily weathering into other sulphate minerals and sulfuric acid. The leached acidity and heavy metals can constitute serious environmental problems, especially toward surface and groundwaters.

Oxides and hydroxides

This group is composed by relatively hard, dense, and refractory minerals characterized by the combination of oxygen or hydroxyl groups with one (simple oxides) or more metals (multiple oxides). The most common minerals that belong to this group are Fe and Al minerals [56] such as goethite ($Fe^{+3}O(OH)$), hematite (Fe_2O_3), and gibbsite ($Al(OH)_3$), which are characteristic of in intensely weathered tropical soils. These minerals usually show pH-depending amphoteric surface

charge properties and can act as chemical binding agents, playing an important role in soil aggregation and structural formation [53].

A high content of Fe-minerals can influence the overall colour of the soil, since under oxidizing conditions they can show bright red to brownish-yellow hues, while under reducing conditions they turn grey due to Fe^{3+} to Fe^{2+} reduction. These changes of colour can be used as indicators in pedogenic (degree of weathering) and land use interpretations (soil drainage classes, septic systems, wetland delineations).

Manganese oxides and hydroxides, often associated with Fe-oxide minerals, are also common components of soils, especially as birnessite and lithiophorite.

Another less abundant group of minerals, usually found in sand and silt fractions as common accessory minerals of igneous and metamorphic rocks, includes titanium oxides, such as rutile, anatase, and ilmenite, which due to their high resistance to weathering are usually used as paedogenic indicators of soil maturity and uniformity.

Halides, sulphates and carbonates

Halides are salts having F^-, Cl^-, Br^- and I^- as main anions, but only some of those containing F^- and Cl^- have any petrogenic significance, such as halite (NaCl), sylvite (KCl), chlorargyrite (AgCl), cryolite (Na_3AlF_6), fluorite (CaF_2), and atacamite. Sulphates, salts of sulfuric acid (H_2SO_4), occur mainly as gypsum ($CaSO_4 \cdot 2H_2O$) and anhydrite ($CaSO_4$) and, rarely, as baryte, kieserite and polyhalite. Carbonates are the salts of carbonic acid and can form several isomorphic structures in the presence of Ca, Mg, Fe, Mn, Zn, Sr, Ba, and Pb, the most important of which are dolomite ($MgCa(CO_3)_2$), calcite and aragonite ($CaCO_3$) [57].

These mineral groups contain some of the most soluble soil minerals, and they are easily susceptible to physical and chemical weathering, thus occurring mainly in arid/semiarid regions or in soils where weathering is limited. While halite is found only in salt affected soils, gypsum is common in both saline soils, either under arid or hydromorphic conditions, and at weathering interfaces where sulphide and carbonate minerals dissolve. Calcite and dolomite, while most common in arid and semiarid climatic zones can also be found in other soil environments where the dissolution of calcareous parent materials causes secondary carbonate precipitation at lower soil depths.

Phosphates

Phosphates are salts of phosphoric acid (H_3PO_4), and only those from the apatite group ($Ca_5(F, Cl, OH)(PO_4)_3$) have petrogenic significance. These minerals are found in only a few soils, and along with their weathering products like Al- and Fe-phosphates, are considered a natural source of P for plants and soil microorganisms. About 90% of the phosphate rocks mined annually is used to produce fertilizers, animal feed supplements and industrial chemicals [53,57].

Silicates

The fundamental building unit of these minerals is a Si-tetrahedron, in which one Si^{4+} cation is coordinated with four apical O^{2-} anions. Different arrangements of individual Si-tetrahedra, linked by sharing one oxygen atom between two adjacent tetrahedra, form more complex structures, consisting of single tetrahedral (neso-silicates), double tetrahedral (soro-silicates), rings (cyclo-silicates), single or double chains (ino-silicates), sheets (phyllo-silicates), or three-dimensional frameworks (tecto-silicates) [53].

Silicates constitute the largest and most important group of soil minerals, accounting for about 40% of the most diffuse minerals in the world. Some of the most important primary silicate minerals that make up the majority of most soils' sand and silt fractions include quartz, feldspars, olivines, pyroxenes, amphiboles, and micas.

Quartz is a tecto-silicate mineral and, due to its high resistance to weathering, it is probably the most abundant mineral found in soils. Even if it is considered a chemically inert skeletal material, poorly crystalline forms of quartz may serve as cementing agents for soil materials.

Feldspars are tecto-silicate minerals where some of the Si^{4+} cations are replaced by Al^{3+} ions with extra base cations like Ca^{2+}, Na^{+} or K^{+} to re-establish neutrality. Their weathering stability decreases in the sequence Na < Ca < K, producing secondary minerals that are important sources of K and Ca in soils. The most abundant types of feldspars are: $KAlSi_3O_8$ (orthoclase and microcline), $NaAlSi_3O_8$ (albite), and $CaAl_2Si_2O_8$ (anorthite).

Secondary silicate minerals (i.e. phyllo-silicates) are composed by multiple stacks of Si-tetrahedral sheets and Al-octahedral sheets held together either by weak van der Waals bonds strong hydrogen bonding. Si-tetrahedral and Al-octahedral sheets can bond either in 1:1 or in 2:1 structural arrangement, where the interlayer space can be occupied by water, hydrated or un-hydrated cations, cations coordinated with hydroxyls or other molecules. Various isomorphous substitutions, limited by the cation's size, within the tetrahedral or octahedral sheets are possible, involving in particular Al^{3+} for Si^{4+} in the in the tetrahedral sheet and Fe^{2+}, Fe^{3+} and Mg^{2+} for Al^{3+}in the octahedral sheet. In some cases, other cations may be involved in these substitutions as long as they have coordination numbers of 4 or 6 for tetrahedral vs. octahedral substitutions, respectively. This can produce a net charge, which is balanced by free ions, which is the cause of these minerals' ion exchange capacity.

Since many phyllo-silicates' structural configurations are very similar to each other, the stack of layers making up a mineral particle may consist of a mixture of two or more minerals, characterized by a periodic sequence (regular inter-stratification) or by random layers (random inter-stratification). Randomly interstratified mineral assemblages are far more common in soil environments than regularly interstratified minerals

1.2.2.2. Soil water

Precipitation and groundwater are the two principal sources of water in soil, contributing to a delicate dynamic equilibrium which depends mainly on climatic conditions and on the water balance between the atmosphere and the plant-soil system [14].

The amount of vapour transferred from the soil into the atmosphere by evaporation or by plant transpiration is also closely related to the way water is held in the soil. In particular, it is very important to distinguish between the water available for root uptake (capillary water, held in the soil by surface tension and cohesive forces), the water unavailable to plant roots (hygroscopic water, forming thin films on the surface of colloidal soil particles by hydrogen bonds) and the water percolating downward to join the groundwater reservoir (gravitational water) [58].

Soil water can contain a wide range of dissolved and/or suspended organic, mineral, and gaseous substances. The mayor constituent of these solutions includes dissolved salts and gaseous compounds, such as O_2 and CO_2. The latter may come from the atmosphere by being dissolved in precipitation, from the soil gas as a product of soil organisms' respiration or as a product of organic matter decomposition. The most common ions found into the soil water include cations such as Ca^{2+}, Na^{+}, K^{+}, and NH^{4+}, as well as anions like NO^{3-}, PO_4^{3-}, and Cl^{-}. These ions can be introduced into the soil solution by both external sources, such as air borne marine salts and acid deposition, and by internal chemical processes taking place within the soil (i.e. weathering, diagenesis, decomposition and synthesis of organic matter) [59]. Under acidic conditions, Fe^{2+}, Fe^{3+} and Al^{3+}ions may also constitute a considerable part of the cations dissolved into the soil water [60].

Minor constituents of soil solution also include small amounts of soluble and suspended organic compounds, dissolved silica and heavy metals.

The overall concentration of ions in the soil water, however, depends mainly on the soil-pH, its oxidation status and the affinity to processes such as adsorption, precipitation and desorption. Lower pH-values cause the adsorption of a lower quantity of substances, which will in turn lead to higher metal concentrations in the solution [14].

The concentration of CO_2 in the soil solution is important factor that influences the soil pH since, for example, soil water in equilibrium with the CO_2 present in soil air has pH-values often below five. This acidity is mainly caused from the processes like organic acids' production during degradation of organic matter, nitrification processes, release of H^{+} ions by plants in exchange for nutritive base cations, sulphide oxidation, and pollution.

1.2.2.3. Soil air

Soil air, soil atmosphere, or soil gas are the characteristic names used to identify the mixtures of gases filling the soil pores, where these are not already occupied by interstitial water, and moving in the vadose zone above the water table. The composition of these gasses depends on the relative magnitude of both the sources and the sinks of the various gas components, the interchange between soil air and atmospheric air, and the partitioning of the gases between the gaseous, liquid, and solid (mineral and organic matter) phases of the soil [61]. In particular, the mass flow of these gases in the aerated zone will be controlled by atmospheric factors such as temperature, pressure, and moisture conditions. The composition of these gasses is slightly different from that of atmospheric air, containing 1–6% less oxygen by volume since O_2 is consumed in soil by plant root and microbial respiration and through chemical reactions. and about 10 to 150 times more CO_2 [14].

These differences of CO_2 and O_2 concentration between soil air and the atmosphere cause partial pressure gradients between the two systems along which O_2 moves from the atmosphere to the soil, while CO_2 flows in the opposite direction. Gas exchange between soil air and the atmosphere may also take place along temperature gradients and in places where rainwater introduces atmospheric gases into the soil. Minor or trace amounts of other gases may be also found in the soil gas, originating from deep-seated sources or as products of organic or mineral reactions in the soil environment, such as CH_4, H_2, H_2S, CO and C_2S [62,63].

1.2.3. Sediment constituents

Sediment can also be considered as a three-dimensional system, made of a solid, a liquid and a gaseous phase, each in an amount depending both on the abundance of its constituents and the complex series of interactions leading to its formation. Sediments can be constituted by particles originating from the weathering and erosion of minerals (described above) or from skeletal remains of marine organisms [64].

While a multitude of plants and animals can contribute to the organic matter that accumulates in marine sediments, only a relatively limited group of organisms are significantly responsible for the production of biogenic deep-sea sediments, which are mainly composed by either calcareous or siliceous oozes. Both distribution and accumulation of biogenic oozes in oceanic sediments can depend by several factors, like the production rate of biogenic particles in the surface waters, the dissolution rates of those particles in the water column, and the rates of dilution by terrigenous sediments after they reach the bottom [65].

The abundances and distributions of the organisms producing biogenic sediments are closely related to several environmental factors, such as nutrient supply and water temperature. Dissolution rates are

dependent upon both the chemistry of the waters through which the skeletal remains settle and that of the bottom and interstitial waters in contact with the remains. Moreover, all these factors are also heavily dependent upon the rates of deep ocean circulation and the length of time that the bottom water has been accumulating CO_2 and other by-products of biotic activities [64].

1.2.3.1. Carbonate Oozes

Most carbonate or calcareous oozes are mainly produced by the two different groups of organisms. The first group is composed by phytoplankton of the marine algal group, the Coccolithophoridae, which tends to produce tiny (less than 10 μm) calcite plates called nanofossil or coccolith ooze. The second group is composed by planktic protists belonging to the Foraminiferida family and produces sand-sized (> 63 μm in diameter) calcite shells. A lesser contribution to the production of carbonate oozes is given by shells of pteropods and heteropods which are, differently from the previous ones, made of aragonite [66].

Carbonate oozes are the most widespread shell deposits on earth, since almost half the pelagic sediment in the world's oceans is carbonate ooze. Furthermore, because foraminifera and coccolithophorids have been the major producers of pelagic sediment for the past 200 million years, the evolution of species and higher taxa, as well as their fossils, provide the single most important record of earth history over the past 200 million years [65].

The distributions and abundances of living planktic foraminifera and coccolithophorids in the upper few hundred meters of the ocean are dependant from both the nutrient supply and temperature.

The accumulation of carbonates is mainly controlled by dissolution processes in bottom waters rather than by production in surface waters [65]. Since dissolution of calcium carbonate in seawater is influenced by temperature, pressure, and partial pressure of CO_2, these processes are favoured in the deep ocean than in surface waters. In particular, the depth at which surface production of calcium carbonate equals dissolution is called the “calcium carbonate compensation depth” (CCD). Above this depth, carbonate oozes can accumulate while below this threshold only terrigenous sediments, oceanic clays, or siliceous oozes can accumulate [66].

1.2.3.2. Siliceous Oozes

Biogenic siliceous oozes are mainly produced by four contributors.

The two most common siliceous shells are made of opaline silica by diatoms (*Bacillariophyceae*, a species of golden-brown algae) and by a large group of marine protists distantly related to the foraminifera (*Radiolaria*).

Lesser contributions to the production of siliceous oozes are made by silicoflagellates (*Dictyochophyceae*, a minor group of marine algae) and sponge spicules.

Since silica is undersaturated throughout most of the world's oceans, its extraction from seawater for production of silica shells or skeletons requires substantial energy. Moreover, the preservation of siliceous sediments requires them to deposited in waters close to saturation with respect to silica and a quick burial. For these reasons, since seawaters around volcanic islands and island arcs tend to have higher concentrations of H_4SiO_4 in solution, this kind of sediments are most common beneath upwelling zones and near high latitude island arcs, particularly in the Pacific and Antarctic. In fact, more than 75% of all oceanic silica accumulates on the sea floor between the Antarctic convergence and the Antarctic glacial marine sedimentation zone [67].

Since conditions favouring deposition of silica or calcium carbonate are quite different, the patterns of carbonate and silica deposits reflect different processes of formation and preservation, resulting in carbonate oozes that are poor in biogenic silica and vice versa.

Most siliceous oozes remain unconsolidated after burial, but a fraction can dissolve and reprecipitate as chert beds or nodules forming beds that are very difficult to drill, since chert is very hard and impermeable.

1.3. Remediation of contaminated soils and sediments

While heavy metals can be naturally present in both soils and sediments, with concentrations depending on both the paedogenic or weathering processes of the parent materials, and the hydrological conditions of the water bodies involved [3,68], organic pollutants are mainly introduced into the environment by anthropogenic activities. Moreover, these activities (i.e. mining and smelting of metals, combustion of fossil fuels, agricultural use of fertilizers and pesticides, and disposal of sewage sludge, and municipal and industrial waste [69,70]) can also lead to an increase of heavy metals concentrations in various environmental compartments up to harmful levels for human health, plants, animals, and ecosystems [69,71].

The nature and degree of pollution for each contaminated site may vary widely but, in most cases, these sites do not pose immediate dangers or serious risks to the surrounding population. Instead, the risk associated to polluted sites generally results from exposure to pollutants at low doses over a long period of time, which may even correspond to a lifetime. A polluted site may also become a threat to groundwater or surface waters, endangering both biota and drinking water resources. In any case, damage to a given target is possible only if the risk source and the target are in contact (directly or indirectly) and a transfer of pollutants occurs from the source to the target [72]. For these reasons, when source of pollution, transfer and target are present at the same time, risk does exist, and the

application of suitable risk assessment methodologies is essential, in order to identify the issues of concern and define the suitable actions to be implemented [73].

1.3.1. Risk assessment and management

Risk is a concept that denotes a potential negative impact to an asset. This implies that there must be a source for this potential negative impact, which is generally called a hazard. As far as contaminated sites are concerned, the hazards are the adverse effects on selected targets of soil or groundwater contaminants.

The characterization of potential risks to the environment and human health posed by contaminated soils and sediments can be a very difficult task due to the heterogeneity and complexity of the matrix, a poor understanding of some contaminants' fate, scarcity of toxicological/ecotoxicological data, and variability of matrix-screening levels. However, several different frameworks for simple, cost-effective, and reliable ways to manage contaminated sites on the basis of risk assessment have been developed over the last few decades.

In this context, **Figure 1.1** shows the schematization of one of the most used frameworks for the management of contaminated sites , reported in 1983 by the US National Research Council [74].

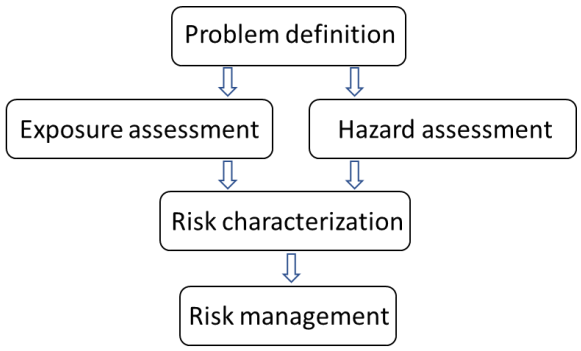

Figure 1.1. The contaminated site management framework, in accordance with [74].

The first step in this framework is to define the problem, identifying the objectives, the issues and the targets involved, while the second step requires to assess the exposure of the selected targets to each contaminant (exposure assessment) and their effects (hazard assessment) for the risk characterization. This is then followed by the application of the appropriate measures to mitigate the detected risks to an acceptable level. Each of these steps will be briefly discussed in the following section.

1.3.1.1. Problem definition

The first step in a contaminated site management project is to define the problems, clearly describe the scope and identify all the factors involved (issue framing). In addition, it is also very important to define the relevant time frame, since the factors impacting risks can change over time. Considering the definition of risk, it is fundamental to determine the nature and value of the asset that

need to be protected. Regarding contaminated sites, several targets needing to be protected have been recognised. While human health has always been considered the most important one, many studies proved the importance of soil ecosystem, groundwater and food safety, together with the extent of their influence on human health [75–83]. In addition to the targets, the level of protection also needs to be defined, and the combination of these two parameters is often referred to as the 'endpoint'. An important factor that affects both the risks and the degree to which they are evaluated, is the use planned for the considered contaminated site, since it influences the type, duration and mechanism of exposure of each target to the various pollutants. The selection of appropriate protection targets and level of protection in regulatory frameworks is primarily a policy decision but, since the protection targets' significance and the appropriate levels of protection are often difficult to understand, these decisions need to be supported by ample scientific investigation [84].

1.3.1.2. Exposure assessment

Exposure assessment can be considered as the process of characterizing, estimating, measuring, and modelling the magnitude, frequency, and duration of contact with an agent as well as the size and characteristics of the population exposed [85]. In particular, exposure is defined as the concentration or amount of a particular agent that reaches a target in a specific frequency for a defined duration [86], implying that it could represent a rate, expressed as mass per unit of body weight and time ($mg \cdot kg_{bw}^{-1} \cdot d^{-1}$), but also as concentration, expressed as mass per unit of volume (mg/L) [84]. Exposure is usually estimated using various multimedia models [87–92] to correlate the concentration of each contaminant found in the polluted matrix with both the transport mechanisms involved and the selected targets. The most common courses (exposure pathway) that a hazardous agent can travel from a source to a receptor (i.e. human being, animal, plant, algae …) via environmental carriers or media generally involve transport through air (volatile compounds, particulates) or water (soluble compounds), while the most frequent mechanisms by which the transfer occurs (exposure route, or intake pathway) are inhalation, ingestion, and/or dermal contact [93].

1.3.1.3. Hazard assessment

Hazard assessment can be divided into two steps, namely, hazard identification and hazard characterisation [84,86]. While the first one focuses on determining both the possible effects of each specific contaminant on the selected targets and the time frame for which these effects take place, the second deals with assessing a dose-response relationship, relating exposure to effects in order to determine the "critical exposure" for each contaminant. Hazard identification for a pollution risk assessment usually consists of a review of all relevant biological and chemical information on whether or not an agent may pose a specific threat [93].

The quantification of the adverse effects arising from exposure to a hazardous agent based on the degree of exposure (dose-response or hazard characterisation assessment) is usually expressed mathematically as a plot showing a response (i.e., mortality) in living organisms to increasing doses of the agent. Regarding human risk assessment, most of the information necessary for this process is derived from laboratory studies in which researchers expose laboratory animals (i.e. mice and rats) or microorganisms to increasingly higher doses of these agents and observe their corresponding effects. Responses or effects may be subjected to large variations going from no observable effect, to temporary and reversible effects (i.e. enzyme depression or diarrhoea), to permanent organ injury (i.e. liver and kidney damage), to chronic functional impairment (i.e. bronchitis or emphysema), to death [93]. Due to the high costs involved in the experimental tests need to obtain toxicological data, low-dose responses are usually extrapolated from their high-dose data. Since several mathematical models have been developed [94–97], the most common approach for non-cancerogenic substances is to allow for the existence a certain dose (threshold) below which there is No Observed Adverse Effect (NOAEL) by virtue of the body's natural repair and detoxifying capacity. This threshold is used to estimate the *reference dose* (RfD) of each contaminant, defined as the intake, or dose, of the substance per unit body weight per day (mg kg^{-1} day^{-1}) that is likely to pose no appreciable risk to human populations, including such sensitive groups as children, elders or pregnant women.

The RfD is obtained by dividing the NOAEL by appropriate uncertainty factors (VF_i) (or safety factors) (**Eq. 1.6**), calculated to account for differences in sensitivity between the most sensitive individuals in an exposed human population, for the extrapolation of data to human beings from animal testing, and for the possible lack of data [93].

$$RfD = \frac{NOAEL}{\prod_1^n VF_i} \qquad (Eq.\ 1.6)$$

On the other hand, carcinogens are considered "non-threshold contaminants" under the conservative assumption is that exposure to any amount of these substances can increase the likelihood of cancer. For this reason, the only intake of a carcinogen considered ''safe'' is zero, so the dose–response plot must go through the origin. The parameter used to estimate the hazardousness of carcinogenic pollutants is the slope of the dose–response plot (slope factor, SF) [84].

Toxicity tests are also used to evaluate the effects of the presence of pollutants in several environmental media (i.e. air, water, sediment, soil) on the survival, growth, reproduction, and behaviour of a number of organisms, in order to establish whether those substances are bioavailable and have the potential to cause biochemical damage to the biological tissues and organs of these organisms. If mixtures of pollutants are present in the tested media, the toxicity tests can evaluate the

aggregate toxic effects. Also in this case, the effects on the tested organisms are classified as acute, chronic, lethal or non-lethal. For example, sublethal effects include reduced growth, impaired reproduction, behavioural changes, reduction of size of organisms at the level of communities, disruption of community functions among its species and ecosystem-level functions [98].

1.3.1.4. Risk characterization

Risk characterization can be defined as estimating the potential impact of a hazard on a target based on the severity of its effects and on the amount of exposure under specific conditions.

In the case of non-cancerogenic pollutants, risk is expressed in terms of a hazard quotient (HQ) for a single substance, or hazard index (HI) for multiple substances and/or exposure pathways, following **Eq. 1.7** and **Eq. 1.8**.

$$HQ = \frac{CDI}{RfD} \qquad (Eq.\,1.7)$$

$$HI = \sum_{i=1}^{n} HQ_i \qquad (Eq.\,1.8)$$

where

CDI = chronic daily intake ($mg \cdot kg^{-1} \cdot day^{-1}$);

RfD = reference dose.

The value of HQ and HI has been defined so that if it is less than 1.0, there should be no significant risk or systemic toxicity, while higher values denote unacceptable level of risk.

If the dose-response curve is assumed to be linear at low doses, for cancerogenic substances excess cancer risk (R) can be calculated, following **Eq. 1.9**, as the product of CDI and SF.

$$R = CDI \cdot SF \qquad (Eq.\,1.9)$$

where:

SF = slope factor of the dose-response curve for cancerogenic substances.

If more than one cancerogenic pollutants are present, the cumulative risk (R_{cum}) is calculated as the sum of all the substances involved (**Eq. 1.10**).

$$R_{cum} = \sum_{i=1}^{n} R_i \qquad (Eq.\,1.10)$$

The decision on the acceptable excess cancer risk is a policy decision and values used in Human Health Risk Assessment (HHRA) in regard to contaminated sites range worldwide between 10^{-4} and 10^{-6} [84].

After risk characterization has been carried out, the most appropriate solutions for risk management are selected, depending on the final use of the contaminated site and on the best available

technologies. More in depth contaminated site management frameworks, considering also economic and social issues, are reported in the literature [84,99].

1.3.2. Italian regulatory framework

The Italian approach to the regulation regarding soil contamination is to set the objectives of reclamation according to the intended use of the site (e.g. residential, green, commercial, and industrial use). An implication of this is that the treatment of the contaminated matrix will be accomplished only when its future purpose is established.

Regarding contaminated soils, the first approach used to deal with the management of contaminated sites in Italy followed the application of a "limit value" criterion, as established in the Decree of the Ministry of the Environment No 471 of 03/04/1999 [100]. This law has been repealed in 2006 by the adoption of Legislative Decree No 152 of 03/04/2006 (Consolidated Environmental Protection Code) [101] which, as subsequently modified, contains the Italian contaminated land regime. Differently from the previous legislation, this decree is based on the application of a three tiered risk-based approach [102] for the characterization and management of the contaminated sites.

In detail, Title V, section IV of the Consolidated Environmental Protection Code sets out the legal structure to deal with contaminated land issues. This document i) sets the definition of contaminated land and of land at risk of contamination; ii) sets out the duty to carry out prevention measures to tackle the risk of contamination; iii) regulates the administrative procedures for the approval of plans for monitoring and remediating contamination; iv) determines liability and duties of persons held responsible for contamination and v) allocates and divides the costs of carrying out the clean-up works among the responsible people [103].

On the occurrence of an event that could cause land or groundwater contamination, the Legislative Decree No 152 of 03/04/2006 (Title V, section IV) imposes a series of complex procedures that can be divided into several tiers, which are summarized in the following section and **Figure 1.2**.

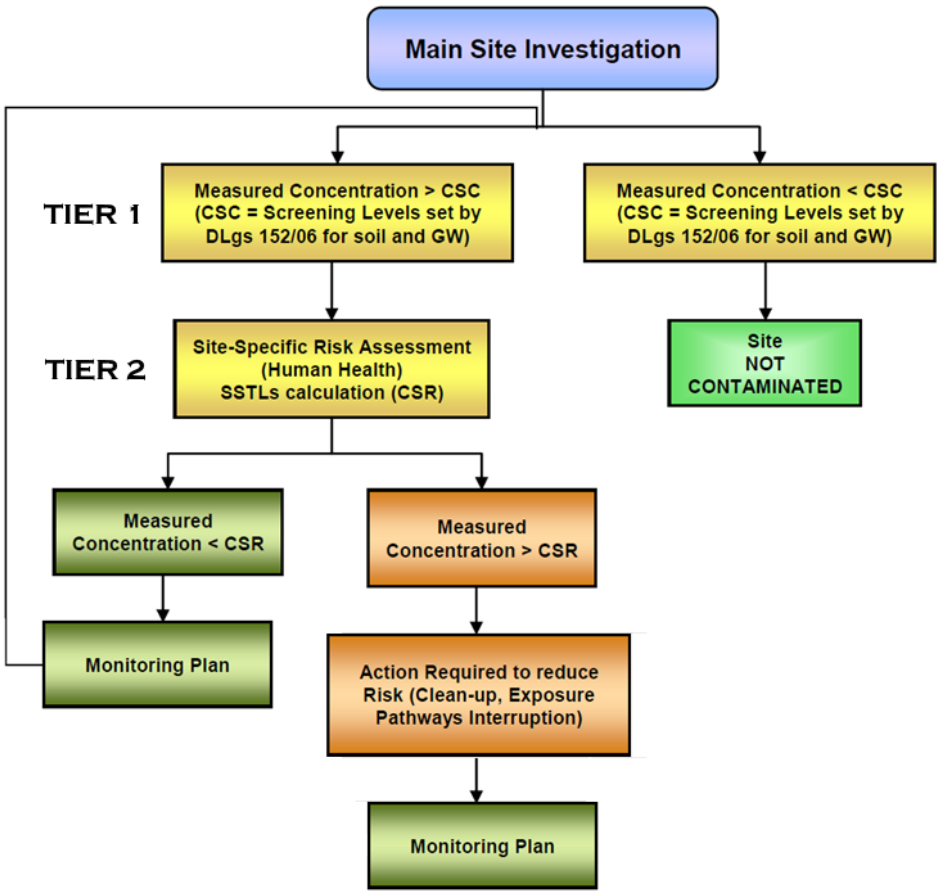

Figure 1.2. Procedures to be adopted in the case of soil or groundwater contamination according to Legislative Decree No 152 of 03/04/2006 (Title V, section IV) [101].

After carrying out the appropriate emergency measures and notifying the contamination to the relevant local authorities of the Ministry of Interiors, the person responsible for the contamination must execute a preliminary investigation (Tier 1) on the site to verify whether the CSC thresholds (*Concentrazioni Soglia di Contaminazione*, screening levels set by the Legislative Decree No 152/2006 for soil and groundwater) for the concentration of organic and inorganic pollutants have been exceeded or not. If the values obtained by analysis are inferior to the CSC threshold, the site is considered non-contaminated, thus concluding the procedure. If the values exceed the CSC thresholds, the responsible person must, after informing the relevant authorities, submit for approval a detailed characterisation plan (Annex 2, section IV, Consolidated Environmental Protection Code). to determine the actual level and extent of contamination. On the basis of the results of the characterisation plan, the site must undergo a site-specific health and environmental risk analysis procedure (TIER 2) in accordance with the general criteria set out in Annex 1, section IV of Legislative Decree No 152/2006 [101]. **Table 1.1** shows CSC concentration thresholds for the inorganic and organic contaminants subject of study in this thesis.

Table 1.1. CSC concentration thresholds for the inorganic and organic contaminants subject of study in this thesis (Table 1 of Annex V to Part IV of Title V of Legislative Decree No 152 of 03/04/2006 [101].

Contaminant	Column A (residential and green use)	Column A (commercial and industrial use)
	$mg \cdot kg^{-1}$ d.w.	
Antimony (Sb)	10	30
Arsenic (As)	20	50
Beryllium (Be)	2	10
Cadmium (Cd)	2	15
Cobalt (Co)	20	250
Chromium (Cr)	150	800
Mercury (Hg)	1	5
Nickel (Ni)	120	500
Lead (Pb)	100	1000
Copper (Cu)	120	600
Selenium (Se)	3	15
Tin (Sn)	1	350
Thallium (Tl)	1	10
Vanadium (V)	90	250
Zinc (Zn)	150	1500
Hydrocarbons C_{12-40}	50	750

During this part of the characterization of the contaminated site, a series of Site-Specific Target levels (SSTLs, or *Concentrazioni Soglia di Rischio* (CSR)) are calculated by the application of site-specific risk analysis (backward application) for both soil and groundwater. An additional level of site-specific risk assessment (TIER 3), even if not required by the regulation, may be carried out to evaluate pollution- and time- related risks to off-site targets by the use of more sophisticated mathematical descriptions of fate and transport phenomena.

If the results of the specific health and environmental risk analysis show that the level of contamination is lower than the CSR thresholds, only further monitoring, to ensure that relevant values do not exceed the CSR thresholds, is needed. On the contrary, if CSR thresholds are exceeded appropriate risk management actions must be taken, such as reclamation, clean-up, or exposure pathways interruption. Moreover, monitoring of the remediated site may be necessary, depending on the technologies applied during the reclamation operations.

Regarding dredged sediments, the Italian legislation includes several alternative provisions describing the criteria used to establish their possible uses, depending on their origin.

In detail, the reuse of sediments dredged inside Italian remediation Sites of National Interest (SNI) is regulated by the Law n° 84 of 28/01/1994 [104], which refers to the Ministerial Decree No 172 of 15/07/2016 [105] and to the Ministerial Decree of 7th November 2008 [106] for the technical

requirements. The management of sediments not dredged from a SIN is regulated by the Legislative Decree No 152 of 03/04/2006 (Article 109, paragraph 2) [101], which refers to the Ministerial Decree No 173 of 15/07/2016 [107] for the technical requirements. Moreover, the management of sediments dredged from other sites of crucial environmental concern, such as the lagoon of Venice, is governed by specific *ad-hoc* regulations [108]. In addition, the Water Framework Directive (WFD) 2000/60/EC [109], the Directive 2008/1/EC concerning integrated pollution prevention and control [110] and the Directive 2013/39/EU on priority substances in the field of water policy [111]

introduced several environmental quality standards regarding the good management of the European waster bodies. The aforementioned Directives have been transposed in Italy by the Legislative Decree No 172 of 13/10/2015 [112]. If the criteria mentioned above are not met, the dredged sediments are considered as waste and are subjected to the legislation that regulates waste management (Ministerial Decree of 5th February 1998) [113]. In particular, those sediments are classified as "dredging sludge" (code 170506), while contaminated soils are classified as "excavated soils and rocks" (code 170504) [113]. They can be reused in environmental rehabilitation operations as filling material, in the construction of embankments and in road foundations after being subjected to an appropriate treatment that must lead to a final material complying with the limits on the leaching of contaminants established in the Ministerial Decree No 186 of 05/04/2006 (Table 1 of Annex III) [114] (**Table 1.2**).

Table 1.2. Regulatory limits for the leaching test UNI12457-2:2004 for the reuse of contaminated wastes after appropriate treatment, in accordance to Ministerial Decree No 186 of 05th April 2006 (Table 1 of Annex III) [114].

Contaminant		**Contaminant**	
	$\mu g \cdot L^{-1}$		$mg \cdot L^{-1}$
Arsenic (As)	50	**Nitrates (NO^{3-})**	50
Barium (Ba)	1000	**Fluorides (F^-)**	1.5
Beryllium (Be)	10	**Sulfates (SO_4^{2-})**	250
Cadmium (Cd)	5	**Chlorides (Cl^-)**	50
Cobalt (Co)	250	**Asbestos**	30
Chromium (Cr)	50		
Mercury (Hg)	1		$mg \cdot L^{-1}O_2$
Nickel (Ni)	10	**COD**	30
Lead (Pb)	50		
Copper (Cu)	50	**pH**	5.5-12.0
Selenium (Se)	10		
Vanadium (V)	250		
Zinc (Zn)	3000		
Cyanides	50		

1.3.3. Remediation technologies

Soils and sediments are the major sink for many of the pollutants released into the environment by both natural and anthropogenic sources, such as weathering of bedrock and ore bodies, volcanic eruptions, forest fires, sea-salt sprays, industrial emissions, improper disposal of mine tailings and wastes, lead gasoline and paints, application of pesticides, fertilizers, animal manures, sewage sludge, wastewater irrigation, fossil fuel combustion, spillage of petrochemicals, and atmospheric deposition [115]. Unlike many organic contaminants which can oxidized to carbon dioxide by microbial action, most heavy metals do not undergo microbial or chemical degradation [116] and thus their total concentration in soils usually persists for quite a long time after their introduction in the environment [117]. For this reason, many technologies have been developed to reclaim polluted sites, making them available for a future use and, at the same time, conserving land resources, improving the environmental condition at the sites, as well as reducing the risk to humans and the environment.

This entails the need for relevant efforts for environmental risk assessment and management, which should take into account the implications of different remediation approaches.

The planning of the most suitable management strategy must consider the combination of: i) the nature and distribution of the contamination, ii) the characteristics of the polluted matrix, iii) the availability and applicability of suitable remediation technologies and iv) the necessity of evaluation and monitoring technologies to verify the performance and to ensure the sustainability of the remediation processes [118]. In this context, remediation can be defined as a set of actions taken to clean up, mitigate, correct, abate, minimize, eliminate, control and contain or prevent a release of contaminants, in order to protect human health and the environment, including actions to study or assess any actual or suspected release [119].

Remediation technologies can be classified in many ways, according to the scope of application, as *in-situ* (performed directly on the site without excavating the soil) and *ex-situ* technologies (including excavation and transport of the contaminated soil to a treatment plant) [120], or taking into account the processes used, such as biological, physical, chemical, physical-chemical, thermal, and containment techniques [119].

In general, bioremediation technologies use either microbiological metabolism, to transform or degrade pollutants into less hazardous substances (ranging from carbon dioxide and water to fatty acids and other organic degradation products), or plants, to extract or fix heavy metals present in contaminated soil (phytoremediation). Physical and chemical treatment technologies, on the other hand, are based on the physical and/or chemical properties of the contaminants as well as on the contaminated media to chemically convert, separate, or contain the contamination [121]. Moreover, biological and chemical methods can be applied together depending on the type of metal, soil, plant

and chemical substances involved. The effectiveness of different phytoremediation techniques can be enhanced by microbial-, chelate- and genetic-assisted remediation. **Figure 1.3** shows the most used remediation technologies for heavy metals, which will be briefly discussed in the following section.

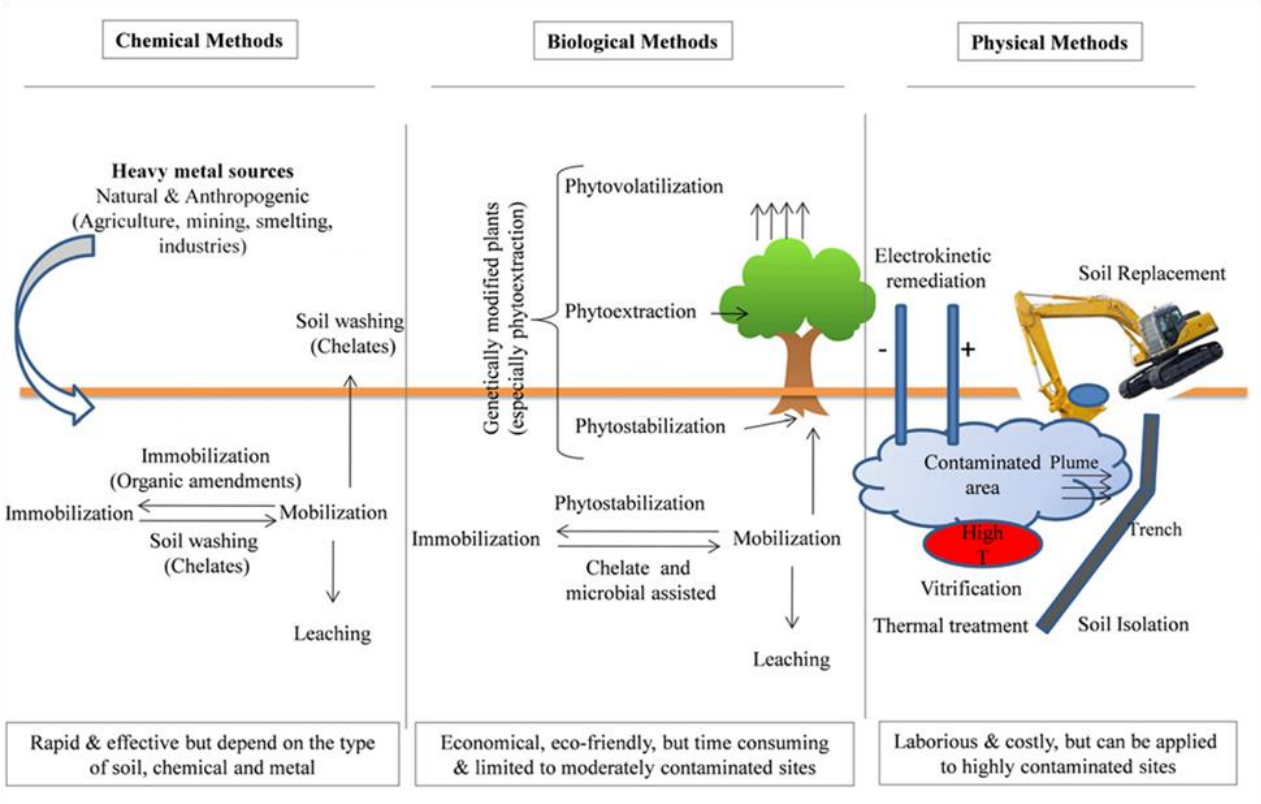

Figure 1.3. Comparison of different soil clean-up methods. Soil remediation methods can be broadly divided into three categories: physical, chemical and biological. Physical remediationmethods include soil replacement, soil isolation, vitrification, thermal treatment, and electrokinetic. Biological methods generally include phytostabilization, phytoevaporation, and phytoextraction. Chemical methods contain immobilization, and soil washing [122].

1.3.3.1. Physical remediation

Soil replacement

Soil replacement refers to the use of non-contaminated soil to completely or partly replace polluted soil to dilute the total concentration of heavy metals and organic contaminants, in order to increase the soil environmental capacity, thus increasing soil functionality [123]. The replaced soil can be either treated to remove heavy metals or, in some cases, disposed into a landfill. The most common methods used to apply this technique are soil spading and new soil importing. Specifically, in the case of soil spading the contaminated site is dug deeply and the contaminated soil is mixed with the unpolluted deep soil, while new soil importing refers to the addition of clean soil to the contaminated one. Prior to 1984, excavation, off-site disposal and soil replacement were the most commonly method used to clean-up contaminated sites, but these methods are feasible only for small

volumes of heavily polluted shallow soil situated in relatively small areas. Moreover, soil replacement is not a sustainable alternative for the remediation of contaminated sites both for the high quantity of virgin resources needed and for the costly handling and disposal of the contaminated soil, which is often considered as a hazardous waste [124,125].

Soil isolation

Soil isolation processes are used to prevent off-site movement of pollutants by restricting them within a specified area [126], through the separation of contaminated soils from the surrounding uncontaminated soils and water reservoirs [127] Subsurface barriers are usually used to separate the contaminated water or soil by restricting the flow of ground and/or surface water at the contaminated site [128]. These vertical barriers can be installed either downstream, upstream, or completely surrounding the site, usually in combination with a capping system to restrict uncontaminated surface water infiltration. These barriers cannot be installed into deep soil and are often limited to around 30 ft depth. Moreover, in order to effectively isolate the contaminated part of soil, the barrier should be continuous with a low-permeability layer [122].

Vitrification

Vitrification can be defined as a high temperature process in which soil organic matter is incinerated and mineral matter is melted, thus leading to heavy metals' sequestration in a small volume of vitreous material [129]. This process can be applied both *in-situ* and *ex-situ* by using fossil fuels' combustion or electrical energy (through the Joule effect, electric arc, induction, or plasma processes) to provide the necessary heat [130]. Some elements, , such as Hg and Se, may be volatilized due to the high temperatures involved, thus additional steps for their recovery and disposal may be required. Vitrification can be carried out *in-situ* by applying an electric current through the soil using a vertical array of electrodes planted into the contaminated area, and *ex-situ* by using especially designed installations [131]. However, dry soil may not provide enough conductance for vitrification and high alkali content (1.4 wt%) may also hinder good electrical conduction [132]. The vitrified material can then be mixed with various additives like clay, clean soil or sand to prepare a product with certain characteristics, which may improve the effectiveness of this technology. While fuel- or electrical- based heating is often cost-prohibitive, the use of solar technology may bring remarkable energy saving [133].

Electrokinetic remediation

Electrokinetic remediation operates on the principle that, if an electric field gradient of suitable intensity is established on two sides of an electrolytic tank containing saturated soil, the heavy metal present can be separated via electrophoresis, electric seepage, electroosmosis, electrolysis or

electro-migration [123]. This process can also be applied in combination with other techniques such as microbial- [134], chemical- [135], redox- [136], and phyto- remediation [137]. The removal of contaminants having poor conductivity (e.g. sulfides) or present in metallic form (e.g. Hg) may also require a preliminary dissolution, obtained by the use of appropriate electrolytes such as distilled water, organic acids or synthetic chelates. Electro-migration is one to two orders of magnitude faster than the other mechanisms, and thus is the dominant mass transfer mechanism for heavy metals [138], while the dominant electron transfer reaction occurring at electrodes during the electrokinetic process is the electrolysis of water, which may cause significant changes in soil pH [124]. Electrokinetic remediation can be economically effective because it is easy to install and operate (Virkutyte et al., 2002), does not modify the original nature of the soil [139], and produces no or little by-products. However, it is only applicable for saturated soil with low groundwater flow, it only removes a part of leachable heavy metals, it is less effective for heterogeneous soils, and the energy cost can be prohibitive especially when higher removal is needed [124].

Thermal treatment

Thermal treatment processes are based on the volatility of both organic and inorganic contaminants. While this technology is more suitable for the removal of volatile organic compounds, it has been often used for the remediation of soils and sediments polluted by volatile metals such as Hg [140].

This technology is performed by heating the contaminated matrix via steam, microwave, or infrared radiation without combustion or melting of the media or contaminants. The volatilized pollutants are then collected under negative pressure or with a carrier gas. Compared to vitrification or incineration, thermal treatment consumes much less energy and can simultaneously remove volatile compounds that are often co-present with heavy metals. The main components of a thermal desorption system usually include a pre-treatment and material handling unit, a desorption unit, and a post-treatment unit for the treatment of both off-gas and processed soil. The pre-treatment consists of removing extraneous matter (i.e. plastic, rubber or other detritus) and dewatering to achieve suitable moisture content. At ambient pressure, thermal desorption units can be employed in a wide range of temperature, usually from 320 to 700 °C [141], but the application of vacuum conditions can allow the use of much lower temperatures (< 150°C) [140]. In fact, the overall cost of the process, as well as the decontamination efficiency, are mainly determined by the temperature, pressure and treatment time employed [142,143]. In addition, thermal treatment at high temperatures may cause the change of the physical and mineralogical characteristics of the treated soil, as well as some changes of the heavy metals' speciation and partitioning [124].The major problems of this class of processes are the high energy consumption and the capital costs caused by the necessity of specialized facilities.

1.3.3.2. Biological remediation

Phytoremediation

Phytoremediation can be defined as a class of technologies that uses specific plants to fix, adsorb or degrade contaminants, in order to remove them from soil or reduce their environmental impacts, thus remediating and revegetating contaminated sites. The use of metal-accumulating plants to clean up contaminated sites was first formally presented in 1983, but its first applications date back to the 1600s. These methods are considered environmentally friendly, aesthetically pleasing, non-invasive, energy efficient, and cost-effective ways to clean up the sites characterized by low-to-moderate concentrations of heavy metals [144]. In addition, they can also be used effectively in combination with several other traditional remediation techniques. In detail, the efficiency of these processes can vary depending on many plant and soil factors, like the physico-chemical properties of the soil, the bioavailability of metals in soil, and the capacity of plants to take up, accumulate, sequester, translocate and detoxify heavy metals. The term phytoremediation can include several techniques and applications, which are distinguished from each other based on the processes/mechanisms involved to immobilize or remove heavy metals (i.e. phytostabilization, phytoextraction, and phytovolatilization)

In particular, phytostabilization can be defined as the use of plants capable to decrease the bioavailability or/and mobility of contaminants through adsorption by roots, reduction of soil erosion, chemical precipitation, or complexation in the root zone [145]. Since this process does not reduce the concentration of heavy metals present in the contaminated soil, but it prevents their off-site movement, long-living plants such as poplar trees or perennial grass are often employed [146]. Moreover, phytostabilization is only effective for a depth limited to the extent the roots can reach and, since heavy metals remain in the soil or plants, regular monitoring of the site is usually required [145].

Phytoextraction refers to the uptake of contaminants from soil by plant roots and their translocation and accumulation in the aboveground harvestable biomass, which can more easily recycled, disposed of, treated or oxidized compared to soil. The translocation of heavy metals is a crucial biochemical process to obtain an effective phytoextraction, since the harvest of the root biomass is generally not feasible. Phytoextraction can permanently remove heavy metals from contaminated soil, but it is suitable only for sites that are polluted by low or moderate concentrations of metals, since most plant species are not able to survive in heavily polluted sites [147,148]. This technique is highly economical, comparatively less disruptive to the soil and environment, and needs no excavation or disposal of the contaminated soil [149,150], but it depends on the growing conditions essential for plants and microorganisms, and on plant tolerance to heavy metals. In addition, large

scale applications need considerable experience and expertise in the use of agricultural equipment and require relatively long times to completely remediate the contaminated site [124]. Since this process is usually limited by the low heavy metal availability, uptake and translocation [149–151], chelate-assisted phytoremediation has gained significant consideration, with a number of investigations on the use of ammonium fertilizers, low molecular weight organic acids, EDDS, EDTA, nitrilo triacetic acid (NTA), hydroxyethylene diamine triacetic acid (HEDTA) and humic substances as potential chelating agents [124,152].

Phytovolatilization involves the uptake of heavy metals from soil by selected plants (i.e. *Arabidopsis thaliana, Brassica juncea*, and *Chara canescens*) and their subsequent transformation into volatile forms, which are released into the atmosphere through stomata [153]. This technique is primarily useful for Se, Hg and As, which may exist as gaseous specie [154]. However, the practical application of this technique for soil remediation seems questionable, since once the metals have been volatilized, they may be recycled back into to the soil by precipitation.

Microbial remediation

Microbial remediation refers to a group of processes that use microorganisms (i.e., bacteria, fungi, and algae) to lower the availability of heavy metals present in a polluted soil through adsorption, precipitation, oxidation or reduction. The contaminated soil is usually inoculated with selected microorganisms, which may be indigenous to the contaminated area or may be isolated from elsewhere, by spray irrigation, infiltration galleries or injection wells. The most applied microbial remediation techniques include biosorption, bioprecipitation, bioleaching, biotransformation, and biovolatilization [124].

Biosorption is a process used to trap heavy metals on the cellular structure of the microorganisms through sorption onto the binding sites of the cell wall binding sites of the cell wall, like polysaccharides, lipids, and proteins, through their carboxylate, hydroxyl, amino and phosphate groups. While bioprecipitation processes transform heavy metals' soluble species into insoluble hydroxides, carbonates, phosphates, and sulfides through microbial metabolism, bioleaching refers to the dissolution of metallic minerals and to the release of the associated heavy metals. The most used microorganisms for these applications include chemoautotrophic bacteria and fungi, such as *Leptospirillum ferrooxidans*, *Acidithiobacillus thiooxidans*, *Acidithiobacillus ferrooxidans*, and *Aspergillus niger* [124].

Biotransformation processes are used to change the chemical speciation of heavy metals, and thus alter their mobility, toxicity and bioavailability, particularly in the case of heavy metals whose toxicity varies with different oxidation states. For example, the mercury-resistant bacteria *Organomercurial lyase* has been reported to convert methyl mercury to Hg(II), which is one hundred-

fold less toxic [155]. Biovolatilization, similarly to phytovolatilization, involves turning a soluble contaminant into a more volatile state, but it is only applicable to Se and Hg [146,155,156]
Microbial remediation can be considered a safe, easy, and effective technology with relatively low energy requirements, low operation costs, and no environmental and health hazards, but it is effective only when environmental conditions permit the desired microbial growth and activity. Moreover, both the addition of nutrients, oxygen, and other amendments and the combination with physical-chemical techniques are usually required to stimulate microbial activity and enhance bioremediation, since these processes are usually slow and time consuming [124].

1.3.3.3. Chemical remediation

Chemical stabilization

Chemical stabilization refers to a class of remediation processes in which several immobilizing agents are added to a contaminated soil to decrease heavy metals' mobility and bioavailability through surface complexation, chemical precipitation, ion exchange, and adsorption [157]. The most commonly used amending agents include clay minerals, phosphate compounds, liming materials, organic composts, metal oxides, and biochar [158–161] but recent studies also highlighted the potential applications of low-cost industrial residues such as industrial eggshell [162] and red mud [163]. Chemical stabilization can be considered a relatively cost effective, simple, and rapid remediation technology but, since it does not remove the contaminants from soil, long-term stability needs be monitored.

Clay minerals can function as natural scavengers of heavy metals through a multitude of mechanisms (i.e. ion exchange, adsorption, precipitation, nucleation, and crystallization) with quite good performances, as shown in various field studies. The best results were reported for the use of aluminosilicates, sepiolite, palygorskite, and bentonite [160,164,165].

Soluble phosphate compounds (i.e. phosphate salts and phosphoric acid) and particulate phosphate minerals (i.e. natural and synthetic apatite and hydroxyapatite) have been widely studied for immobilization of heavy metals by direct metal adsorption, substitution, surface complexation, and chemical precipitation [166,167].

The most commonly used liming materials include oyster shells and eggshells [168], lime and limestone [169]. These materials enhance sorption and/or precipitation of heavy metals by increasing soil pH and increasing the negative surface potential of soil particles.

Metal oxides, such as oxides of Fe, Mn, and Al, due to their extensive active surface areas and their amphoteric nature, can strongly bind heavy metals via specific sorption, co-precipitation, and inner-sphere complexation, thus decreasing their mobile, bioavailable, and bio-accessible fractions.

Good results have been reported for the application of iron oxides and oxyhydroxides for immobilization of various heavy metals (i.e., Sb, Pb, and As) [170,171].

Most metal oxides can be added into soil only in the form of powder or granular particles through mechanical mixing, which largely impedes their application to deeper soil or *in-situ* remediation uses. In the case of phosphates, liming materials and metal oxides the use of soluble compounds has the advantage of a faster reaction rate, but reactive lifetime is limited by the wash out caused by rainwater and groundwater.

Organic composts include mainly biosolids (solid residues generated during the treatment of domestic sanitary sewage) and animal manure (mainly from chicken, swine, beef cattle, dairy, and poultry wastes) usually containing cellulose and lignin as the main constituents, together with hemicellulose, proteins, lipids, starches, simple sugars, hydrocarbons, and many other compounds that contain a number of functional groups which can bind various transition metals [172]. These materials can immobilize heavy metals in soil through various mechanisms, such as adsorption, formation of metal hydroxides, prevention of sulfide oxidation/hydrolysis and formation of stable complexes [144,173,174], but their performance can vary over time due to organic matter decomposition.

Biochar is a carbon rich and porous charcoal manufactured during the pyrolysis of organic residues such as municipal waste, animal wastes, wood, crop residues and biosolids, and recent studies showed its ability to immobilize heavy metals thanks to a highly porous structure, the presence of many active functional groups, elevated pH, and suitable cation exchange capacity [175,176]. Biochar amendments have many positive effects like carbon sequestration, agronomic benefits (i.e. improved soil mechanical strength and enhanced soil capacity for retaining nutrients and water), metal immobilization and reuse of solid waste, but its application is restricted to shallow soil due to a limited adsorption capacity, difficult deliverability into the soil and slow reaction rate.

Soil washing

The term “soil washing” refers a group of processes used to remove heavy metals from various contaminated matrixes by using various reagents, such as water, inorganic acids (i.e. hydrochloric, sulfuric, nitric, phosphoric, fluorosilicic acid), inorganic bases (i.e. sodium hydroxide), inorganic salts (i.e. calcium chloride, ferric chloride, ammonium chloride, ammonium acetate, sodium acetate), organic acids (i.e. formic, acetic, oxalic, citric, tartaric , polyglutamic acid), organic solvents (i.e. isopropyl alcohol and acetone), organic chelating agents (i.e. EDTA, DTPA, NTA, EDDS), humic substances, surfactants and cyclodextrins [177–186]. The contaminated soil is dug out and mixed with a suitable extractant solution for a specified time depending on the type of metals and soil, thus removing part of the heavy metals present through dissolution, ions exchange, chelation or desorption

[187]. If the treated soil is fulfilling the necessary regulatory criteria, it can be either backfilled to the original site or reused for other applications. The choice of the best reagent to use for soil washing is usually established on a case-by-case basis, depending on the specific application and on the heavy metals involved, since efficiency can be subjected to large variations. In this context, many chelators have been tested to enhance removal efficiency, but the most used are EDTA and EDDS, thanks to their strong chelating ability for various heavy metals (i.e. Cd, Cu, Pb, and Zn.) in a wide pH range [122,188]. However, several studies investigated also the performances of other bio-degradable chelating agents (i.e. iminodisuccinic, glutamate-N,N-diacetic, glucomonocarbonic polyaspartic acid), since EDTA has been shown to be poorly biodegradable and highly persistent in the soil environment [189]. The combined use of different chelators gave good results, especially for multi-metal contaminated soils [185]. Soil washing is one of the few permanent processes that can be used on large scale to remove heavy metals from soil in a relatively rapid and effective way, allowing, in some cases, also the recovery of the metals[184].

Solidification/Stabilization

Solidification/Stabilization (S/S) is one of the most commonly used technologies for the remediation of heavy metal contaminated soils and sediments, due to its relatively low cost and easy implementation. In particular, solidification refers to processes that encapsulate the waste in a monolithic solid of high structural integrity, thus restricting contaminants' migration by vastly decreasing the surface area exposed to leaching and/or by isolating the wastes within through encapsulation in the solid matrix. Solidification does not necessarily involve a chemical interaction between the wastes and the solidifying reagents but may mechanically bind the waste into the monolith. On the other hand, stabilization refers to those processes that reduce the hazard potential of a contaminated material by converting the pollutants into less soluble, mobile, or toxic forms without necessarily change the physical nature and handling characteristics of the material [190–192]. Solidification/Stabilization processes can be applied either by injecting the S/S reagents into the ground, using a soil-mixing equipment or by pressure injection (*in-situ* application), or applied to excavated soil either on site or off site (*ex-situ* application). The major advantages of *ex-situ* systems compared with *in-situ* ones include improved process conditions' control, better homogenization, and easier control of the emissions and wastes produced. However, *ex-situ* applications need the excavation of the contaminated soil or sediment before treatment, which may increase the mobility of the contaminants [193].

The first uses of S/S technology date back to the late '50s, when in some nuclear plants they began to use Portland cement to encapsulate radioactive liquid waste into monoliths [194]. In order to reduce the amount of cement necessary to form these blocks, and to avoid the transudation of water

from them, it was tried to add mineral sorbents such as vermiculite to the mixture waste/cement. However, this expedient was not sufficient to reduce in a significant way the volume of materials produced, constraining to abandon this technology in favor of calcination and vitrification processes. The first industrially competitive processes exploiting the S/S technology were developed in the late '70s, after the approval of the "Resource Conservation and Recovery Act (RCRA - 1976)" [191]. Some examples are the process developed and patented by Chemfix Inc., which used Portland cement and sodium silicate for the treatment of sewage from a mine drainage, and that developed by Conversion System Inc. for the treatment of sewage from desulfurization plants, which used lime and ash [195]. After the approval of RCRA, companies, universities and environmental protection bodies have showed an increased interest toward this field, leading to many in depth-studies on a multitude of new binding systems, both inorganic (i.e. cement, lime, alkali-activated binders) and organic (i.e. bitumen, polymers). [195].

The most commonly used cementitious binder is Ordinary Portland Cement (OPC), due to its relatively low costs, commercial availability and generally good performance [196], but the application of other cementitious systems (i.e. calcium aluminate cement (CAC), pozzolanic cement, sulfoaluminate cement) also showed great promise. The use of OPC, as well as that of other cements, involves i) chemical fixation of contaminants thanks to their chemical interactions with cement's hydration products; ii) physical adsorption of contaminants on the surface of hydration products; and iii) physical encapsulation of contaminants due to the low permeability of the hardened pastes.

Cements are mainly composed of a mixture of several aluminates and silicates, depending on the starting materials used, to which several additions can be made (i.e. gypsum, calcite, blast furnace slag, fly ashes).

In particular, Portland cement's mayor components are tricalcium silicate ($3CaO{\cdot}SiO_2$, abbreviated as C_3S), dicalcium silicate ($2CaO{\cdot}SiO_2$, abbreviated as C_2S), tricalcium aluminate ($3CaO{\cdot}Al_2O_3$, abbreviated as C_3A), tetracalcium aluminoferrite ($4CaO{\cdot}Al_2O_3{\cdot}Fe_2O_3$, abbreviated as C_4AF) and gypsum ($CaSO_4{\cdot}2H_2O$). Between the various other cementitious binders investigated as an alternative to OPC, very promising results have been obtained for the application of calcium aluminate cement [197–202], which is mainly composed of monocalcium aluminate ($CaO{\cdot}Al_2O_3$, abbreviated as CA) and monocalcium dialuminate ($CaO{\cdot}2Al_2O_3$, abbreviated as CA_2).

In the presence of water calcium silicates (C_3S and C_2S) present in cement hydrate to form an amorphous calcium silicate hydrate gel (C-S-H gel) and $Ca(OH)_2$, while C_3A and C_3AF react with water and $CaOH_2$ to produce tetracalcium aluminate hydrate ($3CaO{\cdot}Al_2O_3{\cdot}Ca(OH)_2{\cdot}12H_2O$) and calcium aluminoferrite hydrates ($6CaO{\cdot}Al_2O_3{\cdot}Fe_2O_3{\cdot}12H_2O$), respectively (**Eq. 1.11-1.14**). On the other hand, the hydration of CA and CA_2 can cause the precipitation of several hydrates as a function

of time and temperature (i.e. $CaO{\cdot}Al_2O_3{\cdot}10H_2O$ (CAH_{10}), $2CaO{\cdot}Al_2O_3{\cdot}6H_2O$ (C_2AH_8), $3CaO{\cdot}Al_2O_3{\cdot}6H_2O$ (C_3AH_6), and $Al(OH_3)(AH_3)$) [201,203].

$$3(3CaO \cdot SiO_2) + 6H_2O \rightarrow 3(3CaO \cdot SiO_2 \cdot 3H_2O) + 3Ca(OH_2) \quad Eq.1.11$$

$$2(2CaO \cdot SiO_2) + 4H_2O \rightarrow 2(3CaO \cdot SiO_2 \cdot 3H_2O) + Ca(OH_2) \quad Eq.1.12$$

$$3CaO \cdot Al_2O_3 + 12H_2O + Ca(OH_2) \rightarrow 3CaO \cdot Al_2O_3 \cdot Ca(OH_2) \cdot 12H_2O \quad Eq.1.13$$

$$4CaO \cdot Al_2O_3 \cdot Fe_2O_3 + 10H_2O + 2Ca(OH_2) \rightarrow 6CaO \cdot Al_2O_3 \cdot Fe_2O_3 \cdot 12H_2O \quad Eq.1.14$$

In the presence of SO_4^{2-} ions, the reactivity of calcium aluminates shifts toward the formation of calcium trisulfoaluminate hydrate ($3CaO{\cdot}Al_2O_3{\cdot}3CaSO_4{\cdot}32H_2O$ - AFt or ettringite), and calcium monosulfoaluminate hydrate ($3CaO{\cdot}Al_2O_3{\cdot}CaSO_4{\cdot}12H_2O$ — AFm or monosulfate) (**Eq. 1.15-1.16**) [204,205].

$$6Ca^{2+} + 2Al(OH)_4^- + 4OH^- + 2(SO_4)^{2-} + 26H_2O \rightarrow 3CaO \cdot Al_2O_3 \cdot 3CaSO_4 \cdot 32H_2O \quad Eq.1.15$$

$$3CaO \cdot Al_2O_3 \cdot 3CaSO_4 \cdot 32H_2O + 2(3CaO \cdot Al_2O_3) + 4H_2O \rightarrow 3(3CaO \cdot Al_2O_3 \cdot 3CaSO_4 \cdot 12H_2O) \quad Eq.1.16$$

As already described above, the hydration of cement is a sequence of overlapping chemical reactions between clinker compounds, calcium sulphate and water, leading to a continuous stiffening and hardening cement paste. The action rate of pure cement phases usually can be arranged in the increasing order $C_3A > C_3S \sim CA > C_4AF > C_2S$ [206]. In the case of solidification/stabilization applications, the actual reaction rates are further complicated by the small grain size of the cement particles, non-regular coordination, deformation of crystal structures and the presence of both heavy metals and the contaminated matrix itself.

The immobilization of heavy metals after solidification/stabilization of the contaminated matrix can involve several different mechanisms, such as:

- precipitation or co-precipitation as low solubility species (i.e. hydroxides, carbonates, sulphates and silicates)[207,208];
- isomorphic substitution inside the structure of cement hydration products, such as CSH, CAH, ettringite, and monosulfate [209–212];

- physical adsorption occurring when contaminants in the pore water are attracted to the surface of particles due to the unsatisfied charges [206];
- chemical adsorption through covalent bonding to the particles' surface [206];
- reduction or oxidation of heavy metals to less mobile and/or toxic forms, such as in the case of the reduction of Cr^{VI} to Cr^{III} [213]

The formation of hydration products, the development of micro-structural features and the adsorption-desorption equilibria depend on many factors such as solution processes, interfacial reactions and solid-state reactions. Therefore, the presence of heavy metals can deeply influence cement hydration, for example by precipitation of insoluble metal colloidal gels on cement grain surfaces [204].
In addition, organic contaminants can exhibit an affinity towards cement particles or cement hydration products by adsorption due to the electrostatic force, hydrogen-bonding interaction, chemical bonding, and hydrophobic force, altering the surface properties of the cement particle and thus its interactions with the solution as well as with other cement constituents.

Moreover, waste forms obtained after cement-based solidification/stabilization are vulnerable to physical and chemical degradation processes, depending to a large extent on factors such as micro-structure, chemical and mineralogical composition and permeability [214].
The most common degradation mechanism in cement-solidified wastes is the carbonation of $Ca(OH)_2$, CSH and other alkaline compounds, but other chemical reactions, like further hydration and ettringite or thaumasite formation [215,216], may also influence the stabilized material's structure and performance [217]. Carbonation decreases the content of $Ca(OH)_2$ and CSH, thus lowering the treated wastes pH and changing the contaminants' leaching behaviour [218–220].

HPSS® process

The HPSS® process (High Performance Solidification/Stabilization), developed by Mapei and In.T.Ec. [221], is an *ex-situ* technology for the treatment of soils, sediments and wastes of predominantly inorganic nature. The process is conducted in suitable mixing and granulation installations, and consists in the treatment of a finely divided contaminated matrix (fraction ≤ 2 mm) with a hydraulic binder (typically Portland cement) and special additives to obtain a hardened granular material characterized by particularly reduced leaching levels of the inorganic contaminants and a mechanical resistance suitable for re-utilization in environmental rehabilitation operations as filling material, as road foundations, and for manufacturing of non-structural concrete items (**Figure 1.4**).

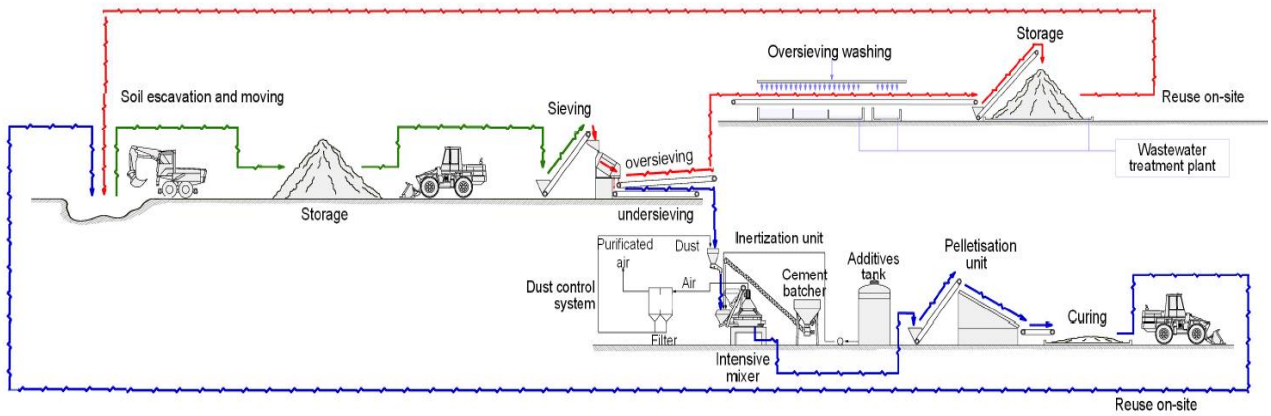

Figure 1.4. Flow scheme of the HPSS® granulation process

This result reflects the combined effect of the cement, which causes the immobilization of metals in the form of poorly soluble compounds (hydroxides, carbonates) and their incorporation in the hydration products (tobermorite gels and aluminosilicate phases AFt and AFm), and of the additives used (superplasticizers and water-repellent), which ensure the formation of a dense solid matrix characterized by a low residual porosity, thus limiting the leaching of pollutants and their transfer towards the environment [222,223].

In the case of wastes contaminated with both organic and inorganic contaminants, the hardened granules obtained from the first stage of the process may be subjected to a further process of distillation in a current of superheated steam (**Figure 1.5**), in order to eliminate any volatile and semi-volatile substances, such as mercury, heavy hydrocarbons (C>12), PCBs, PAHs and PCDD/PCDFs [140].

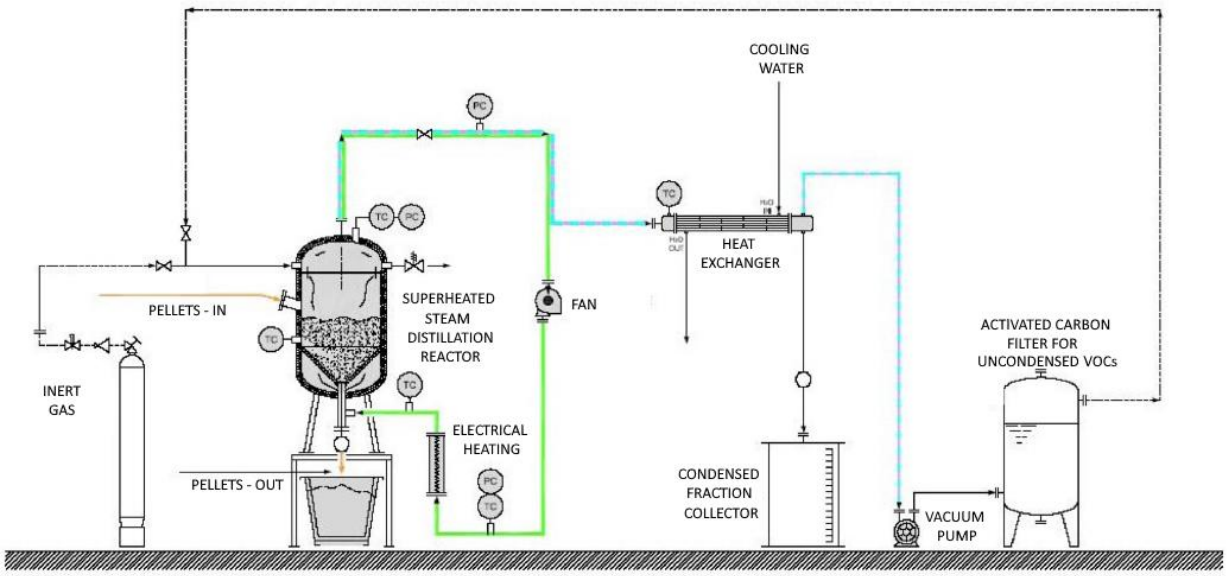

Figure 1.5. Process scheme of the HPSS® superheated steam distillation process.

During distillation, thanks to the previous granulation of the contaminated waste, all the problems deriving from the dragging of dust - which always accompany the heating of powdery materials - are eliminated, thus making expensive and complex dust control systems unnecessary. Furthermore, the decrease of free water presence in the sample, due to cement hydration, significantly reduces the mass of liquid that needs to be evaporated in the distillation phase. Moreover, the use of vacuum conditions for the distillation allows to apply this treatment at relatively low temperatures, ranging from 90°C to 250°C [224]. Since the superheated steam distillation is carried out in a closed system, the only waste of this process consists of a quite low quantity of liquid effluent that can be sent off to a conventional waste-water purification plant for treatment.

In addition, since both installations can be easily moved and set up directly at the reclamation site, the HPSS® process avoids to transport contaminated material off-site, reducing both the emissions of pollutants and the treatment costs to very competitive levels when compared to the other methods currently in use.

2. Chapter 2

Materials and Methods

2.1. Materials

Ordinary Portland cement (OPC) CEM I 42.5 R was purchased from Italcementi S.p.A. (Heidelberg Cement Group, Heidelberg, Germany) for the study reported in chapter 3, while it was purchased from from Barbetti S.p.A., (Gubbio, Italy) for the work reported in chapter 7. Portland cement CEM I 52.5 R, ground granulated blast furnace slag (GGBFS), clinker, lime ($CaOH_2$), and sodium carbonate (Na_2CO_3) were also purchased from Barbetti S.p.A. Metakaolin (MK) "Argical 1000" was acquired from Bal-Co (Sassuolo, Italy), while calcium aluminate cement (CAC) "Gorkal 70" and two water-reducing additives (Mapeplast ECO 1-A and Mapeplast ECO-1B) were purchased from Mapei S.p.A. (Milan, Italy). Mapeplast ECO 1-A is a hydrophobic additive that is used to decrease concrete water adsorption, whereas Mapeplast ECO 1-B is an acrylic-based superplasticizer that is used to better disperse cement particles. MK was activated by using a 4 M NaOH solution, which was obtained by dissolving pellets of NaOH (ACS Reagent, Merck KGaA, Darmstadt, Germany) in ultrapure water.

Sodium citrate tribasic dihydrate ($C_6H_5O_7Na_3 \cdot 2H_2O$), sodium oxalate anhydrous ($C_2O_4Na_2$), sodium acetate anhydrous ($C_2H_3O_2Na$), ferric chloride ($FeCl_3$), ferric sulfate ($FeSO_4$), polyaluminum chloride, H_3PO_4 85 % (w/w) solution (ACS reagent), NaOH 30 % (w/w) solution (technical grade), and sodium hydroxide (semiconductor grade >99.99%) were purchased from Merck KGaA (Darmstadt, Germany).

Quartz sand for sand filter preparation, Macrolite™ and VitroSphere Micro™ were purchased from Enki Ambiente s.r.l. (Venice, Italy).

HCl (35%), HNO_3 (69%), HF (48%) and $B(OH)_3$ were purchased from PanChem (AppliChem GmbH, Darmstadt, Germany) at high purity for trace metal analysis and used without further purification, while ultrapure water with a resistivity of 18.2 MΩcm was obtained with the MilliQ system from Merck KGaA (Darmstadt, Germany). The tap water used was characterized in compliance with UNI EN 1008:2002 standard [225] and was deemed adequate for concrete production.

NIST-SRM 2711a (Montana II soil) and NIST-SRM 981 (Common Lead Isotopic Standard) from NIST (National Institute of Standards and Technology, Gaithersburg, MD, USA) were used as certified standards to validate Inductively Coupled Plasma Mass Spectrometry (ICP-MS) and Inductively Coupled Plasma Optic Emission Spectroscopy (ICP-OES) analytical methodologies.

2.2. Methods

2.2.1. Instrumental analysis

2.2.1.1. Inductively coupled plasma mass spectrometry (ICP-MS) and Inductively Coupled Plasma Optic Emission Spectroscopy (ICP-OES)

The concentration of Be, Cd, Hg, Pb, V, Cr, Ni, Cu, Zn, Ba, Co, As, Se, Sn, Sb and Tl were determined in solids and eluates by ICP-MS (NexION 350D - Perkin Elmer, Waltham, MA, USA), using the instrument in Standard, Collision (Kinetic Energy Discrimination - KED) and Reaction mode (Dynamic Reaction Cell - DRC), depending on the severity of the polyatomic interferences on each of the analytes to achieve the lowest detection limit for each element (instrument settings are reported in **Table 2.1**).

Table 2.1. ICP-MS Instrument's settings.

Component/Parameter	Type/Value/Mode		
Nebulizer	Meinhard quartz microconcentric		
Spry Chamber	Quartz cyclonic		
Triple Cone Interface Material	Nickel/Aluminum		
Plasma Gas Flow	18 L/min		
Auxiliary Gas Flow	1.2 L/min		
Nebulizer Gas Flow	0.96-1 L/min		
Sample Uptake Rate	200-250 µL/min		
Rf Power	1600 W		
Collision Gas Flow (Helium)	4.3 mL/min		
Reaction Gas Flow (Oxygen)	0.8 mL/min		
Analyte	**Symbol**	**Mode**	**Mass (amu)**
Beryllium	Be	Standard	9
Cadmium	Cd	Standard	111
Mercury	Hg	Standard	202
Lead	Pb	KED	208
Vanadium	V	KED	51
Chromium	Cr	KED	52
Nickel	Ni	KED	60
Copper	Cu	KED	63
Zinc	Zn	KED	66
Barium	Ba	KED	137
Cobalt	Co	KED	59
Arsenic	As	DRC	91
Selenium	Se	DRC	93
Tin	Sn	Standard	120
Antimony	Sb	Standard	121
Thallium	Tl	Standard	205

The concentration of heavy metals in solid samples was determined after total microwave-assisted acid digestion. In detail, aliquots of about 10 mg of homogenized solid were digested, by means of a mixture of 5 mL of Milli-Q water, 3 mL of aqua regia (1:3 HCl:HNO_3), and 0,5 mL of 48 % HF solution, in a sealed PFA vessel using Ethos 1600 microwave oven (Milestone, Milan, Italy). After the digestion the remaining HF was neutralized by adding to the samples 1 ml of saturated $B(OH)_3$ solution [226].

Heavy metals' concentrations in the leachates obtained from the wet conditioning process (chapter 3), in the washing water obtained from the pre-treatment of contaminated fly ashes, and in the eluates obtained from alkaline extraction tests (chapter 7) were measured by ICP-OES (Spectro Genesis - AMETEK, Berwyn, PA, USA) according to APAT CNR IRSA 3020 Man 29 2003 standard [227]. In order to reach a low detection limit for each element, the instrument was calibrated and optimized for a 1 g/L solution of CsCl to compensate for the high saline content of the analysed matrix. Spectral lines were selected according to the severity of the interference and relative intensities of each analyte (all the instrumental settings are reported in **Table 2.2**).

2.2.1.2. Ultraviolet-Visible (UV-Vis) spectroscopy

Ultraviolet-Visible (UV-Vis) spectroscopy was performed using a Lambda 3B (Perkin Elmer, Waltham, MA, USA) spectrophotometer equipped with 1-cm path length quartz cuvettes

2.2.1.3. Gas chromatography (GC) and high-performance liquid chromatography (HPLC) analysis

Gas Chromatography (GC) analysis was carried out using an Agilent GC 6890 N (Agilent, Santa Clara, CA, USA) equipped with a DB-5MS UI capillary column using a constant flow of N_2 (1.2 mL/min) as carrier gas (all the instrumental settings are reported in **Table 2.3**).

High-performance liquid chromatography (HPLC) analysis were performed at room temperature using an ERRECI S150 A Ionic Chromatograph (ERRECI, Milan, Italy) with suppressor module, equipped with Dionex IonPac AS29-Fast-4µm analytical column and a Dionex™ IonPac™ NS1 guard Column. The anions were detected using a suppressed conductivity detector, with a full scale of 250 μScm^{-1}, optimized to obtain the maximum signal-to-noise ratio possible for the anions being analysed. The injection volume was 50 µL.

The concentration of soluble anions (i.e. Cl^-, SO_4^{2-} and NO_3^-) in solid samples was determined by using the following procedure: 100.0 mg (d.w.) of the solid sample was placed in 10.0 mL of ultrapure water (solid/liquid ratio = 100) using a 10 mL volumetric glass flask and stirred for 1 hour by using a magnetic stirrer.

The eluate was then filtered at 0.45 µm and analysed by HPLC. The concentration of the soluble anions was then calculated by using the following equation:

$$[Anion]_{solid} = \frac{([Anion]_{eluate} \cdot Volume_{water})}{Mass_{solid}} \quad (Eq.\ 2.1)$$

Table 2.2. ICP-OES Instrument's settings.

Component/Parameter	Type/Value/Mode	
Nebulizer	Meinhard quartz microconcentric	
Spry Chamber	Concentric cross-flow	
Plasma Gas Flow	12 L/min	
Auxiliary Gas Flow	0.80 L/min	
Nebulizer Gas Flow	1.04 L/min	
Sample Uptake Rate	200-250 µL/min	
Rf Power	1340 W	
Analyte	**Symbol**	**Spectral lines (nm)**
Beryllium	Be	313.042; 313.107
Cadmium	Cd	228.002
Mercury	Hg	194.227; 184.950
Lead	Pb	220.353
Vanadium	V	311.071
Chromium	Cr	267.716
Nickel	Ni	231.604; 341.476
Copper	Cu	324,754; 327.396
Zinc	Zn	213.856
Barium	Ba	455.404; 233.527
Cobalt	Co	228.616
Arsenic	As	189.042
Selenium	Se	196.090
Tin	Sn	189.991
Antimony	Sb	217.581
Thallium	Tl	190.864
Sodium	Na	589.592; 588.995
Calcium	Ca	317.933; 393.366; 315.890
Potassium	K	213.618; 214.914
Magnesium	Mg	279.079; 285.213

Table 2.3. GC Instrument's settings.

Component/Parameter	Type/Value/Mode
Inlet	EPC/Splitless
Inlet Temperature	300°C
Inlet Pressure	14.52 psi
Oven's Temperature Ramp	80°C for 1 min, 20°C·min^{-1} for 12 min, 320°C for 20 min
Detector	FID
Detector Temperature	350°C
Detector H_2 Flow	30.0 mL·min^{-1}
Detector Air Flow	400 mL·min^{-1}
Detector N_2 Flow	20 mL·min^{-1}

2.2.1.4. X-ray diffraction (XRD), X-ray fluorescence (XRF) and scanning electron microscopy equipped with energy-dispersive X-ray spectrometry (SEM/EDX).

The mineral composition of powdered samples was determined quantitatively by Rietveld analysis of XRD data by employing the Topas software (Bruker, Billerica, MA, USA). Known amounts of ZnO internal standard (ACS Reagent, Thermo Fisher Scientific Inc., Waltham, MA, USA) were mixed to the samples to quantify the amorphous fractions. Diffraction data were acquired with a X'Pert Pro diffractometer (Malvern Panalytical, Malvern, UK) according to the measurement details reported in **Table 2.4**.

Table 2.4. XRD instrumental settings.

XRD instrumental settings	
Radiation source	Cobalt
Detector	X'Celerator detector
Geometry	Bragg-Brentano geometry
2θ range	3-84°
Step size	0.017°
Time per step	100 s

XRF analysis was performed by using a Wavelength Dispersive Sequential (WDS) Philips PW2400 spectrometer (Spectris, Egham, UK) (Instrumental precision and detection limits are reported in **Table 2.5)**.

Table 2.5. XRF analysis details

XRF analysis details		
Analyte	Instrumental precision	Detection limit
Silicon	0.6%	0.2%
Aluminium	0.6%	0.01%
Magnesium	0.6%	0.01%
Sodium	0.6%	0.01%
Titanium	0.6%	0.005%
Iron	0.6%	0.005%
Manganese	0.6%	0.005%
Calcium	0.6%	0.005%
Potassium	0.6%	0.005%
Phosphorus	0.6%	0.005%

SEM investigations on polished and carbon-coated sections of pellets were performed using a CamScan MX3000 SEM (Applied Beams, Beaverton, OR, USA) equipped with an EDX spectrometer. Samples were dry-polished to avoid further hydration of cement phases and dissolution of the most soluble species. Care was taken in the polishing process by continuously removing the residues on the abrasive papers, to avoid the formation of scratches on the samples surface. Standard-

less elemental mapping and point analyses were performed, and the images were processed with ImageJ software (U.S. National Institutes of Health – NIH). A Merlin^{TM} Field Emission Scanning Electron Microscope (FESEM) (Carl Zeiss, Oberkochen, Germany), equipped with a wavelength dispersive spectrometer (WDS) for elemental analysis was used for more detailed investigations in chapter 4. For the quantitative analysis of Ca, Al, S, O, Pb, Mg, Fe, C and Si the following standards were used: FeS_2, $PbMoO_4$, $CaCO_3$, $CaMgSi_2O_6$ and $KAlSi_3O_8$.

2.2.1.5. Mechanical tests

Uniaxial compressive strength (σ_U) measurements were carried out with a C-094N manual digital point load tester (Matest, Treviolo, Italy), while resistance to fragmentation tests were performed with an A075N abrasion testing machine (Matest, Treviolo, Italy).

2.2.1.6. Particle size distribution

Particle size distribution of the granular materials obtained by applying the HPSS® technology to the contaminated matrixes was measured using a set of stainless-steel sieves with mesh of 63 μm, 1.0 mm, 2.0 mm, 3.15 mm, 4.0 mm, and 10.0 mm.

Particle size distribution measurements of contaminated soils and sediments were conducted with a Malvern MasterSizer 3000 (Malvern Panalytical, Malvern, UK) using both air and water as dispersants. Samples analysed in water were continuously sonicated (35 W, 40 kHz) and stirred (2500 rpm). Particles were assumed as spherical, with an absorption index of 0.01. The refractive index of cement (1.68) was used for both the red laser (632.8 nm) and the blue laser (470 nm). The refractive index of water for both lasers was set to 1.33, while the refractive index of air was set to 1.00. Dispersants' temperature was 20±2°C. Obscuration of the MasterSizer during the experiments was kept between 10% and 20%.

2.2.2. Analytical procedures

2.2.2.1. Leaching tests

Leaching tests were performed applying the UNI EN 12457-2:2004, UNI 12457-4:2004 and the UNI 14429:2015 [228–230] standards. According to the first two standards, the samples were placed in a HDPE bottle with MilliQ water (solid/liquid ratio = 1/10) and shaked with an end-over-end tumbler (10 rpm) for 24 hours. On the other hand, the UNI 14429:2015 leaching test consists of a series of 48 hours long parallel batch extractions (solid/liquid ratio = 1/10) with an increasingly acid or basic leachant, prepared using nitric acid or sodium hydroxide. Each material was analysed in triplicate after applying coning and quartering to obtain an adequate sample. Eluates were filtered at 0.45 μm

and were analysed by applying the following analytical methods: (1) APAT CNR IRSA 2060 Man 29 2003 [231] for pH measurement; (2) APAT CNR IRSA 5130 Man 29 2003 [232] for Chemical Oxygen Demand – COD and (3) ICP-MS analysis for heavy metals quantification. The pH values of the eluates obtained from the UNI 12457-2:2004 and UNI 12457-4:2004 leaching test were considered as the characteristic pH values of each material because these tests were designed to reach equilibrium conditions in a neutral solvent.

2.2.2.2. Mechanical tests

The solidification capabilities of several binders were investigated by studying the unilateral compressing strength (σ_U) of cylindrical test pieces made of the same formulations of the granular materials and applying the ASTM D7012-14 (Method C) [233]standard. Each test piece was prepared by filling a cylindrical HDPE mould (Φ: 20 mm, h: 30 mm) and then ripened for 28 days in wet air (20°C, 95% atmospheric relative moisture content). To account for the soil-binder systems' heterogeneity, each formulation was studied using ten specimens (confidence intervals are reported for $\alpha = 0.05$). The resistance to fragmentation of the cementitious granular materials obtained by applying the HPSS® process to some of the contaminated materials studied was investigated by following the UNI EN 1097-2:2010 standard [234], while their resistance to abrasion was estimated by measuring the fraction of granulate with particle diameter below 63 μm obtained after the UNI EN 12457-2:2004 of the UNI 12457-4:2004 leaching test. For this reason, the sample was sieved at 63 μm and the over-sieved fraction was dried and weighted, and the difference between the weight of the sample prior to the test and that of the over-sieved fraction was considered as the abraded fraction.

2.2.2.3. Pelletization of the contaminated matrixes

As in the already established HPSS® industrial procedure [222], the contaminated matrixes were air dried up to 10% weight/weight (w/w) moisture content and sieved at 2 mm prior to homogenization. Afterwards, the HPSS® technology was applied by adapting at lab-scale the procedure developed by Bonomo et al. [235]. The contaminated matrix and the binder were blended for 5 min in a mechanical mixer (PL40TVARE - Star Mix, Marano Vicentino, Italy) with the proper amount of liquid activator (tap water in the case of cement-containing binders or NaOH solution in the case of metakaolin and GGBFS) to prevent the formation of dust aerosols.

Two water-reducing additives (Mapeplast ECO 1-A and Mapeplast ECO-1B) can be added, each as 2% of cement dry weight to decrease concrete water adsorption and to better disperse cement particles. Since such additives are designed for use in traditional cement/concrete [236] and are known to degrade rapidly in the alkaline solution of geopolymers [237], they were included

exclusively in the OPC and CAC formulations. Then, after 2 min of additional mixing, the mixture was poured into a laboratory granulator plate, where additional water or NaOH solution was added to promote the granulation process until the development of millimeter-sized pellets. The water-to-cement ratio varied from about 0.4 to about 1.5, depending if the two water-reducing additives were used or not, whereas the NaOH solution-to-MK/GGBFS ratio was varied in the range 1-2.6 because of the higher water demand of MK and GGBFS. About 5-10% of each solution (i.e. water and NaOH solution) was added during mixing to prevent the formation of dust aerosol, while the remaining was added during the pelletization stage. The obtained granulates were ripened for 28 days in wet air (20°C, 95% atmospheric relative moisture content) and then characterized.

The specific formulations and dosages used in each study are reported in the respective experimental sections.

3. Chapter 3

Consecutive thermal and wet conditioning treatments of sedimentary stabilized cementitious materials from HPSS® technology: effects on leaching and microstructure

Loris Calgaro[1], Elena Badetti[1], Alessandro Bonetto[1], Silvia Contessi[2], Roberto Pellay[3], Giorgio Ferrari[4], Gilberto Artioli[2], Antonio Marcomini[1*]

[1]Department of Environmental Sciences, Informatics and Statistics, University Ca' Foscari of Venice, Via Torino 155, 30172 Venice Mestre, Italy.

[2]Department of Geosciences, University of Padua, Via Gradenigo 6, 35131 Padua, Italy

[3]Ingegnerie e Tecnologie Ecologiche (In.T.Ec.) s.r.l., Via Romea 8, 30034 Malcontenta di Mira, Venice, Italy

[4]Mapei s.p.a., via Cafiero 22, 20158 Milan, Italy

In this chapter, the results related to the paper "Consecutive thermal and wet conditioning treatments of sedimentary stabilized cementitious materials from HPSS® technology: effects on leaching and microstructure" published on the Journal of Environmental Management are reported.

Among "ex-situ" S/S treatments, the High Performance Solidification/Stabilization (HPSS®) process, developed by Mapei and In.T.Ec. [205,206], for the treatment of soils, sediments, and wastes with a dominant inorganic matrix has already been successfully applied for the reclamation of various sites contaminated by multiple heavy metals [222,223,238]. However, it has been shown that, in the case of soils or sediments contaminated by both organic and inorganic pollutants, the HPSS® technology should be ameliorated to obtain higher quality materials [208].

Within this work, sediments dredged from the Mincio river (Italy) contaminated by mercury and heavy hydrocarbons (C_{12-40}) were treated by applying and implementing the High Performance Solidification/Stabilization technology, aiming to produce safe and reusable cement-based granular materials. Temperature and time of treatment were varied to diminish the degradation of the cementitious phases of the granules (usually related to the high temperatures employed in the process), and a wet conditioning step was introduced to improve their mechanical properties, as well as to further reduce the leaching of contaminants. The physical-chemical properties of the granules and contaminant leaching in water were investigated by Inductively Coupled Plasma Mass and Optical Emission Spectrometry, Ultraviolet–Visible spectroscopy, Gas Chromatography, X-Ray Powder Diffraction, and Scanning Electron Microscopy, in order to identify the optimal parameters for both thermal and wet conditioning processes.

3.1. Experimental

3.1.1. Contaminated site, sampling of contaminated sediment, and preparation of cementitious granular material

The investigated sediments (~ 100 kg) were dredged from the construction site of a new navigation basin along the Mincio river at Valdaro (Italy) and the chemical characterization of the area, which is one of the Italian remediation Sites of National Interest (SNI) [239], pointed out a contamination mainly due to mercury (concentrations up to 10 $mg \cdot kg^{-1}$ d.w.) and to high molecular weight petroleum hydrocarbons ($C_{12–40}$, concentrations up to 1500 $mg \cdot kg^{-1}$d.w.).This pollution is a consequence of poor industrial waste management and accidental spills that affected this area since the 1950s, when several chemical and petrochemical factories and oil refineries were built along the Mincio river. After sampling, the sediment was air-dried, mechanically crushed (by a hammer mill HM/530 B - Ceramic Instruments, Sassuolo, Italy) homogenized, and characterized.

The total content of heavy metals and $C_{12–40}$ petroleum hydrocarbons present in the contaminated sediment are reported in **Table S3.1**, while the XRD analysis of the sediment (**Table S3.2**) highlighted the presence of mainly calcite, quartz and amorphous phases, confirming the previous geological characterization of this area [240]. The sample was also investigated by laser diffraction particle size analysis, showing the presence of a mainly clayey sediment (**Figure S3.1**).

Afterwards, the HPSS® technology was applied as described in chapter 2.2, and the obtained granulate material was characterized to determine heavy metals and heavy hydrocarbons (C12–40) content (**Table S3.1**).

The formulation used is reported in **Table 3.1.**

Table 3.1. Standard HPSS® formulation and dosages used for granular material preparation

Component	% w.t.
Contaminated sediment	72.2
CEM I 42,5 R	26.7
Mapeplast ECO-1A	0.53
Mapeplast ECO-1B	0.53
Water/Cement ratio	0.40

The dosages used were: 20.000 kg (d.w.) sediment; 7.40 kg (d.w.) CEM I 42.5 R; 148 g Mapeplast ECO 1-B and 148 g Mapeplast ECO 1-A (2% of cement d.w.); 3010 g water (300 g at the first addition, 2710 g at the second one).

Leaching tests were also performed following the UNI 12457-2:2004 standard, and the leachates were characterized by ICP-MS (heavy metals) and UV-Vis spectroscopy (Chemical Oxygen Demand – COD).

3.1.2. Thermal desorption process under vacuum

After 28 days of curing, aliquots of 2.5 kg of pellets were subjected to a series of thermal treatments under vacuum at the temperatures of 90°C, 110°C, 150°C and 200°C using a pilot plant, to distill mercury and hydrocarbons. The system was pre-heated up to the operating temperature and the pellets were inserted into the reactor. After reaching the operating temperature, heating was maintained for 15 minutes; then the system was kept for 15 minutes under vacuum. Finally, the system was vented to ambient pressure and the pellets were removed from the reactor (total time required for each sample: ~ 70 min).

The samples, before and after TT, were characterized by SEM and to determine their morphological and mineralogical characteristics and analysed by ICP-MS and GC to measure, their total heavy metal and hydrocarbons ($C_{12–40}$) content, respectively. Moreover, the granulate leaching

behaviour was studied by using the UNI EN 12457-2:2004 leaching test [228], and the leachates were characterized by ICP-MS and UV-Vis.

3.1.3. Wet-conditioning process

The wet-conditioning process was applied to the pellets before and after the TT, in order to hydrate the residual cementitious phases and to remove the Portlandite present in the samples. For each of the conditions investigated (sample before thermal treatment and samples after thermal treatment in the range from 90 to 200°C), 2 kg of the pellets were conditioned in water for 76 days, by using flowing tap water with a solid/liquid ratio of 1 $kg \cdot L^{-1}$ and a flow of 1 L of water per day for each kilogram of pellets. The system was stirred by insufflating compressed air from the bottom of the conditioning tank. During this process, heavy metal leaching was monitored by collecting the overflowing water (2L) every 24 hours. The obtained samples were filtered at 0.45 μm (AXIVA SICHEM BIOTECH Membrane Filters, Delhi, India) and analyzed by ICP-OES.
The wet conditioning was interrupted after 76 days, when the leaching values of Ni, Cr, Cu, and V in the washing water were less than 5 $\mu g \cdot L^{-1}$ for six consecutive days. As for the thermal desorption process, the pellets were characterized by SEM, XRD and ICP-MS analysis, and the leaching behaviour was studied by the UNI EN 12457-2:2004 leaching test [228].

3.2. Results and discussion

Innovative technologies such as HPSS®, taking advantage of the principles of "circular economy", are of great interest from both the environmental and economic point of view, since the reuse of contaminated materials is usually a more sustainable approach than landfill disposal.
In this context, we tried to improve this technology by varying thermal and time conditions of the TT and by adding a wet conditioning step, to further increase the performance of the pellets produced with the established approach [140,222]. In the specific case of the sediments dredged from the Mincio river**,** both Hg and C_{12-40} petroleum hydrocarbons (**Table S3.1**) exceeded both the reclamation thresholds established for this contaminated site by ISPRA - Italian Institute for Environmental Protection and Research [241], and the limits imposed by the Italian regulation for the use of soil for residential purposes [101]. In order to obtain a reusable material, the content of both Hg (average concentration: 8.64±0.55 $mg \cdot kg^{-1}$ d.w.) and C_{12-40} petroleum hydrocarbons (average concentration: 1452±203 $mg \cdot kg^{-1}$ d.w.) had to be reduced, by suitable treatments, below 5.0 and 750 $mg \cdot kg^{-1}$ d.w., respectively. The different steps concerning the management of the contaminated sediments adopted in this study are represented in **Figure. 3.1**.

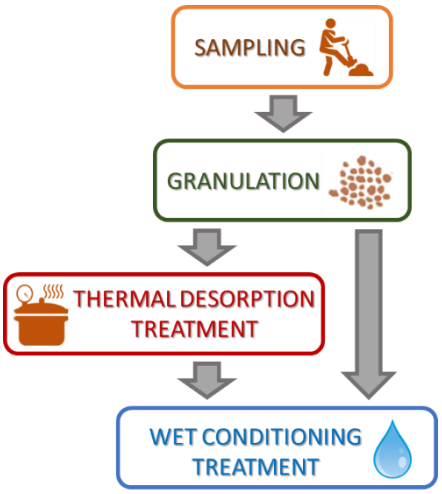

Figure 3.1. Steps of the experimental set-up.

In detail, after sampling the contaminated sediments were granulated and sieved, and the particle size distribution of the obtained granular material showed that most pellets (59% in weight) were in the range 2 - 3.15 mm, about 38% were in the range 3.15 - 4 mm, while ~3% had a size greater than 4 mm (**Table S3.3**). As can be seen in **Table S3.1**, the pellets showed a reduced amount of Hg (6.31±0.32 mg·kg^{-1} d.w.) and $C_{12\text{-}40}$ hydrocarbons (1060±148 mg·kg^{-1}d.w.) with respect to the sediment, according to the amount of cement used for the granulation (c.a. 27%).

Afterwards, the pellets were subjected to a series of thermal desorption treatments at temperatures ranging from 90°C to 200°C, which are the operational temperature limits of the pilot plant used. This step was followed by a wet conditioning (WC) process, aiming at rehydrating the cement-based granules obtained after the TT. This treatment was also performed directly after the granulation step, in order to evaluate the differences between the two routes.

3.2.1. Thermal desorption treatment

3.2.1.1. XRD and SEM analysis

After the TT, the XRD analysis of the pellets showed an increase of the signals corresponding to di-and tricalcium silicates (C_2S and C_3S), tetracalcium alumino ferrite (C_4AF) and tricalcium aluminate (C_3A), together with a decrease of both calcite and amorphous phases' signals, indicating a progressive dehydration of the cement with the increase of the treatment temperature (**Table S3.4** and **Figure 3.2**).

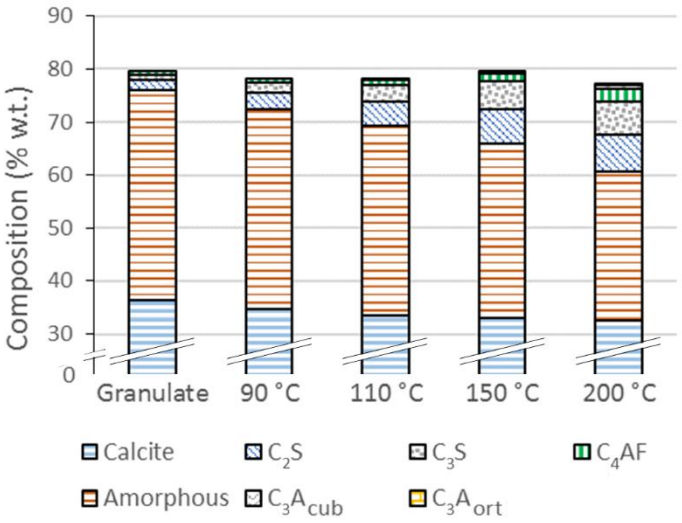

Figure 3.2. Calcite, C_2S, C_3S, C_4AF, cubic C_3A (C_3A_{cub}), orthorhombic C_3A (C_3A_{ort}) and amorphous phases (w.t. %) present in the granulate before and after the thermal treatment at 90°, 110°, 150°, and 200°C.

Moreover, the percentage of ettringite ($C_3A{\cdot}3CaSO_4{\cdot}32H_2O$) decreased from 3% to less than 0.5% (**Table S3.4**), with slightly lower values at the highest temperatures of TT, since this mineral is known to be unstable over 50°C [242]. In addition, as far as Portlandite ($Ca(OH)_2$) is concerned, the amount found by XRD after TT increased almost linearly with the temperature (**Table S3.4**).

SEM images (**Figure S3.2**) revealed how the dehydration process shifted from the surface of pellets to the core as a function of temperature (deeper dehydration at higher temperatures), as shown also in the example reported in **Figure 3.3**.

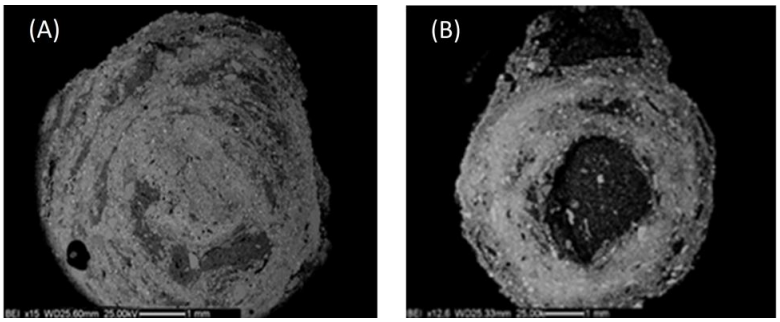

Figure 3.3. Section of pellets after 28 days of curing (A), subjected to vacuum thermal treatment at 150°C (B)

2.2.1.2. Hg and C12-40 petroleum hydrocarbons removal

The removal of Hg and $C_{12\text{-}40}$ after the TT is illustrated in **Figure 3.4** and **Table S3.5**. As already reported in the literature [140], the amount of $C_{12\text{-}40}$ hydrocarbons and Hg decreased with increasing the distillation temperature from 90 to 200°C, with a higher reduction at the maximum temperature used. The results showed that the Hg content was compliant with the Italian regulation on soil use in industrial areas [101] already at 90°C (reduction of ca. 45% with respect to pellets before TT), while for $C_{12\text{-}40}$ hydrocarbons a temperature of 110°C was required to achieve a reduction

of 47%. This temperature can therefore be considered as a good compromise between operational costs and performances.

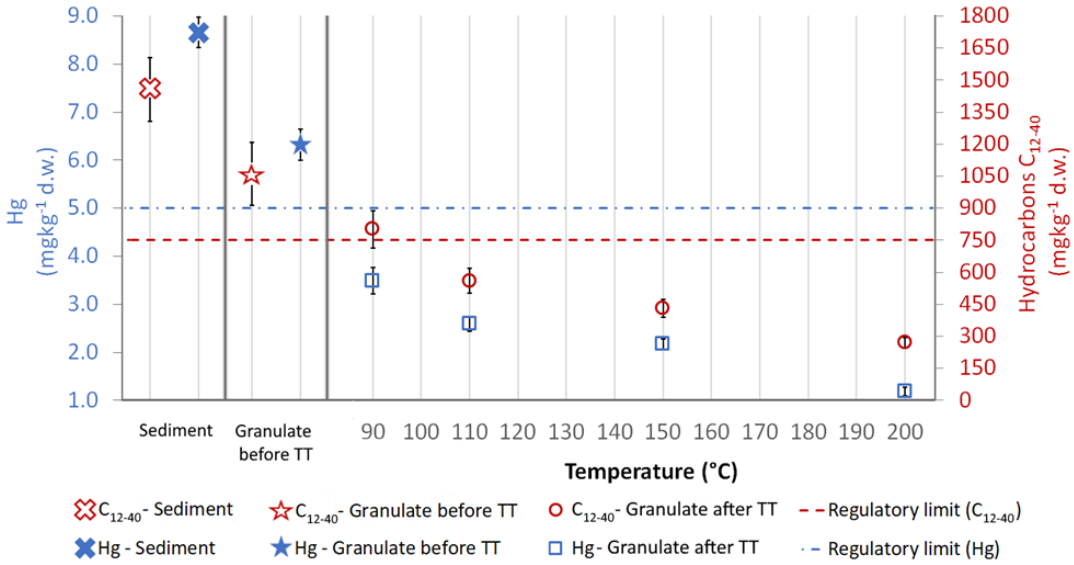

Figure 3.4. Hg and Hydrocarbons C_{12-40} in the dredged sediment and in the granulate before and after the thermal treatment. Error bars indicate confidence intervals ($\alpha = 0.05$).

2.2.1.3. Leaching test

After the morphological and chemical characterization, the leaching behaviour of the granulated material was investigated by ICP-MS and UV-Vis. The overall results are reported in **Table 3.2** together with the regulatory limits required by the Italian legislation [101] for the end-of-waste classification (Sn, Sb, and Tl were also investigated even though they are not regulated).

A slight increase of pH from 11.9 to 12.3 was measured for leachates after the TT (**Table 3.2**), which can be attributed, according to XRD analysis, to the increase of C_2S, C_3S, C_4AF, C_3A, and Portlandite. As far as leaching is concerned, granules treated at 200°C showed the highest release of each metal investigated, except for Ba, which remained practically constant and for Cd, Cr and As, which showed a significant variation already at 90°C. These increases of metal leaching can be attributed to both an increased abrasion of the pellets, caused by the end-over-end tumbler shaking that lead to the formation of fine particles with a higher specific area, and the increase of the leachates' pH, which increased the solubility of amphoteric heavy metals [243].

Moreover, the temperature may also affect this process, since the presence of more dehydrated cement can induce a reduction of the mechanical properties. As far as Se, Hg, Pb, Be, Sn, Sb and Tl are concerned, their concentrations were always below the respective detection limits (< 0.1-1 $\mu g \cdot L^{-1}$). Finally, COD values were used to estimate the leaching of organic substances from the pellets in the aqueous matrix; as shown in **Table 3.2**, an increase of these values was observed within the whole

temperature range investigated, which could be ascribed to the degradation of heavy organic molecules (e.g. humic acids) to more soluble compounds [140].

Table 3.2. Results of the leaching test UNI EN 12457-2:2004 of granulated material before and after the TT.

Parameter	Granulate	Granulate after TT at 90°C	Granulate after TT at 110°C	Granulate after TT at 150°C	Granulate after TT at 200°C	Regulatory Limit*
Analyte ($\mu g \cdot L^{-1}$)						
Be	< 0.1	< 0.1	< 0.1	< 0.1	< 0.1	10
Cd	0.15±0.02	0.19±0.04	0.21±0.03	0.21±0.02	0.21±0.03	5
Hg	< 0.5	< 0.5	< 0.5	< 0.5	< 0.5	1
Pb	< 0.5	< 0.5	< 0.5	< 0.5	< 0.5	50
V	0.70±0.18	0.78±0.17	0.81±0.28	0.93±0.55	1.14±0.58	250
Cr	13.3±0.7	17.3±1.1	19.4±3.9	20.1±0.8	24.8±2.3	50
Ni	59.5±6.1	60.1±6.9	64.5±6.1	75.2±4.0	78.7±4.7	10
Cu	91.0±12.0	90.5±7.1	92.8±5.2	108±12	105±4	50
Zn	< 0.5	< 0.5	< 0.5	< 0.5	< 0.5	3000
Ba	655±121	581±109	491±75	467±89	483±97	1000
Co	2.44±0.58	2.68±0.57	3.86±0.36	4.90±1.40	5.07±0.64	250
As	1.05±0.09	1.42±0.07	1.63±0.20	2.17±0.15	3.10±0.67	50
Se	< 1	< 1	< 1	< 1	< 1	10
Sn	< 0.1	< 0.1	< 0.1	< 0.1	< 0.1	-
Sb	< 0.1	< 0.1	< 0.1	< 0.1	< 0.1	-
Tl	< 0.1	< 0.1	< 0.1	< 0.1	< 0.1	-
COD ($mg \cdot L^{-1}O_2$)	119±10	174±10	211±12	327±45	413±37	30
pH	11.91±0.04	12.27±0.04	12.37±0.12	12.32±0.02	12.27±0.04	5.5-12.0

*Regulatory limit: Table 1 of Annex III of Ministerial Decree No 186 of 05th April 2006 [114]

3.2.2. Wet conditioning

3.2.2.1. Leaching during the wet conditioning process

The wet conditioning process was performed to rehydrate the pellets after TT and to reduce their Portlandite content, which, together with other components, is responsible of increasing the pH values during the leaching test. The water where the pellets were immersed was analyzed daily to monitor the leaching of metals and the pH: the overall data (**Figure S3.3-S3.7**) revealed that leaching occurred only for Ni, Cr, Cu, Ba, and V, and that it was closely linked to the wash water pH.

In detail, the maximum leaching of Ni, Cr, Cu, and Ba, due to the high pH value of the washing water, occurred in the first 18 days of wet conditioning. As commented before, these pH values were due to the formation of Portlandite and, once the hydration of the granules was completed, a slow decrease of pH values was detected within six days, due to the gradual wash-out of calcium hydroxide. Once

the wash water pH stabilized at values between 8.0 and 8.5, the leaching for each metal decreased to less than 5 $\mu g \cdot L^{-1}$ (per day) in the next 50 days, except for Ba, which was around 50 $\mu g \cdot L^{-1}$.
The leaching observed for almost all samples was similar, regardless of the temperature employed in the TT. In the case of Ba, the sample not subjected to TT showed leaching of one order of magnitude greater than those of samples subjected to TT, suggesting that this metal was mainly leached from the hydrated cementitious phases. On the other hand, V leaching increased sharply after pH decreased below 9.5 and reached a maximum value after 10-20 days. At this point, in accordance with the results already reported in the literature for V leaching from concrete [244,245], the leaching started to decrease when pH dropped below 8.5**.** ICP-MS analysis of the pellets after microwave-assisted acid digestion was performed, confirming these results (**Table S3.6**). As an example, Cr and V leaching from the sample subjected to TT at 150°C, together with the pH values, is reported in **Figure 3.5**.

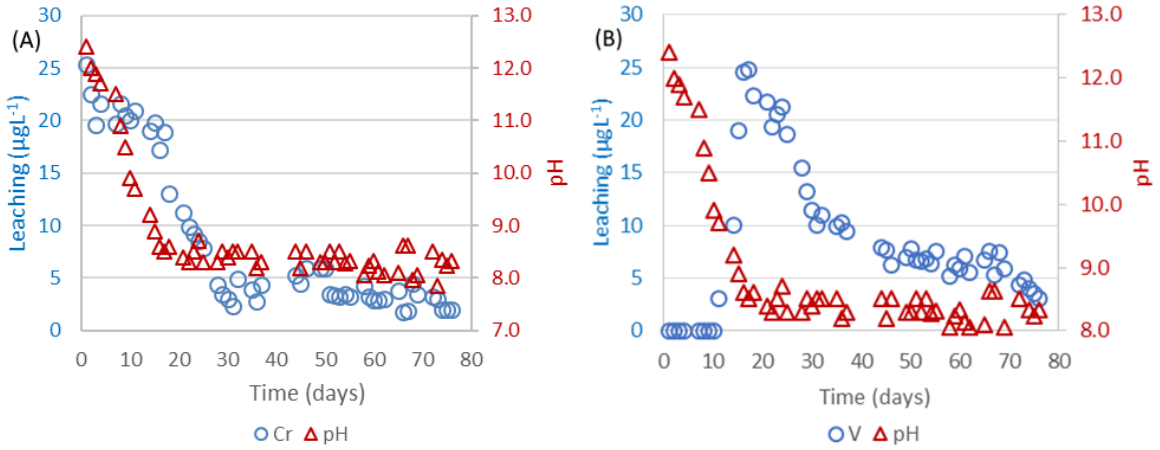

Figure 3.5. pH of the washing water alongside leaching of Cr (A) and V (B) for the sample of granules subjected to WC process after TT at 150°C.

3.2.2.2. XRD and SEM analysis after the WC process

XRD results (**Table S3.7**) showed partial rehydration of the pellet's cementitious phases for all the samples investigated. In fact, after the WC process, the weight percent (wt %) of di-and tricalcium silicates (C_2S and C_3S), tetracalcium alumino ferrite (C_4AF) and tricalcium aluminate (C_3A) phases decreased by about 40-80%, with respect to the same materials analysed after the TT. This reduction was more pronounced for the pellets that were subjected to the TT at higher temperatures, since these conditions caused an increase of their dehydration, as well as of their porosity. This probably allowed a better diffusion of water within the granule's microstructure, which facilitated the rehydration of the pellets during the WC process. These results were also confirmed by the increase of the calcite percentage (ca. 5-35%) measured by XRD analysis, which can be partly ascribed to the carbonation of the calcium silicate hydrates (C-S-H phase) formed during the

hydration of the pellet's cementitious phases [246]. Moreover, an increased content of ettringite and an almost complete wash out of Portlandite were observed from the XRD spectra of all the samples treated with WC.

SEM analysis (**Figure 3.6**) showed the formation on the pellets' surface of an outer film of calcite, which was less porous compared to the rest of the granulate and, in addition, slightly thicker for the pellets treated at 150 and 200 °C. These microstructure variations improved both the mechanical and leaching properties of the treated pellets.

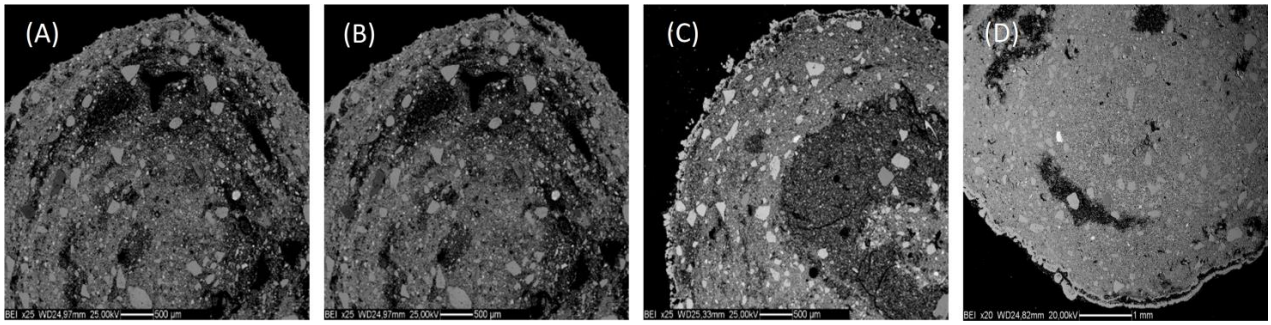

Figure 3.6. Section of pellets subjected to wet conditioning after thermal treatment at 90°C (A), 110°C (B), 150°C (C) and 200°C (D).

3.2.2.3. Leaching test after the WC process

The leaching of the pellets after WC was investigated by following the same procedure described in paragraph 3.1.3. for TT. From the results reported in **Table 3.3**, it can be seen that the WC treatment caused a significant variation of all the samples' leaching, whenever they were subjected to TT or not. In detail, all the metals investigated showed a decreased leaching, except for Be, Cd, Sn, Hg, Sb, Tl, Se and Zn, whose variations were negligible, and V, which increased from 3 to 5 times with respect to leaching before WC. As for leaching observed during WC, the behaviour of V can be related to the eluates' pH [244,245], which decreased from 12.3 to 11.3. This pH reduction probably influenced also the decrease in leaching observed for the other metals (i.e. Ni, Cu, Cd, Cr), since it reduced the solubility of the corresponding salts and hydroxides by nearly 5-10 times [243]. A decrease of the leaching of organic contaminants, estimated on the basis of the COD value, was also observed. The overall results of this leaching test, therefore, showed that the WC process led to materials that can be classified as "end of waste", accomplishing the limits established by Italian law for reuse [114].

Table 3.3. Results of the leaching test UNI 12457/2 of granulated material after WC.

Parameter	Granulate WC	Granulate WC 90°C	Granulate WC 110°C	Granulate WC 150°C	Granulate WC 200°C	Regulatory limit*
Analyte ($\mu g \cdot L^{-1}$)						
Be	< 0.1	< 0.1	< 0.1	< 0.1	< 0.1	10
Cd	< 0.1	< 0.1	< 0.1	< 0.1	< 0.1	5
Hg	< 0.5	< 0.5	< 0.5	< 0.5	< 0.5	1
Pb	< 0.5	< 0.5	< 0.5	< 0.5	< 0.5	50
V	26.2±2.5	28.2±1.7	32.8±2.2	35.4±1.5	38.7±1.8	250
Cr	8.32±0.82	7.88±0.54	7.12±0.38	6.32±0.61	4.08±0.42	50
Ni	9.7±0.9	9.5±0.6	8.6±0.7	6.0±1.1	4.6±0.8	10
Cu	32.5±0.7	30.1±3.2	28.6±1.6	26.4±1.2	24.5±1.8	50
Zn	<0.5	<0.5	<0.5	<0.5	<0.5	3000
Ba	96.2±4.5	100±10	93.0±9.1	90.0±7.2	91.1±5.1	1000
Co	1.79±0.20	1.43±0.25	1.38±0.27	1.53±0.19	1.32±0.12	250
As	< 0.1	< 0.1	< 0.1	< 0.1	< 0.1	50
Se	< 1	< 1	< 1	< 1	< 1	10
Sn	< 0.1	< 0.1	< 0.1	< 0.1	< 0.1	-
Sb	0.53±0.16	0.53±0.12	0.59±0.13	0.55±0.15	0.63±0.16	-
Tl	< 0.1	< 0.1	< 0.1	< 0.1	< 0.1	-
COD ($mg \cdot L^{-1} O_2$)	24±5	< 10	< 10	< 10	< 10	30
pH	11.29±0.09	11.19±0.08	11.23±0.09	11.35±0.04	11.24±0.03	5.5-12.0

*Regulatory limit: Table 1 of Annex III of Ministerial Decree No 186 of 05/04/2006 [114].

3.2.2.4. Mechanical properties

The mechanical properties of the pellets obtained after the various treatment steps were also investigated. In particular, the resistance to fragmentation was evaluated by using the UNI EN 1097-2:2010 test [234], which was carried out on pellets treated with the TT at 110 °C, before and after the WC process (**Table S3.8**). The crushed fraction (particle diameter < 1.6 mm) obtained after the test showed a decrease from 38.8 % to 30.6 % after the WC process.

The resistance to abrasion was also estimated by quantifying the fraction with particle diameter < 63 μm in the granulate sample recovered after the UNI EN 12457-2:2004 leaching test [228]. To this purpose, the sample was sieved at 63 μm and the over-sieved fraction was dried and weighed, and the difference between the weight of the sample prior to the test and that of the over-sieved was considered as the abraded fraction. The results, reported in **Table S3.9**, showed a decrease of the pellets abrasion of nearly 50 % after the WC process. This enhancement in the mechanical properties of the granulated materials was most likely due to the decrease of unreacted cement, to the increase of calcite content, and to the formation of a carbonated layer on the surface of the pellets. All these factors contributed to reduce the fragmentation and abrasion of the pellets, and consequently the formation of small particles and fragments.

3.3. Implications for environmental management

With the aim of limiting the unsustainable practice of landfill disposal for contaminated soil and sediments, the development, testing and application of innovative and efficient techniques for their treatment are needed. Sustainable practices should promote those technological approaches that allow to maintain soil or sediment quality or that are capable of transforming the contaminated matrices into reusable products, following the principles of the circular economy.

This research will contribute to improve the knowledge on the performance of a state-of-the-art technique for the treatment of contaminated soil and sediment, thus helping to extend the pool of available technologies that can be applied to develop sustainable remediation strategies.

3.4. Conclusions

In this study, the HPSS® (High Performance Solidification/Stabilization) technology developed by Mapei and In.T.Ec. was successfully applied to remediate freshwater sediments from the Mincio river, contaminated by Hg and C_{12-40} petroleum hydrocarbons. The technology was improved by adding a wet conditioning process to a thermal treatment, in an attempt to produce granulated materials accomplishing all the Italian regulatory requirements for reuse. The thermal treatment yielded good results already at 110 °C, allowing to obtain for both contaminants concentrations below the regulatory limits. In addition, the wet conditioning process was shown to improve the leaching and mechanical characteristics of the granular material.

The results from this study demonstrated that HPSS® is a promising technology to address soil and sediment pollution issues, since it allowed for the removal of volatile and semi-volatile pollutants (Hg and hydrocarbons C_{12-40}) and the trapping of the other heavy metals in a reusable stabilized cementitious material. This technology can give the contaminated sediments and soils (otherwise destined to landfill disposal) a second life, offering a valuable option for addressing the long-term management of these polluted matrices. To the best of our knowledge, this is the first time in which a wet conditioning step has been added to the HPSS® process, with and without prior thermal treatment of the pellets. It is therefore highly recommended to improve the performances of cement-based granulated materials deriving from the HPSS® technology, also in the case of pellets not subjected to the thermal treatment.

3.5. Acknowledgments

The authors are grateful to In.T.Ec. s.r.l. for founding the Ph.D. fellowship of L. C. and to Mapei spa for additional support. Dr. Elisa Giubilato and Dr. Cinzia Bettiol (University Ca' Foscari of Venice) are acknowledged for useful discussions.

3.6. Supplementary information

Table S3.1. Heavy metals and hydrocarbons C_{12-40} content of contaminated sediments and granulate. Concentrations exceeding the regulatory limits are highlighted.

Contaminant	Sediment	Granulate	Regulatory Limit
	$mg \cdot kg^{-1}$ d.w.		
Be	0.17±0.02	0.15±0.02	2**
Cd	< 0.5	0.52±0.04	0.6*
Hg	**8.64±0.55**	**6.31±0.32**	**1***
Pb	27.0±1.8	22.0±1.5	120*
V	30.0±2.8	36.2±5.3	42*
Cr	54.1±4.2	68.0±3.2	70*
Ni	37.2±2.0	53.0±2.9	75*
Cu	20.9±1.1	64.8±3.5	120*
Zn	65.1±5.4	74.0±6.1	150*
Ba	201±8	280±7	-
Co	5.86±0.47	7.55±0.61	20**
As	4.53±0.31	8.53±0.58	20*
Se	< 0.5	< 0.5	3*
Sn	0.84±0.11	0.73±0.09	1**
Sb	< 0.5	2.29±0.12	10**
Tl	0.39±0.04	0.58±0.12	1*
Hydrocarbons C_{12-40}	**1452±203**	**1060±148**	**50****

*Regulatory limit: Thresholds for reclamation established for this contaminated site by the Italian Institute for Environmental Protection and Research (ISPRA)[241]. **Regulatory limit: Column A (residential and green use) of Table 1 of Annex V to Part IV of Title V of Legislative Decree No 152 of 03/04/2006 [101]

Table S3.2. Results of the mineralogical characterization of the dredged sediment.

	Sediment
	% w.t.
Calcite	43.1±2.0
Clinochlore	2.7±0.3
Dolomite	3.2±0.4
Quartz	8.8±1.0
Muscovite	3.8±0.4
Lizardite	0.7±0.3
Albite	2.9±0.3
Orthoclase	1.0±0.2
Amorphous phases	33.9±1.7

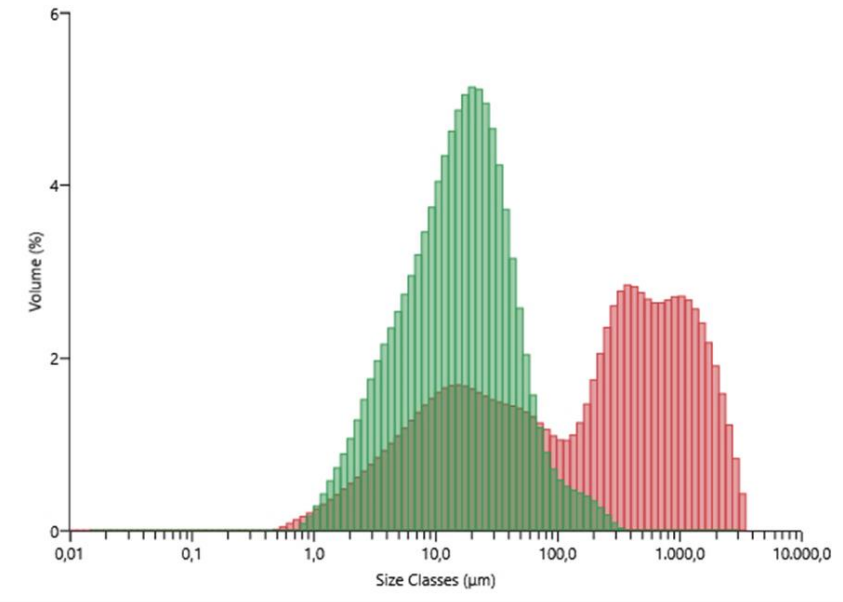

Figure S3.1. Particle size distribution of the contaminated sediment after homogenization using air (red) and water (green) as dispersants.

Table S3.3. Particle size distribution of the granular material obtained from the contaminated sediments.

Particle size	Granulate
	% w.t.
Φ < 2.0 mm	0
2.0 mm > Φ > 3.15 mm	55.0
3.15 mm > Φ > 4.0 mm	38.2
Φ > 4.0 mm	2.8

Table S3.4. XRD analysis of granulate before and after thermal treatment. (l.o.d.: limit of detection).

	Granulate	Granulate after TT at 90°C	Granulate after TT at 110°C	Granulate after TT at 150°C	Granulate after TT at 200°C
	% w.t.				
Calcite	36.4±1.1	34.7±1.9	33.5±1.0	33.1±0.8	32.5±1.1
Clinochlore	2.0±0.2	2.5±0.2	2.3±0.2	2.2±0.1	2.4±0.3
Dolomite	2.3±0.4	2.8±0.3	2.6±0.4	3.0±0.2	2.9±0.3
Quartz	6.4±1.1	7.1±0.6	6.5±0.5	6.4±0.5	6.2±0.7
Muscovite	2.8±0.4	3.3±0.3	3.5±0.3	3.1±0.3	3.2±0.3
Lizardite	0.5±0.1	0.6±0.2	0.5±0.1	0.6±0.2	0.6±0.2
Albite	2.1±0.3	2.8±0.3	2.4±0.2	2.0±0.2	2.1±0.2
Orthoclase	0.7±0.2	0.7±0.2	0.8±0.3	0.7±0.2	0.8±0.1
C_2S	2.0±0.3	3.2±0.3	4.6±0.4	6.5±0.3	7.1±0.3
C_3S	1.0±0.2	2.0±0.2	3.0±0.2	5.3±0.5	6.2±0.4
C_3A_{Cub}	< l.o.d.	< l.o.d.	0.2±0.1	0.4±0.1	0.7±0.1
C_3A_{Ort}	< l.o.d.	< l.o.d.	< l.o.d.	< l.o.d.	0.1±0.05
C_4AF	0.8±0.2	0.9±0.1	1.1±0.1	1.6±0.1	2.5±0.2
Ettringite	3.1±0.5	0.5±0.1	0.3±0.1	0.3±0.1	0.2±0.1
Portlandite	0.4±0.1	1.3±0.2	1.8±0.2	2.1±0.2	2.9±0.3
Amorphous	39.5±1.7	37.6±1.3	35.8±1.5	32.8±1.2	28.1±1.0

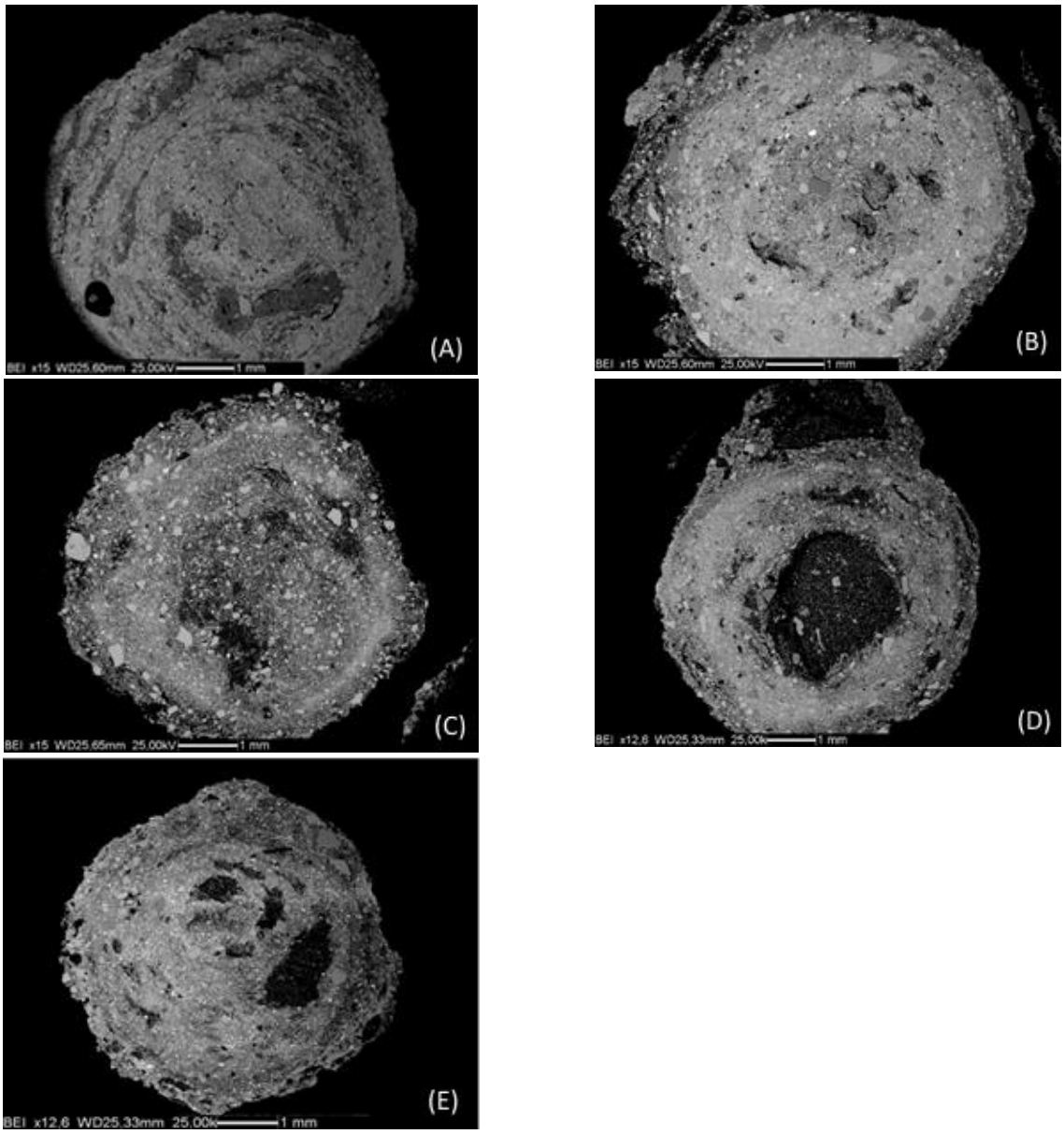

Figure S3.2. Sections of pellets before (A) and after thermal desorption treatment at 90°C (B), 110°C (C), 150°C (D) and 200°C (E).

Table S3.5. Hg and Hydrocarbons contained in the pellets before and after TT. Concentrations exceeding the regulatory limits are highlighted.

	Granulate	**Granulate after TT at 90°C**	**Granulate after TT at 110°C**	**Granulate after TT at 150°C**	**Granulate after TT at 200°C**	**Regulatory Limit***
Analyte ($mg \cdot kg^{-1}$ d.w.)						
Hg	**6.31±0.32**	3.49±0.27	2.59±0.15	2.17±0.11	1.18±0.09	**5**
Hydrocarbons C_{12-40}	**1060±148**	**801±67**	559±58	430±42	272±23	**750**

*Regulatory limit: Column B (commercial and industrial use) of Table 1 of Annex V to Part IV of Title V of Legislative Decree No 152 of 03/04/2006 [101].

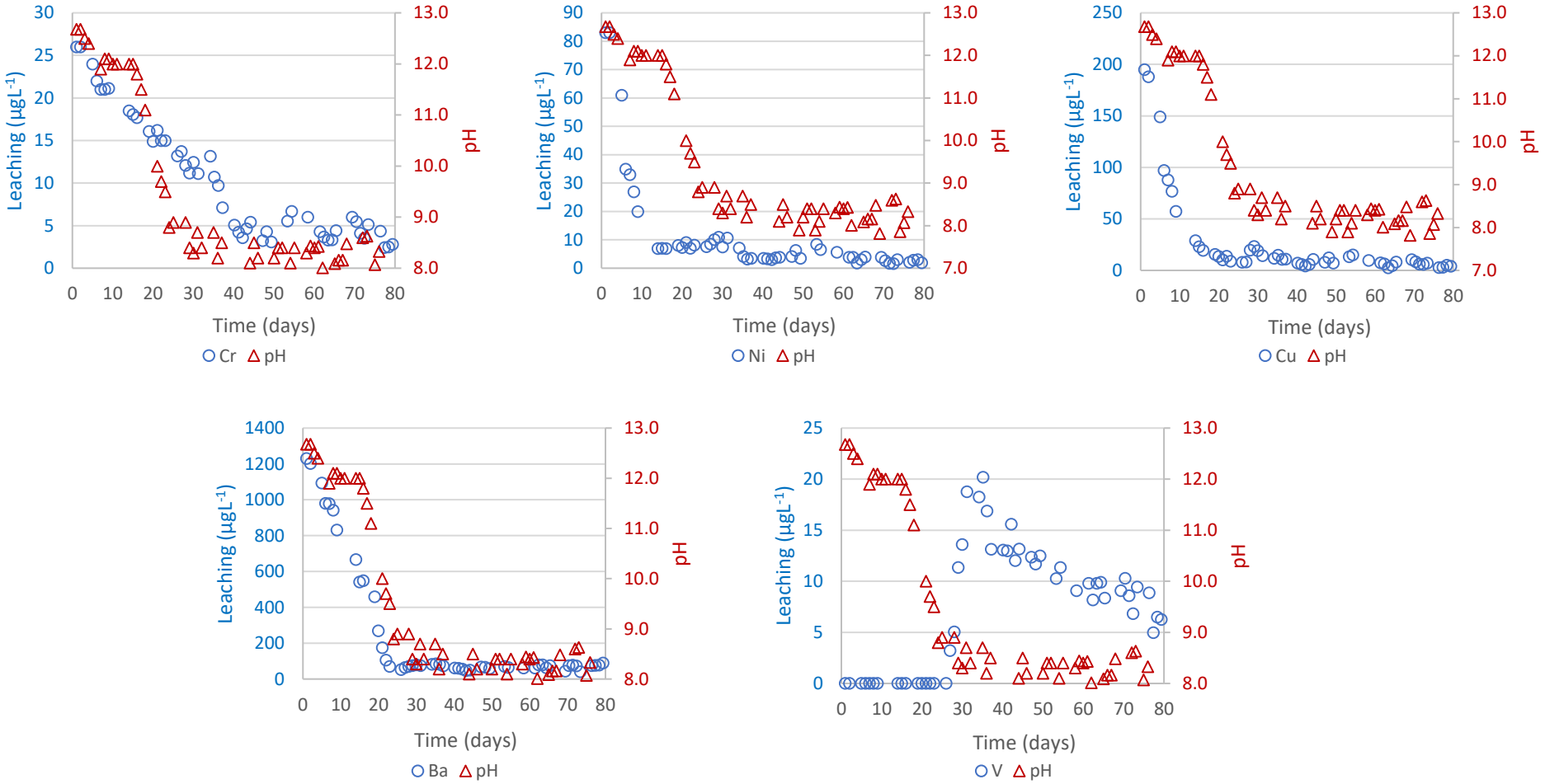

Figure S3.3. pH of the of the washing water alongside leaching of Cr, Ni, Cu, Ba and V for the sample of granules subjected to WC process without thermal treatment.

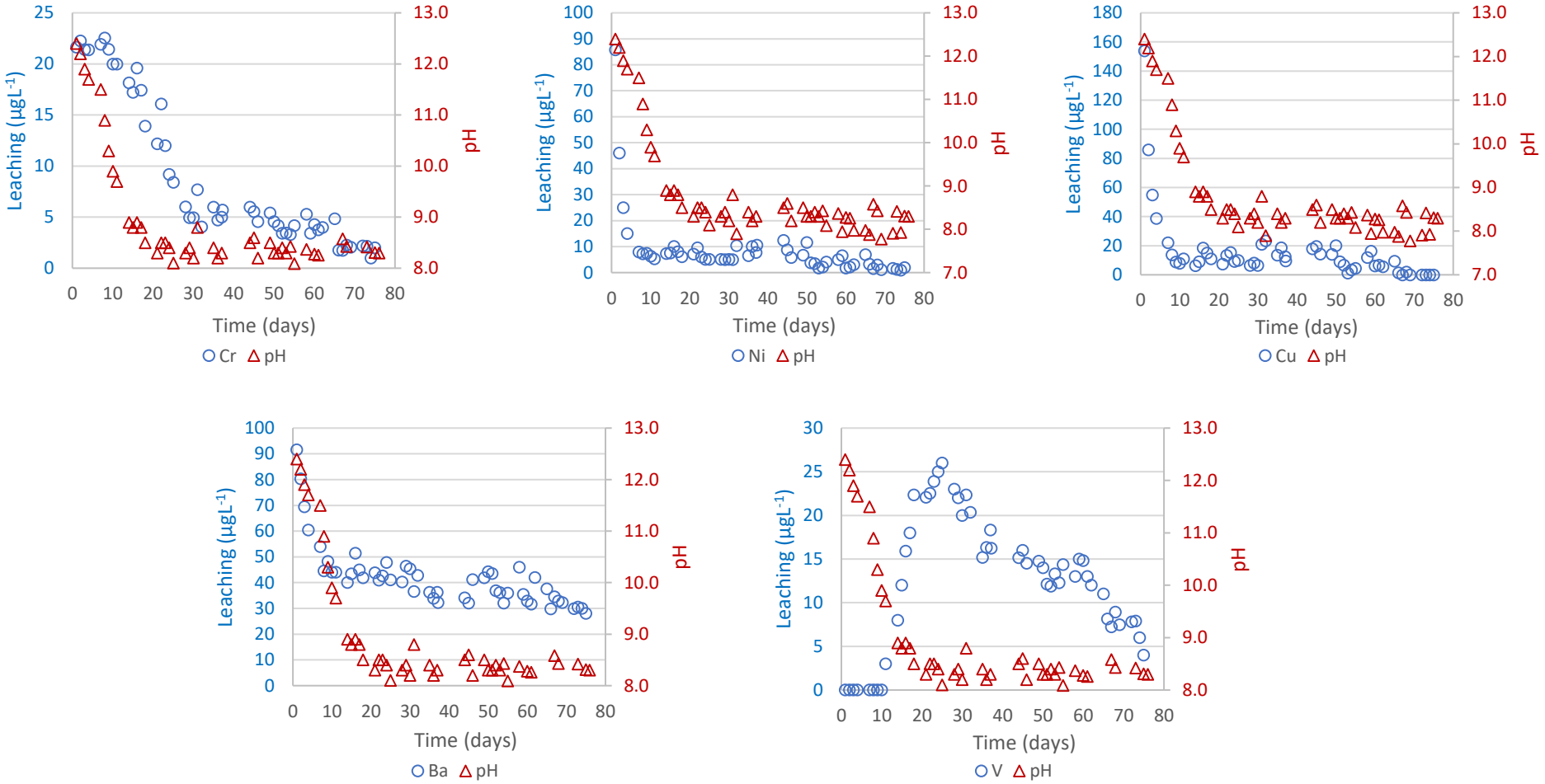

Figure S3.4. pH of the of the washing water alongside leaching of Cr, Ni, Cu, Ba and V for the sample of granules subjected to WC process after thermal treatment at 90°C.

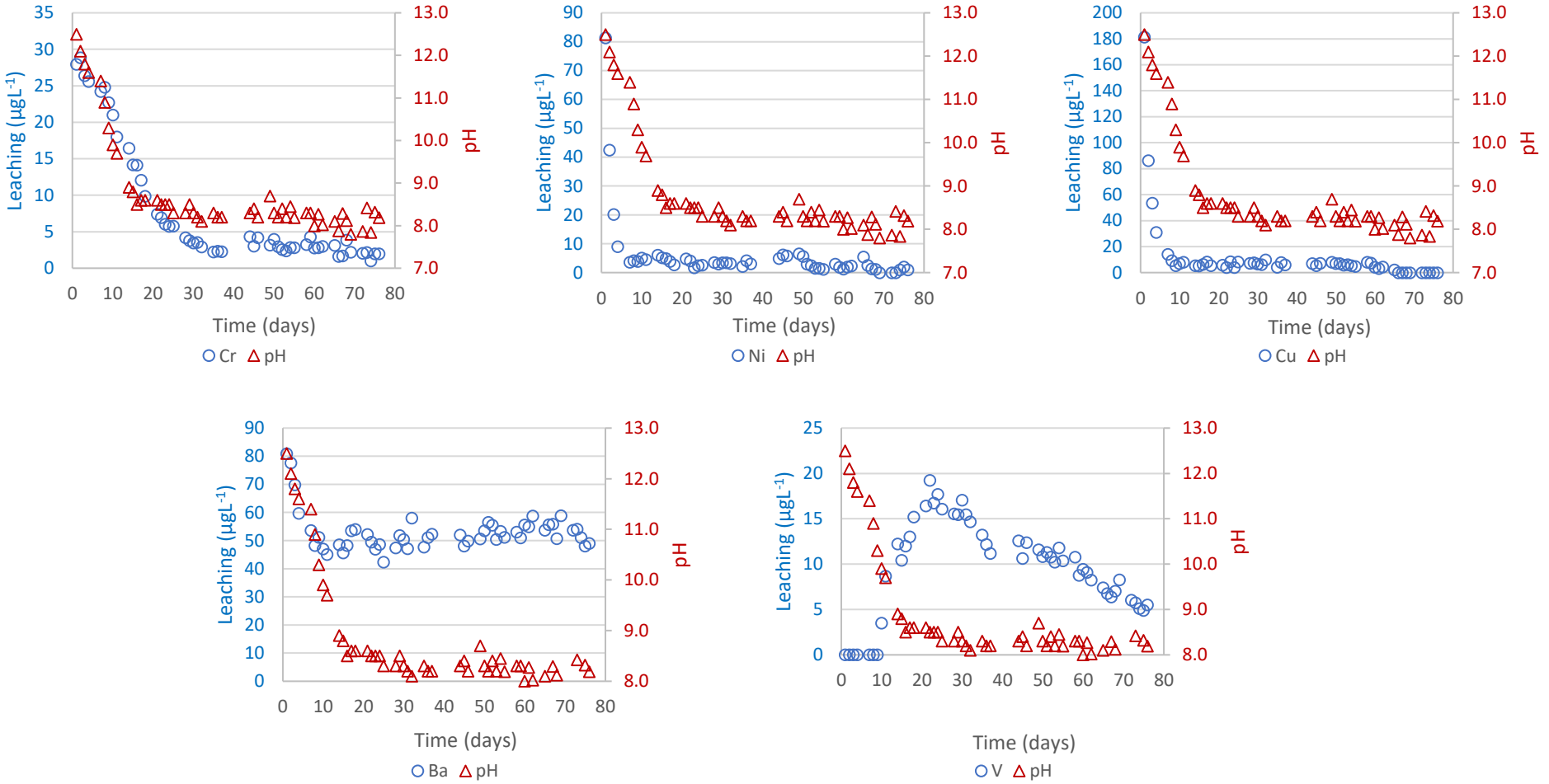

Figure S3.5. pH of the of the washing water alongside leaching of Cr, Ni, Cu, Ba and V for the sample of granules subjected to WC process after thermal treatment at 110°C.

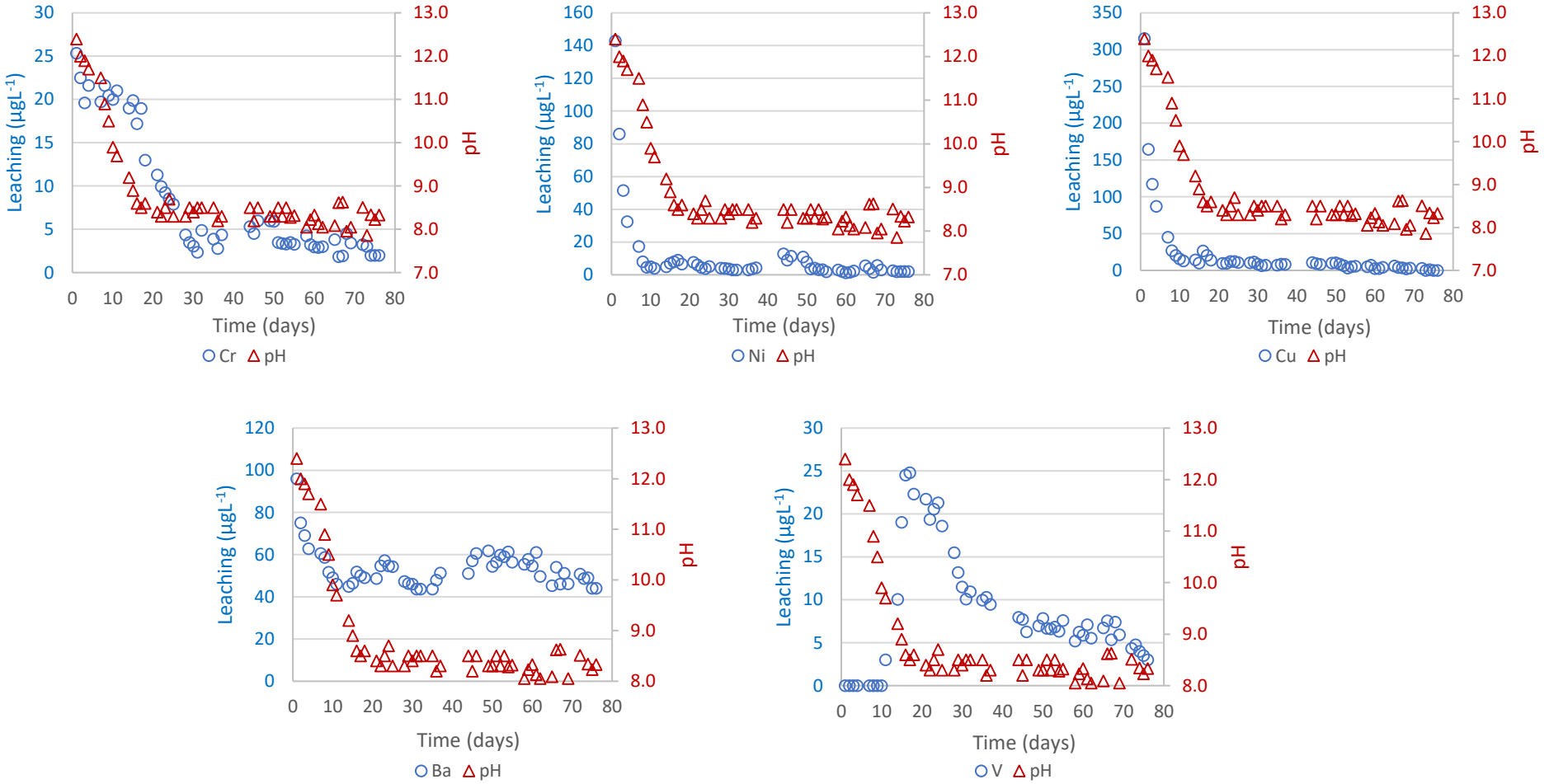

Figure S3.6. pH of the of the washing water alongside leaching of Cr, Ni, Cu, Ba and V for the sample of granules subjected to WC process after thermal treatment at 150°C.

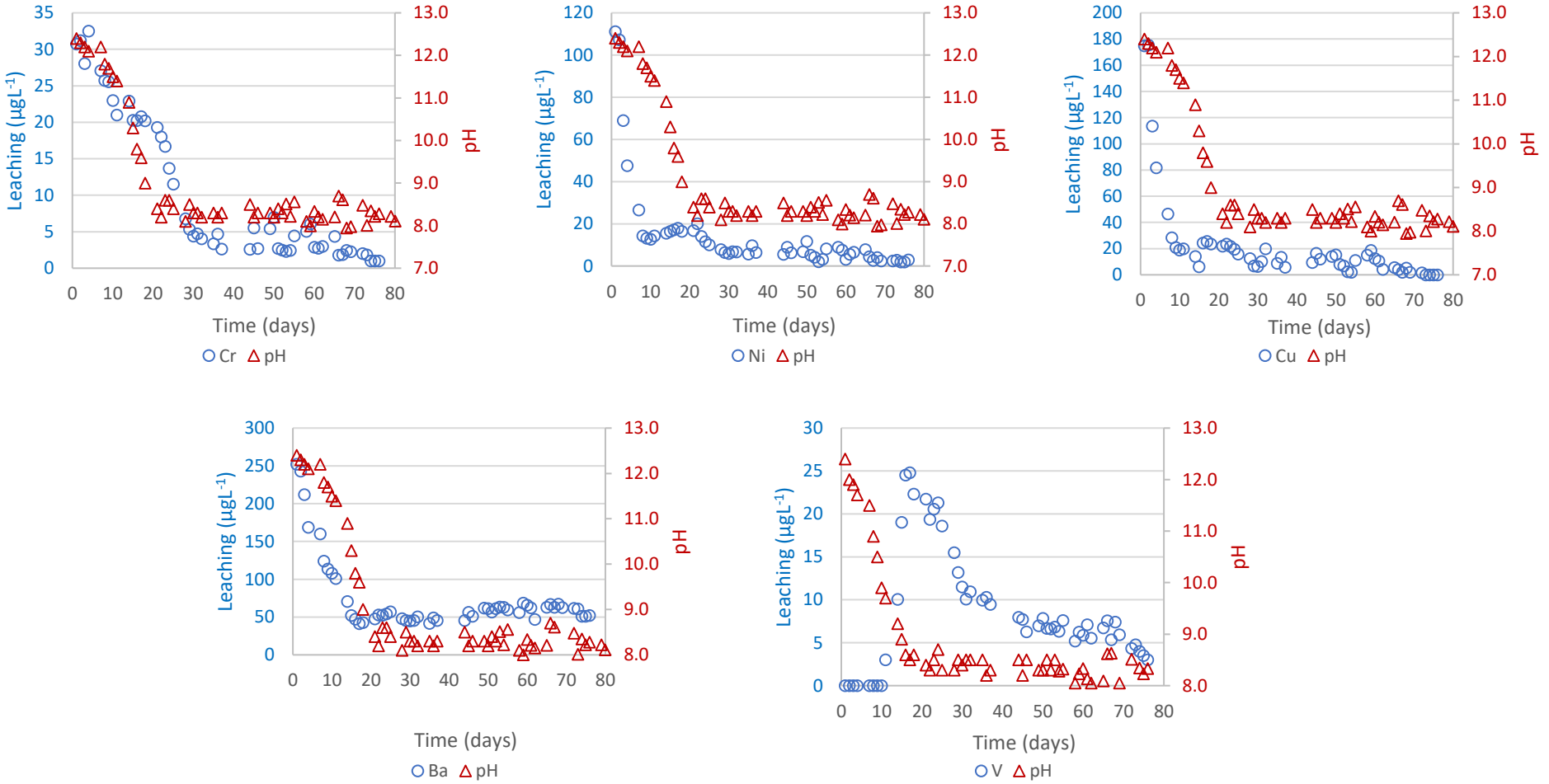

Figure S3.7. pH of the of the washing water alongside leaching of Cr, Ni, Cu, Ba and V for the sample of granules subjected to WC process after thermal treatment at 200°C.

Table S3.6. Heavy metals content of granulate after WC process. Concentrations exceeding the regulatory limits are highlighted.

Parameter	Granulate WC	Granulate WC 90°C	Granulate WC 110°C	Granulate WC 150°C	Granulate WC 200°C	Regulatory Limit*
	$mg \cdot kg^{-1}$ d.w.					
Be	0.81±0.04	0.85±0.04	0.82±0.04	0.84±0.04	0.89±0.04	10
Cd	0.49±0.04	0.48±0.04	0.51±0.04	0.50±0.04	0.51±0.04	15
Hg	**6.35±0.48**	3.52±0.29	2.55±0.25	2.13±0.19	1.21±0.11	**5**
Pb	21.0±1.4	22.7±1.5	22.8±1.5	21.4±1.4	21.6±1.5	1000
V	35.1±4.1	35.2±2.5	35.3±2.9	35.7±2.8	35.8±3.1	250
Cr	67.0±4.1	67.5±3.2	67.6±3.7	66.8±3.3	67.5±2.2	800
Ni	51.3±2.8	52.0±2.8	52.0±2.8	51.8±2.8	51.9±2.8	500
Cu	63.3±2.4	63.9±3.0	64.7±3.3	63.2±3.6	62.8±2.3	600
Zn	72.1±4.0	72.7±4.8	73.1±4.3	73.5±5.2	72.6±4.4	1500
Ba	265±9	277±6	278±5	278±8	275±5	-
Co	7.31±0.59	7.25±0.59	7.43±0.60	7.51±0.61	7.50±0.61	250
As	8.40±0.67	8.50±0.38	8.61±0.42	8.65±0.49	8.43±0.50	50
Se	< 0.5	< 0.5	< 0.5	< 0.5	< 0.5	15
Sn	0.75±0.08	0.81±0.17	0.73±0.13	0.68±0.12	0.75±0.11	350
Sb	2.32±0.12	2.39±0.12	2.26±0.12	2.36±0.12	2.33±0.12	30
Tl	0.55±0.14	0.48±0.15	0.57±0.14	0.52±0.15	0.53±0.13	10

*Regulatory limit: Column B (commercial and industrial use) of Table 1 of Annex V to Part IV of Title V of Legislative Decree No 152 of 03/04/2006 [101].

Table S3.7. XRD analysis of granulate after wet conditioning treatment (l.o.d.: limit of detection).

	Granulate WC	Granulate WC 90°C	Granulate WC 110°C	Granulate WC 150°C	Granulate WC 200°C
	% w.t.				
Calcite	37.9±1.3	38.5±2.0	40.2±1.5	42.6±1.4	44.4±1.2
Clinochlore	2.1±0.4	2.5±0.6	2.5±0.6	2.8±0.7	3.0±0.8
Dolomite	2.0±0.9	3.2±1.0	2.4±0.5	2.5±0.3	2.6±0.3
Quartz	6.3±1.1	6.98±1.2	7.4±1.3	7.1±0.5	7.6±0.5
Muscovite	2.3±0.4	3.8±0.4	3.1±0.4	3.3±0.2	3.3±0.2
Lizardite	0.6±0.2	0.8±0.2	0.7±0.3	0.5±0.1	0.6±0.1
Albite	2.0±0.6	2.5±0.6	2.6±0.8	2.6±0.3	2.6±0.3
Orthoclase	0.7±0.2	0.9±0.2	1.0±0.3	0.9±0.6	1.8±0.7
C_2S	1.6±0.2	1.7±0.4	1.8±0.3	2.0±0.3	1.7±0.2
C_3S	0.8±0.2	0.9±0.2	0.8±0.3	0.9±0.3	0.7±0.2
C_3A_{Cub}	< l.o.d.	< l.o.d.	< l.o.d.	< l.o.d.	0.2
C_3A_{Ort}	< l.o.d.	< l.o.d.	< l.o.d.	< l.o.d.	< l.o.d.
C_4AF	0.4±0.1	0.4±0.1	0.4±0.1	0.4±0.1	0.5±0.1
Ettringite	4.6±0.9	0.6±0.1	1.5±0.3	1.8±0.2	2.2±0.2
Portlandite	0.1±0.05	< l.o.d.	< l.o.d.	< l.o.d.	< l.o.d.
Amorphous	38.6±1.0	37.9±1.3	35.4±1.6	31.5±1.6	28.7±1.4

Table S3.8. UNI EN 1097-2 test for resistance to fragmentation on pellets subjected to TT at 110°C before and after WC.

Parameter	Before WC	After WC
Resistance to fragmentation (Los Angeles) (%)	38.8 ± 1.3	30.6 ± 1.1

Table S3.9. Fraction of granulate with particle diameter < 63 μm produced during UNI 12457/2 leaching test.

	Granulate	Granulate after TT at 150°C	Granulate WC 150°C	Granulate WC
Fraction of granulate with particle diameter < 63 μm (%)	16.8 ± 0.9	22.3 ± 1.1	10.8 ± 0.5	11.5 ± 0.6

4. Chapter 4

Stabilization of lead contaminated soil with traditional and alternative binders

Silvia Contessi[1], Loris Calgaro[2], Maria Chiara Dalconi[1], Alessandro Bonetto[2], Maurizio Pietro Bellotto[3], Giorgio Ferrari[4], Antonio Marcomini[2] and Gilberto Artioli[1]

[1]Department of Geosciences, University of Padua, Via Gradenigo 6, 35131 Padua, Italy
[2]Department of Environmental Sciences, Informatics and Statistics, University Ca' Foscari of Venice, Via Torino 155, 30172 Venice Mestre, Italy.
[3]Department of Chemistry, Materials and Chemical Engineering, Polytechnic of Milan, piazza Leonardo da Vinci 32, 20133, Milan, Italy
[4]Mapei s.p.a., via Cafiero 22, 20158 Milan, Italy

As reported in chapter 1.3.3., among the several technologies developed for the treatment of materials contaminated by heavy metals, solidification/stabilization processes based on OPC showed good performances, but despite the well-understood chemistry of this binder as a building material, the mechanisms that control the immobilization of heavy metals in these systems are not well elucidated. In addition, the use of this binder poses several environmental issues, like high CO_2 emissions and consumption of virgin resources (e.g. limestone, clay, sand).

According to theory, S/S with cement results in the precipitation or coprecipitation of metal ions as hydroxides or in their uptake by cement hydration products, e.g., in calcium silicate hydrate, or ettringite and/or monosulfate-type phases [247–249]. However, experimental attempts to prove this theory do not provide comprehensive ex-post direct evidence of such immobilization mechanisms but, in most cases, refer to ex-ante synthesis and characterization of prepared materials [206,249–254]. The occasional formation of new mineralogical phases containing toxic metallic cations or oxyanions has been reported [250,255–258], but the role of these phases in the retention of toxic elements is not always evident and clear. Many studies have been published regarding the hydration of metal-doped OPC or single cement phases [212,258–261], but although highly informative in assessing the effect of different hazardous elements on hydration reactions and leaching properties, these studies are hardly representative of real contamination conditions.

In this context, this chapter reports the paper "Stabilization of lead contaminated soil with traditional and alternative binders", in which the performance of CAC and an alkali activated metakaolin binder for the treatment of a Pb contaminated soil was evaluated *vs* ordinary Portland cement. In particular, the phase composition of the stabilized products was investigated by XRD and correlated to the internal microstructure obtained by SEM-EDX imaging. Leaching tests were performed to ascertain the effectiveness of the proposed binders in the S/S of the contaminated soil, and Pb release was evaluated for each binding system.

4.1. Experimental

4.1.1. Contaminated site, soil sampling and preparation of stabilized granular materials

One cubic meter of soil was excavated from a brownfield located in an abandoned production and storage site located in Bagnolo Mella (BS, Italy). This industrial site devoted to fertilizer production, operational between 1898 and 1985, included a sulfuric acid production plant by means of pyrite (FeS_2) roasting process. The contaminated soil sample was collected from the surface to 1.5 meters depth, air-dried up to 10% weight/weight (w/w) moisture content and sieved at 2 mm prior to

homogenization, as in the already established HPSS® industrial procedure [222]. The fraction of soil with particles with a diameter higher than 2 mm was about 35%, while the undersieve showed the particle size distribution reported in **Figure S4.1.** The sampled contaminated soil was an unsaturated soil mainly composed of sandy-gravelly material, as determined also by the geological survey prior to the reclamation activities. At the same time, subsamples of different layers of the subsoil were collected with the sampling criterion being variation in color. This allowed us to distinguish an upper layer with bricks and other debris (layer a), an underlying zone composed of a purple layer (layer b), a light-yellow layer with pale brown intercalations (layer c), and a brown-colored layer (layer d) (**Figure S4.2**). A sample of soil was collected in an area that was found not contaminated, according to the regulatory limits imposed by the Italian regulation for the use of soil and sediments for industrial purposes [101], during the initial characterization of the property and used to represent the mineralogical composition of the soil prior to contamination. The sample was collected at a depth between 15 and 35 cm, air-dried, sieved at 2 mm and characterized.

Afterwards, the HPSS® technology was applied to the homogenized sample of contaminated soil as described in chapter 2.2, and the obtained granulated materials were characterized. The mineralogical compositions of the binders used are reported in **Table S4.1**.

The formulations used are reported in **Table 4.1 and Table 4.2.**

Table 4.1. HPSS® formulation used for granular materials preparation with OPC and CAC as binders

Component	% w.t.
Contaminated soil	72.2
Cement	26.7
Mapeplast ECO-1A	0.53
Mapeplast ECO-1B	0.53
Water/Cement ratio	0.4-0.6

Table 4.2. HPSS® formulation used for granular material preparation with MK as binder.

Component	% w.t.
Contaminated sediment	73
Metakaolin	27
Mapeplast ECO-1A	0
Mapeplast ECO-1B	0
NaOH solution/Cement ratio	0.9

The dosages of each granulation resulted in 3.650 kg d.w. of soil, 1.350 kg of binder and 27.0 g of each additive. About 5% of the activator used (tap water or 4 M NaOH solution) was added during mixing to prevent the formation of dust aerosol, while the remaining amount was added during the pelletization stage. The pellets were cured in sealed plastic bags at ambient temperature for 28 days, then sieved following the UNI EN 933-1 standard [262]. For this study, only the fraction of pellets

with diameters between 2 and 10 mm was considered. This range of particle sizes is normally produced during industrial scale applications of the HPSS® process, while pellets outside this range are reprocessed after milling. The leaching of heavy metals from the contaminated soil and the stabilized granular materials was studied by applying the UNI 12457-4:2004 standard for all samples, while the UNI 14429:2015 leaching test was carried out only on the contaminated soil and on OPC pellets since it is time consuming and costly.

4.2. Results and discussion

After a detailed chemical and mineralogical characterization, the contaminated soil was pelletized with the selected binders (i.e. OPC, CAC and MK) to obtain stabilized granular materials. The mineralogical composition, microstructure and leaching behavior of these products were investigated. Since Pb is the only heavy metal present in the contaminated soil at high enough concentration to be identified by XRD and SEM-EDX mapping, only its leaching was considered in this work. The results are detailed below.

4.2.1. Soil characterization

The mineralogical composition of the homogenized sample of contaminated soil is reported in **Figure 4.1** and **Table S4.2,** together with the mineralogy of the uncontaminated soil sample collected outside the contaminated area. The results of XRF analysis performed on the contaminated soil are reported in **Table S4.3**. The heavy metal content of the polluted soil is presented in **Table S4.4**, showing a very high concentration of Pb (40430±3210 mg·kg^{-1}), together with minor amounts of As (383±24 mg·kg^{-1}) and Se (362±28 mg·kg^{-1}).

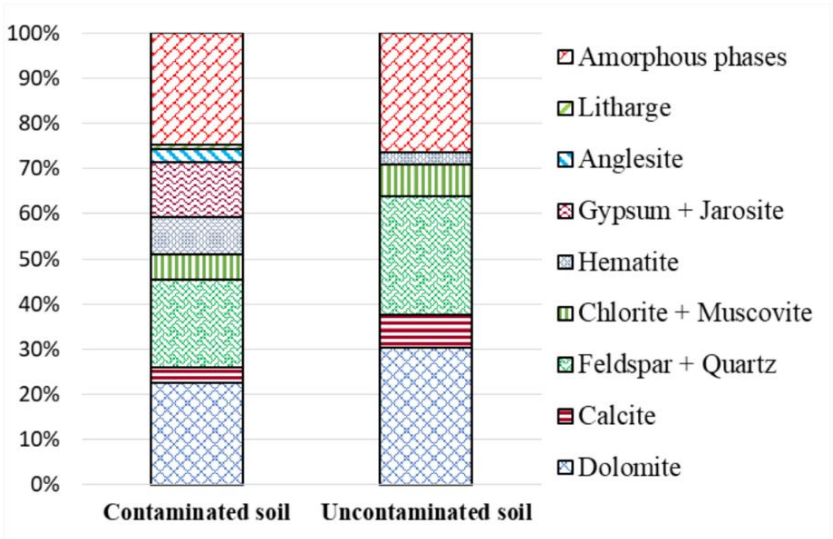

Figure 4.1. Mineralogical composition of contaminated and uncontaminated soil obtained by XRD quantitative analysis.

Soil mineralogy was a combination of primary components (i.e., the aluminosilicate, silicate and carbonate minerals initially present in the soil) and secondary phases that were produced by the industrial activities and weathering processes in the area, namely hematite (Fe_2O_3), gypsum ($CaSO_4 \cdot 2(H_2O)$), anglesite ($PbSO_4$) and jarosite ($KFe^{3+}{}_3(SO_4)_2(OH)_6$). Since the amorphous fraction of soil accounted for one fourth of the composition, an attempt to characterize such phase was made. The comparison between the chemical composition of the crystalline fraction of soil calculated by XRD quantitative analysis and the bulk chemical composition of soil obtained with XRF analysis yielded information about the nature of the amorphous fraction of the soil. These results, reported in **Table S4.5**, indicated a chemical composition resembling iron oxides and aluminosilicate minerals. SEM/EDX images of the contaminated soil are displayed in **Figure 4.2**.

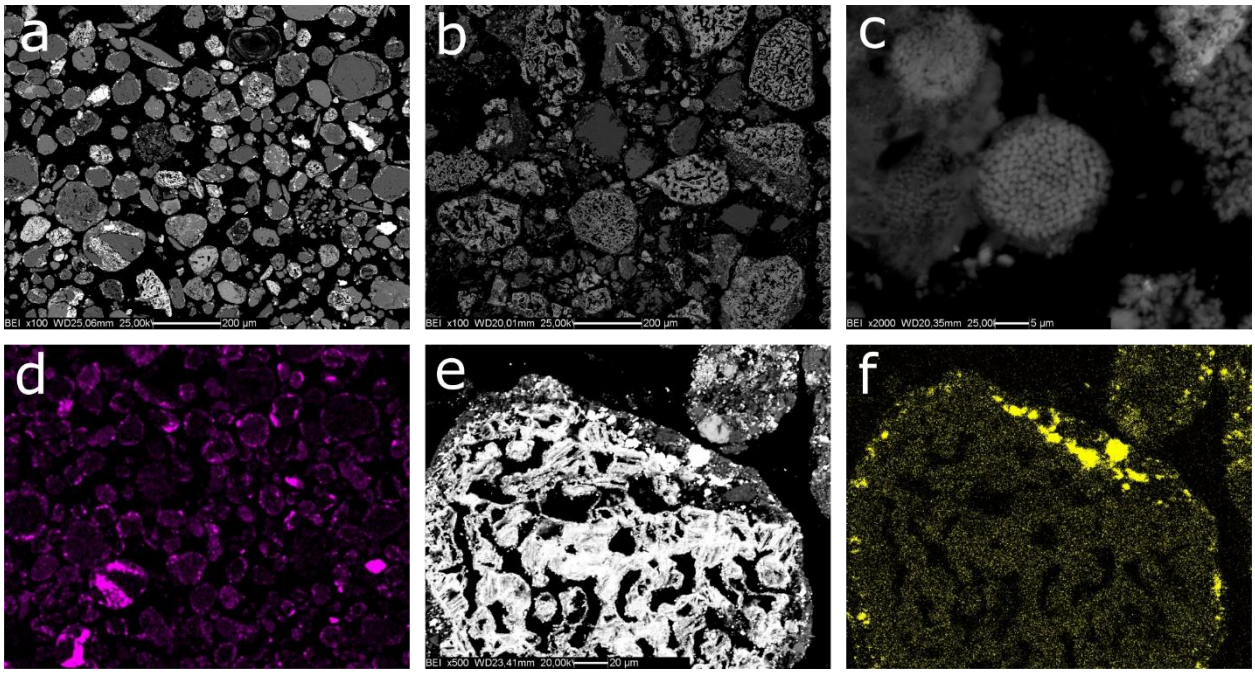

Figure 4.2. SEM micrographs of the contaminated soil. (a) Back-scattered electron image of the bulk soil; (b) back-scattered electron image of the material sampled from the purple layer, showing a large amount of iron oxides; (c) back-scattered electron image of framboidal pyrite found in the light yellow layer; (d) map of the Pb distribution relative to image (a); (e) iron oxide particle; and (f) Pb mapping showing the metal adsorption on the particle in image (e).

A detailed analysis of the sample from the purple layer (layer b) revealed a large number of Fe phases, possibly hematite, jarosite and amorphous iron oxides, the latter being residues of the pyrite roasting process (**Figure 4.2b**). Sulfate-containing phases were also detected and were identified as gypsum and natrojarosite ($NaFe^{3+}{}_3(SO_4)_2(OH)_6$) on the basis of the information derived from XRD data. The underlying light-yellow layer (layer c) was mainly composed of gypsum, jarosite and natrojarosite. In this layer, SEM images showed the presence of some framboidal pyrite particles

(**Figure 4.2c**) that have not yet been oxidized. The lower investigated layer (layer d) contained many aluminosilicate minerals as well as carbonates and silicon oxide and seemed to be mostly untouched by contamination. XRD quantitative analyses of layers b, c and d are reported in **Table S4.5**.

4.2.2. Reconstruction of the contamination scenario

In the investigated area, pyrite was present as a raw material for sulfuric acid manufacturing. It is well-known that the oxidation of sulfide minerals can lead to acid sulfate water production [263]. The resulting acidity can be considered the main reason for the mobilization of heavy metals in the studied soil, similarly to what is observed during acid mine drainage [264]. These conditions led to the precipitation of minerals in the soil that are typically found in acid sulfate soils, such as sulfates and hydroxysulfates. Jarosite is one of these phases and it was abundant in the light-yellow layer of the contaminated soil. Jarosite forms in a pH range of 1-3 [265]. Other phases having similar behaviors are gypsum and anglesite, which together accounted for more than 13% of the bulk soil mineralogy. The pH of the contaminated sample (7.5) showed how the high amount of carbonate minerals (26% of soil mineralogy) contributed to neutralization of soil acidity. The remarkable concentration of Pb found in the contaminated soil can be related to the use of lead-lined ovens and Pb-rich raw materials for sulfuric acid manufacturing. Lead is highly enriched in pyrite ores (ranging from 813 to 11377 $mg \cdot kg^{-1}$ with an average of 4030 $mg \cdot kg^{-1}$) compared to lead abundance in Earth's crust, that is limited to 10 $mg \cdot kg^{-1}$ [266]. Additionally, galena (PbS) has been reported as a Pb host in pyrite ores [267]. Due to pyrite oxidation, it is likely that the acid Fe^{III}-rich solution promoted the dissolution of galena, as reported in the following reaction:

$$PbS + 2Fe^{3+} + 3SO_4^{2-} + \frac{3}{2}O_2 + H_2O \rightarrow PbSO_4 + 2Fe^{2+} + 2H^+ + 3SO_4^{2-} \qquad (Eq.\,3.1)$$

leading to formation of anglesite, which is very weakly soluble in acidic conditions [268]. In addition to anglesite, Pb was also found adsorbed onto the amorphous iron oxide particles (**Figures 4.2e**, **f**).

4.2.3. Pelletization with OPC

XRD analysis of OPC-pellets after 28 days of curing (**Figure 4.3a** and **Table S4.7**) showed the presence of soil phases and cement phases, both hydrated and unhydrated. The comparison of XRD patterns of contaminated soil and OPC-pellets (**Figure S4.3**) showed that Pb-containing minerals (i.e., anglesite) were completely dissolved by the high pH values reached after mixing with cement. Measure of pH of the eluate at the end of the UNI 12457-4 leaching test indicated a value of 12.3. No newly formed crystalline phases containing Pb were detected by XRD analysis in the OPC-pellets. Also gypsum, initially detected in the soil, was consumed leading to the formation of ettringite

($Ca_6Al_2(SO_4)_3(OH)_{12}\cdot 26(H_2O)$), one of the first products that forms during cement hydration [269]. While ettringite normally forms in purely cementitious systems because of the reaction between calcium aluminates and sulfates in the presence of water, in this hybrid system composed of soil and cement, ettringite may also precipitate from the dissolved sulfate ions derived from the dissolution of gypsum and anglesite, which were present in the contaminated soil. Even if not directly detectable by the presence of diffracted Bragg peaks (because of their amorphous structures), calcium silicate hydrates (C-S-H phase) were present in OPC-pellets based on quantitative analysis with internal standard and quantified as ca. 20% of the bulk pellet. This percentage was calculated by subtracting the amorphous counterpart present in soil from the entire amorphous fraction in the OPC-pellet. The C-S-H phase in OPC is formed by reaction of tricalcium silicates (Ca_3SiO_5, abbreviated C_3S) with water through a dissolution process liberating calcium and silicate ions in solution followed by the precipitation of the C-S-H phase on C_3S surfaces [204].

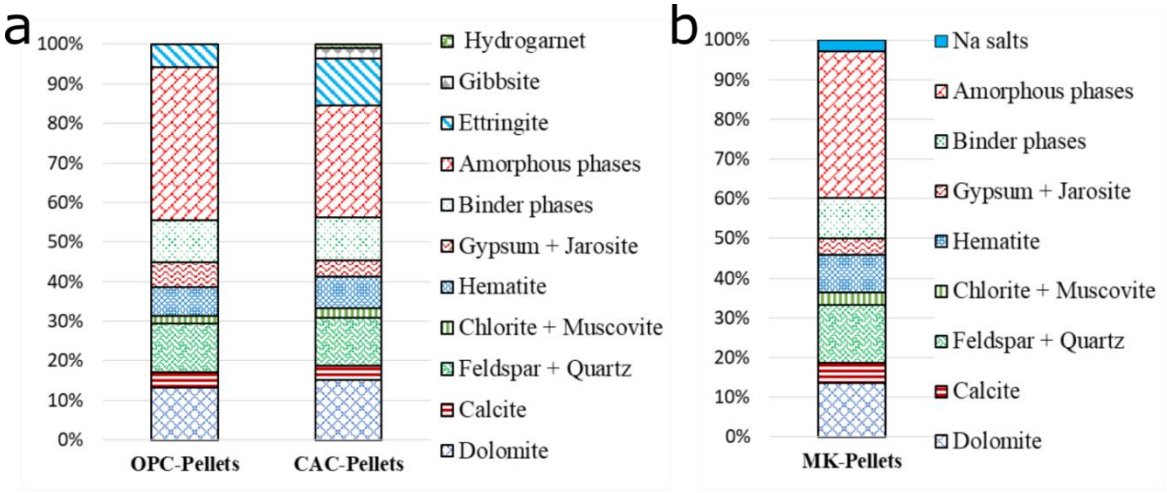

Figure 4.3. Mineralogical compositions of OPC-pellets (a), CAC-pellets (a) and MK-pellets (b) expressed as weight percent (w.t.%) for every phase. Binder phases encompass unreacted clinker phases. Amorphous phases in OPC and CAC-pellets are constituted both by the amorphous fraction of soil and the newly formed amorphous hydration products. Amorphous phases in MK-pellets are the sum of the amorphous fraction of soil, the amorphous metakaolin and the newly formed geopolymeric products.

Portlandite ($Ca(OH)_2$ or CH according to cement chemistry notation), which normally forms after C_3S hydration, was not detected in the OPC-pellets. It is likely that the pore solution did not reach the level of Ca^{2+} saturation required for CH precipitation as a consequence of pozzolanic reactions between Ca^{2+} and siliceous counterparts derived by the dissolution of amorphous silica, leading to. additional C-S-H precipitation. Amorphous silica, which was likely included in the amorphous fraction of soil, is known to increase its dissolution kinetics at a pH above 9 [270]. The considerable amount of unhydrated cement (37% of the total added cement) indicates a limited hydration degree of cement paste. Normally after 28 days of curing, the percentage of unhydrated

OPC is approximately 5-15% [206]. Despite this, the amount of C-S-H phase found was relatively high, supporting the hypothesis of pozzolanic reactions producing additional C-S-H. The drastic deceleration of clinker hydration was particularly true for the C_3A and C_2S phases, whose amounts were almost the same as the pre-hydration scenario. While C_2S is known to have slow hydration kinetics, C_3A is rapidly reactive with water [204]. The simultaneous presence of C_3A and ettringite - the latter normally forming upon C_3A dissolution - suggests that other aluminum suppliers were dissolving, yielding aluminate ions for ettringite formation. It is suggested that clay minerals with particle sizes < 0.2 μm were likely included in this amorphous counterpart of soil, and that their dissolution in the alkaline pH induced by cement could have supplied aluminate ions. The internal microstructure of OPC-pellets, investigated through SEM analysis, was composed of soil minerals embedded within an amorphous matrix of cement hydration products (**Figure 4.4a, b**). EDX analysis performed on different points of the cementitious matrix revealed the presence of Pb together with elements that are typical of cement phases (i.e., Ca, Si, Al and Mg).

Elemental mapping showed that Pb was well dispersed within the matrix and was particularly concentrated on the surfaces of unhydrated cement particles (**Figure 4.4c**, **d**). This Pb-rich layer on cement grains was also visible in back-scattered electron images as a white halo on light gray particles (**Figure 4.4e**, **f**). Since the Kα emission line of S (2.30 eV) almost coincides with the Mα line of Pb (2.34 eV), the actual presence of Pb was determined thanks to its Lα line (10.5 eV). Experiments conducted by Ahn and coworkers [271], who hydrated cement in the presence of $Pb(NO_3)_2$, showed the rapid formation of a gelatinous coating of lead nitrates and sulfates around cement particles, which had a protective effect that inhibited hydration. In our system after the dissolution of anglesite due to the high pH, Pb^{2+} ions may have formed such a coating on clinker particles, preventing and slowing the hydration reactions. The low hydration degree could also be related to the scarce availability of water for cement particles due to the presence of soil, which may have adsorbed part of the water otherwise available for cement hydration.

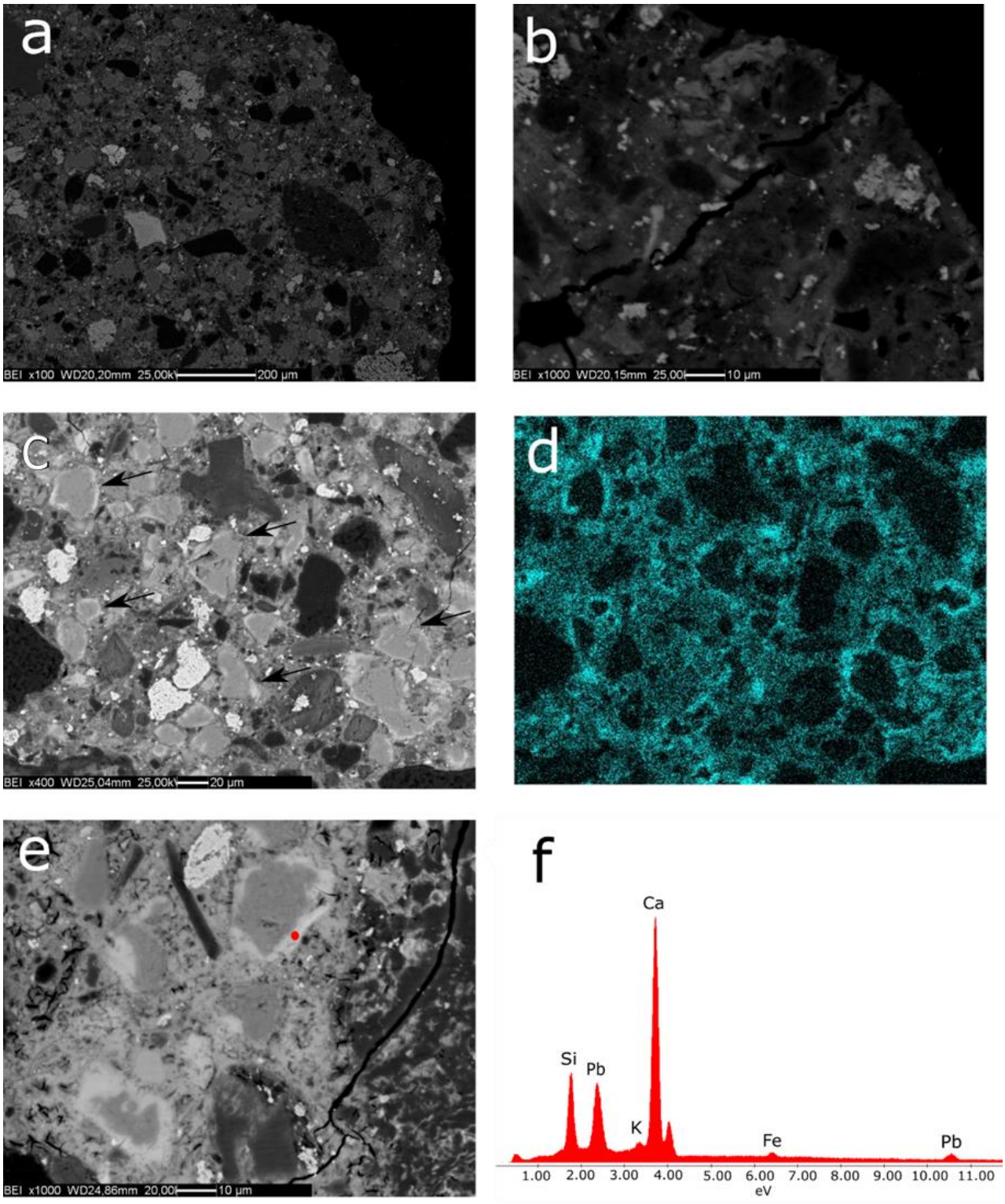

Figure 4.4. SEM micrographs of polished sections of OPC-pellets. (a) Internal microstructure with soil particles embedded within the amorphous matrix given by cement; (b) soil particles dissolving in the alkaline medium; (c) internal microstructure showing unhydrated clinker particles (arrows); (d) map of Pb relative to image c obtained by choosing only the Pb signal at 10.5 eV to exclude S interferences; (e) high magnification image showing cement particles surrounded by a Pb-rich white halo; and (f) EDX spectrum correspondent to the red point in image (e).

The 24-hour leaching test in ultrapure water (UNI 12457-4:2004) resulted in a Pb concentration in the eluate of 2040±90 $\mu g \cdot L^{-1}$, indicating retention of about 99.93% of the total Pb, with pH of 12.3. The results of the UNI 14429 leaching test performed at various pH values, ranging from 2.0 to 12.7, are reported in **Figure 4.5** and **Table S4.8** for both the untreated soil and the OPC-pellets.

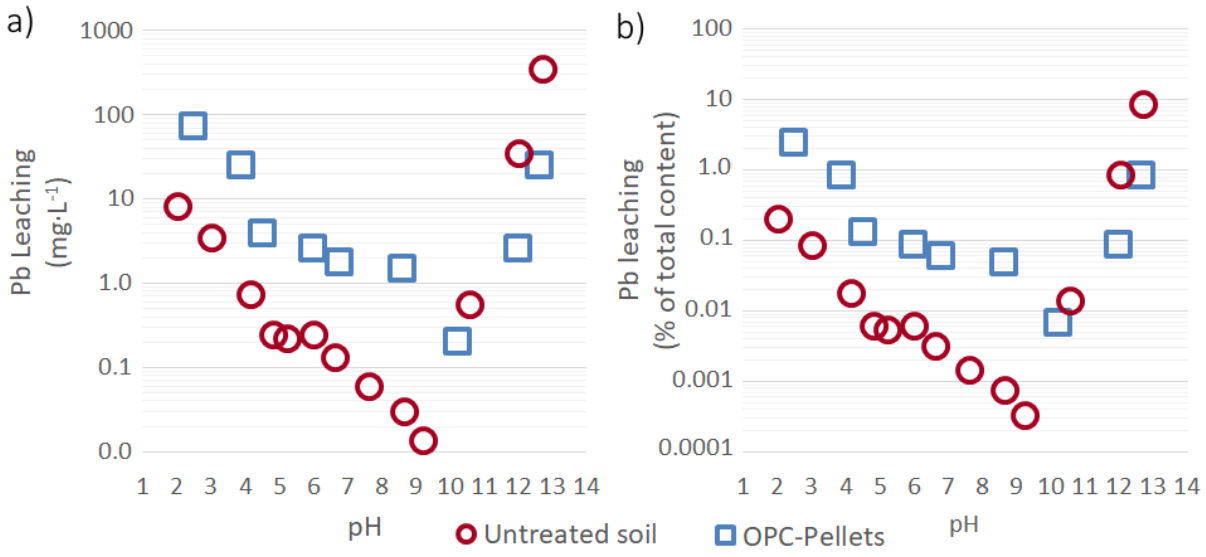

Figure 4.5. Pb leaching as a function of pH – comparison of untreated soil and OPC-pellets. The release is expressed as $mg \cdot L^{-1}$ of Pb in the eluate (a) and as percentage of leached Pb with respect to total amount in the starting material (b).

Pb behavior was highly pH-dependent, as expected based on its amphoteric nature, exhibiting lower mobilization at circum-neutral pH. In the case of the untreated soil, the minimum for Pb leaching (i.e., 0.01 $mg \cdot L^{-1}$) was reached at a pH of ca. 9, while between pH 7.0 and 4.5 Pb release was stable approximately at 0.2 $mg \cdot L^{-1}$. A clear increase was found for both pH lower than 4 and higher than 9, where the highest release from the contaminated soil was reached between pH 12 and 13. As observed in **Figure 4.5,** the pelletization with OPC provided a reduction in Pb mobility within the pH range 10-13 by nearly an order of magnitude. Treatment with OPC also shifted the minimum solubility to a pH of 10. In both untreated soil and OPC-pellets, Pb release was enhanced at highly acid and alkaline pH levels. However, the ratio between its mobility in those extreme pH ranges was different in the two systems, as reported in the right-hand part of **Figure 4.5**. While 8.6% of the total Pb was leached from untreated soil at pH 12.7, only 0.9% was released from pellets in the same pH conditions. In an acidic environment, the situation was reversed: the percentage of leached Pb from OPC-pellets was higher with respect to untreated soil (2.5% versus 0.3% of the total Pb content, respectively). These differences indicate the stabilization of Pb within the S/S matrix, with a change

in its geochemical speciation after treatment with OPC. As the stabilized material was maintained within a range of pH that is suitable for C-S-H phase stability (i.e., within 10 and 13), Pb was well-retained by the cementitious matrix, even if the pH was unsuitable for anglesite stability. This is because the metal underwent a change in its physical-chemical form with cement constituents, in which anglesite was no longer stable. When pH dropped below 4, the greater sensitivity of the C-S-H phase to acidic conditions with respect to anglesite led to a greater leaching of Pb. These leaching tests can also be considered as a qualitative estimate of long-term leaching behavior of both materials. In fact various contaminated materials stabilized with OPC have been reported to shift towards less alkaline pH due to carbonation [272,273], and soils subjected to acid mine drainage phenomena have been found to reach pH values lower than 3 [274]. The results reported in **Figure 4.5** indicate that OPC-pellets have higher long-term environmental compatibility than untreated soil. In particular, if they are used in a non-acidic environment such as in concreate preparation or as filling material in environmental rehabilitation operations, their Pb leaching decreases with the gradual lowering of pH, while the release of Pb from the untreated soil continues with progressing acidification due to acid mine drainage phenomena [275,276].

4.2.4. Pelletization with CAC

XRD analysis of CAC-pellets is reported in **Figure 4.3a** and **Table S4.7**. The amount of ettringite was doubled in comparison to that detected in the OPC-pellets. Ettringite does not usually form from the hydration of pure CAC because of the absence of sulfates. In CAC-soil system, calcium and aluminate ions derived from the dissolution of $CaAl_2O_4$ (CA) and $CaAl_4O_7$ (CA_2) reacted with the $(SO4)^{2-}$ ions present in the soil to produce ettringite. CAC promoted ettringite formation with respect to OPC as it supplied more aluminate ions, which were the limiting factor for its formation in the OPC system. Other CAC hydration phases found were gibbsite ($Al(OH)_3$), hydrogarnet ($Ca_3[Al(OH)_6]_2$) and a metastable calcium aluminum hydrate ($CaAl_2[OH]_8[H_2O]_{5.4}$). As expected, the amount of amorphous fraction was lower with respect to OPC-pellets, as the C-S-H phase typically is not a product of CAC hydration. Unhydrated CAC phases (~ 40% of the total cement) were quantified in an amount comparable to that observed in the OPC system, indicating the same degree of hydration's reduction. SEM analysis showed, as in the case of OPC-pellets, that the internal microstructure was composed of soil minerals and clinker particles surrounded by an amorphous matrix (**Figure 4.6a**). The cracks observed throughout the analyzed areas (**Figure 4.6b**) could be attributed to the high vacuum condition reached during the analysis, which promoted the dehydration of ettringite with subsequent shrinkage and cracking of the cement matrix. This phenomenon, which is known in the literature [277], was also ascertained by conducting an additional investigation with

an environmental scanning electron microscope (ESEM) not reported in this paper. EDX analysis also confirmed the existence of ettringite in correspondence to areas with intense cracking.

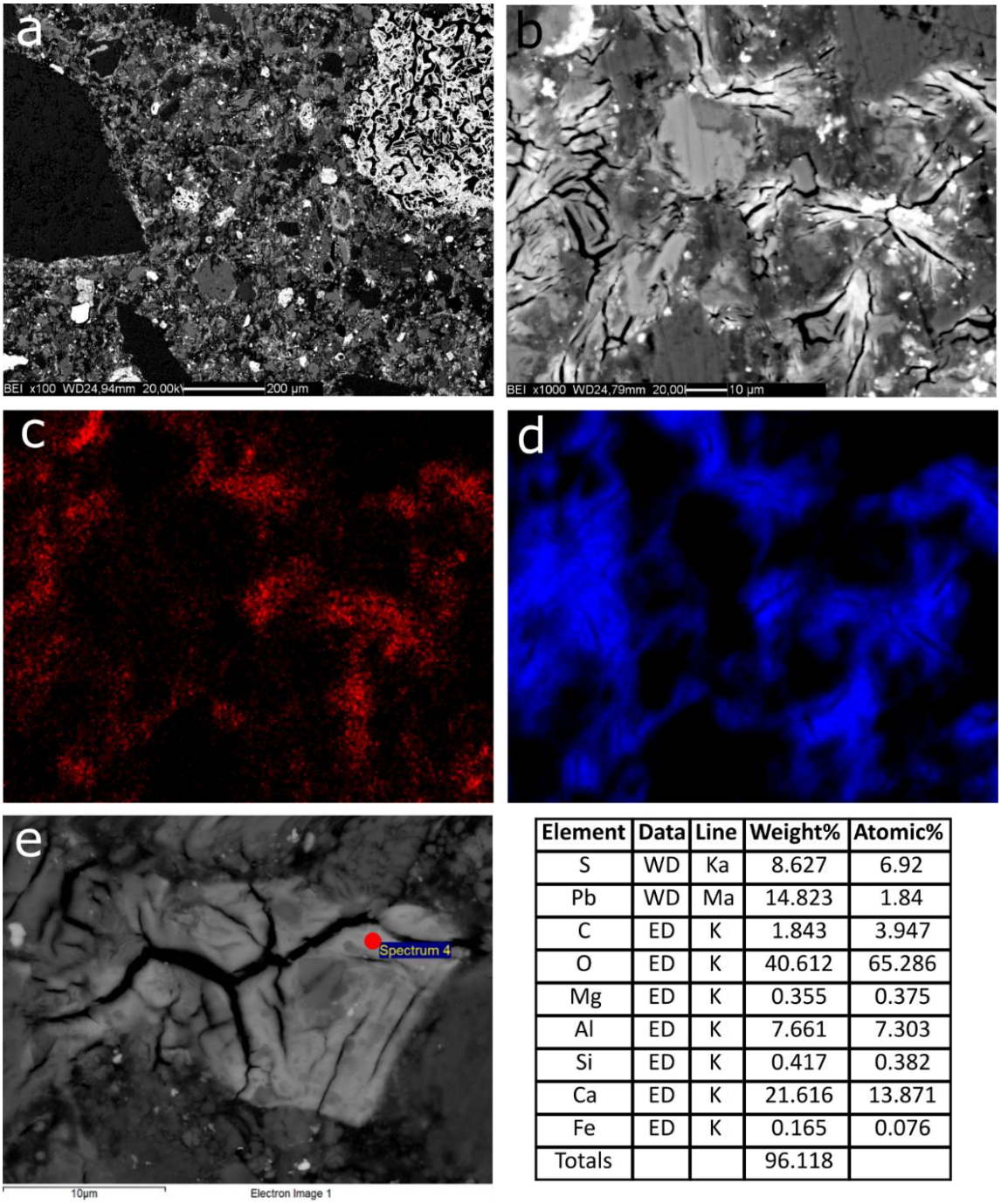

Element	Data	Line	Weight%	Atomic%
S	WD	Ka	8.627	6.92
Pb	WD	Ma	14.823	1.84
C	ED	K	1.843	3.947
O	ED	K	40.612	65.286
Mg	ED	K	0.355	0.375
Al	ED	K	7.661	7.303
Si	ED	K	0.417	0.382
Ca	ED	K	21.616	13.871
Fe	ED	K	0.165	0.076
Totals			96.118	

Figure 4.6. SEM micrographs of polished sections of CAC-pellets. (a) Internal microstructure; (b) Internal microstructure at higher magnification showing the cracks for the dehydration of ettringite in the high vacuum conditions; (c) map of Pb relative to image (b); (d) map of S relative to image (b); (e) FESEM image of ettringite with the chemical composition of the red point reported (WD = wavelength dispersive, ED = energy dispersive).

Elemental mapping of lead and sulfur relatively to **Figure 4.6b** is reported in **Figure 4.6c** and **d**. Pb appeared associated with S in the cracked regions of ettringite. A detailed investigation of the

cracked domains with a FESEM equipped with WDS (**Figure 4.6e**) indicated a chemical composition compatible to ettringite with a certain degree of substitution of Pb^{2+} for Ca^{2+} [247]. Contrary to the OPC-pellets, where Pb formed a coating on clinker particles, in CAC-pellets no Pb-enrichment was observed on CA and CA_2 clinker phases. A delayed hydration in CAC doped with $Pb(NO_3)_2$ was observed in recent studies [202,278], but the mechanisms involved are still not completely understood.

The results of the leaching test in ultrapure water revealed a Pb concentration of 73.2 ± 9.4 $\mu g \cdot L^{-1}$, meaning an almost complete retention of Pb, consistently with results reported in the literature [200,202,279,280]. The pH of CAC-pellets was slightly lower compared to OPC-pellets (12.0 vs 12.3, respectively, as measured after the 24-hour leaching test) indicating a more favorable condition for Pb immobilization. However, the small difference in pH values hardly explains the significant lowering of Pb leaching after treatment with CAC. We hypothesized that the increased and rapid precipitation of ettringite has promoted the sequestration of Pb ions from the pore solution in the early phases of hydration. XRD analysis, coupled with the results of the leaching test clearly attest that ettringite represents the low-solubility species that trapped Pb, as confirmed by WDS data indicating that Pb is associated with ettringite structural elements. For these reasons, our proposed interpretation involves both physical encapsulation and chemical fixation as mechanisms involved in Pb immobilization after treatment with CAC in the presence of sulfates. Despite various studies reporting the influence of pH, temperature, soluble components and dissolved CO_2 on ettringite stability [281–284], these data are not enough to fully predict ettringite durability in this case study, since substituted ettringite showed different behavior compared to the unsubstituted form [210,211,285,286]. In light of this we are aware that investigations on Pb-substituted ettringite stability are needed.

4.2.5. Pelletization with metakaolin

The treatment of the contaminated soil with NaOH-activated metakaolin produced pellets with the composition reported in **Figure 4.3b** and **Table S4.7**. Given the amorphous nature of both metakaolin and the derived geopolymeric gel, the phase assemblage was difficult to characterize with XRD analysis alone. The only new crystalline phases formed in MK-pellets were thenardite (Na_2SO_4), mirabilite ($Na_2SO_4 \cdot 10H_2O$) and burkeite ($Na_6(CO_3)(SO_4)_2$), which were derived from the interaction between sulfates from the soil and NaOH. These pellets presented an internal microstructure characterized by high porosity and a less-dense structure (**Figure 4.7a**), which caused a very low mechanical resistance. This could be ascribed to both highly hygroscopic salts (thenardite) leading to expansion phenomena [287] and to a limited dissolution of metakaolin due to relatively

low molarity of the activating solution (4 M NaOH). In addition, the lack of readily available silica may have also impeded the formation of a well-developed geopolymeric gel [288].

An in depth investigation of the microstructure revealed the presence of Pb inside some aggregates with dimensions of ca. 100-200 μm (**Figure 4.7b**) that were composed of clusters of soil minerals (grey particles in **Figure 4.7b**) surrounded by an amorphous Pb-rich gel-like phase, white-colored at back-scattered electron detection (**Figure 4.7c)**.

Despite the loosely bound structure, the results of leaching test showed a concentration of Pb in the eluate of 194±10 $\mu g \cdot L^{-1}$, which is similar to the leaching of Pb from the untreated soil at similar pH (**Table S4.8**). This result demonstrates how the eluate pH (10.4, as measured at the end of the 24 hours leaching test) played a fundamental role in the retention of this heavy metal [243,289], despite the high surface area exposed to leaching due to the pellets low mechanical resistance. We hypothesize that an amorphous phase with a high Pb concentration may also have contributed, together with the mild alkaline pH of the eluate, to the low release observed from the MK-pellets. Given the amorphous character of the geopolymeric binder, XRD data were of limited utility in elucidating the mechanism implied in Pb retention. Further work on MK systems is required for a better comprehension of this promising binder in S/S applications.

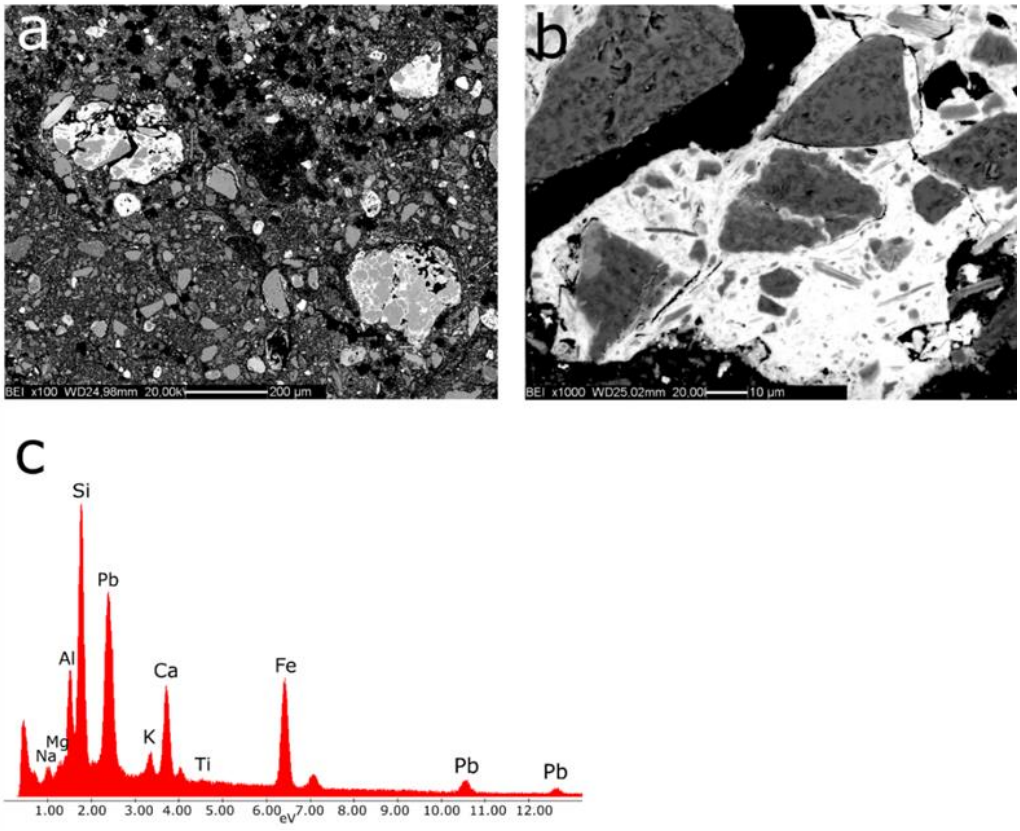

Figure 4.7. SEM micrographs of the polished sections of MK-pellets. (a) Internal microstructure showing high porosity and light gray/white aggregates; (b) aggregate composed of soil phases (gray) embedded in a matrix (white); and (c) elemental composition of the white-colored phase in image (b).

4.3. Conclusions

In this study the use of three different binders (OPC, CAC, MK) for the solidification/stabilization of Pb were investigated, showing how the various hydration products provided different immobilization mechanisms and performances. With OPC the C-S-H formation could host Pb ions likely adsorbed on its surface. The analysis of this system at different pH permitted to indicate an optimal pH for Pb retention, which revealed to be close to 10. The pH of a carbonated cementitious material decreases with respect to the initial pH values, suggesting that the Pb-retention in OPC-pellets can increase in the long term. In the case of CAC binder, the high concentration of sulfates in the soil drastically shifted the reactivity toward ettringite formation, where Pb^{2+} was found replacing part of calcium in the crystalline structure. The lowering of Pb mobilization in CAC system and SEM-WDS analyses indicated that ettringite had a leading role in the retention of this contaminant. NaOH-activated metakaolin was studied for exploring the use of geopolymers in S/S applications, including only one precursor (MK) and one alkaline activator (NaOH solution) to limit the number of variables involved. The high retention of Pb in MK-pellets was partly related to the relatively low pH of the system and we also hypothesize the role of an amorphous phase contributing with chemical fixation. Despite the promising results of the leaching test with regard to Pb, we are aware that future research is needed to overcome the lack of solidification. Additionally, the use of a different alkaline solution for metakaolin activation could be a way to avoid the formation of unwanted Na salts. As far as the other heavy metals present in the contaminated soil, further work is in progress to assess the performance of the discussed binders for their immobilization.

4.4. Acknowledgements

The authors thank Federico Zorzi (University of Padua) for XRF analyses. Andrea Cavallo (Certema) is kindly acknowledged for the FESEM/WDS analyses. The authors are grateful to In.T.Ec. s.r.l. for founding the Ph.D. fellowship of L. C. This work was performed with financial support of the Mapei S.p.A-UniPd research agreement, Intec S.r.l. and Ca' Foscari University of Venice.

4.5. Supplementary Information

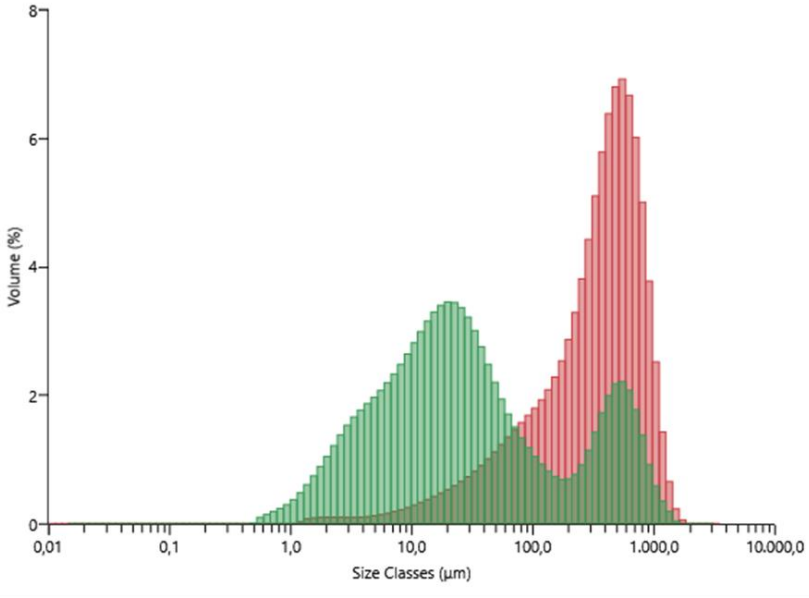

Figure S4.1. Particle size distribution of the contaminated soil after sieving at 2 mm using air (red) and water (green) as dispersants.

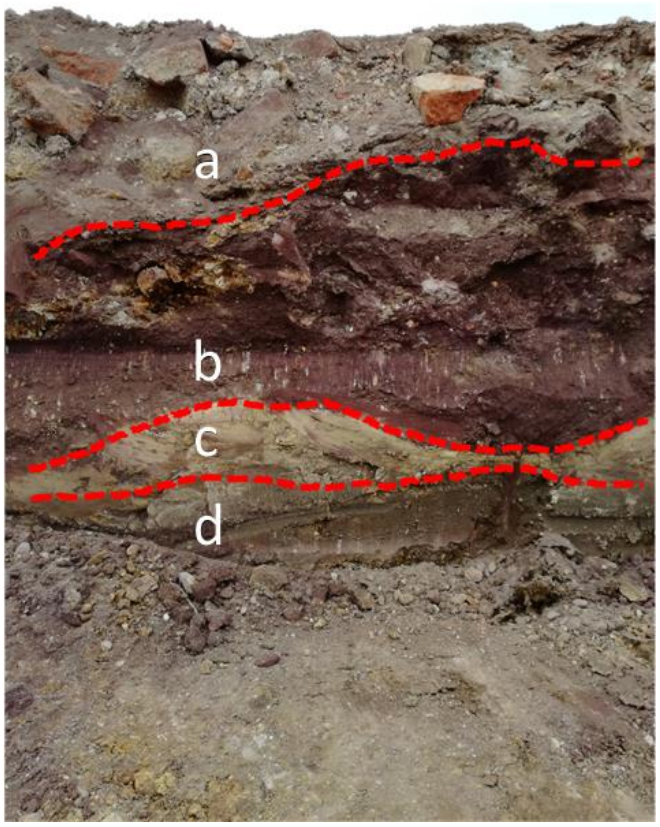

Figure S4.2. Picture of the contaminated soil before excavation, showing the different layers identified by a discrimination based on the color.

Table S4.1. Mineralogical composition of the investigated binding systems, obtained with XRD quantitative analysis with Rietveld refinement, using ZnO internal standard. For OPC and CAC, phases are reported with the abbreviations used in cement chemistry notation. (wt% = weight %)

Ordinary Portland Cement		**Calcium Aluminate Cement**		**Metakaolin**	
	(wt%)		(wt%)		(wt%)
C_3S	52.8±0.5	**CA_2**	37.3±1.2	**Quartz**	9.1±0.5
C_2S	6.4±0.1	**CA**	52.0±2.1	**Anatase**	0.3±0.1
C_3A	10.4±0.1			**Illite**	2.1±0.1
C_4AF	3.7±0.5			**Kaolinite**	7.3±0.2
Gypsum	1.4±0.2				
Anhydrite	1.1±0.4				
Amorphous fraction	24±0.4	**Amorphous fraction**	10.7±0.3	**Amorphous fraction**	81±2.3

Table S4.2. Mineralogical composition of the homogenized sample of contaminated and uncontaminated soil, expressed as weight %. (l.o.d.: limit of detection)

	Bulk contaminated soil (fraction <2 mm)	**Uncontaminated soil (fraction <2 mm)**
	wt.%	wt.%
Dolomite	22.6±1.0	30.1±1.3
Quartz	16.5±0.1	19.7±0.3
Muscovite	4.5±0.1	3.1±0.2
Chlorite	< 1	4±0.5
Calcite	3.5±0.2	7.2±0.3
Feldspar	3.2±0.2	6.4±0.6
Hematite	8.5±0.7	2.6±0.1
Gypsum	10.6±0.2	< l.o.d.
Jarosite	1.7±0.4	< l.o.d.
Anglesite	2.7±0.1	< l.o.d.
Litharge	< 1	< l.o.d.
Amorphous fraction	25.2±1.3	26.2±1.0

Table S4.3. Chemical composition of the homogenized bulk sample of contaminated soil obtained by XRF analysis, expressed as weight % of the oxides.

	Bulk contaminated soil (fraction <2 mm)
	wt.%
SiO_2	32.1
TiO_2	0.4
Al_2O_3	5.6
Fe_2O_3	20.9
MnO	0.1
MgO	6.9
CaO	19.2
Na_2O	0.6
K_2O	1.4
P_2O_5	0.4

Table S4.4. Heavy metals content of the bulk contaminated soil (fraction <2 mm), as obtained by ICP-MS analysis of the digested sample.

Analyte	Bulk contaminated soil (fraction <2 mm)	Regulatory limit*
	$mg \cdot kg^{-1}$	$mg \cdot kg^{-1}$
Al	10170±1030	-
As	383±24	50
Ba	300±16	-
Be	0.85±0.11	10
Cd	2.38±0.22	15
Co	42.3±2.1	250
Cr	45.2±4.1	800
Cu	311±21	600
Fe	144170±15830	-
Hg	8.27±0.47	5
Ni	31.8±1.3	500
Pb	40430±3210	1000
Sb	41.0±3.3	30
Se	362±28	15
Sn	76.3±12.9	350
Tl	1.90±0.22	10
V	47.3±5.0	-
Zn	500±62	1500

*Regulatory limit: Column B (commercial and industrial use) of Table 1 of Annex V to Part IV of Title V of Legislative Decree n°152 of 03/04/2006 [101].

Table S4.5. Comparison between soil chemical composition, as calculated by XRD quantitative analysis, and as obtained by XRF analysis. The difference (Δ) was calculated by using the following equation: $\Delta = wt.\%_{XRD} - wt.\%_{XRF}$.

Oxides	Calculated by XRD quantitative analysis	Obtained by XRF analysis	Δ
	w.t.%	w.t.%	
SiO_2	20.9	32.1	-11.2
Na_2O	0.4	0.6	-0.2
CaO	12.5	19.2	-6.7
Al_2O_3	2.4	5.6	-3.2
K_2O	2.2	1.4	+0.8
Fe_2O_3	9.4	20.9	-11.5
MgO	5.1	6.9	-1.8

Table S4.6. Mineralogical composition of layers b, c and d of the contaminated soil, as shown in the picture of **Figure S4.1**, expressed as weight %.

Layer b (purple)		Layer c (yellow)		Layer d (brown)	
	w.t.%		w.t.%		w.t.%
Quartz	5.5	**Natrojarosite**	25.7	**Feldspar**	6.2
Gypsum	4.3	**Muscovite**	3.7	**Calcite**	< 1
Hematite	72.1	**Feldspar**	3.1	**Chlorite**	8.3
Jarosite	2.6	**Quartz**	16.4	**Dolomite**	26.2
Natrojarosite	7.5	**Gypsum**	20.5	**Gypsum**	< 1
Anglesite	< 1	**Chlorite**	1.4	**Muscovite**	2.7
Plumbojarosite	< 1	**Jarosite**	10.5	**Quartz**	30.2
Amorphous fraction	7.3	**Amorphous fraction**	18.7	**Titanite**	2.7
				Brushite	< 1
				Amorphous fraction	23.0

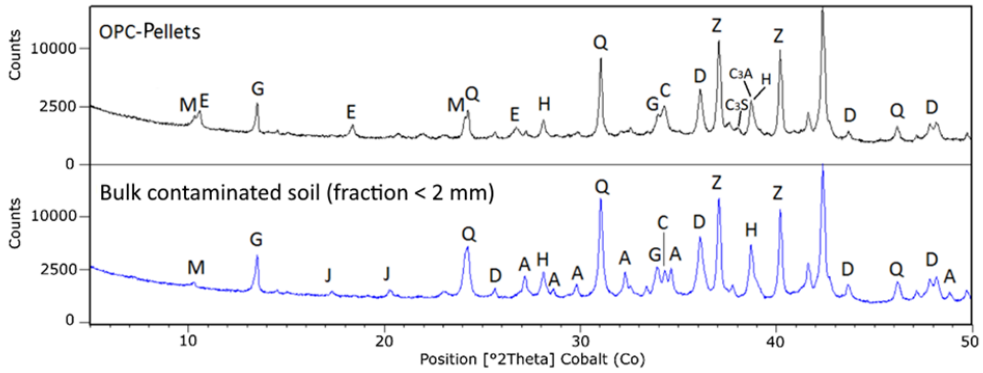

Figure S4.3. XRD spectra of OPC-pellet and untreated soil. M=muscovite, E=ettringite, G=gypsum, J=jarosite, Q=quartz, D=dolomite, H=hematite, A=anglesite, C=calcite, Z=zincite.

Table S4.7. Mineralogical composition of OPC-Pellets, CAC-Pellets, and MK-Pellets expressed as weight %. [a]Amorphous phases are constituted both by the amorphous fraction of soil and the newly formed amorphous hydration products. [b]Amorphous phases are the sum of the amorphous fraction of soil, the amorphous metakaolin and the newly formed geopolymeric products.

OPC-Pellets		**CAC-Pellets**		**MK-Pellets**	
	w.t. %		w.t. %		w.t. %
Soil phases:		***Soil phases:***		***Soil phases:***	
Feldspar	2.7±0.4	**Feldspar**	2.1±0.4	**Feldspar**	1.3±0.5
Calcite	3.7±0.7	**Calcite**	3.6±0.6	**Calcite**	5.1±0.2
Dolomite	13.2±1.9	**Dolomite**	15.2±2.0	**Dolomite**	14.3±0.6
Gypsum	5.3±1.0	**Gypsum**	2.8±0.8	**Gypsum**	3.3±0.1
Hematite	7.2±1.1	**Hematite**	8.1±1.2	**Hematite**	9.7±0.1
Jarosite	< 1	**Jarosite**	1.2±0.4	**Jarosite**	1.0±0.6
Quartz	9.7±0.7	**Quartz**	10.0±0.7	**Quartz**	13.8±0.1
Muscovite	1.7±0.1	**Muscovite**	2.3±0.3	**Muscovite**	1.3±0.5
Clinker phases:		***Clinker phases:***		**Chlorite**	2.2±0.1
C_3A	2.4±0.1	**CA**	5.7±0.2	***Metakaolin phases:***	
C_2S	2.0±0.3	**CA_2**	5.2±0.6	**Kaolinite**	**< 1**
C_3S	5.1±1.4	***Cement hydration products:***		***Hydration products:***	
C_4AF	< 1	**C_3AH_6**	< 1	**Thenardite**	**< 1**
Cement hydration products:		**AH_3**	2.7±0.2	**Mirabilite**	**< 1**
Ettringite	5.9±1.6	**CAH_{10}**	< 1	**Burkeite**	**< 1**
Amorphous phases[a]	38.3±1.5	**Ettringite**	11.8±2.6	**Amorphous phases[b]**	45.2±0.3
		Amorphous phases[a]	28.3±1.0		

Table S4.8. Leaching of Pb from bulk contaminated soil (fraction <2 mm) and OPC-Pellets at various pH, obtained from the UNI 14429 leaching test [230].

Bulk contaminated soil (fraction <2 mm)		**OPC-Pellets**	
pH	$mg \cdot L^{-1}$	pH	$mg \cdot L^{-1}$
12.6	348.9±21.9	12.6	25.9±0.3
12	35.0±2.7	12	2.65±0.03
10.5	0.575±0.050	10.2	0.207±0.008
9.2	0.0136±0.0012	8.6	1.49±0.23
8.6	0.0307±0.0044	6.7	1.81±0.10
7.6	0.0607±0.0013	5.9	2.65±0.13
6.6	0.13±0.01	4.5	4.03±0.05
5.9	0.25±0.02	3.8	25.7±0.3
5.1	0.22±0.01	2.4	73.8±0.6
4.6	0.25±0.02		
4.0	0.75±0.04		
2.9	3.53±0.45		
1.9	8.20±0.24		

5. Chapter 5

Calcium aluminate cement as an alternative to ordinary Portland cement for the remediation of a heavy metals contaminated soil: mechanisms and performance

Loris Calgaro[1], Silvia Contessi[2], Alessandro Bonetto[1], Elena Badetti[1], Giorgio Ferrari[3], Gilberto Artioli[2], Antonio Marcomini[1]

[1]Department of Environmental Sciences, Informatics and Statistics, University Ca' Foscari of Venice, Via Torino 155, 30172 Venice Mestre, Italy

[2] Department of Geosciences, University of Padua, Via Gradenigo 6, 35131 Padua, Italy

[3]Mapei s.p.a., Via Cafiero 22, 20158 Milan, Italy

Thanks to the promising results obtained for the stabilization of Pb with the use of CAC reported in Chapter 3, we decided to study the mineralogy, microstructure and leaching behavior of the granular materials obtained by treating the same contaminated soil from Bagnolo Mella, with different combinations of OPC and CAC. In particular, Chapter 4 reports the draft of the manuscript "Calcium aluminate cement as an alternative to ordinary Portland cement for the remediation of a heavy metals contaminated soil: mechanisms and performance". In this work, leaching and mechanical tests were carried out to evaluate the S/S performance of the proposed binders on the immobilization of other heavy metals of environmental concern (e.g. Ba, As, Be, Cd, Co, Cr, Cu, Hg, Ni, Sb, Se, Sn, Tl, V, and Zn). In addition, to better elucidate the mechanism involved, XRD analysis and SEM/EDX imaging were used to investigate the phase composition and internal microstructure of the pellets obtained.

5.1. Experimental

5.1.1. Contaminated site, soil sampling and preparation of stabilized granular materials

As already shown in chapter 4.2, a sample of contaminated soil was excavated, from the surface to 1.5 meters depth, from a brownfield located in an abandoned production and storage site located in Bagnolo Mella (BS, Italy). Afterwards the sample was air dried up to 10% (w/w) moisture content and sieved at 2 mm. The passing fraction was homogenized and characterized by ICP-MS, XRD and SEM analysis [37].

The HPSS® technology then was applied to the air-dried, sieved and homogenized contaminated soil by applying the procedure reported in chapter 2.2. The formulation of each granulated material is reported in **Table 5.1.**

Table 5.1. Design of the tested formulations. The nomenclature used for the samples' label indicates the percentage of the two cements in the formulation (P = OPC, A =CAC), excluding the soil counterpart (i.e. 90P-10A is the formulation with 90% of OPC and 10% of CAC as binder).

Sample	Soil	OPC	CAC	Mapeplast Eco 1A/1B	Water/Cement ratio
	% (d.w. / d.w.)				
100P	72.2	26.7	0	0.53	0.58
95P-5A	72.2	25.4	1.3	0.53	0.53
90P-10A	72.2	24.0	2.7	0.53	0.53
85P-15A	72.2	22.7	4.0	0.53	0.57
70P-30A	72.2	18.7	8.0	0.53	0.64
60P-40A	72.2	16.0	10.7	0.53	0.62
40P-60A	72.2	10.7	16.0	0.53	0.58
100A	72.2	0	26.7	0.53	0.54

The dosages of each granulation resulted in 3.650 kg d.w. of soil, 1.350 kg of binder and 27.0 g of each additive. About 5% of tap water used was added during mixing to prevent the formation of dust aerosol, while the remaining amount was added during the pelletization stage.
The pellets were cured in sealed plastic bags at ambient temperature for 28 days, then sieved following the UNI EN 933-1 standard [262]. For this study, only the fraction of pellets with diameters between 2 and 10 mm was considered. This range of particle sizes is normally produced during industrial scale applications of the HPSS® process, while pellets outside this range are reprocessed after milling.

5.2. Results and discussion

Due to the recent attention given to the research aimed at individuating sustainable alternatives to the landfill disposal of soils, sediments and wastes polluted by heavy metals, innovative processes permitting the reuse of these materials, such as the HPSS® technology, are of great interest from both environmental and economic point of view. The contaminated soil and the binders were initially characterized by means of XRD, SEM, and ICP-MS analysis to study their mineralogical composition and their total heavy metals' content. Then, XRD, SEM and ICP-MS analysis were performed to investigate the influence of CAC, used instead of OPC, in binder formulations (0, 5, 10, 15, 30, 40, 60, and 100 % d.w./d.w. of CAC in the binder formulation). For each of the granulated material obtained, the leaching behavior, microstructure and mechanical properties were investigated with the aim to better elucidate the mechanisms involved in the retention of heavy metals. Since Pb was the only heavy metal present in the contaminated soil at a high enough concentration to be identified by XRD and SEM-EDX mapping, particular attention was given to its immobilization in the various materials studied. In particular, the mechanical characteristics and leaching behavior of the granules obtained were compared as a function of the Binder's CAC Content (BCC), and the results are reported below.

5.2.1 Characterization of contaminated soil and binders

XRD analysis of the contaminated soil, as reported in chapter 4, (**Table S4.2** and **Figure 4.1**) showed the presence of both natural and anthropogenic mineralogical phases. The main natural minerals found were dolomite and quartz, together with lower amounts of muscovite, albite and calcite, while the anthropogenic minerals identified in the soil were gypsum, hematite, anglesite, jarosite and litharge. Moreover, SEM investigations (**Figure S5.1**) reported the presence of abundant amorphous iron oxides of anthropogenic source as well.

By comparing the contaminated soil heavy metals' content (**Table 5.2**), obtained after microwave assisted total digestion and ICP-MS analysis, with the Italian regulatory limits for soil's commercial and industrial use [101], the elements found exceeding the contamination threshold concentrations were Pb (40430±2000 mg·kg^{-1} d.w.), As (383±24 mg·kg-1 d.w.), Se (362±28 mg·kg^{-1} d.w.), Hg (8.27±0.47 mg·kg^{-1} d.w.), and Sb (41.0±3.3 mg·kg^{-1} d.w.). After the chemical and morphological characterization, the release of heavy metals from the contaminated soil was investigated by ICP-MS, and the results (**Table S5.1**) showed soil pH being slightly alkaline (pH of 7.77±0.02) [290]. Moreover, despite the high concentrations found in the contaminated soil, only very low quantities of Pb, Ba, Se, As, Zn, Ni and Cu, together with traces of Cd, Co and Hg, were leached, while the leaching of Be, Cr, Sn, Tl, and V was below the instrumental detection limit (<0.1 µg·L^{-1}).

XRD analysis of OPC (**Table S5.2**) confirmed the presence of di- and tricalcium silicates (C_2S, C_3S), tetracalcium alumino ferrite (C_4AF) and tricalcium aluminate (C_3A), together with minor amounts of gypsum, anhydrite, calcite and quartz, while the main constituents found for CAC were monocalcium aluminate (CA) and dicalcium aluminate (CA_2). ICP-MS analysis of the binders (**Table 5.2**) revealed that OPC contained more heavy metals than CAC, in particular Ba, Tl, Sb, Sn, Ni, Co, Pb, Cr and As, with a difference ranging from 2 (As, Cr) to 500 times (Ba) more. These data were used to calculate the theoretical heavy metals content (**Table S5.3**) of each granulate produced with the different binders, following the formulations reported in the experimental section.

Table 5.2. Heavy metals' content of contaminated soil and cements.

Contaminant	Contaminated soil[a]	OPC	CAC	Regulatory Limit*
		mg·kg^{-1} d.w.		
Ba	300+12	1463±59	2.10±0.19	-
As	**383±24**	4.32±0.50	7.99±0.92	**50**
Be	0.85+0.09	0.81±0.13	0.93±0.14	10
Cd	2.38+0.22	0.45±0.10	< 0.1	15
Co	42.3+2.1	19.6±1.2	0.4±0.1	250
Cr	45.2±7.1	73.3±11.5	31.2±4.9	500
Cu	311±11	137±9	29±1.01	600
Hg	**8.27±0.47**	< 0.1	< 0.1	**5**
Ni	31.8±1.32	119±7	2.4±0.10	800
Pb	**40430±2000**	38±5	1.20±0.15	**1000**
Sb	**41.0±3.3**	6.2±0.50	< 0.1	**30**
Se	**362+28**	0.50±0.1	< 0.1	**15**
Sn	76.3+12.9	6.10±1.03	0.17±0.06	350
Tl	1.90±0.22	8.03±1.03	< 0.1	10
V	47.3±10.0	170±18	4.22±0.91	250
Zn	500±62	101±13	91±11	1500

[a]From Contessi *et al.* [291].

* Regulatory limit: Column B (commercial and industrial use) of Table 1 of Annex V to Part IV of Title V of Legislative Decree No 152 of 03/04/2006 [101]

5.2.2 Pelletisation

After the contaminated soil pelletisation, the cementitious granular materials obtained were ripened for 28 days in wet air (20°C, 95% atmospheric relative moisture content) and then their mineralogical composition, microstructure and leaching behavior were investigated using XRD, SEM and ICP-MS analysis. The mechanical characteristics of these samples were also investigated by following ASTM D7012-14 (Method C) standard and by quantifying the abraded fraction after the UNI 12457/4 leaching test.

5.2.2.1. XRD and SEM

The mineralogical composition of the different pellets after 28 days of curing is reported in **Table S5.4** and **Figure 5.1**. The mineralogical phases identified by XRD analysis could be included into three groups: soil phases, clinker phases, and newly formed cement hydration products.

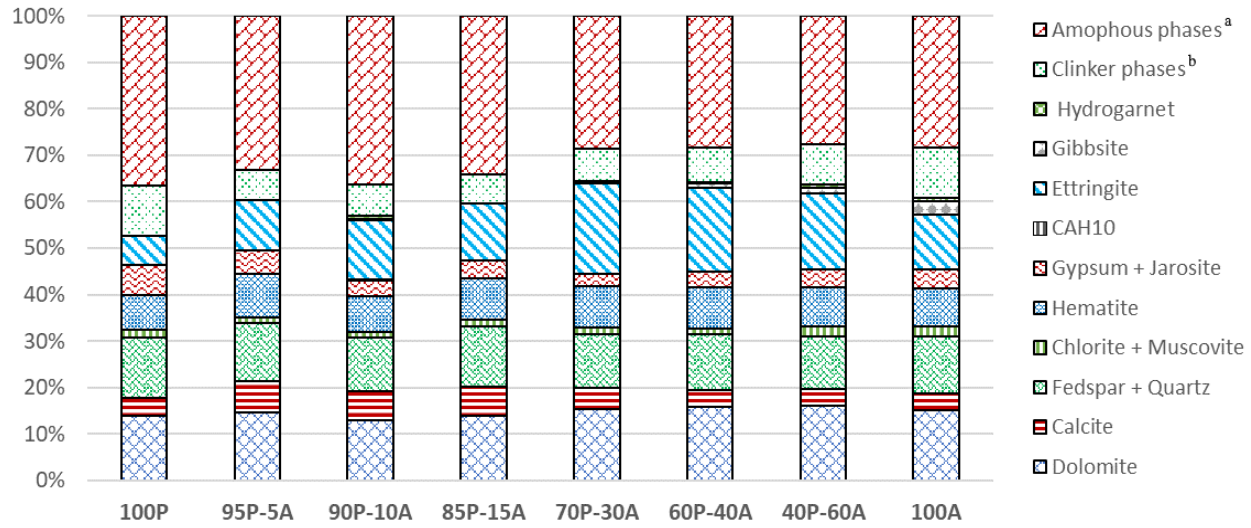

Figure 5.1. Mineralogical composition of the pellets after 28 days of curing obtained by XRD quantitative analysis. [a] Amorphous phases encompass both the amorphous fraction of the contaminated soil and the newly formed amorphous hydration products. [b] Clinker phases represent the sum of the unreacted calcium silicates and calcium aluminates.

Regarding the Pb-minerals detected in the soil, no signals corresponding to anglesite and lithargite were detected in the pellets, probably because of the dissolution processes induced by the high pH (> 12.0) caused by cement hydration [291]. Numerous cement hydration products were also observed in all granulated samples, with ettringite being the most abundant one. This mineral was produced by the reaction of SO_4^- ions, yielded by the dissolution of gypsum, with calcium and aluminate ions provided by both OPC and CAC, as described by the following reactions:

$$CaSO_4 \cdot 2H_2O = Ca^{2+} + SO_4^{2-} + 2H_2O \quad \text{(dissolution of gypsum)} \qquad (Eq.\ 4.1)$$

$$6Ca^{2+} + 2Al(OH)_4^- + 4OH^- + 2(SO_4)^{2-} + 26H_2O = Ca_6[Al(OH)_6]_2 \cdot (SO_4)_3 \cdot 26H_2O$$

(precipitation of ettringite) (*Eq.* 4.2)

In accordance to this, as reported in **Table S5.4** and **Figure 5.1**, the greater the precipitation of ettringite, the lower the quantity of residual gypsum found in the pellets' composition. Ettringite usually does not form from the hydration of CAC, because sulphates are not present but, when combined with sulphates from the contaminated soil, calcium and aluminate ions derived by the dissolution of CA and CA_2 from CAC are able to precipitate ettringite. A small quantity of gibbsite ($Al(OH)_3$) was also found in some CAC-containing pellets, due to the following reaction:

$$3(CaO \cdot Al_2O_4) + 3CaSO_4 \cdot 2H_2O + 32H_2O \rightarrow Ca_6[Al(OH)_6]_2 \cdot (SO_4)_3 \cdot 26H_2O + 4Al(OH)_3$$

(precipitation of ettringite and gibbsite) (*Eq.* 4.3)

Other CAC hydration products detected were hydrogarnet ($3CaO \cdot Al_2O_3 \cdot 6H_2O$) and a calcium aluminium hydrate (CAH_{10}), the latter characterized by a low degree of crystallinity. In OPC-containing pellets, calcium silicate hydrates (C-S-H phase) were also present, resulting from the hydration of calcium silicates (C_3S and C_2S). Even if not directly detected by the presence of diffracted Bragg peaks, because of its amorphous structure, the presence of C-S-H phase was identified thanks to XRD quantitative analysis with internal standards by subtracting the amorphous counterpart present in the contaminated soil to the whole amorphous fraction observed in the pellets (**Table S5.5**).

Portlandite ($Ca(OH)_2$), which usually is a by-product of calcium silicates hydration, was not detected in any of the pellets, regardless of the binder composition, meaning that pore solution did not reach the level of Ca^{2+} saturation required for its precipitation. This could be ascribed to pozzolanic reactions between Ca^{2+} ions and siliceous/aluminous counterparts, deriving by the dissolution of clay minerals (unstable at alkaline pH), which led to additional C-S-H precipitation [270,292].

SEM analysis of polished and carbon-coated sections of the pellets (**Figure S5.2**) showed a microstructure mainly constituted by an amorphous matrix (cement hydration products) where soil particles and unreacted binder particles were dispersed. The cracks observed in **Figure S5.2** could be attributed to the high vacuum condition reached during the analysis, which promoted the dehydration of ettringite with subsequent shrinkage and cracking of the cement matrix [277,291]. Indeed, the soil particles from sample 100P displayed in **Figure 5.2** , mainly composed by aluminosilicate minerals and dolomite, showed shaded borders that suggested an ongoing dissolution process, while in **Figure 5.3** is reported the map of Si distribution in the internal microstructure of 100P and 85P-15A pellets, showing that this element was contained not only in the aluminosilicate minerals, but it was also dispersed in the matrix. These evidences strongly support the hypothesis that both dissolution and pozzolanic reactions occurred.

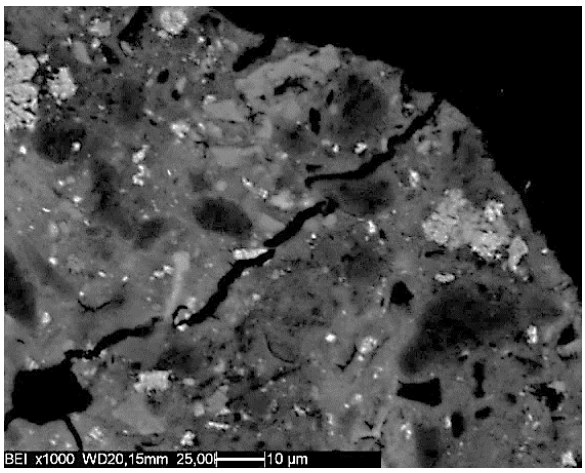

Figure 5.2. SEM image of a polished section of 100P pellets, displaying minerals with shaded borders, indicating that dissolution processes of these phases occurred.

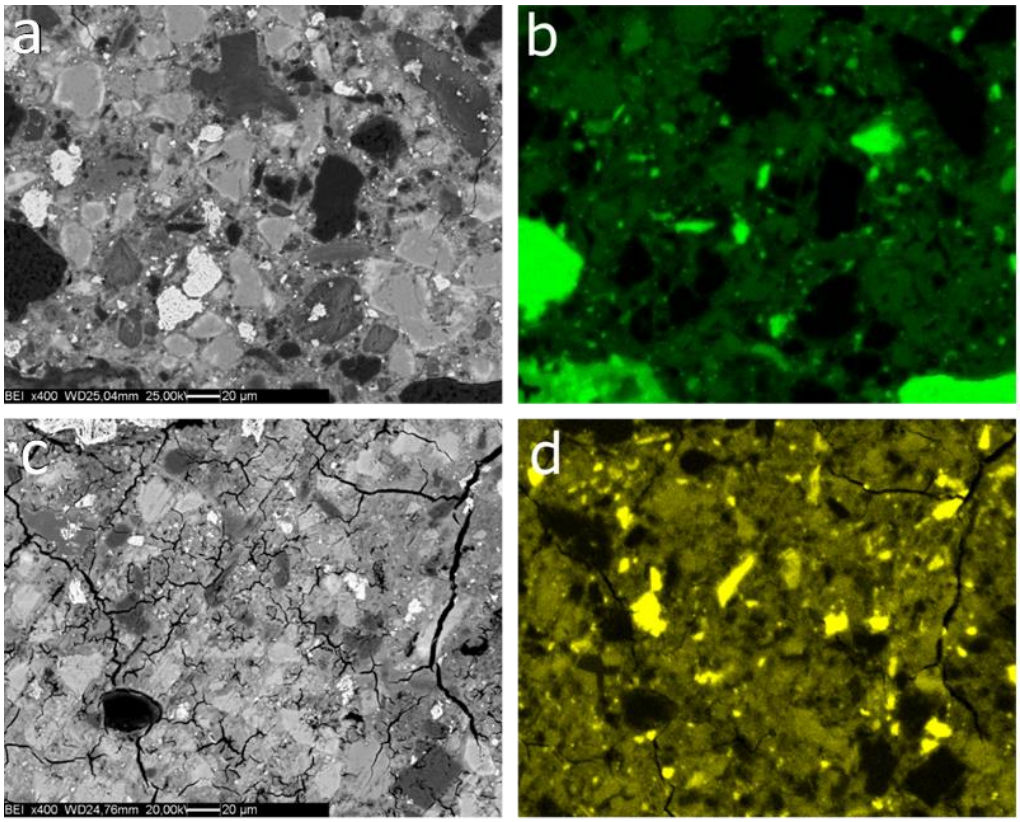

Figure 5.3. SEM images of polished sections of pellets 100P (a) and 85P-15A (c), with the relative map of distribution of Si (b and d), obtained by EDX investigations.

Despite the precipitation of the hydration products described, XRD analysis showed a consistent quantity of residual unhydrated cement phases in all samples (**Figure 5.1**, **Table S5.4**). This delay of clinker hydration, which was more accentuated for samples 100 P and 100A (ca 40% of unhydrated cement), could be ascribed both to the presence of Pb salts [202,278] and to the scarce availability of water for cement particles due to the presence of soil, which may have adsorbed part of the water

otherwise available for cement hydration [202,278,291]. In all the pellets, except for sample 100A, SEM/EDX analysis showed numerous unreacted clinker particles whose external surface was covered by a coating, white-coloured at back-scattered electrons detector (**Figure 5.4a-c**), which resulted enriched in Pb, as shown by the map of Pb distribution (**Figure 5.4d**).

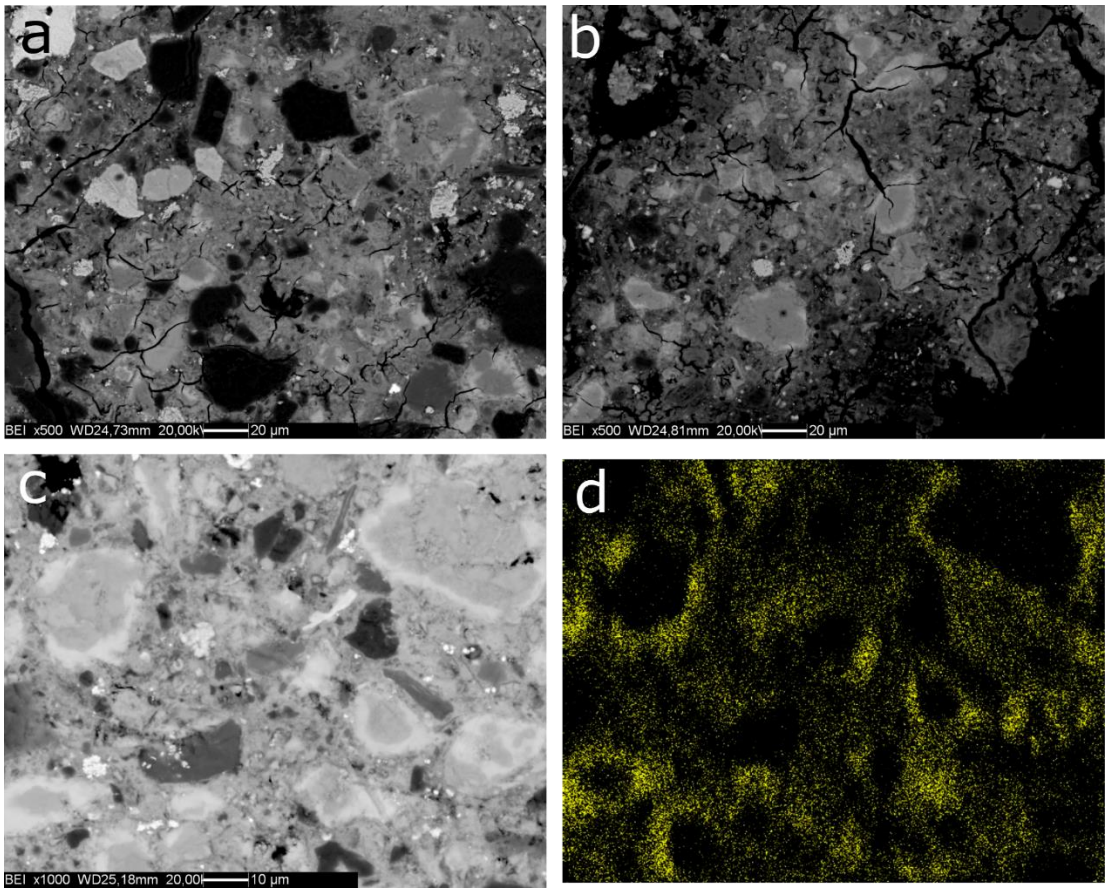

Figure 5.4. SEM images of polished sections of pellets: 95P-5A (a), 85P-15A (b) and 100P (c). Map of Pb distribution (d) relative to image (c)

Pb was also found dispersed throughout the amorphous matrix of all OPC-based samples, where C-S-H and ettringite were precipitated. Moreover, in sample 100A no Pb-rich coating was observed on clinker particles, instead Pb was quite well distributed in the hydrated matrix, and also seldom found in some residual crystalline forms (i.e. anglesite and/or litharge) not detected by XRD analysis [291]. As shown by XRD (**Figure 5.1**, **Table S5.4**) the quantity of unreacted binder found in samples 95P-5A, 90P-10A, 85P-15A, 70P-30A¸60P-40A¸and 40P-60A was significantly lower than that found in the pellets obtained by using pure OPC and CAC as binders. This could be ascribed to the higher quantity of ettringite detected in these samples (**Figure 5.1**, **Table S5.4**), which could have encapsulated Pb^{2+} ions in its structure [209], leading to a reduced delay in the hydration of OPC-clinker particles, which is usually caused by the presence of Pb. EDX analysis (**Figure 5.5b**) supports this hypothesis, since Pb has been found among the elements constituting the ettringite (i.e. Al, Ca,

and S) as showed by the presence of the characteristic Pb Lα line at 10.5 eV. The other characteristic Pb signal (Mα emission line at 2.34 eV) resulted superimposed to Kα line of S at 2.30 eV [291].

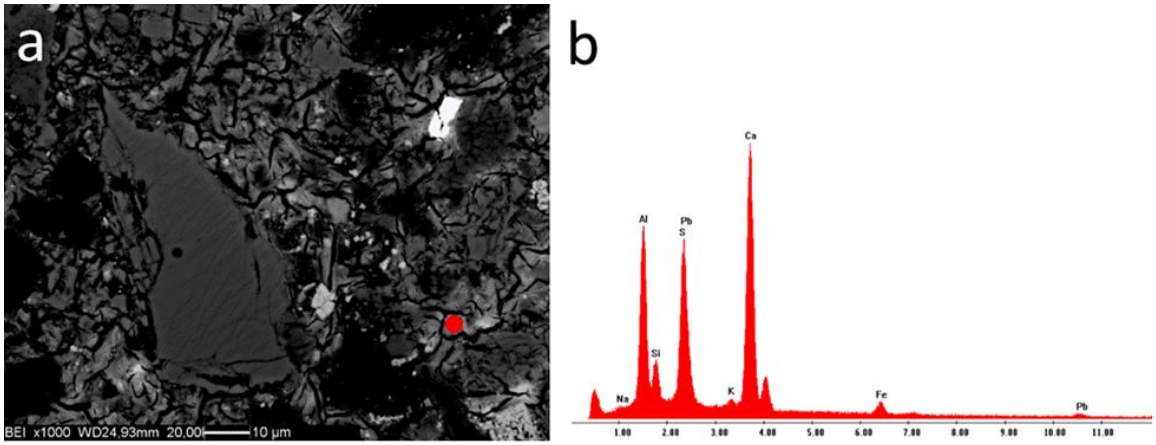

Figure. 5.5. SEM image of a section of 85P-15A pellets (a) and elemental composition of the red point (b), showing Pb together with ettringite structural elements.

5.2.2.2. Mechanical characteristics

To further elucidate the mechanisms involved in the heavy metals' solidification/stabilization process, the effects of the changes in the binder formulation on the granulate's mechanical properties were investigated. In detail, the uniaxial compressive strength (σ_U) of cylindrical test pieces made of the same formulation of the various granular materials, and the fraction of granulate with particle diameter below 63 µm obtained after the UNI EN 12457/4 leaching test, are reported in **Figure 5.6**, **Table S5.6** and **Table S5.7**.

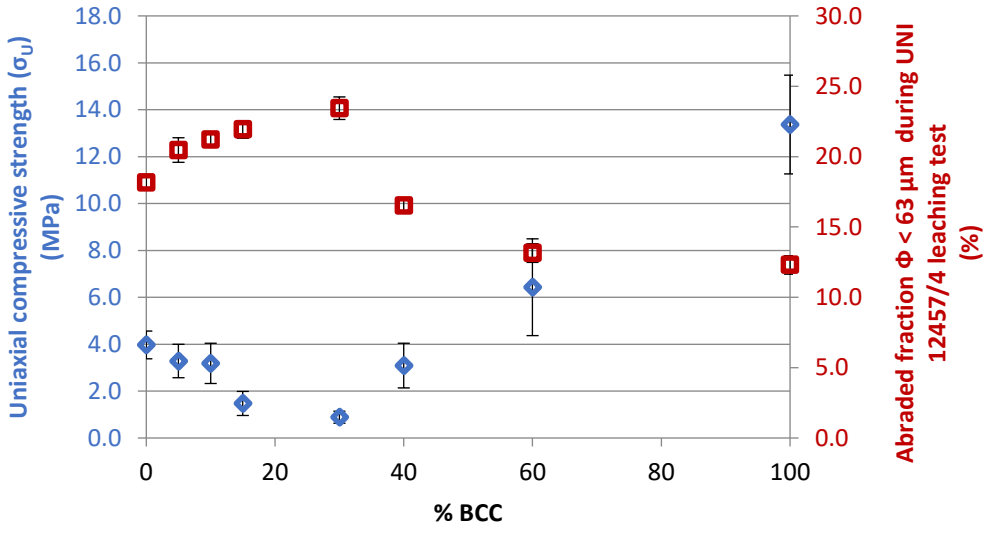

Figure 5.6. Uniaxial compressive strength (σ_U) of cylindrical test pieces (Φ: 20 mm, h: 30 mm) made with the same formulation of the granulates and fraction of granulate with particle diameter below 63 µm obtained after the UNI 12457/4 leaching test as a function of the Binder's CAC Content (BCC).

Figure 5.6 shows that the use of low quantities of CAC in the binder formulation (0-30 % BCC range) caused a decrease of σ_U from 3.9±0.6 MPa to 1.5±0.3 MPa, while when using more CAC as binder (40-100 % BCC range) the test pieces' mechanical resistance increased up to 13.4 MPa.
The fraction of granulate with particle diameter below 63 μm obtained after UNI EN 12457/4 leaching test showed a specular behaviour, increasing from 18.2±0.4% to 23.2±0.6% in the 0-30 % BCC range and then decreasing to 12.3±0.5 using only CAC as binder. These trends are similar to the one showed by ettringite precipitation (**Figure 5.1** and **Table S5.4**), which is known to decrease the mechanical properties of OPC-based cementitious systems [246]. Moreover, CAC has already been reported to develop high early strength and abrasion endurance [293].

5.2.2.3. Leaching tests

The effects of each formulation on the pellets leaching behaviour was investigated by the UNI 12457-4 leaching test and ICP-MS analysis (**Table 5.3a-b**), showing that the addition of CAC to OPC in the binder formulation caused important changes in the retention of heavy metals. In order to account for the difference between each binder contaminants' content, the concentrations of heavy metals measured in the eluates were normalized to the respective total contents (**Figure 5.7**) calculated for each granulate shown in **Table S5.3**

Table 5.3a. Leaching of samples 100P, 95P-5A, 90P-10A, and 85P-15A after 28 days of curing following the UNI EN 12457/4:2004 standard.

Parameter	100P	95P-5A	90P-10A	85P-15A
pH	12.35±0.02	12.25±0.02	12.21±0.02	12.18±0.03
	$\mu g \cdot L^{-1}$			
Ba	274±21	325±14	362±27	421±33
As	1.73±0.22	1.69±0.20	1.65±0.23	1.75±0.29
Be	< 0.1	< 0.1	< 0.1	< 0.1
Cd	< 0.1	< 0.1	< 0.1	< 0.1
Co	7.56±0.48	5.59±0.91	5.03±0.19	4.45±0.92
Cr	43.2±1.7	35.6±3.1	27.4±2.3	25.2±2.4
Cu	90.2±11.0	95.2±8.3	114±11	146±10
Hg	< 0.1	< 0.1	< 0.1	< 0.1
Ni	75.3±3.4	62.6±4.4	47.2±3.0	36.0±3.9
Pb	2040±90	1842±111	1647±100	1348±93
Sb	0.21±0.05	0.23±0.07	0.28±0.05	0.24±0.03
Se	19.0±1.9	19.1±1.6	22.9±2.0	29.5±3.8
Sn	< 0.1	< 0.1	< 0.1	< 0.1
Tl	1.31±0.07	1.24±0.17	1.23±0.08	1.07±0.12
V	0.86±0.11	0.95±0.11	1.52±0.35	2.05±0.17
Zn	2.50±0.17	1.59±0.29	1.55±0.25	1.54±0.25

Table5.3b. Leaching of samples 70P-30A, 60P-40A, 40P-60A, and 100A after 28 days of curing following the UNI EN 12457/4:2004 standard.

Parameter	70P-30A	60P-40A	40P-60A	100A
pH	12.05±0.02	12.02±0.02	12.01±0.03	12.00±0.03
	$\mu g \cdot L^{-1}$			
Ba	277±25	211±10	153±12	86.8±5.6
As	1.77±0.23	1.29±0.25	1.11±0.15	1.02±0.19
Be	< 0.1	< 0.1	< 0.1	< 0,1
Cd	< 0.1	< 0.1	< 0.1	< 0,1
Co	2.62±0.33	0.68±0.08	0.28±0.01	< 0,1
Cr	23.0±3.0	20.6±1.2	12.5±0.8	1.62±0.18
Cu	186±17	113±5	71.1±5.2	27.8±2.3
Hg	< 0.1	< 0.1	< 0.1	< 0.1
Ni	14.6±1.8	2.44±0.21	0.99±0.29	0.59±0.33
Pb	1094±93	877±82	617±36	73.1±9.2
Sb	1.12±0.05	1.38±0.13	1.65±0.22	2.24±0.22
Se	37.0±2.9	28.0±3.1	19.1±1.2	11.8±1.4
Sn	< 0.1	< 0.1	< 0.1	< 0.1
Tl	0.32±0.06	0.19±0.03	0.18±0.03	0.17±0.03
V	4.36±0.96	3.60±0.51	2.94±0.23	< 0,1
Zn	1.18±0.32	0.81±0.24	< 0,1	< 0,1

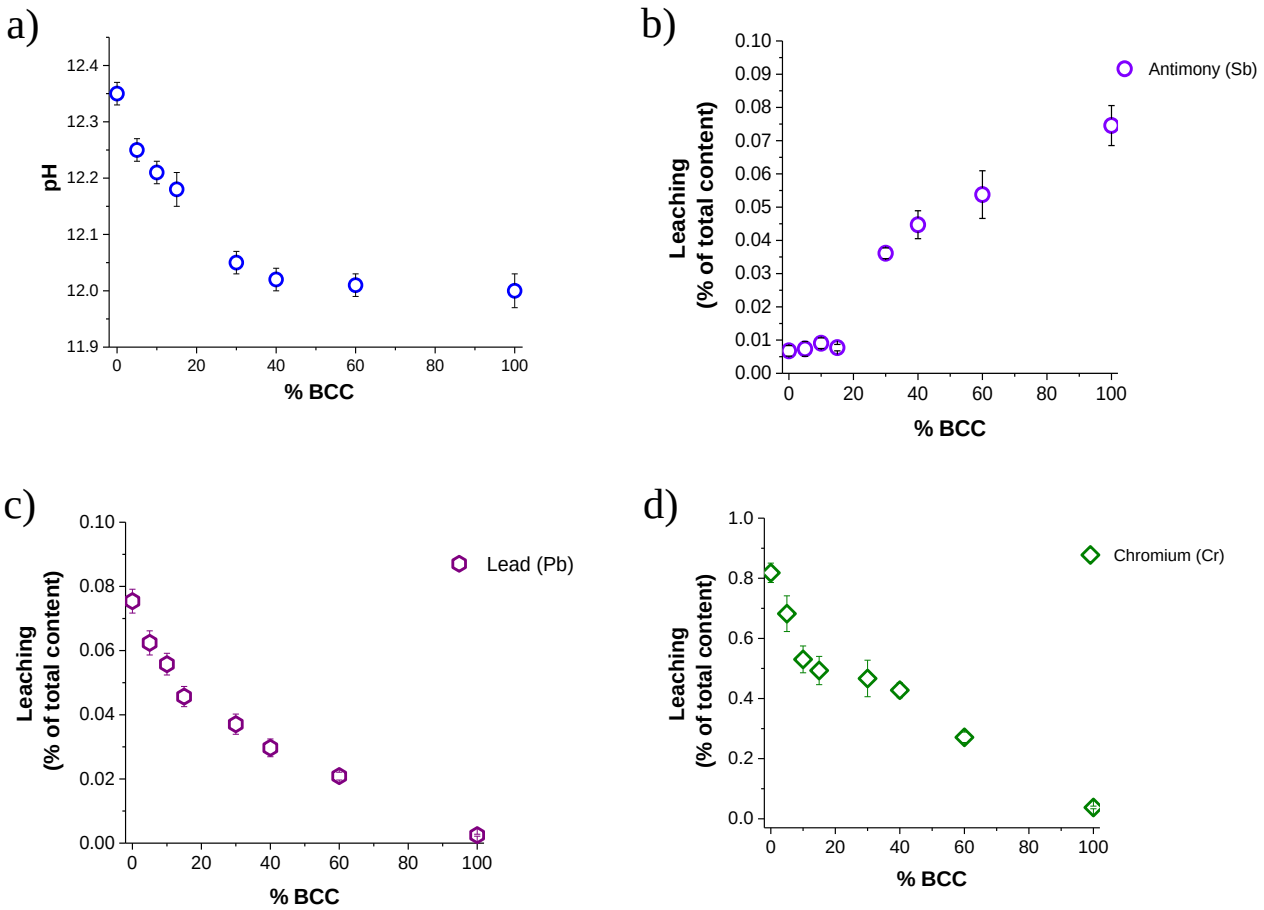

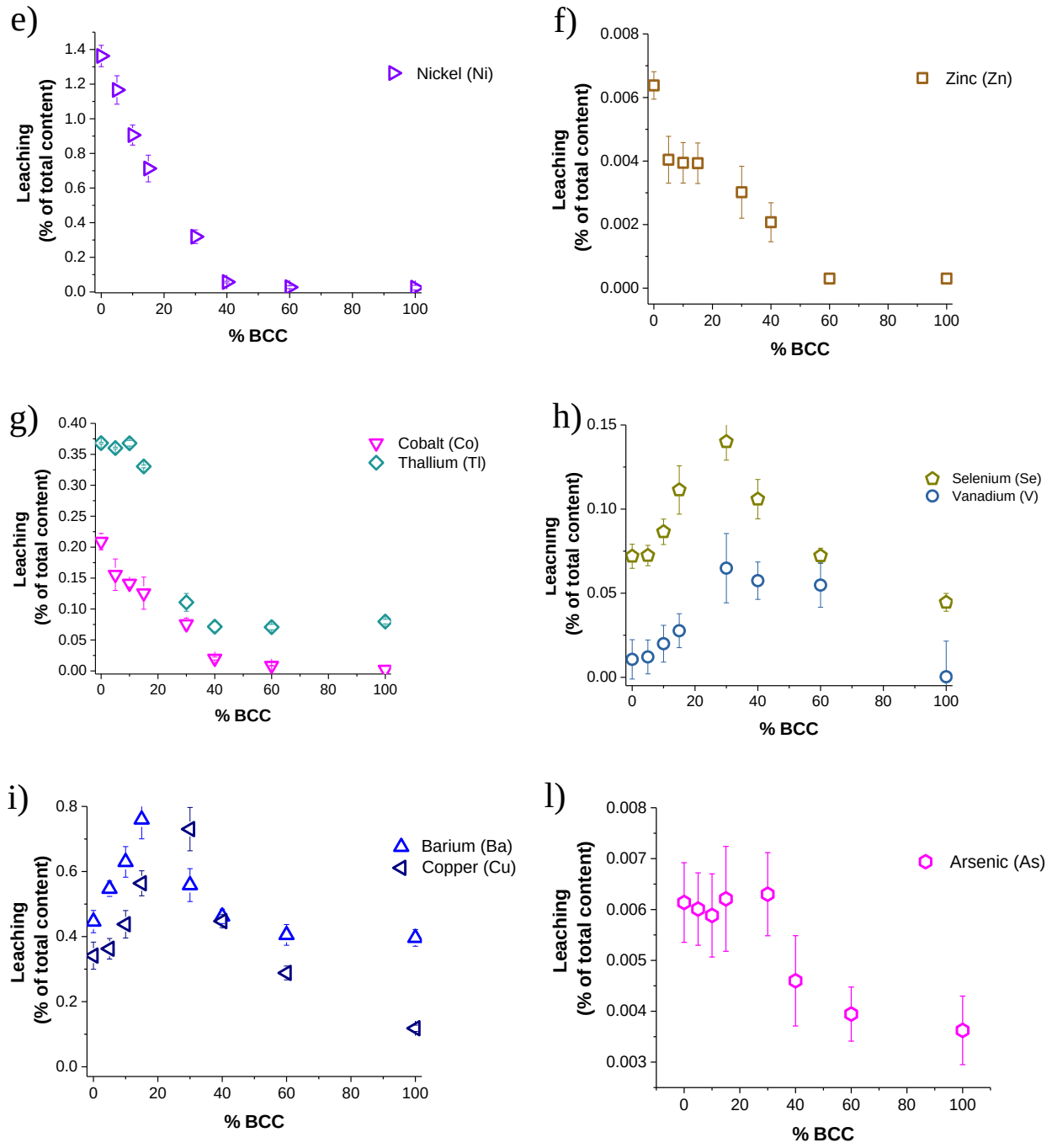

Figure 5.7. Results of the leaching test UNI EN 12457/4:2004 of the granulated materials as a function of the Binder's CAC Content (BCC), normalized with the calculated heavy metal content of each sample reported in **Table S5.3**.

In detail, due to the slightly less alkaline pH that characterize CAC with respect to OPC [197], the final pH of the eluates changed significatively in the range from 0 to 40 % BCC, decreasing from 12.35 to 12.05, and then remaining constant for the rest of the examined pellets (**Figure 5.7a**). Comparing the leaching of the two samples obtained using pure binders (i.e. 100P and 100A), we found that CAC gave the best immobilization of all the studied metals save for Sb, whose leaching increase of about eleven times, while the leaching of Be, Cd, Hg, and Sn remained below the detection limit (< 0.1 $\mu g \cdot L^{-1}$) for all the samples investigated. In detail, the difference was the highest for Co,

Cr, Ni, Pb and Zn (decrease of 95-99 % with respect to OPC-pellets), slightly less pronounced for V, Tl and Cu (decrease of 65-72% with respect to OPC-pellets), and of about 40 % for As and Se. The slightest improvement was found for Ba, with a decrease of ca. 12 %.

The study of each contaminant's leaching from the samples obtained using binders with a mixed composition provided important information to better elucidate the mechanisms involved in their retention.

When the quantity of CAC in the binder exceeded the 15%, we observed an increased leaching of Sb from the pellets, going from about 0.24 to 2.24±0.22 μgL^{-1}(**Figure 5.7b**). This could be attributed to the decrease of CSH content in the pellets, whose importance in the retention of this metal was established by Salihoglu *et al.* [294]. Despite the observed increase in the leaching of this heavy metal, the amount of Sb released is still modest probably because of the relatively high amount of ettringite, which, as suggested by the same authors, is able to incorporate Sb by replacing Ca ions in its structure [294].

The leaching of Cr, Pb, Ni, Co, Zn, and Tl (**Figure 5.7c-g** and **Table 5.3a-b**) varied between 1 and 2 orders of magnitude, clearly decreasing when the percentage of CAC used in the binder's formulation increased. In addition, their leaching showed similar trends, indicating that they may be subjected to similar immobilization mechanisms. This decrease in the leaching of these contaminants could be related to the increase of the percentage of ettringite observed for samples 95P-5A, 90P-10A, 85P-15A, and 70P-30A (0-40% BCC range), indicating the fundamental role of this mineralogical phase in these heavy metals' retention [286,295,296]. The further decrease of their mobilization for the samples characterized by a slightly lower ettringite content (i.e. 60P-40A, 40P-60A, and 100A) could be ascribed both to a more favourable pH of the eluate, which corresponds to a decrease in solubility of these metals of nearly 3-5 times [243,297] and to the lower surface area exposed during the leaching test, thanks to the increase of these pellets resistance to abrasion (**Figure 5.7**, **Table S5.6** and **Table S5.7**). In the case of Pb, the fundamental role of ettringite in the stabilization performance of the different binders was also supported by SEM/EDX data, which showed this contaminant together with ettringite constituent elements like S, Ca and Al (**Figure 5.5**).

The leaching of Se, Cu, Ba and V increased with BCC from 0 % to 15-30 %, then decreased almost linearly, reflecting the granulated materials' resistance to abrasion and their mechanical strength. This could indicate their retention to be mainly controlled by diffusion phenomena, closely related to their physical encapsulation and the different amounts of superficial area exposed to the eluent during the leaching test. The retention of As was quite efficient for all the samples studied (i.e. > 99.993%) due to its precipitation as less soluble compounds and immobilization inside both CSH and ettringite structure [249,251,298], but showed also significant increase for the formulations having higher CAC

content (i.e. 60P-40A, 40P-60A, and 100A). This indicates the importance of pH and diffusion phenomena in the retention of this heavy metal.

5.3. Conclusions

In this work we studied the performance of both Ordinary Portland Cement (OPC) and Calcium Aluminate Cement (CAC), as well as several binders prepared with different combinations of these two cements, for the solidification/stabilization of a soil contaminated by several heavy metals of environmental concern (i.e. Ba, As, Be, Cd, Co, Cr, Cu, Hg, Ni, Pb, Sb, Se, Sn, Tl, V, and Zn), highlighting the different mechanisms involved in the retention of these pollutants. To the best of our knowledge, this is one of the few studies evaluating the S/S performance of the proposed binders for the treatment of a real polluted soil, characterized by an increased complexity than artificially doped systems. Despite this complexity we managed to obtain data useful to better elucidate the mechanisms involved. Our results showed that CAC gave better performances than OPC for most of the investigated metals, representing a good alternative to improve immobilizations treatments based on hydraulic binders. In detail, XRD and SEM/EDX analysis demonstrated that the high sulphates content of the contaminated soil sharply shifted the reactivity of CAC-containing binders towards the precipitation of ettringite. This mineral showed a leading role in the retention of Cr, Pb, Ni, Co, Zn, and Tl, while the leaching of Se, Cu, Ba and V was observed to be dependant from both the pellets' mechanical performances (i.e. unilateral compressive strength and resistance to abrasion) and pH, showing the importance of these contaminants' physical encapsulation to obtain a successful immobilization.

5.4. Acknowledgements

The authors are grateful to In.T.Ec. s.r.l. for founding the Ph.D. fellowship of L. C.. This work was performed with financial support of the Mapei S.p.A-UniPd research agreement, Intec S.r.l. and Ca' Foscari University of Venice.

5.5. Supplementary Information

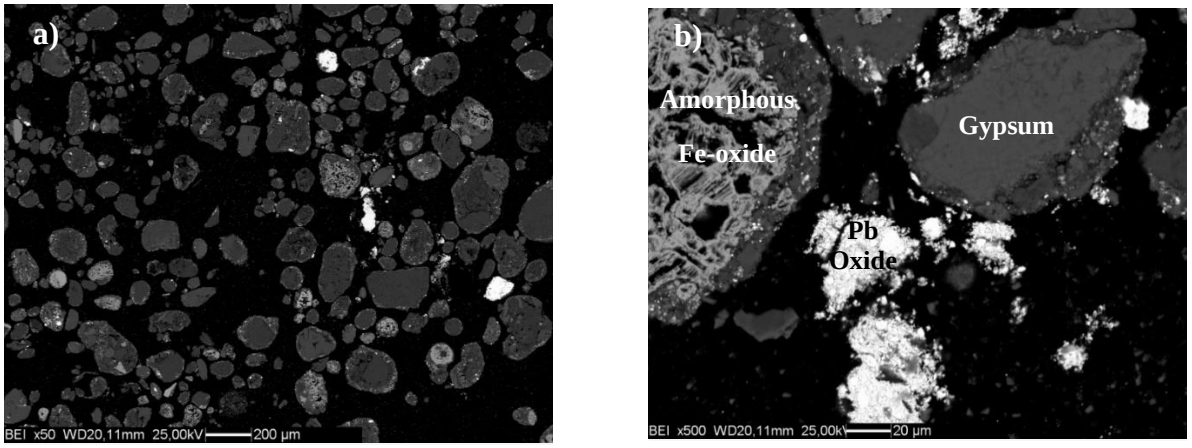

Figure S5.1. SEM images of the contaminated soil at a) 50x and b) 500x.

Table S5.1. Leaching of contaminated soil following UNI EN 12457/4:2004 standard.

Parameter	Contaminated soil		
pH	7.77±0.02		
	µg·L^{-1}		µg·L^{-1}
Ba	18,4±0,8	**Ni**	1,35±0,32
As	5,36±0,32	**Pb**	40,5±6,9
Be	< 0,1	**Sb**	3,65±0,10
Cd	0,41±0,06	**Se**	11,6±1,3
Co	0,32±0,05	**Sn**	< 0,1
Cr	< 0,1	**Tl**	< 0,1
Cu	1,75±0,26	**V**	< 0,1
Hg	0,22±0,08	**Zn**	11,1±1,7

Table S5.2. XRPD analysis of OPC and CAC. (l.o.d. = limit of detection)

Phase	OPC	CAC
	w.t. %	
Calcite $Ca(CO_3)$	0.4±0.2	< l.o.d.
Quartz SiO_2	0.2±0.1	< l.o.d.
Gypsum $CaSO_4 \cdot 2(H_2O)$	1.4±0.2	< l.o.d.
Anhydrite $CaSO_4$	1.1±0.4	< l.o.d.
C_3A $Ca_3Al_2O_6$	13.4±0.1	< l.o.d.
C_2S Ca_2SiO_4	9.4±0.1	< l.o.d.
C_3S Ca_3SiO_5	58.3±0.5	< l.o.d.
C_4AF $Ca_2(Al,Fe)_2O_5$	3.7±0.5	< l.o.d.
CA $CaAl_2O_4$	< l.o.d.	37.3±0.9
CA_2 $CaAl_4O_7$	< l.o.d.	52.0±1.2
Amorphous phases	12.1±0.4	10.7±0.3

Table S5.3. Calculated heavy metals content of each granulate, obtained using the following approximation:

$$[Sample] = 0.73 \cdot [Soil] + 0.27 \cdot \{\%OPC \cdot [OPC] + \%CAC \cdot [CAC]\}.$$

Parameter	100P	95P-5A	90P-10A	85P-15A	70P-30A	60P-40A	HP010	100A	Δ % 100A-100P
	mg·kg^{-1} d.w.								%
Ba	614	594	574	555	495	456	377	219	-64.3
As	281	281	281	281	281	281	282	282	+0.32
Be	0.84	0.84	0.84	0.84	0.85	0.85	0.86	0.87	+2.85
Cd	1.86	1.85	1.85	1.84	1.82	1.81	1.79	1.74	-6.29
Co	36.2	35.9	35.7	35.4	34.6	34.1	33.1	31.0	-14.3
Cr	52.8	52.2	51.6	51.1	49.4	48.2	46.0	41.4	-21.6
Cu	264	263	261	260	255	252	246	235	-11.1
Hg	6.05	6.05	6.05	6.05	6.05	6.05	6.05	6.05	0
Ni	55.2	53.7	52.1	50.5	45.8	42.7	36.4	23.9	-56.7
Pb	29525	29524	29524	29523	29522	29521	29519	29515	0
Sb	31.6	31.5	31.5	31.4	31.1	31.0	30.6	30.0	-5.16
Se	265	265	265	264	264	264	264	264	0
Sn	57.3	57.3	57.2	57.1	56.9	56.7	56.4	55.7	-2.80
Tl	3.55	3.45	3.34	3.23	2.91	2.70	2.27	1.41	-60.2
V	80.6	78.4	76.1	73.9	67.1	62.6	53.6	35.6	-55.8
Zn	393	393	392	392	392	391	391	390	-0.75

Table S5.4. XRD analysis of granulate after 28 days of curing (l.o.d. = limit of detection).

Phase	100P	95P-5A	90P-10A	85P-15A	70P-30A	60P-40A	40P-60A	100A
	% w.t.							
Feldspar	2.7±0.4	1.4±0.2	1.4±0.2	2.1±0.3	1.4±0.2	1.4±0.2	1.2±0.2	2.1±0.4
Calcite	3.7±0.7	6.6±1.3	6.1±1.0	6.1±1.0	4.4±0.7	3.6±0.6	3.5±0.6	3.6±0.6
Dolomite	13.2±1.9	14.3±1.8	12.9±1.6	14.0±1.8	14.9±1.9	15.3±1.9	15.5±2.0	15.2±2.0
Hematite	7.2±1.1	9.1±1.1	7.8±0.9	8.8±1.1	8.7±1.1	8.8±1.1	8.0±1.0	8.1±1.2
Jarosite	0.8±0.3	1.2±0.4	< l.o.d.	< l.o.d.	1.2±0.4	1.9±0.7	1.8±0.6	1.2±0.4
Quartz	9.7±0.7	10.8±0.7	10.1±0.6	11.0±0.7	9.8±0.6	10.2±0.6	9.8±0.6	10.0±0.7
Muscovite	1.7±0.1	1.2±0.1	1.1±0.1	1.4±0.1	1.4±0.1	1.1±0.1	2.1±0.2	2.3±0.3
Gypsum	5.3±1.0	3.8±0.5	3.3±0.5	3.8±0.6	1.4±0.2	1.4±0.3	2.1±0.3	2.8±0.8
Ettringite	5.9±1.6	10.4±1.1	12.8±1.0	12.2±1.2	19.0±1.7	17.4±1.2	15.7±1.3	11.8±2.6
Hydrogarnet	< l.o.d.	< l.o.d.	0.7±0.1	< l.o.d.	0.2±0.1	0.2±0.1	0.8±0.1	0.7±0.1
Gibbsite	< l.o.d.	< l.o.d.	0.1±0.05	0.1±0.05	0.1±0.05	1.0±0.2	1.1±0.2	2.7±0.2
CAH_{10}	< l.o.d.	< l.o.d.	0.1±0.05	0.1±0.05	< l.o.d.	< l.o.d.	< l.o.d.	0.1±0.05
Amorphous phases	34.9±2.1	32.3±1.9	36.0±1.2	34.0±2.1	27.7±1.5	27.6±1.4	26.7±1.4	28.3±1.0
C_3S	5.1±1.4	3.1±0.4	2.6±0.5	2.1±0.4	3.8±0.5	4.6±0.6	3.8±0.3	< l.o.d.
C_2S	2.0±0.3	0.9±0.2	1.4±0.4	1.8±0.4	0.4±0.1	< l.o.d.	< l.o.d.	< l.o.d.
C_3A	2.4±0.1	1.9±0.3	1.1±0.2	0.7±0.2	0.6±0.1	0.8±0.1	0.3±0.1	< l.o.d.
C_4AF	0.9±0.3	0.5±0.1	0.4±0.1	0.1±0.05	0.3±0.1	< l.o.d.	0.1±0.05	< l.o.d.
CA	< l.o.d.	< l.o.d.	1.1±0.2	1.4±0.2	1.2±0.2	0.8±0.1	1.9±0.3	5.7±0.2
CA_2	< l.o.d.	< l.o.d.	0.1±0.05	0.2±0.1	0.5±0.1	0.9±0.2	2.2±0.3	5.2±0.6
Unreacted Cement	10.4±2.1	6.4±1.1	6.7±1.4	6.3±1.3	6.8±1.3	7.1±1.1	8.3±1.0	10.9±0.8

Table S5.5. Estimated CSH content of each granulate, obtained using the following approximation:

$$w.t.\%_{CSH} = w.t.\%\ amorphous_{\ Pellet} - 0.73\ w.t.\%\ amorphous_{Soil}\ .$$

Phase	100P	95P-5A	90P-10A	85P-15A	70P-30A	60P-40A	40P-60A
$\%_{CSH}$	% w.t.						
	16	14	18	16	9	9	8

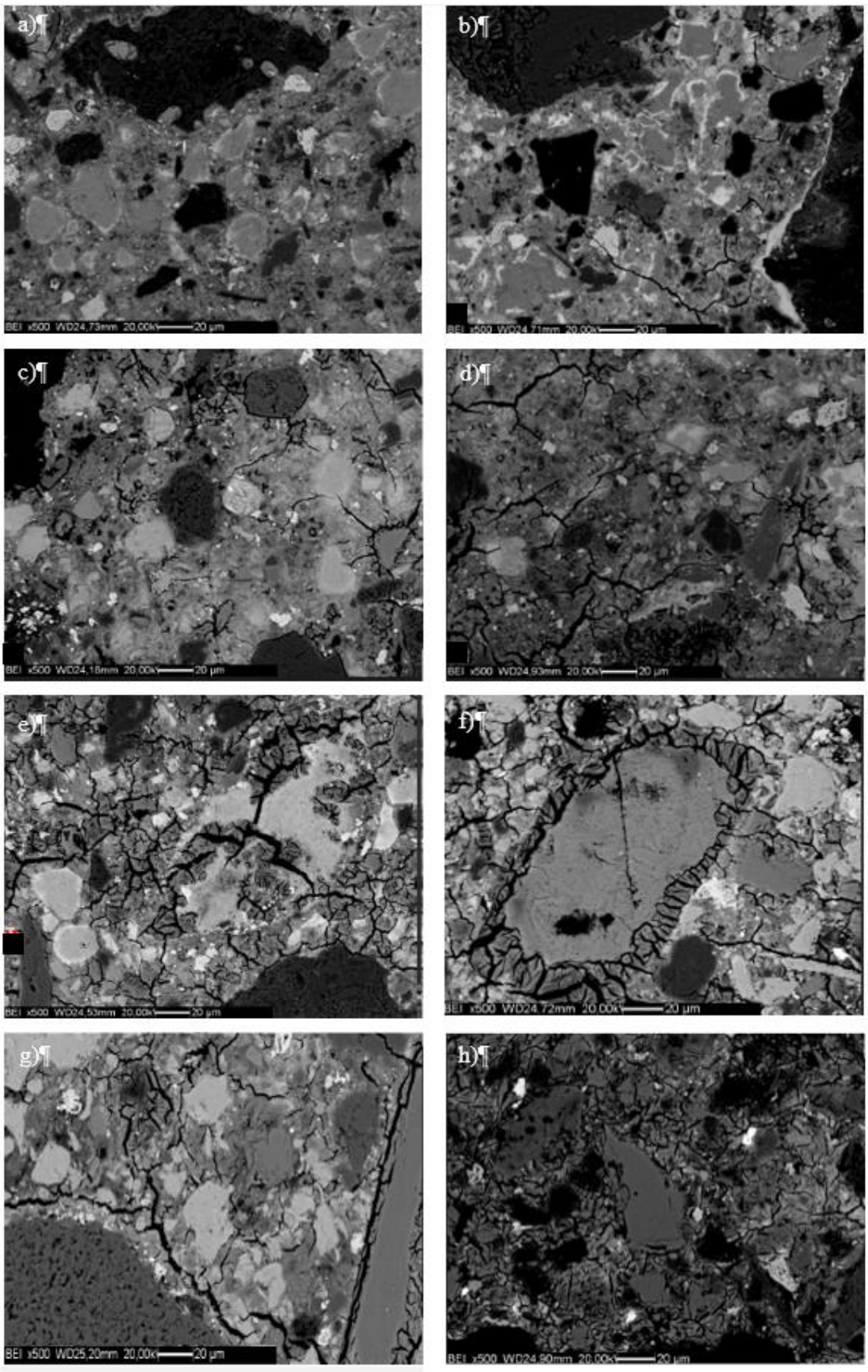

Figure S5.2. Sections of pellets after 28 days of curing: a) sample 100P, b) sample 95P-5A, c) sample 90P-10A, d) sample 85P-15A, e) sample 70P-30A, f) sample 60P-40A, g) sample 40P-60A, h) sample 100A

Table S5.6. Uniaxial compressive strength (σ_U) of cylindrical test pieces made of the same formulation of the pellets

Parameter	100P	95P-5A	90P-10A	85P-15A	70P-30A	60P-40A	40P-60A	100A
Uniaxial compressive strength (σ_u)	MPa							
	3.97±0.59	3.28±0.71	3.18±0.86	1.47±0.51	0.89±0.26	3.09±0.95	6.43±2.06	13.37±2.10

Table S5.7. Fraction of granulate with particle diameter < 63 μm produced during UNI 12457/4 leaching test after 28 days of curing.

Parameter	100P	95P-5A	90P-10A	85P-15A	70P-30A	60P-40A	40P-60A	100A
Fraction of granulate with particle diameter < 63 μm	%							
	18.2±0.4	20.5±0.5	21.2±0.4	21.9±0.4	23.2±0.8	16.5±0.5	13.1±0.5	12.3±0.5

6. Chapter 6

Past environmental pollution in an industrial site: using stable lead isotopic analysis to identify multiple contamination sources

Alessandro Bonetto[1], Loris Calgaro[1], Silvia Contessi[2], Elena Badetti[1], Gilberto Artioli[2], Antonio Marcomini[1]

[1]Department of Environmental Science, Informatics and Statistics, University Ca' Foscari Venice, via Torino 155, 30172, Mestre (VE), Italy
[2]Department of Geosciences, University of Padua, via G. Gradenigo 6, 35129, Padua, Italy

This chapter presents the manuscript “Past environmental pollution in an industrial site: using stable lead isotopic analysis to identify multiple contamination sources”, where a lead-polluted industrial site in Bagnolo Mella (Italy) was investigated to establish if the contamination has spread into the surrounding area.

The RBCA (Risk Based Corrective Action) approach, where the identification of applicable risk factors on a site-specific basis is followed by the implementation of appropriate corrective measures in a timeframe necessary to prevent unsafe conditions [299] is one of the of the most applied remediation and reclamation procedures. One of RBCA’s fundamental steps is to establish the exposure pathways between the pollution and its surrounding, in order to correctly evaluate the possible risks posed to both the environment and human health [102,300]. For this reason, identifying the sources, the release’s timing and the distribution of contaminants in the environment is essential for estimating the extent of the damage and to define the areas that may need specific remediation treatments [301,302]. While the historical analysis of the areas based on information retrieved from the local authorities can be a good starting point, sometimes the lack of archived data can lead to a wrong estimation of pollution sources and consequently of the contamination’s entity. Moreover, the identification of heavy metals pollution sources is a difficult task in a typical industrial setting because of the large number of possible sources such as direct emissions from industrial sites, inappropriate waste disposal, exhaust from fuel combustion or spills, pesticides and the natural geological background.

To solve this problem, there are three methods currently used to discriminate pollution sources: i) the geochemical mapping method [303–305], ii) the statistical method [306–308], and iii) the isotopes’ tracing method [309,310]. The first two methods are generally applied to analyze and evaluate the total concentration of heavy metals and their speciation in soils and plants, usually requiring the use of large databases and sophisticated statistic models. However, these methods can give results that may be misinterpreted due to poor correlation between variables or the possible presence of confounding factors. For these reasons it can be quite difficult to effectively trace multiple pollution sources by using these two techniques [302,311]. On the other hand, isotopic measurement tools, combined with the contaminants’ concentration mapping of the polluted site, have already been successfully used to trace multi-source contamination of sites characterized by reduced available data or limited areas [312,313], and to trace heavy metals’ mobility in soils’ profiles [311] and into the surrounding acquirers and groundwaters [314].

In this case, since the analysis of various historical documents revealed that this area was subjected to a heavy lead pollution, probably originated from the inappropriate disposal of wastes and

tailings of a plant for sulfuric acid production which used the pyrite roasting process, particular attention was given to investigate the lead contamination present in the selected site, especially focusing on the possible diffusion of Pb (and other heavy metals metals) into the nearby fields, both at the superficial level and in depth.

6.1. Experimental

6.1.1. Research area

Located in the southern part of the Brescia province, northern Italy, the city of Bagnolo Mella has been, at the beginning of the 20th century, one of the first Italian industrial centres for the large-scale production of sulphate and perphosphate fertilizers [315]. Attracted by this development, other industries settled in this area, moving from steel smelting and manufacturing to tanning and plastic production.

Bagnolo Mella is located on a plain in the transition zone between predominantly gravel-sandy fluvioglacial deposits with pebbly levels and differently cemented horizons. This region is characterized by a humid subtropical climate, with annual mean precipitations of around 800 - 1000 mm/m^2 and winds primary from NNE to SSW.

In particular, the production of fertilizers has been carried out in an agrarian consortium situated near the SW border of the city, between various smelting and steel manufacturing factories. The site included installations dedicated to different activities, from sulphuric acid production thought pyrite roasting (lead chambers process) to fuel and mineral oil storage [291].

The plant for the synthesis of sulphuric acid has been operational from 1897 to 1985, while other activities (i.e. fuel and mineral oil storage, bagging and storing of fertilizers) continued until 1999.

Historical research and preliminary surveys confirmed this property to be affected by heavy metal pollution, due to tailings and wastes' disposal practices that could be considered inappropriate for today's standards. Moreover, this particular area can be considered of high environmental concern, since the contaminants can by diffusion reach the nearby aquifer, which is relatively shallow, and the cropland destined to human consumption.

6.1.2. Sampling, sample preparation and analysis

Topsoil (from 15 to 30 cm depth, series "T") and subsoil (from 130 to 150 cm depth, series "S") samples from the contaminated site and the surrounding area were collected as shown in **Figure 6.1.**

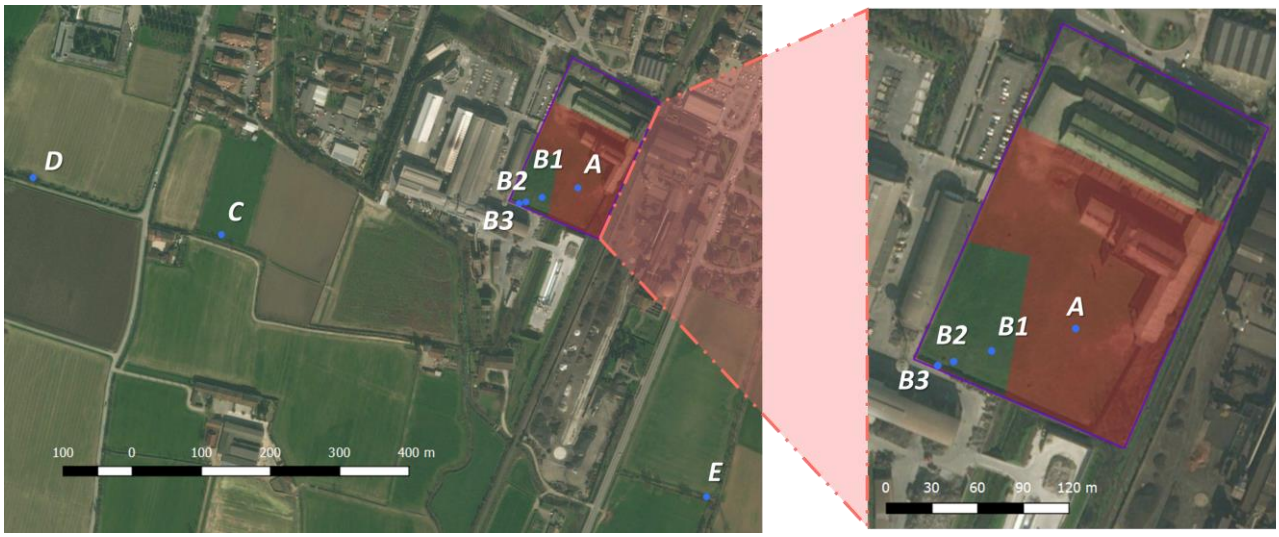

Figure 6.1. Map of the sampling campaign. The red area represents the contaminated area, as determined from historical documentation and preliminary characterization of the property.

The depth of the superficial samplings was selected to account for the presence of rubble and other debris in the first soil layer within the contaminated zone.

Sample A was taken in the middle of the contaminated zone, while samples B (B_1, B_2, B_3) were excavated outside from this area at different distances moving towards the property's boundaries (at 55, 75 and 90 m from sample A, respectively). Sample C was collected from a lawn, which has remained like this for the last 30 years, at 500 m from the contaminated site while samples D and E were excavated from two other cultivated fields at a distance of 600 and 800 m, respectively. All samples were collected using a manual auger, dried at 105 °C for 24 h and sieved at 2 mm. The under sieve, after being quartered and homogenized to obtain a suitable sample, was manually ground into a fine powder using a ceramic mortar.

Heavy metals content and Pb isotope ratios ($^{208}Pb/^{206}Pb$ and $^{207}Pb/^{206}Pb$) were determined by ICP-MS after total microwave-assisted acid digestion. In detail, Pb isotope ratios were determined by analysing the same digested samples used for quantitative analysis. The analytical conditions were adapted from already published methods [316,317], by setting the instrument in Ratio mode, in which the voltages on the Universal Cell are decreased significantly to minimize the energy imparted to the ions in the cell. Moreover, a low flow of helium was introduced into the cell to equilibrate the ions' energy distribution. In order to increase the precision of the isotope ratio measurements, the signal intensities were recorded 200 times over 24×10^{-3} s, 18×10^{-3} s and 6×10^{-3} s for ^{206}Pb, ^{207}Pb and ^{208}Pb respectively. These ratios were used because ^{204}Pb both accounts only for a low percentage of Pb total abundance [318] and it is more difficult to measure by using mass spectroscopy due to the interference from ^{204}Hg [319].

The NIST SRM 981 isotopic ratios were used to correct for the mass discrimination of the ICP-MS by following the procedure reported by Barbaste *et al* [320].

6.2. Results and discussion

The presence of dumps or deposits of sulfate-rich materials, wherever they originated from the inappropriate disposal of sulfuric acid production's tailings or from the oxidation of sulfide minerals (i.e. pyrite, galena), upon exposure to air, microbial activities, or water is known to cause severe negative effects on the nearby environment, also posing risks for human health [321]. These effects include, for example, a very high acidity of water (i.e. pH 2-3) and the leaching of both sulphates and heavy metals (i.e. Cd, Co, Cr, Ni, Pb, Se, As, Tl, and Zn) [264,322]. Since these negative phenomena can last for hundreds of years, the management of such sites is of great importance, especially those, like our case study, which are situated in zones characterized by the presence of nearby swallow aquifers, surface waters or cultivated land [276].

6.2.1. Chemical and mineralogical characterization

Starting from the historical documents related to the past activities that have been conducted in this industrial area, and availing of some preliminary analysis, the parts of the property which have been used for the disposal of the contaminated tailings and wastes (red area in **Figure 6.1**) have been identified.

The characterization of a sample collected from the surface to 1.5 meters depth in the contaminated area has already been reported in chapter 4, showing the presence of a serious contamination, evident from both the heavy metals' content (i.e. Pb, As, Se, Hg and Sb) exceeding Italian regulations for industrial use of soils and sediments [101], and from the presence of clearly anthropogenic mineralogical phases (i.e. gypsum, anglesite, lithargite, jarosite, hematite and amorphous iron oxides).

The sample of topsoil taken from the center of the contaminated area (Sample A_T) showed a clear contamination (**Table S6.1**), with slightly higher concentrations of As, Be, Co, Cr, Cu, Hg, Pb, Sb, Sn and Zn with respect to the above-mentioned sample [291]. Similarly, XRD analysis of this sample (**Figure 6.2** and **Table S6.2**) highlighted both a slightly higher content of anthropogenic minerals and a lesser quantity of carbonates (dolomite and calcite) and silicates (quartz and muscovite). This difference can be attributed to the fact that sample A_T did not contain part of the less polluted soil found at higher depths. Regarding the other samples dug from the polluted site, ICP-MS analysis of sample A_S (**Table S6.3**) showed concentrations of heavy metals indicating the vertical percolation of

some pollutants, in particular of As, Hg, Pb, Sb, Se and Zn. The effects of this percolation could also be observed in the mineralogical composition of this sample (**Figure 6.2** and **Table S6.2**), which showed the presence of a minor quantity (ca. 4 w.t.%) of anthropogenic phases (i.e. hematite, gypsum, brushite, and fosfoferrite). Moreover, the effects of this percolation on the soil underneath the contaminated waste can be seen also from the lower content of calcite and dolomite observed in this sample compared to the quantity found in the nearest sample (30.4 and 45.3 w.t.%, respectively) taken at the same depth outside the contaminated zone (B_{1S}) (**Figure 5.2** and **Table S6.2**). These phenomena have already been observed as an effect of acid mine drainage and can be attributed to the acid behavior of the contaminated soil present above [322].

XRD analysis of sample B_{1T} (**Figure 6.2** and **Table S6.2**) highlighted only the presence of natural minerals (i.e. quartz, dolomite, calcite, albite , clinochlore, anorthite and muscovite), while the comparison with the spectra of a sample excavated at the same depth nearly 500 m outside the contaminated property (sample C_T) showed that no particular effect, save for a slight decomposition the carbonated minerals (i.e. calcite and dolomite), was caused on sample B_{1T} mineralogy by the presence of the contaminated waste.

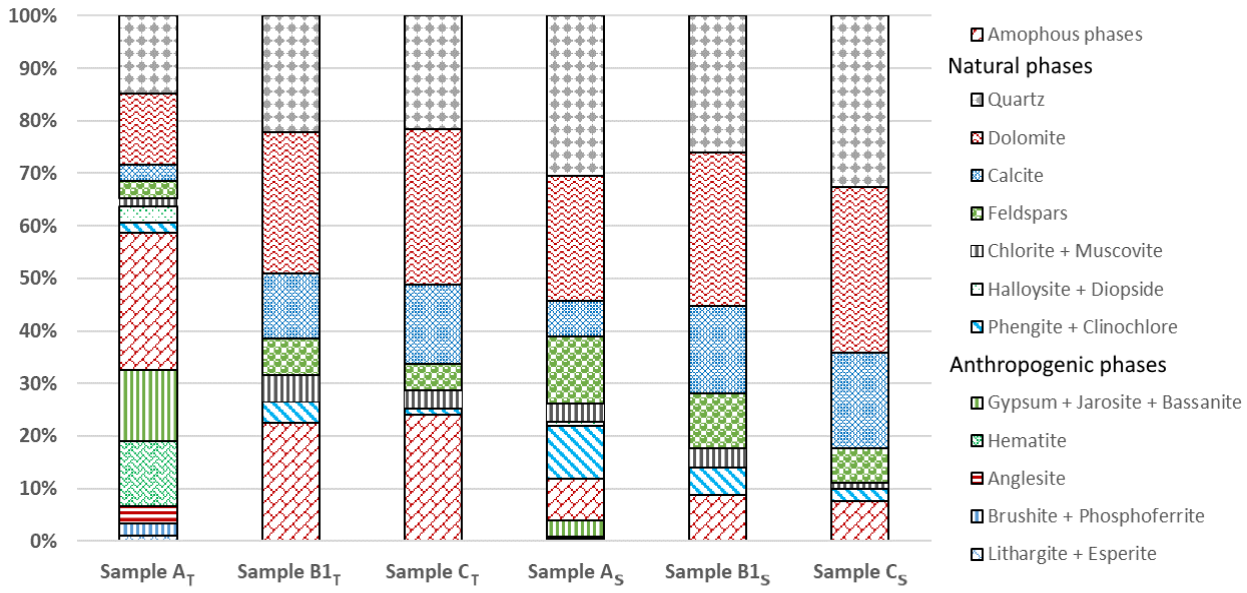

Figure 6.2. Mineralogical composition of samples taken from points A, B_1 and C.

A similar vertical gradient in the concentration of several heavy metals (i.e. As, Co, Hg, Pb, Sb, Se and Zn) from topsoil to subsoil can be observed also for the other sampling points, both inside and outside the property.

In addition, the migration of several contaminants from the contaminated waste to the surrounding area could also be observed from the concentrations observed in the other samples taken inside the site (samples $B_{1,2,3}$), both at surface level and at depth (**Table S5.1** and **Table S6.3**).

The concentrations of As, Cd, Cu, Pb, Sb, and Zn found at both depths on the edge of the property (sample B_3) were very similar to those observed in the samples from outside the property (samples C, D, and E), indicating either high natural background levels of these contaminants, their possible diffusion from the contaminated waste or the presence of other pollution sources such as deposition of smelting residues originating from the nearby smelters [323], combustion of leaded gasoline or the use of leaded pesticides [324,325].

Figure 6.3 shows, as an example of these gradients, the concentrations of Pb found for the different soil samples both inside the contaminated site and in the surrounding fields.

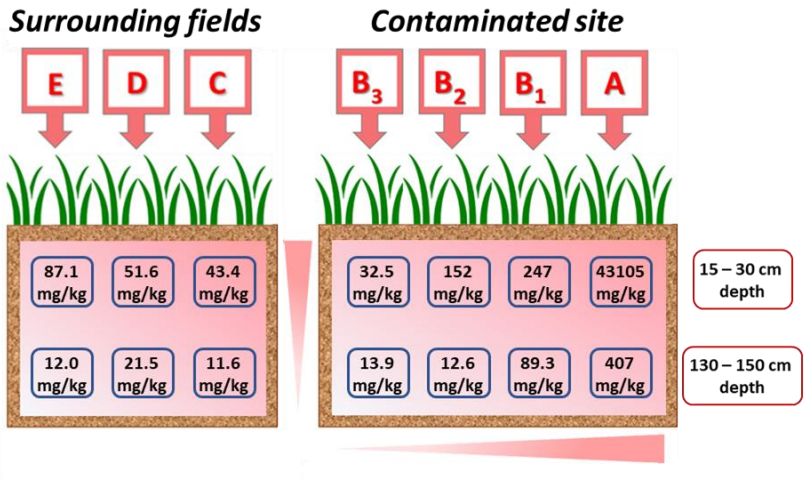

Figure 6.3. Pb concentrations observed inside and outside the contaminated property.

6.2.2. Isotopic analysis

In similar cases, to solve problems regarding the uncertain attribution of pollution to specific sources, isotopic fingerprinting has already been established as a useful tool to better trace pollution sources regarding different environmental compartments like soils, water, plants, animals and aerosols [319].

In this case, given the nature of the contamination, the Pb isotopic fingerprints of the various samples were used, together with a binary mixing model [326], as trackers to determine the origin of the pollution found in the lands near the dismissed industrial site.

In detail, the results are reported in **Table S6.4** and in the isotopic distribution plot $^{208}Pb/^{206}Pb$ vs $^{207}Pb/^{206}Pb$ (**Figure 6.4**), where four distinct areas can be recognized.

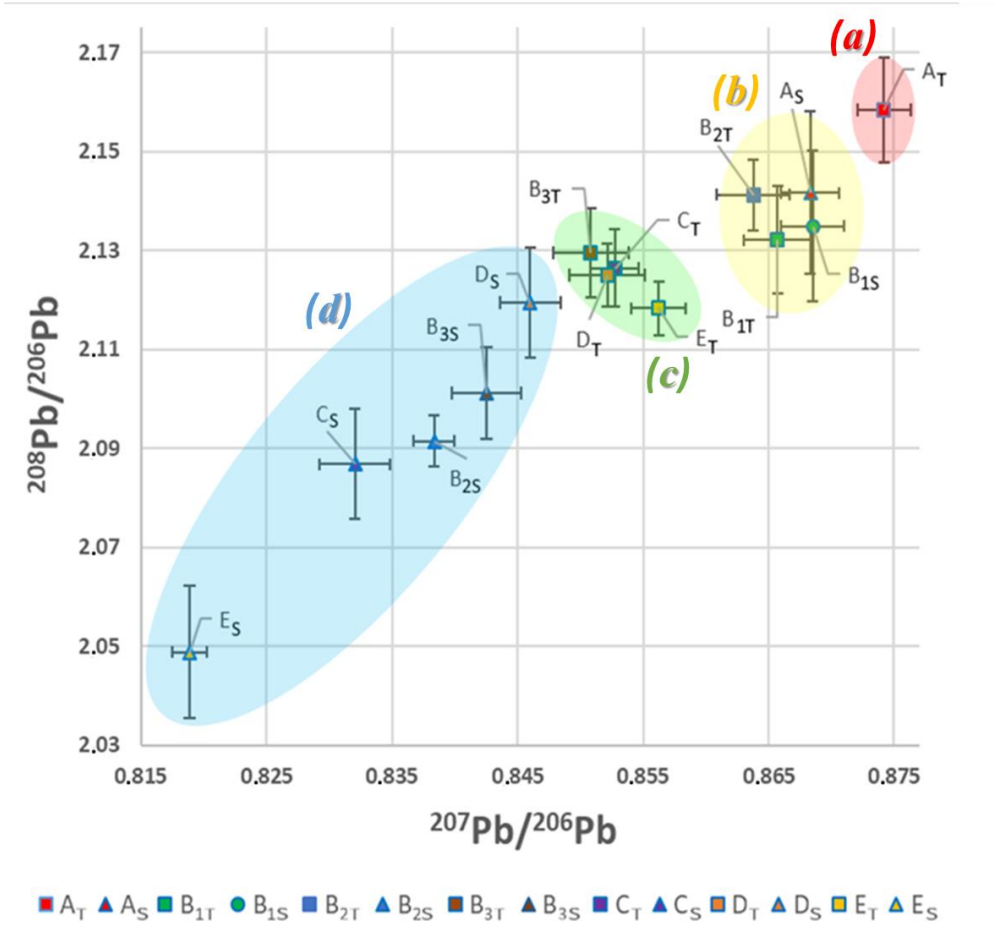

Figure 6.4. Isotopic distribution plot $^{208}Pb/^{206}Pb$ vs $^{207}Pb/^{206}Pb$.

The identification of well-defined areas in the isotopic ratio's graph, means that each geographical area, both within and outside the industrial site, has been subjected to a specific anthropogenic alteration. In detail, the red area ***(a)*** can be attributed to the industrial waste (sample A_T), while the yellow one ***(b)*** contains the isotopic fingerprints corresponding to the soils more affected by the presence of the industrial waste (samples A_S, $B_{1T\text{-}1S}$, and B_{2T}). The green area ***(c)*** groups together the isotopic fingerprints of both the topsoil sample inside the contaminated site nearest to the property's edge (sample B_{3T}) and the topsoil samples taken outside the polluted property (samples C_T, D_T, and E_T). The blue area ***(d)*** identifies the samples collected at 150 cm depth both in the field outside the property (samples C_S, D_S, and E_S) and near the property border (samples B_{2S} and B_{3S}).

As expected, since samples A_S, B_{1T}, B_{1S} and B_{2T} fall together inside area ***(b)*** their high heavy metals' concentrations can be attributed to the migration of contaminants from the nearby waste.

On the contrary, the low heavy metals' concentrations observed for samples B_{2S}, B_{3S}, C_S, D_S, and E_S, which are similar to those reported as background values in the literature [327], and the fact that the isotopic ratios of samples B_{2S} and B_{3S} fell into area ***(d)*** together with samples C_S, D_S and E_S, instead

of in area ***(b)*** with samples A_S and $B_{1T,S}$, indicates that no diffusion of pollution occurred between the contaminated site and the surrounding fields at that depth (130-150 cm).
Moreover, the significant difference between the isotopic ratios and the heavy metals' concentrations of samples B_{3S}, C_S, D_S, and E_S and those of the samples taken at the same places but at lower depth (samples B_{3T}, C_T, D_T, and E_T) confirms an increased contribution of pollutants deriving from anthropogenic activities, while the fact that all isotopic fingerprints of these top-soils fell together in area ***(c)*** indicates a common origin for their contamination.

To further investigate these findings and determine if this contamination has been caused by the run off from the contaminated waste or by other sources (i.e. fuel combustion, smelting emissions or use of pesticides and fertilizers), we applied a two sources model [326] to simulate the isotopic ratio of samples B_{1T}, B_{1S}, B_{2T}, B_{3T}, C_T, D_T, and E_T. In detail, we applied the following equation:

$$R_S{}^* = R_C \cdot \left(1 - ([Pb]_B/[Pb]_S)\right) + R_B \cdot ([Pb]_B/[Pb]_S) \qquad \text{(Eq. 6.1)}$$

where:

$R_S{}^*$: simulated isotopic ratio of the sample;

R_C: isotopic ratio of the contamination;

R_B: isotopic ratio of the background;

$[Pb]_B$: Pb concentration in the background;

$[Pb]_S$: Pb concentration in the sample.

We considered the $^{208}Pb/^{206}Pb$ and the $^{207}Pb/^{206}$ Pb ratios obtained for sample A_T as the contamination's isotopic fingerprint, while the means of the isotopic fingerprints and of the Pb concentrations observed for samples C_S, D_S and E_S were used an approximation of the respective background values. The results of this simulation ($B_{1T}{}^*$, B_{1S}*, B_{2T}*, $B_{3T}{}^*$, $C_T{}^*$, D_T, and $E_T{}^*$) are reported in **Figure 6.5** and compared with the results obtained by means of ICP-MS analysis.

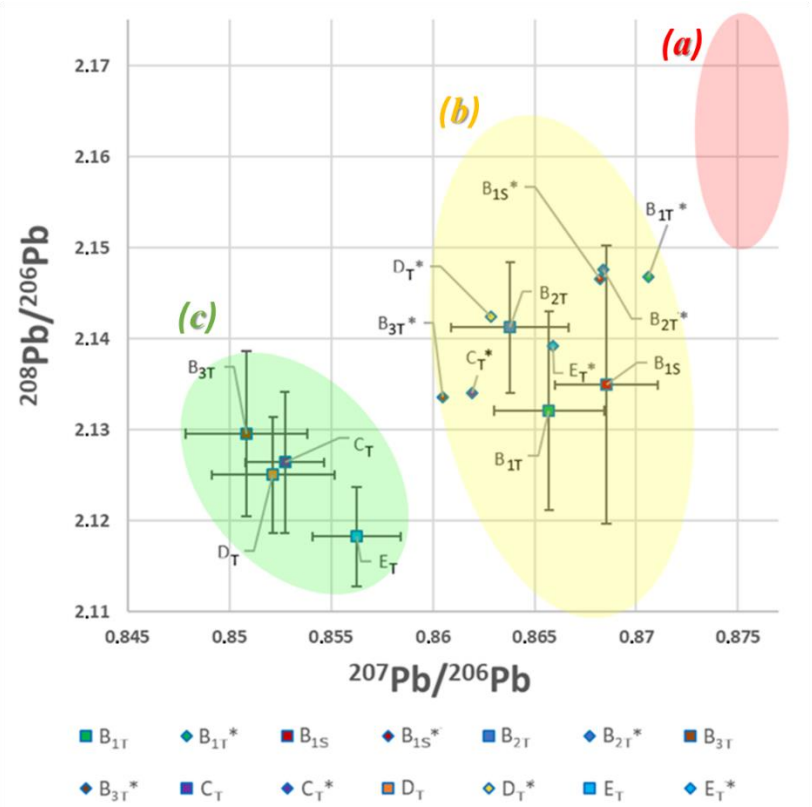

Figure 6.5. Isotopic distribution plot $^{208}Pb/^{206}Pb$ vs $^{207}Pb/^{206}Pb$.

The isotopic ratios simulated for sample B_{2T} (B_{2T}*) and B_{1T} (B_{1T}*) showed good agreement with the experimental data, confirming the migration of Pb and other heavy metals from the buried tailings. On the contrary, the simulated isotopic fingerprints of samples B_{3T} (B_{3T}*), C_T (C_T*), D_T (D_T*), and E_T (E_T*) fall within area ***(b)*** instead of area ***(c)***, showing very poor agreement with the experimental data. For this reason, we can conclude that the contamination of these samples is not directly attributable to the polluted waste buried in the industrial site, but was probably caused by other sources like pesticides, fuel combustion, smelting emissions or other non-point sources.

6.3. Conclusions

In this study stable Pb isotopes analysis was successfully applied, together with concentration mapping and XRD analysis, to ascertain the diffusion into the surrounding area of several heavy metals from a dismissed industrial plant devoted to sulfuric acid production where Pb-rich wastes were improperly disposed of.

While concentration mapping and XRD analysis of several samples taken at different depths both inside and outside the contaminated area clearly showed the percolation of several pollutants, the two techniques employed were not sufficient to establish with certainty if heavy metals migration from the waste occurred also outside the property.

The isotopic distribution plot $^{208}Pb/^{206}Pb$ vs $^{207}Pb/^{206}Pb$ and a two-source model were used to investigate the pollution sources responsible for the similar levels of contamination found both at the edge of the contaminated site and in the fields nearby. The results obtained from the simulation of these samples isotopic ratios lead to exclude the transport of heavy metals from the contaminated waste and attributed this contamination to other non-point sources like fuel combustion or emissions from the nearby smelters.

6.4. Supplementary Information

Table S6.1. Heavy metals content of the topsoil samples excavated from 15 to 30 cm depth (series "T").

Parameter	Sample A_T	Sample B_{1T}	Sample B_{2T}	Sample B_{3T}	Sample C_T	Sample D_T	Sample E_T	Regulatory Limit*
	mg·kg^{-1} d.w.							
As	453±20	34.6±1.3	37.5±1.5	17.0±0.7	15.29±0.6	21.3±0.9	21.0±0.9	50
Be	2.60±0.14	1.86±0.12	1.03±0.15	0.98±0.17	1.57±0.12	1.88±0.19	1.32±0.08	10
Cd	2.44±0.22	1.64±0.17	0.76±0.19	0.55±0.16	0.54±0.12	0.62±0.13	0.61±0.11	15
Co	53.3±4.4	13.5±1.3	14.3±1.3	7.2±0.7	12.6±1.1	17.6±1.6	10.4±0.9	250
Cr	111±7	90.9±7.4	93.0±6.9	82.3±6.1	83.2±6.2	72.9±5.4	67.6±5.0	500
Cu	339±22	96.5±8.7	112±8.7	31.0±2.4	36.0±2.8	41.6±3.2	34.3±2.6	600
Hg	9.09±0.68	0.44±0.10	0.31±0.11	0.22±0.10	0.14±0.05	0.20±0.11	0.28±0.08	5
Ni	39.2±3.1	22.2±1.4	27.4±1.9	25.0±1.8	30.8±2.2	32.5±2.3	29.1±2.1	800
Pb	43105±1200	248±15	152±7	32.1±1.4	43.4±1.9	51.6±2.3	87.1±3.9	1000
Sb	54.3±3.3	4.32±0.44	3.94±0.31	2.01±0.24	1.97±0.20	2.38±0.23	3.09±0.25	30
Se	393±26	1.88±0.21	1.02±0.10	0.67±0.10	0.58±0.12	0.32±0.09	0.42±0.08	15
Sn	90.3±6.0	8.80±1.21	3.96±0.4	2.78±0.3	3.94±0.4	5.01±0.5	4.55±0.46	350
Tl	2.13±0.44	0.86±0.10	0.81±0.1	0.75±0.1	0.68±0.1	0.79±0.10	0.73±0.12	10
V	58.2±4.9	79.0±5.2	76.0±5.7	60.9±4.6	90.6±6.8	102±7.6	98.1±7.4	250
Zn	574±36	420±29	173±11.4	145±9.5	150±9.9	161±10.6	162±11	1500

* Regulatory limit: Column B (commercial and industrial use) of Table 1 of Annex V to Part IV of Title V of Legislative Decree No 152 of 03/04/2006 [101].

Table S6.2. Mineralogical composition of samples taken from points A, B_1 and C. (l.o.d.: limit of detection).

Phase	Formula	Sample A_T	Sample B_{1T}	Sample C_T	Sample A_S	Sample B_{1S}	Sample C_S
		w.t. %					
Quartz	SiO_2	14.9±1.1	21.7±1.3	21.6±1.5	30.4±1.8	25.8±1.3	32.5±2.1
Dolomite	$MgCa(CO_3)_2$	13.5±0.9	26.1±1.2	29.6±1.4	23.7±1.3	28.9±1.0	31.5±1.4
Calcite	$CaCO_3$	3.0±0.4	12.2±0.8	15.3±0.9	6.7±0.7	16.4±1.0	18.3±0.8
Albite	$NaAlSi_3O_8$	3.3±0.4	6.8±0.5	3.8±0.4	4.8±0.3	7.0±0.8	3.1±0.5
Chlorite	$(MgFeAl)_8(SiAl)_8O_{20}(OH)_{16}$	< l.o.d.	< l.o.d.	< l.o.d.	3.3±0.4	3.5±0.3	< l.o.d.
Phengite	$K_2Al_4(Si_6Al_2O_{20})(OH)_4$	< l.o.d.	< l.o.d.	< l.o.d.	6.6±0.5	5.3±0.6	< l.o.d.
Orthoclase	$KAlSi_3O_8$	< l.o.d.	< l.o.d.	< l.o.d.	1.5±0.5	3.5±0.4	< l.o.d.
Clinochlore	$(Mg,Fe^{+2})_5Al(Si_3Al)O_{10}(OH)_8$	1.8±0.3	4.0±0.3	3.0±0.4	3.4±0.2	< l.o.d.	2.5±0.4
Anorthite	$CaAl_2Si_2O_8$	< l.o.d.	< l.o.d.	1.2±0.3	4.9±0.5	< l.o.d.	3.4±0.4
Microcline	$KAlSi_3O_8$	< l.o.d.	< l.o.d.	< l.o.d.	1.7±0.3	< l.o.d.	< l.o.d.
Muscovite	$KAl_2(Si_3Al)O_{10}(OH,F)_2$	1.6±0.5	4.9±0.6	3.4±0.4	< l.o.d.	< l.o.d.	1.1±0.4
Halloysite	$Al_2Si_2O_5(OH)_4$	1.1±0.5	< l.o.d.	< l.o.d.	0.9±0.4	< l.o.d.	< l.o.d.
Diopside	$CaMgSi_2O_6$	2.1±0.3	< l.o.d.	< l.o.d.	< l.o.d.	< l.o.d.	< l.o.d.
Amorphous	-	26.3±1.5	21.9±1.4	24.1±1.2	7.9±0.6	8.6±0.7	7.5±0.5
Anglesite	$PbSO_4$	3.4±0.4	< l.o.d.	< l.o.d.	< l.o.d.	< l.o.d.	< l.o.d.
Haematite	Fe_2O_3	12.4±0.8	< l.o.d.	< l.o.d.	0.4±0.2	< l.o.d.	< l.o.d.
Jarosite	$KFe_3\ (SO_4)_2(OH)_6$	2.8±0.4	< l.o.d.	< l.o.d.	< l.o.d.	< l.o.d.	< l.o.d.
Gypsium	$CaSO_4{\cdot}2(H_2O)$	10.1±0.8	< l.o.d.	< l.o.d.	3.1±0.2	< l.o.d.	< l.o.d.
Esperite	$PbCa_3Zn_4(SiO_4)_4$	0.7±0.2	< l.o.d.	< l.o.d.	< l.o.d.	< l.o.d.	< l.o.d.
Brushite	$CaHPO_4{\cdot}2(H_2O)$	1.6±0.3	< l.o.d.	< l.o.d.	0.3±0.1	< l.o.d.	< l.o.d.
Phosphoferrite	$(Fe^{2+},Mn^{2+})3(PO_4)_2{\cdot}3H_2O$	0.6±0.2	< l.o.d.	< l.o.d.	0.1±0.05	< l.o.d.	< l.o.d.
Lithargite	PbO	0.4±0.2	< l.o.d.	< l.o.d.	< l.o.d.	< l.o.d.	< l.o.d.
Bassanite	$CaSO_4{\cdot}0,5(H_2O)$	0.5±0.3	< l.o.d.	< l.o.d.	< l.o.d.	< l.o.d.	< l.o.d.

Table S6.3. Heavy metals content of the subsoil samples excavated from 130 to 150 cm depth (series "S")

Parameter	Sample A_S	Sample B_{1S}	Sample B_{2S}	Sample B_{3S}	Sample C_S	Sample D_S	Sample E_S	Regulatory Limit*
	$mg \cdot kg^{-1}$ d.w.							
As	49.0±4.0	15.2±2.3	10.1±1.2	6.54±0.75	10.0±1.1	12.0±1.0	8.97±1.0	50
Be	1.24±0.13	1.00±0.16	0.59±0.08	0.82±0.11	0.75±0.10	0.89±0.12	0.44±0.06	10
Cd	0.72±0.12	0.34±0.06	0.28±0.05	0.24±0.04	0.16±0.03	0.27±0.05	0.20±0.03	15
Co	11.2±1.2	7.27±1.0	5.47±0.66	3.49±0.49	5.07±0.71	3.23±0.45	2.13±0.30	250
Cr	51.5±4.3	45.8±1.5	32.8±2.8	28.5±2.5	34.0±2.9	36.6±2.2	22.1±1.9	500
Cu	52.7±4.8	43.5±1.3	8.01±0.54	10.9±0.7	13.7±0.9	11.0±0.7	10.2±0.6	600
Hg	0.94±0.11	0.21±0.05	< 0.1	< 0.1	<0.1	< 0.1	< 0.1	5
Ni	23.6±1.9	15.4±0.3	13.2±1.5	10.5±1.1	11.8±1.3	15.7±1.2	12.9±1.5	800
Pb	407±10	89.3±5.5	12.6±0.7	13.9±0.8	11.6±0.6	21.5±0.7	12.0±0.7	1000
Sb	4.25±0.32	2.57±0.40	0.96±0.11	1.66±0.19	0.99±0.11	1.50±0.17	1.15±0.13	30
Se	4.01±0.38	0.59±0.10	0.42±0.06	0.37±0.06	0.22±0.08	0.28±0.07	0.23±0.09	15
Sn	4.51±0.57	2.22±0.12	1.80±0.22	2.07±0.16	1.27±0.22	1.38±0.18	1.56±0.19	350
Se	0.40±0.08	0.28±0.03	0.14±0.04	0.26±0.05	0.23±0.07	0.33±0.05	0.26±0.06	10
V	44.1±2.0	44.5±2.7	45.2±2.4	46.5±2.2	42.3±2.1	58.8±3.0	37.9±2.0	250
Zn	174±7	102±8	52.9±4.5	55.5±4.8	46.3±3.1	53.7±4.6	42.7±3.7	1500

* Regulatory limit: Column B (commercial and industrial use) of Table 1 of Annex V to Part IV of Title V of Legislative Decree 152 of 03/04/2006 [101].

Table S6.4. Isotopic ratios $^{208}Pb/^{206}Pb$ and $^{207}Pb/^{206}Pb$ for all the investigated samples.

Sample	$^{208}Pb/^{206}Pb$	$^{207}Pb/^{206}Pb$		$^{208}Pb/^{206}Pb$	$^{207}Pb/^{206}Pb$
Sample A_T	2.1584±0.0106	0.8742±0.0021	**Sample A_S**	2.1416±0.0164	0.8683±0.0023
Sample $B1_T$	2.1321±0.0109	0.8657±0.0027	**Sample B_{1S}**	2.1349±0.0153	0.8685±0.0025
Sample $B2_T$	2.1412±0.0072	0.8638±0.0029	**Sample B_{2S}**	2.0914±0.0052	0.8383±0.0016
Sample $B3_T$	2.1295±0.0091	0.8508±0.0030	**Sample $B3_S$**	2.1012±0.0094	0.8425±0.0028
Sample C_T	2.1264±0.0078	0.8527±0.0019	**Sample C_S**	2.0868±0.0112	0.8320±0.0028
Sample D_T	2.1250±0.0064	0.8521±0.0030	**Sample D_S**	2.1195±0.0110	0.8460±0.0024
Sample E_T	2.1183±0.0054	0.8563±0.0022	**Sample E_S**	2.0488±0.0134	0.8189±0.0014

7. Chapter 7

HPSS-NanoExtra: a new integrated process for heavy metals' recovery from stabilized matrixes

Loris Calgaro[1], Petra Scanferla[2], Roberto Pellay[3], Antonio Marcomini[1]

[1]Department of Environmental Sciences, Informatics and Statistics, University Ca' Foscari of Venice, Via Torino 155, 30172 Venice Mestre, Italy.
[2]Fondazione Università Ca' Foscari, Ca' Dolfin, Calle Larga Ca' Foscari, Dorsoduro 3859/A, 30123 Venice
[3]Ingegnerie e Tecnologie Ecologiche (In.T.Ec.) s.r.l., Via Romea 8, 30034 Malcontenta di Mira, Venice, Italy

Metals and metalloids have become one of the most widespread sources of pollution in the world, affecting both soils and waters, and making the management of contaminated materials a significant issue in the last decades. For example, more than 50% of the 10 million contaminated sites reported worldwide resulted polluted by metals and metalloids [328], and it has been estimated that nearly 10-20% on a weight basis of all the sediments dredged every year for the maintenance of harbors, canals and other waterways are also contaminated [329].
This kind of contamination is not limited to soils and sediments, but also affects a relevant amount of the municipal solid waste (MSW) produced worldwide.

For these reasons, sustainable and environmentally acceptable strategies for the management of these materials are needed. In this context, the design of modern sanitary landfills can guarantee an environmentally acceptable way of waste disposal, provided they are properly operated. However, the introduction of increasingly stringent laws on landfill liners and emissions (i.e. leachate and landfill gas collection and control systems) and long-term closure requirements caused a dramatic increase in the cost of landfilling. In addition, finding suitable locations for landfill sites close to cities of urbanized areas is becoming more and more difficult due to public pressure and the diffusion of the Not-In-My-Back-Yard (NIMBY) attitude, which have increased the difficulty of many communities in the siting and permitting of these new landfills.
Consequently, as existing landfill capacity has been reduced, interest has increased in the concept of recovering energy and recyclable materials from contaminated wastes rather than relying on sanitary landfilling as the primary long-term method of solid waste disposal [330,331], as demonstrated by the Circular Economy Package adopted by the EU Commission at the end of 2015. Most contaminated wastes in Italy are usually sent to landfill disposal, either as they are or after some pre-treatments.

One of the most used technologies used to treat these matrixes are solidification/stabilization (S/S) treatments, which only in a few rare cases allow to obtain a reusable material.
The HPSS® process (High Performance Solidification / Stabilization) [221]) is an established technology for the "on-site" treatment of soils, sediments and waste of predominantly inorganic nature capable to obtain a reusable hardened granular material. However, this technology does not currently allow the recovery of the heavy metals present in the treated matrix, leading both to the loss of a potential source of precious metals, whose demand is constantly increasing, and to their potential release in the environment over time, though in concentrations below the regulatory limits set for waste recovery [114].

In this context, my work was developed within the HPSS-NANOEXTRA project (Veneto Region, POR FESR 2014-2020- ID 10052461), which aimed at the development of an innovative

technology for the treatment of special/hazardous waste (i.e. contaminated soil and sediments, fly ash, bottom ash, sewage sludge from chemical-physical treatment of wastewater) that, coupled with the already established HPSS® process, allowed to produce re-usable materials and to recover heavy metals by extraction. In particular, the decontamination process was applied:

- to the stabilized granulate produced by using the HPSS® technology, according to the consolidated formulation, in order to produce a granular material having a reduced content of heavy metals but still maintaining both the mechanical and leaching characteristics necessary to be classified as a reusable material [221].
- to the treated matrix in order to produce a no longer contaminated material, according to the limits imposed by the Italian legislation for commercial and industrial use of soils and sediments [101]

This project therefore proposed the development of an extraction process allowing the removal of the heavy metals contained in the granulate obtained from the use of HPSS® technology, coupled with a system for recycling the extractant solution and recovering heavy metals.

The granulation step (amount of binder and additives), each step of the extracting process (i.e. extractant composition, time of contact with the contaminated material), of the recycling process (i.e. pre-treatment and membrane filtration of the leachate) and of the heavy metals recovery (i.e. pH of precipitation, use and dosage of coagulating additives) has been optimized in order to properly design a *bench scale* prototype. Moreover, the use of various alkali-activated binders was investigated as a more sustainable alternative compared to Ordinary Portland Cement (OPC).

The research has been divided into the following work packages (WPs):

WP1. Bibliographical research

Both patent and scientific literature has been used to identify the most promising lines of research to be used as a starting point for the design and optimization of the HPSS-NanoExtra process. This research focused on:

- Soil washing: processes to extract organic and inorganic contaminants from polluted materials by using physical or chemical separation technologies.
- Membrane separation: processes used to concentrate or purify mixtures of various substances by utilizing semipermeable membranes as separation barriers to divide two phases and restrict the transport of various components in a selective manner.
- Removal of heavy metal ions from wastewater: processes used to remove heavy metal ions from wastewater producing a recoverable metal-rich sludge.
- Alkali-activated binders: a class of inorganic materials, obtained from the chemical reaction between aluminosilicate oxides and alkaline silicates, characterized by the

formation of polymeric Si-O-Al bonds, which can be used as binders as an alternative to Ordinary Portland Cement.

WP2. Process design

The information obtained from the literature has been used to identify the most promising techniques for each step of the process and to design each treatment step.

WP3. Selection and characterization of binders and contaminated materials

During this phase, the contaminated materials to be used for this research have been chosen and characterized, together with each component of the various proposed binders.

Macro samples of each contaminated material have been prepared and, based on the contamination present, the metals of interest have been identified.

WP4. Preliminary experiments

During this phase, the selected contaminated materials were treated with the HPSS® technology, following the formulations discussed in chapter 6.3.1., and the obtained granular materials were used to run a series of preliminary tests to optimize the extraction process. In particular, the influence of binder formulation, of leachant concentration and of chelating agents' use were investigated. The obtained results were used to optimize the proposed bench scale prototype.

WP5. Bench scale testing

Based on the results produced in the previous phases of the study, the final design and operating conditions of the bench-scale plant were selected. The effectiveness of the nanofiltration step for NaOH recovery was investigated, followed by the optimization of the treatment to recover heavy metals from the concentrated fraction. These results were used to test the effectiveness of the entire process on one of the contaminated materials previously selected. In addition, the effects of the wet conditioning process were investigated for the granulate produced following the standard formulation.

7.1. WP1: Bibliographical research

The information obtained from both patent and scientific literature used to identify the most promising lines of research to be considered as a starting point for the design and optimization of the HPSS-NanoExtra process is reported below.

7.1.1. Soil washing

The term "soil washing" refers to *ex situ* technologies that use physical and/or chemical procedures to extract contaminants (metallic or organic) not only from contaminated soils and sediments, but also from other wastes.

Physical Separation processes are used to concentrate the contaminants in a smaller volume of material, exploiting the differences in some physical characteristics between the metal-bearing particles and the matrix's particles (i.e. dimensions, density, magnetism, hydrophobicity and hydrophilicity). Chemical Extraction techniques aim to solubilize contaminants from the contaminated material into an aqueous extracting fluid containing chemical reagents such as acids, bases or chelating agents [332]. In general, physical separation processes are mainly applicable when heavy metals are in the form of discrete particles, while chemical extraction is usually suitable when they are present in adsorbed ionic forms or as non-detrital metals. Physical separation processes generally use technologies deriving from the mining sector and the mineral processing industry (i.e. mechanical screening, hydrodynamic classification, concentration by gravity, foam flotation, magnetic separation, electrostatic separation and friction washing) to extract metal particles from the contaminated matrix [333]. These techniques cannot usually be applied if: (1) the heavy metals are strongly bound to the contaminated matrix particles; (2) the density or the surface properties of metal-bearing particles and soil do not differ significantly; (3) the contaminants are present in a multitude of different chemical forms; (4) the heavy metals are found in all particle size fractions of the polluted matrix; (5) the soil contains more than 30–50% w/w of silt or clay; (6) the soil present a high humic content and (7) the soil contains very viscous organic compounds [332].

Chemical extraction processes use an extracting fluid containing one or more chemical reagents (acids/bases, surfactants, chelating agents, salts or red-ox agents) to transfer the contaminant from the polluted matrix to the leaching solution, either by dissolving the phases to which the contaminants are bound, or by converting the contaminants into more soluble forms.

To better estimate the effectiveness of these processes, sequential extraction procedures [334,335] are often applied to the treated soils and sediments, showing that the most easily removed metals by chemical leaching are those of the exchangeable fraction and those associated with carbonates and reducible Fe-Mn oxides [336]. In particular, the extraction of metals associated with the exchangeable and carbonate fractions is quite faster than the extraction of metals linked to Fe-Mn oxides [337,338]. Factors that may limit the applicability and effectiveness of chemical extraction processes include: (1) high content of clay, silt and humic acids; (2) high content of Fe and Ca; (3) high calcite content or high acid neutralization capacity; (4) simultaneous presence of cationic and anionic contaminants;

(5) high soil heterogeneity; (6) presence of metals associated with the residual fraction of the soil, incorporated in the mineral lattices, or in the form of discrete particles [339,340]. In large-scale operations, chemical extraction processes are mainly classified as percolation leaching, if the leach solution is sprayed on a heap/pile of material and allowed to percolate downward through the heap, or as agitated leaching if the process is carried out under turbulent flow conditions into specifically designed reactors [341]. These processes can become significantly more convenient if the chemical reagents are not hazardous and can be recycled or regenerated. However, several disadvantages must be considered, such as the fact that the treated soil may not be appropriate for revegetation or on-site reuse due to a change of its physical, chemical and microbiological properties, or that the presence of toxic chemical agents in the final products (treated matrix, residual sludge and exhausted extraction fluid) can cause various problems for disposal. Moreover, the presence of some chemical agents in the extraction fluid can make recycling and treatment more complex, thus increasing the overall costs of the process [332].

In the following paragraphs the main applications of these processes will be briefly discussed.

7.1.1.1. Acid extraction

Acid extraction is an already established technology for the treatment of contaminated soils, sediments, and sludges, with many operational industrial scale units.

There are several mechanisms involved in the extraction of metals using an acid solution, like the desorption of metal cations via ion exchange, the dissolution of metal compounds and the dissolution of soil mineral components (i.e. carbonates, sulphates, phosphates, and Fe–Mn oxides) which may contain metal contaminants [342,343]. The use of both strong mineral acids (HCl, H_2SO_4, HNO_3 and H_3PO_4) and weak organic acids (acetic acid) has been reported, with different results depending on the contaminants, the soil geochemistry, and the reagents concentrations [177].

Moreover, the co-dissolution of various soil components is a fundamental parameter from an environmental and an economic point of view, because these treatments may cause the loss (up to 50%) of the soil minerals [340] and organic matter [344], therefore increasing the acidity of the treated soil [344], the consumption of acid reagent and the complexity of the wastewater treatment [340]. For these reasons, acid leaching is not suitable for materials that have a high buffering capacity such as calcareous soils or cementitious materials [339]. In addition, although these processes are efficient in extracting metals from contaminated materials, their full-scale application presents various disadvantages, such as damaging the soil microbiology and fertility, the need to neutralize wastewater and processed soils, the production of big amounts of new toxic residues and the problems related to their disposal.

7.1.1.2. Basic extraction

The use of basic solutions for the removal of heavy metals has been studied, exploiting both the amphoteric characteristics of some contaminants (i.e. Ni, Cr, Cu, Pb, Se) and the hydroxide ions' propensity to replace the metal compounds adsorbed on the surface of the contaminated particles. The removal of As, Cr and Cu from a contaminated soil by using a heated (80°C) NaOH 1 M solution has been reported by Reynier *et al* [345], while Dalgren *et al.* [346] reported that As is better removed using alkaline (pH = 12) rather than acid (pH = 3) solutions (35% and 1 % removal, respectively). Jang *et al.* reported the complete removal of As from the tailing of a closed iron mine by using highly concentrated NaOH solutions (1-2 M) with a solid/liquid ratio of 1/5 [347]. It has also been reported that the use of NaOH to extract Cr and Cu leads to the formation of highly soluble chromate and hydroxycuprate species [348,349]. The use of alkaline leaching solutions does not cause the degradation of carbonated or cementitious minerals, but they may be subjected to carbonation problems due to atmospheric CO_2 dissolution. This last fact may offer a relatively cheaper way to neutralize both the treated materials and the spent solutions than the use of other acids.

7.1.1.3. Chelant extraction

The ability of some compounds to form stable and not absorbable metal complexes offers a promising method to remove these contaminants from polluted materials but, while the application of these reagents can improve the removal efficiency, it may also cause problems if toxic or non-biodegradable products are used. The best removal efficiency has been obtained using ethylenediaminetetraacetic acid (EDTA) nitrilotriacetic acid (NTA) and citric acid together with various inorganic acids, while gluconate, oxalate, ammonium acetate showed less satisfactory results [336]. EDTA is particularly effective in removing metallic cations bound to the exchangeable, carbonate ang organic fractions, but is less efficient for those bound to reducible Fe-Mn oxides and tends to form stable complexes also with Fe^{3+} and Ca^{2+} ions [338,350,351].
Moreover, various processes have been developed to recycle these reagents, in order to make the overall treatment more convenient. The most used include precipitation and chelant regeneration by adding chemical agents, electrochemical procedures, ion exchange processes, and nanofiltration [352].

7.1.1.4. Extraction using diluted acid solutions containing chloride salts

The use of diluted acid solutions containing chloride salts has been investigated as an alternative to the use of concentrated mineral acids, because they would not affect soil mineralogy by lessening both co-dissolution and acidification phenomena [332]. These treatments exploit the

dissolution of heavy metals due to the formation of soluble Cl-complexes and ion-exchange with monovalent cations (i.e. Na^+ and K^+) [353]. The overall costs of these treatments can be significantly decreased by recycling the leaching solution, as shown by Meunier *et al*, who studied the recovery of a spent $NaCl/H_2SO_4$ solution by means of chemical precipitation, coagulation and electrochemical precipitation [354].Good performances have been reported by Nedwed *et al.* [353] for the removal of Pb, but the careful control of both pH and redox potential needed to avoid the formation of insoluble compounds makes the large scale implementation of these processes quite difficult.

7.1.2. Membrane separation

The need to separate, concentrate and purify mixtures of various substances is one of the major problems encountered in many sectors of today industry, such as food, pharmaceuticals and other high-grade materials production, as well as in the removal/recovery of toxic or valuable components from wastewaters. To this purpose, a multitude of conventional separation methods have been developed (i.e. distillation, precipitation, crystallization, extraction, adsorption, and ion-exchange), but these have been also supplemented by a family of processes utilizing semipermeable membranes as separation barriers to separate two phases and restrict the transport of various components in a selective manner.[355]

The first introduction of membranes and membrane processes can be traced back to the development of analytical tools in chemical and biomedical laboratories, which was followed by the development of many products and methods characterized by significant technical and commercial impact [356–359]. Today, membrane technology is used for a large number of large-scale applications such as the production of potable water from sea and brackish water, the purification of industrial effluents, the recovery, concentration and purification of valuable substances or macromolecular mixtures in the food and drug industries. These systems are also key components in energy conversion and storage systems, in chemical reactors, in artificial organs and in drug delivery devices [360].

Membranes can be classified using various systems, according to the nature of their materials, morphology, geometry, preparation methods, and to the driving force of the separation process.

According to the driving force applied, membrane processes can be classified as pressure-driven processes (microfiltration (MF), ultrafiltration (UF), nanofiltration (NF), reverse osmosis (RO)), partial-pressure-driven processes (pervaporation), concentration/gradient-driven processes (dialysis), temperature-driven processes (membrane distillation) and electrical potential-driven processes (electrodialysis). **Figure 7.1** shows the pore sizes, working pressures and the ranges of applications for the pressure-driven membrane processes used for the treatment of water, wastewater and other liquid feeds [355].

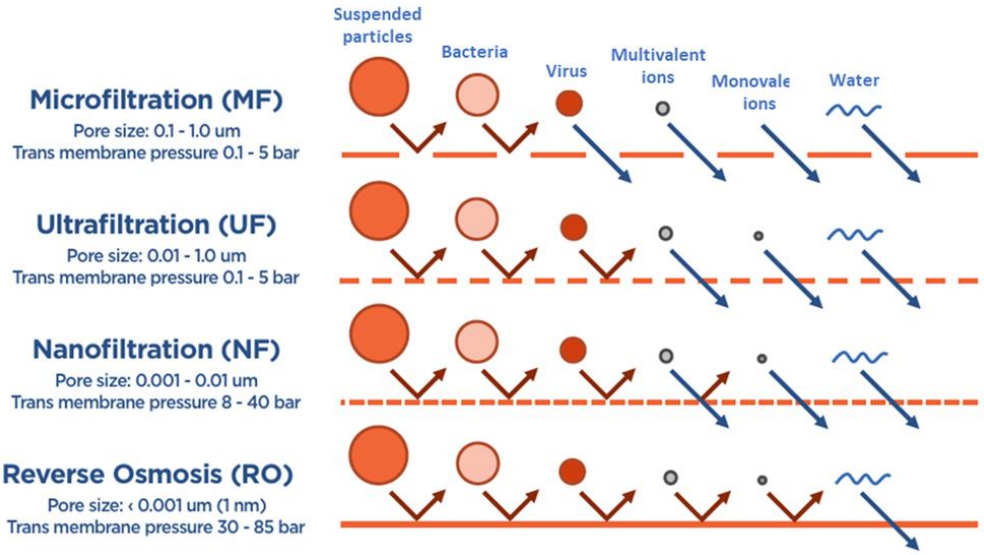

Figure 7.1. Pressure-driven membrane processes used for the treatment of water, wastewater and other liquid feeds.

Membrane filtration can be operated basically in two modes: dead-end and crossflow.

In dead-end mode, the feed flows perpendicularly to the membrane, causing the retained particles and other components to accumulate and deposit on its surface, while in crossflow mode the feed stream moves parallel to the membrane surface, so that only a portion passes through the membrane under the driving pressure. This can result in higher permeation fluxes and lower fouling in comparison with dead-end mode, since the stream continuously removes retained material. Moreover, the deposited material can be removed by using various methods, such as backwashing or ultrasonic vibrations. However, higher set-up and operational costs are required by the crossflow mode due to the more complex equipment and to the energy required to circulate the feed flow.

The main problems found for this technology are the decrease of the membrane's efficiency due to fouling phenomena and the costs related to membrane cleaning and replacement. Membrane fouling can be defined as the deposition of material on or within the structure of membranes that cannot be readily reversed by simply releasing the pressure or by backwashing. These very complex phenomena are closely related to the feed solution properties (ionic strength, concentration, pH and component interactions), the nature of the membrane (charge, roughness, hydrophobicity, pore size, pore size distribution and porosity) and the operating conditions (temperature, transmembrane pressure (TMP) and crossflow velocity)[361,362].

Most of the membranes used today for water and wastewater treatment are prepared by using a large variety of crystalline, amorphous or glassy organic polymers, such as cellulose, cellulose acetate, polysulfone, polyethersulfone, polyacrylonitrile, polyvinylidene fluoride, polyetherimide, polycarbonate, polyamide, polyimide and polyether ether ketones [363].

7.1.2.1. Nanofiltration

The term “nanofiltration” was first introduced by FilmTec in the second half of the 1980s, indicating a reverse osmosis (RO) process capable to selectively and purposely allow some ionic solutes in the feed water to permeate through, even if membrane characterized by a selectivity between RO and ultra-filtration (UF) have been known since the 1960s [364,365].

Differently from RO membranes, which have a non-porous structure and a transport mechanism based on solution-diffusion phenomena, nanofiltration (NF) membranes are characterized by the presence of both porous and non-porous layers and can work with both sieving and diffusion transport mechanisms.

These properties enable NF membranes to be operated at higher water fluxes with much lower pressure compared to RO membranes, resulting in significant energy saving and costs reduction. In addition, most NF membranes can also be surface charged to add electric interactions to the transport mechanisms that control their selective rejection behaviour [355].

Nanofiltration membranes are characterized by high permeability for monovalent salts (e.g. NaOH, NaCl and KCl), but they can also near completely retain multivalent salts and remove relatively small organic molecules [366]. In particular, nanofiltration has been already used to recover sodium hydroxide from the effluents and wastewaters produced in a multitude of processes, such as mercerization [367,368], hemicelluloses extraction from wheat bran [369], polyester fabrics production [370], chitin processing [371] and alkaline cleaning [372].The most used nanofiltration membranes for these applications are asymmetric thin-film composite membranes with a dense active surface layer and a porous support layer usually made from polysulfone, polyethersulfone and poly (vinylidene fluoride) [373].

Nanofiltration has already been applied with good results for the treatment of acid leachates obtained from conventional soil washing processes to recover heavy metals [374–377], while the treatment of the leachate obtained from alkaline soil washing has been comparatively much less investigated.

Nanofiltration membranes have been reported to be sensitive to fouling phenomena caused by the precipitation and accumulation of insoluble compounds on their surface, in particular in the case of Ca^{2+} and Mg^{2+}.

7.1.3. Removal of heavy metals ions from wastewaters

Due to the increasingly stringent regulations applied for the discharge of metal contaminants in the environment, many methods for their removal from wastewaters and other effluents have been

developed, including chemical precipitation, ion-exchange, adsorption, membrane filtration, and electrochemical treatment technologies.

In particular, chemical precipitation methods are very effective and by far the most widely used industrial processes [378] due to their relative inexpensiveness and simplicity of use. In these processes, chemicals react with heavy metal ions to form insoluble precipitates, which can be separated from the water by filtration or flocculation and sedimentation. The two most used conventional chemical precipitation processes are hydroxide precipitation and sulphide precipitation. Between the two, hydroxide precipitation is the most widely applied due to its relative simplicity, lower cost and ease of pH control [379]. Due to the low cost and ease of handling, lime ($Ca(OH)_2$) is the preferred choice of base used in hydroxide precipitation at industrial settings [380].The addition of coagulants such as alum, iron salts and organic polymers can enhance heavy metals removal from wastewater [381], in particular for those of environmental concern, such as As, Pb, Cd, Ni, Hg, Co and Cu [382].

Although widely used, hydroxide precipitation presents various problems. For example, it generates large volumes of relatively low density sludge, which can be difficult to dewater and dispose of [383]. Secondly, due to the amphoteric behaviour of some metal hydroxides, the ideal pH for one metal may put another metal back into solution. Thirdly, the presence of complexing agents in the treated water may seriously inhibit metal hydroxides' formation and precipitation [384].

Sulphide precipitation is also an effective process for the precipitation of many metals' ions. One of the primary advantages of this process is that sulphide precipitates have a much lower solubility compared to the respective hydroxides and are not amphoteric. For these reasons, sulphide precipitation processes can achieve a higher percentage of removal over a broader pH range compared with hydroxide precipitation. Moreover, metal sulphide sludges also exhibit better thickening and dewatering characteristics than the corresponding metal hydroxide sludges.

Good results were obtained for the removal of Cu. Cd, Zn Ni, As ,Se and Pb from various effluents and wastewaters by the use of Na_2S, FeS_2 and other sulphides [385,386]. However, these techniques present some serious disadvantages, such as the possible formation of toxic H_2S fumes if applied in acid conditions, and the tendency to produce colloidal precipitates that may cause separation problems in either settling or filtration processes [384].

Due to the more stringent environmental regulations approved in the last few years, chemical precipitation technologies alone may not be sufficient to meet the required limits. For this reason, various solutions have been developed.

The combination of chemical precipitation with other methods, such as electro-Fenton processes [387], ion-exchange treatments [388], coagulation/sedimentation [389] and nanofiltration [390], has been shown to be very effective.

As an alternative, many applications of chelating precipitants to remove heavy metals from aqueous systems have been reported. The most commercially used compounds include trimercaptotriazine, K/Na-thiocarbonate and Na-dimethyldithiocarbamate [382], but other molecules such as 1,3-benzenediamidoethanethiol, [391] N,N'-bis-(dithiocarboxy)piperazine and 1,3,5-hexahydrotriazinedithiocarbamate, [392,393] and K-ethyl xanthate [394] have shown good performances.

Other techniques used for the treatment of wastewaters are coagulation and flocculation, usually followed by the sedimentation and filtration of the produced sludges.

Coagulation is defined as the destabilization of colloids due to the neutralization of the forces that keep them apart. Some of the most widely used coagulants in conventional wastewater treatment processes are aluminium salts, ferrous sulphate and ferric chloride [384]. This process can effectively remove wastewater particulate matter and impurities by neutralizing the particles' surface charge and by including the impurities in the formed amorphous metal hydroxide precipitates.

Flocculation is defined as the formation of bonds between the flocs to bind the particles into large agglomerates or clumps due to the action of specific polymers. Many flocculants are employed for the industrial treatment of wastewaters (e.g. polyaluminium chloride (PAC), polyferric sulfate (PFS) and polyacrylamide (PAM)); however, the direct removal of heavy metals by their use is nearly impracticable. To solve this problem various flocculants composed by organic macromolecules (i.e. of mercaptoacetyl chitosan [395], poly (acrylamide)-co-sodium xanthate [396], polyampholyte chitosan derivatives and N-carboxyethylated chitosans [397]) have been investigated, showing good results for the removal of heavy metals from wastewaters. Generally, coagulation and flocculation are not able to completely remove heavy metals from the feed water, so they are coupled with other treatments, such as chemical precipitation [398].

In conclusion, although many treatment techniques can be used to remove heavy metals from contaminated waters, each of them has its own inherent advantages and limitations, depending on many factors such as the initial metals concentration, the composition of the feed, capital investments, operational costs, plant flexibility and reliability, and their environmental impact [399].

7.1.4. Alkali-activated binders

Concrete is the most widely used building material in the world, due to its cheapness and its high mechanical strength, but it also poses several environmental problems. Cement production

industry contributes substantially to anthropogenic CO_2 emissions, consumes great amounts of virgin resources (clay, limestone, etc.) [400] and requires high temperatures (~1400 °C), with a consequent high dispersion of energy and emission of pollutants. In particular, the amount of carbon dioxide released during the calcination of limestone and the combustion of the necessary fossil fuels is about one ton for each ton of cement produced [401].

For these reasons more sustainable and ecological substitutes for concrete are needed, in order to reduce greenhouse gas emissions and the consumption of virgin resources[402]. In this context, alkali-activated binders can be defined as a class of inorganic materials obtained from the chemical reaction between aluminosilicate oxides and alkaline silicates, characterized by the formation of polymeric Si-O-Al bonds [403].Research carried out in recent years in this field has led to the development of new binders based on natural materials (mainly kaolinite and metakaolin) or industrial wastes, with particular attention to fly ashes deriving from coal combustion and blast furnace slag.

The use of fly ash and blast furnace slag as raw materials has various environmental benefits, such as the reduction in the consumption of natural resources and the decrease of CO_2 production. It has been estimated that the synthesis of these binders emits 5-6 times less CO_2 compared to the preparation of Portland cement [404]. Furthermore, landfill disposal of these wastes is not considered a sustainable management strategy, so it is essential to develop new technologies enabling its recycling into reusable products. The most common method used to synthetize alkali activated binders consists in combining an alkaline solution with a reactive aluminosilicate powder, such as metakaolin, blast furnace slag or fly ashes. This results in the formation of an amorphous alkaline aluminosilicate gel, known also as "geopolymeric gel". Inside this phase, the solid particles of unreacted precursors are incorporated, and the water used in the mixing of the precursors is contained in the structure formed by the gel pores [403].

Most alkaline solutions used as activators for the synthesis of these materials are composed by sodium hydroxide, potassium hydroxide and sodium silicate but, due to their high corrosivity and viscosity, their handling can be difficult. Moreover, these materials' rheology can be quite complex and difficult to control due to the formation of sticky and thick pastes, particularly in the case of systems where sodium is the source of alkali [403]. For these reasons these materials still struggle to find widespread commercial applications [405]. The use of solid reagents, to be activated by the addition of water to the reactive aluminosilicate powder mixture, can be considered a viable solution to these problems. In particular, promising results have been obtained by using calcium hydroxide, calcium carbonate and anhydrous sodium silicate in combination with both fly ashes and blast furnace slag [406–408]. The application of these materials as binding agents for toxic metals has long been a

topic of study [409,410], obtaining good results for a multitude of heavy metals (e.g. Ni, Pb, Cd, Zn, Cr, Cu and As) depending on the nature of the contaminated matrix and the formulation of the employed binder [410–412].

7.2. WP2: Process design

The bibliographical research reported above allowed to identify the most promising lines of research to be used as a starting point for the design and optimization of the various steps of the HPSS-NanoExtra process.

The main steps that constitute this process are:

- Application of the HPSS® process to the contaminated material
- Leaching of heavy metals from the granules by using soil washing technology
- Recycling of the leaching solution
- Recovery of the extracted heavy metals.

7.2.1. Application of the HPSS® process

The decontamination process has been applied to the granular material produced by applying the HPSS® technology according to:

- the consolidated formulation (**Table 7.1**), to reduce its heavy metals content while maintaining both the mechanical and leaching characteristics necessary to classify it as a reusable material.
-

Table 7.1. Consolidated formulation of the stabilized cementitious granular material produced using the HPSS® technology.

Component	% w.t.
Contaminated material	72.2
CEM I 42,5 R	26.7
Mapeplast ECO-1A	0.53
Mapeplast ECO-1B	0.53
Water/Cement ratio	0.30 – 0.45

- a low binder content formulation (**Table 7.2**), to produce a no longer contaminated material according to the limits imposed by the Italian legislation for commercial and industrial use of soils and sediments [101]. Since this granular material does not require particular mechanical performances, the use of alkali-activated binders as an alternative to OPC was investigated by using the formulations reported in **Table 7.2** and **Table 7.3**

Table 7.2. Low binder content formulation of the stabilized cementitious granular material produced using the HPSS® technology.

Component	% w.t.
Contaminated material	85
Binder	15
MAPEPLAST ECO-1A/1B	0
Activator/Binder ratio	1 – 3

Table 7.3. Alkali-activated binders' formulations.

Component	GEO 1	GEO2	GEO3	GEO4
	% w.t.			
GGBFS	100	92.0	73.0	89.0
$CaCO_3$	0	4.7	0	5.0
$Ca(OH)_2$	0	3.3	0	0
Clinker	0	0	27.0	6.0
Activator	NaOH 4M	H_2O	H_2O	H_2O

7.2.2. Leaching of heavy metals from the granules by using soil washing technology

The use of acid solutions (HCl, H_2SO_4, H_3PO_4, HNO_3…) as extraction fluids for soil washing can lead to the partial dissolution of the carbonate phases possibly present, and to significant emissions of carbon dioxide, thus requiring appropriate abatement and capture systems.

Furthermore, these solutions cannot be used for the treatment of cement-based materials like the granulate produced with the HPSS® process, due to the consequent degradation of the cementitious phases present, which are fundamental both for the immobilization of the pollutants and for obtaining the desired mechanical characteristics in the granulate.

To solve this issue, the use of a basic extraction fluid was selected and NaOH solutions at different concentrations were tested, allowing for the removal of the heavy metals contained in the granulate obtained from the use of the HPSS® technology without damaging their microstructure or emitting CO_2.

Following what reported in the literature, the use of chelating agents to enhance heavy metals removal was investigated. Some of the commonly used chelating agents are EDTA, sodium citrate, sodium acetate and sodium oxalate [336].

Although EDTA is considered one of the best chelating agents for the removal of many heavy metals [352,413,414], its use has two main disadvantages:

- its low biodegradability causes the addition of further treatment steps to the process, increasing the overall costs.

- its tendency to complex Ca^{2+} ions present in solution [351] makes it unsuitable for the treatment of cementitious matrices, such as the granulate produced with the HPSS® technology.

For these reasons, the research on chelating agents' effects was carried out using sodium citrate, sodium acetate and sodium oxalate.

7.2.3. Recycling of the leaching solution

The ability of nanofiltration to selectively allow the permeation of small monovalent ions (Na^+, K^+, OH^-) while retaining heavy metals has already been exploited in many fields to recover sodium hydroxide from spent caustic solutions and effluents, by using various polymeric membranes. The use of a hollow fibre membrane composed by a thin composite asymmetric film of functionalised polyethersulfone precipitated on a porous support layer was selected for this step. Due to the high ionic strength of the treated solutions, this membrane module's configuration was chosen for its high operational fluxes, to increase the fouling resistance of the system.

The efficiency of the separation process was investigated at different volumetric concentration (VCR) ratios ($1.75 < VCR < 8.0$) to find the optimal conditions.

7.2.4. Recovery of the extracted heavy metals

To recover the heavy metals in the concentrated fraction obtained from the nanofiltration step, a chemical precipitation process applying both hydroxide precipitation and coagulation/sedimentation was selected. In detail, the heavy metals recovery process was divided into the following steps:

- Acidification of the concentrate using H_3PO_4
- Addition of the coagulating additive until sludge formation
- Addition of $Ca(OH)_2$ up to reaching pH values between 11.8 and 12.0
- Precipitation of residual Ca^{2+} ions with the addition of Na_2CO_3
- Addition of flocculating additive
- Sedimentation and filtration of the metal-rich sludge.

The initial acidification step has been introduced in the process after preliminary testing, when all the proposed coagulating additives precipitated upon addition to the concentrate, due to its high pH.

The coagulating additives selected for this study were commercial solutions of $FeCl_3$, $Fe_2(SO_4)_3$ and polyaluminum chloride (PAC). Moreover, Na_2CO_3 was used as sequestrant for Ca^{2+} ions to lower membrane fouling during further treatments of the regenerated leaching solution, while an anionic flocculating additive was employed to ensure a faster and more efficient separation of the metal-rich

sludge. To complete the recycling of the extraction solution, the clarified solution obtained after this treatment was added to the permeated fraction, together with the amount of commercial fresh sodium hydroxide solution needed to reach its original concentration.

7.3. WP3: Selection and characterization of binders and contaminated materials

In this WP the contaminated matrices of interest were selected, and the different binders used were characterized. Based on the usual applications of the HPSS® process, several contaminated materials (i.e. soils, sediments, sludges from wastewater treatment, and fly ashes produced by the combustion of urban solid waste) were considered for testing, to establish the performances and the potential of the HPSS-NanoExtra process.

As far as contaminated soils and sediments are concerned, the following three contaminated matrixes were taken into consideration:

- Soil 1: Contaminated soil from a dismissed sulfuric acid production plant, situated in Bagnolo Mella (BS – Italy);
- Sediment: Contaminated sediment from the excavation of a new navigation basin along the Mincio river near Valdaro (MN - Italy);
- Soil 2: Contaminated soil from a dismissed glassmaker factory situated in Murano (VE – Italy)

The documents regarding the characterization of each site have been examined in order to preliminarily identify the main contaminants (**Table 7.4**) and the location of the hot spots for sampling. The contaminated sediment was not considered for this study because among the metals it contained, only Hg was found to exceed the regulatory limits, while Soil 2 was excluded because it resulted mainly contaminated by As, Hg and Cd, which were present as inclusions inside glass fragments, and therefore not suitable for soil washing using chemical extraction. The contaminated soil from the dismissed sulfuric acid production plant was deemed appropriate for this study because of the high heavy metals content and the absence of contaminants in the form of discrete particles.

In addition, the analysis of various sludges produced from wastewater treatment reported in the literature [415–417] showed that for this kind of materials contamination usually involves only few metals, as for example, the case of a galvanic company's sewage sludge.

Table 7.4. Main contaminants found during the preliminary characterization of the contaminated soils and sediment considered for this study.

Contaminants	Soil 1	Sediment	Soil 2	Regulatory limit*
	mg·kg^{-1} d.w.			
As	306	254	153	50
Hg	7.8	17.2	7,5	5
Pb	48160	120	2019	1000
Cu	292	120	453	600
Se	400	< 0.5	51	15
Zn	584	< 0.5.	76	1500
Cd	2.9	< 0.5	85	15

*Regulatory limit: Column B (commercial and industrial use) of Table 1 of Annex V to Part IV of Title V of Legislative Decree No 152 of 03/04/2006 [101].

For this reason, these matrixes were deemed not significant enough for evaluating the performance of the HPSS-NanoExtra process. On the other hand, since the fly ashes produced from the incineration of coal, municipal solid wastes and other hazardous materials are usually substantially contaminated a multitude of heavy metals (i.e. Cd, Cr, Cu, Hg, Ni, Zn, Pb, Sn and Sb), a sample of fly ashes obtained from the combustion of municipal solid waste was selected as a suitable contaminated material for this study.

7.3.1. Experimental

7.3.1.1. Sampling and samples' preparation

One cubic meter of soil (Soil 1) was excavated from a brownfield located in an abandoned production and storage site located in Bagnolo Mella (BS, Italy). This site was operational for the production of sulfuric acid and fertilizers between 1898 and 1985, when it was closed and dismissed until recent reclamation operations started. The contaminated soil sample was collected from the surface to 1 meter depth with an excavator, air-dried up to 10% weight/weight (w/w) moisture content and sieved at 2 mm prior to homogenization thus obtaining a 100 kg sample.

Fly ashes were obtained from an Italian incinerator for the combustion of municipal solid waste (MSW). The fly ashes produced from the combustion of MSW usually contain high concentrations of chlorides, which are known to interfere in the setting and hardening reactions of cementitious binders [418]. For this reason, it was necessary to remove these salts from the sample in order to obtain a material that could be treated with the HPSS® technology. For this purpose, fly ashes were mixed with tap water (solid/liquid ratio of 1/10) and stirred in a tank reactor for 30 minutes, then the water was removed after decanting. This procedure was repeated several times, until the washing water reached a chloride concentration lower than 10 mg/L and then the sample

was dried up to 10% weight/weight (w/w) moisture content, mechanically crushed (by a hammer mill HM/530 B - Ceramic Instruments, Sassuolo, Italy), and homogenized, thus obtaining a 100 kg sample.

7.3.2. Results and discussion

The chemical and mineralogical characterization of Soil 1, reported in **Table 7.5** and **Table 7.7**, showed a clear contamination that can be traced back to the inappropriate disposal of the tailings and wastes of an industrial plant for the production of sulphuric acid. In particular, XRD analysis showed the presence of both natural and anthropogenic mineralogical phases. The main natural minerals found were dolomite and quartz, together with lower amounts of muscovite, albite and calcite. The anthropogenic minerals identified in the soil were gypsum, hematite, anglesite, jarosite and litharge. SEM investigations reported also the abundant presence of amorphous iron oxides of anthropogenic origin. The heavy metals whose concentration was found to exceed the Italian regulatory limits for soil and sediment commercial and industrial use were: As, Hg, Pb, Se and Tl.

Table 7.5. Heavy metals content of contaminated soil and fly ashes after pre-treatment. Concentrations exceeding the regulatory limits are highlighted in bold.

Contaminants	Soil 1	Fly Ash	Regulatory limit*
	$mg \cdot kg^{-1}$ d.w.		
As	**306±26**	15.0±2.0	**50**
Be	0.53±0.03	0.36±0.04	10
Cd	2.86±0.30	133±15	15
Co	26.3±2.5	12.3±2.1	250
Cr	18.5±1.5	123±9	800
Cu	292±5.6	**679±38**	**600**
Hg	**7.86±1.00**	**6.97±0.43**	**5**
Ni	15.0±1.3	167±21	500
Pb	**48160±2960**	**1889±139**	**1000**
Sb	12.5±1.2	**771±74**	**30**
Se	**400±18**	11.4±1.4	**15**
Sn	33±2.6	**455±39**	**350**
Tl	**13.4±1.2**	0.38±0.05	**10**
V	29.0±2.1	27.4±2.8	250
Zn	584±49	**8801±686**	**1500**

*Regulatory limit: Column B (commercial and industrial use) of Table 1 of Annex V to Part IV of Title V of Legislative Decree n°152 of 03/04/2006 [101].

The chemical characterization of the fly ashes obtained after the pre-treatment procedure (**Table 7.5**), determined that this material can be classified as a hazardous filtration residue deriving from the treatment of fumes (CER code: 190105(*)) [101]. In addition, **Table 7.6** shows that the pre-treatment was successful in removing soluble sulfates and chlorides from the sample.

Table 7.6. Content of soluble Cl^- and SO_4^{2-} salts of fly ashes before and after pre-treatment.

Contaminants	Before pre-treatment	After pre-treatment
	g·kg^{-1} d.w.	
$Cl^-_{(soluble)}$	160±2	< 0.001
$SO_4^{2-}_{(soluble)}$	10.5±0.3	< 0.001

Table 7.7. Mineralogical characterization of soil 1.

Phase	Soil 1
	w.t. %
Quartz SiO_2	16.5±1.3
Hematite Fe_2O_3	8.5±0.9
Dolomite $Mgca(CO_3)_2$	22.6±1.5
Calcite $Ca(CO_3)$	3.5±0.5
Gypsum $CaSO_4 \cdot 2(H_2O)$	10.6±0.4
Jarosite $KFe_3^{+3}(SO_4)_2(OH)_6$	1.75±0.3
Anglesite $PbSO_4$	2.75±0.4
Albite $NaAlSi_3O_8$, $KAlSi_3O_8$	3.2±0.5
Muscovite $KAl_2(Si_3Al)O_{10}(OH,F)_2$	4.5±0.5
Chlorite $(Fe_5Al)(AlSi_3)O_{10}(OH)_8$	0.5±0.3
Amorphous Phases	25.2±0.7

The heavy metals content of CEM I 42.5 R and of each starting material used to prepare the various alkali-activated binders is reported in **Table 7.8**.

Table 7.8. Heavy metals content of CEM I 42.5 R from Barbetti S.p.A. and of each starting material used to prepare the various alkali-activated binders.

Contaminants	CEM I 42.5 R	GGBFS	Clinker	Lime	Sodium carbonate
	mg·kg^{-1} d.w.				
As	4.58±0.78	1.40±0.27	4.42±0.04	0.61±0.07	0.36±0.03
Be	1.08±0.06	0.75±0.23	0.52±0.03	< 0.1	< 0.1
Cd	0.79±0.24	0.11±0.01	0.42±0.01	0.30±0.02	0.29±0.05
Co	18.6±0.6	0.9±0.1	22.6±0.5	< 0.1	0.37±0.11
Cr	65.0±2.8	73.4±3.1	90.7±0.8	0.53±0.06	0.42±0.09
Cu	63.0±5.0	9.4±1.0	47.4±0.6	1.19±0.20	0.96±0.10
Hg	< 0.1	< 0.1	< 0.1	< 0.1	< 0.1
Ni	109±5	19.7±1.3	131±7	0.27±0.02	0.18±0.06
Pb	24.3±3.2	0.58±0.28	13.9±0.7	3.01±0.23	1.32±0.22
Sb	6.30±0.67	0.43±0.16	0.69±0.15	0.30±0.07	0.41±0.06
Se	< 0.5	8.37±0.98	< 0.5	< 0.5	< 0.5
Sn	4.15±0.52	0.79±0.18	2.37±0.08	0.16±0.05	< 0.1
Tl	< 0.1	< 0.1	< 0.1	< 0.1	< 0.1
V	176±8	14.3±0.3	216±2	0.70±0.09	0.13±0.06
Zn	104±6	6.71±2.09	77.6±3.1	< 0.1	6.25±0.43

7.3.3 Acknowledgments

The authors are grateful to Maurizio Pietro Bellotto (Polytechnic of Milan) for his help for the geopolymers formulation.

7.4. WP4: Preliminary Experiments

Within this WP, after applying the HPSS® process to the selected contaminated matrices, the influence of binder's formulation, leachant concentration, time of contact between the granules and the leachant and of chelating agents' used were investigated. The information gathered was useful to determine the most efficient conditions to properly design and dimension a bench-scale prototype.
Improving the HPSS® performances by including a wet conditioning step to the process, was already shown to increase the mechanical performances and to lower the leaching of contaminants from the granular material produced with this technology [238]. For this reason, its effects on the removal of contaminants and the possibility of replacing it with the extraction step were studied.
Since the pre-treatment of the contaminated fly ashes may remove up to one third (w/w) of the initial material [419] and use a large volume of water, a process to recycle the washing water and recover the removed salts was developed and tested at bench scale.

7.4.1. Experimental

7.4.1.1. Washing water recycling and salt recovery

The water obtained from the first wash of the contaminated fly ashes was analysed to determine its content of heavy metals, Ca, Na, K, Mg, Cl^-, SO_4^{2-}, F^- and NO_3^-.
A 15 L sample of water was stirred using a mechanical mixer (FALC AT-M 20) and subjected to a chemical-physical treatment to precipitate the heavy metals present. After treatment the solution was left to settle and manually filtered using a sleeve filter having a 5 μm mesh size to remove the sludge. In detail, the treatment included the following steps:

- Addition of $FeCl_3$ solution until sludge formation.
- Addition of NaOH up to reaching pH values between 11.8 and 12.0.
- Precipitation of residual Ca^{2+} ions with the addition of Na_2CO_3.
- Addition of flocculating additive.
- Sedimentation and filtration of the sludge.

After the removal of the sludge, a 10 L aliquot of water was subjected to reverse osmosis, by using a MMS SW18 System (MMS AG, Urdorf, Switzerland) equipped with a spiral wound 1812 module RO membrane (99% NaCl rejection) and a high pressure pump.

RO was terminated after reaching a water recovery of about 70-75 %, then a 1 L sample of the concentrated fraction was concentrated by evaporation under vacuum (~ 80C°, ~ 350 mbar) until a pumpable salt sludge was obtained. The evaporated fraction was condensed, analysed and combined with the permeated fraction obtained from RO, while the salt was filtered on a glass Gooch filter, oven-dried at 105°C for 24 hours and then weighted.

7.4.1.2. Preparation of granular material from contaminated materials by applying the HPSS® process

The HPSS® process shown in chapter 2.2 was used with the formulations reported in **Table 7.9-12**.

Table 7.9. List of the samples of granulated materials used in this study.

Sample	Contaminated material	Formulation	Binder	Activator	Activator/Binder ratio
NanoExtra01 (NE01)	Soil 1	Standard	CEM I 42,5 R	H_2O	0,37
NanoExtra02 (NE02)	Soil 1	Low-binder content	CEM I 42,5 R	H_2O	1,00
NanoExtra04 (NE04)	Fly ashes	Standard	CEM I 42,5 R	H_2O	0.76
NanoExtra05 (NE05)	Fly ashes	Low-binder content	CEM I 42,5 R	H_2O	1,39
NanoExtra07 (NE07)	Soil 1	Low-binder content	GEO 4	H_2O	1,00
NanoExtra09 (NE09)	Fly ashes	Low-binder content	GEO 4	H_2O	2,40
NanoExtra11 (NE11)	Fly ashes	Low-binder content	GEO 1	NaOH 4 M	2,87
NanoExtra13 (NE13)	Fly ashes	Low-binder content	GEO 2	H_2O	2,13
NanoExtra15 (NE15)	Fly ashes	Low-binder content	GEO 5	H_2O	2,56
NanoExtra18 (NE18)	Soil 1	Low-binder content	GEO 1	H_2O	1,07
NanoExtra19 (NE19)	Soil 1	Low-binder content	GEO 2	H_2O	0,97
NanoExtra20 (NE20)	Soil 1	Low-binder content	GEO 5	NaOH 4 M	1,08

Table 7.10. Standard HPSS® formulation and dosages used for granular material preparation.

Component	% w.t.	Dosage (Kg)
Contaminated material	72.2	10.95
CEM I 42,5 R	26.7	4.05
Mapeplast ECO-1A/1B	0.53	0.081

Table 7.11. Low-binder content formulation and dosages used for granular material preparation.

Component	% w.t.	Dosage (Kg)
Contaminated material	85	10.1
Binder	15	1.8
Mapeplast ECO-1A/1B	0	0

Table 7.12. Alkali-activated binders' formulations.

Component	GEO 1	GEO2	GEO3	GEO4
	% w.t.			
GGBFS	100	92.0	73.0	89.0
Sodium carbonate	0	4.7	0	5.0
Lime	0	3.3	0	0
Clinker	0	0	27.0	6.0
Activator	NaOH 4M	H_2O	H_2O	H_2O

7.4.1.3. Extraction tests

Preliminary extraction tests were carried out by placing 330 g d.w. of granules and 1.650 L of extracting solution (solid/liquid ratio of 1/5) into 2 L closed jars. Stirring was maintained using a Jar Test apparatus (JLT6 Jar Test - VELP Scientifica, Usmate, Italy) operating at 70 rpm.

The following parameters were tested:

- NaOH concentration (0.1, 0.5, 1.0 M) tested on samples NE01 and NE02.
- Residence time of the granules within the extractant: sampling (10 mL) after 2, 4, 8, 24, 48, 72, 96 and 168 hours.
- Binder: extraction of samples made from both contaminated materials following the low-binder formulation and using NaOH 1M solution as the leachant.

Effects of chelating agents' addition to the extracting solution (NaOH 1 M solution) using sodium citrate, sodium oxalate and sodium acetate (0.15 M) [420].

For each test the heavy metals removal ($HM_{Removal}$) was estimated by using the following procedure:

- The heavy metals content of each alkali-activated binder was estimated by using the following approximation:

$$[HM]_B = \sum_{i:1}^{n} [\%C_i \cdot [HM]_{C_i}] \quad \text{(Eq 7.1)}$$

where:

$[HM]_B$: Heavy metals concentration in the binder

$\%C_i$: % of each component of the binder formulation

$[HM]_{C_i}$: Heavy metals concentration in each component of the binder formulation

- The heavy metal content of each sample was estimated by using the following approximation:

$$[HM]_S = \%CM \cdot [HM]_{CM} + \%B \cdot [HM]_B \quad \text{(Eq 7.2)}$$

where:

$[HM]_S$: Heavy metals concentration in the granulate sample

$\%CM$: % of contaminated material in the applied formulation

$[HM]_{CM}$: Heavy metals concentration in the contaminated material

$\%B$: % of binder in the applied formulation

$[HM]_B$: heavy metals concentration in the binder

- The removal of heavy metal was estimated by using the following approximation

$$HM_{Removal} = \{[([HM]_{Extr.}/1000) \cdot (S/L)]/[HM]_S\} \cdot 100 \quad \text{(Eq 7.3)}$$

where:

$HM_{Removal}$: Heavy metals removal from the granulate (%)

$[HM]_{Extr.}$: Concentration of heavy metals in the extractant, expressed in µg/L

(S/L): Solid/Liquid ratio used

$[HM]_S$: Heavy metals concentration in the granulate sample

7.4.2. Results and discussions

7.4.2.1. Washing water recycling and salt recovery

The first batch of washing water (Sample W) obtained from the pre-treatment of the contaminated fly ashes was characterized by using ICP-OES and HPLC (**Table 7.13**), and the results showed the solubilization of more than 90% of the soluble salts present, together with a minor quantity of As, Cr, Cu, Pb, Sb, Tl, and Zn. ICP-OES analysis also showed Na, K, and Ca to be the major counterions for Cl^-. Analysis of the water after the physical-chemical treatment (Sample W2) showed that heavy metals were almost completely precipitated and that the addition of Na_2CO_3 led to the complete removal of Ca, while the concentration of Cl^- ions remained mostly unchanged.

Sample W2 was subjected to RO, whose efficiency was studied as a function of the Volumetric Concentration Ratio (VCR), as defined by the following equation:

$$VCR = V_S/[V_S - (w_P \cdot \rho_P)] \quad \text{(Eq 7.4)}$$

where:

V_S: starting volume of the sample subjected to RO

w_P: weight of the permeated fraction

ρ_P: density of the permeated fraction, as measured by a hydrometer

RO was terminated after reaching a VCR ratio of about 4 (water recovery of nearly 75 %), to avoid precipitation of salts and the consequent clogging of the membrane.

Analysis of the concentrated (Sample RO-C) and permeated (Sample RO-P) fractions showed the complete separation of the remaining heavy metals and a high recovery (~ 97%) of salts.

The salty fraction obtained after having evaporated around 90% of sample RO- C was isolated by filtration, dried and weighted, showing a recovery of about 85%.

The condensed fraction (Sample EV-C) accounted for about 90 % of the evaporated water and its analysis showed only low concentrations of Na, K, and Cl, which can be attributed to dragging phenomena during the evaporation.

The saturated solution obtained from the filtration of the salt sludge was dried overnight and the remaining salt was recovered, showing an overall yield of about 95 %.

This procedure was demonstrated to be effective in recycling the washing water, as well as in recovering the salt, which could be sold as road salt [421] to amortize the process' costs.

Table 7.13. Concentrations of heavy metals, Na, Ca, K, Mg, Cl^-, and SO_4^{2-} in the washing water used for fly ashes pre-treatment during the recycling process.

Contaminants	Sample W	Sample W2	Sample RO-C	Sample RO-P	Sample EV-C
	$\mu g \cdot L^{-1}$				
As	9.2±1.1	< 5	< 5	< 5	< 5
Be	< 5	< 5	< 5	< 5	< 5
Cd	< 5	< 5	< 5	< 5	< 5
Co	< 5	< 5	< 5	< 5	< 5
Cr	108±6	12.3±2.4	41.7±1.9	< 5	< 5
Cu	79.5±4.2	7.5±1.1	25.4±0.9	< 5	< 5
Hg	< 5	< 5	< 5	< 5	< 5
Ni	< 5	< 5	< 5	< 5	< 5
Pb	2420±35	< 5	< 5	< 5	< 5
Sb	46.4±3.5	< 5	< 5	< 5	< 5
Se	< 5	< 5	< 5	< 5	< 5
Sn	6.6±1.0	< 5	16±2.1	< 5	< 5
Tl	10.4±0.9	< 5	38.4±1.2	< 5	< 5
V	< 5	< 5	< 5	< 5	< 5
Zn	446±11	17.1±2.0	55.7±2.4	< 5	< 5
	$mg \cdot L^{-1}$				
Na	6330±18	9535±14	34610±150	184±5	6.3±0.3
Ca	2280±13	< 1	2.1±0.3	< 1	< 1
K	3650±31	3260±25	12850±65	60±3	2.4±0.3
Mg	457±17	385±13	1430±17	25±2	< 1
Cl^-	15200±190	15050±160	58170±930	180±9	16±1
SO_4^{2-}	930±15	470±11	1860±13	7±1	<1

7.4.2.2. Extraction tests

The concentrations of heavy metals estimated for each sample of granulated material are reported in **Table 7.14**.

Table 7.14a. Concentrations of heavy metals estimated for samples NE01, NE02, NE04, NE05, NE07, and NE09.

Contaminants	NE01	NE02	NE04	NE05	NE07	NE09
	mg·kg^{-1}d.w.					
As	225	261	12.2	13.5	260	13.1
Be	0.7	0.6	0.6	0.5	0.5	0.4
Cd	2.3	2.6	97	113	2.5	113
Co	24.2	25.2	14	13	23.6	11.7
Cr	31.2	25.6	108	115	23.6	113
Cu	231	258	513	587	254	583
Hg	5.8	6.7	2.9	3.4	6.7	3.4
Ni	40.4	29.1	153	160	20.0	151
Pb	35161	40936	1386	1609	40934	1607
Sb	10.8	11.6	565	657	10.7	656
Se	292	340	8.3	9.7	341	10.3
Sn	25.2	28.6	334	388	28.2	387
Tl	9.8	11.4	0.3	0.3	11.4	0.3
V	68.9	51.2	67.7	49.8	41.1	39.8
Zn	455	512	453	7497	503	7487

Table 7.14b. Concentrations of heavy metals estimated for samples NE11, NE13, NE15, NE18, NE19, and NE20.

Contaminants	NE11	NE13	NE15	NE18	NE19	NE20
	mg·kg^{-1}d.w.					
As	13	13.0	13.0	260	260	260
Be	0.4	0.4	0.4	0.6	0.6	0.6
Cd	113	113	113	2.4	2.4	2.4
Co	10.6	10.6	10.8	22.5	22.5	22.7
Cr	116	115	115	26.7	25.9	26.3
Cu	579	579	579	250	250	250
Hg	3.4	3.4	3.4	6.7	6.7	6.7
Ni	147	146	147	15.7	15.5	16.6
Pb	1606	1606	1606	40933	40933	40933
Sb	655	656	656	10.7	10.7	10.7
Se	11.0	10.9	10.8	341	341	341
Sn	387	387	387	28.1	28.1	28.1
Tl	0.3	0.3	0.3	11.4	11.4	11.4
V	25.4	25.3	27.1	26.8	26.6	28.5
Zn	7482	7482	7482	497	497	498

The concentration of heavy metals in the leaching solution was monitored to determine the efficiency of the extracting process, while the concentration of Ca, Mg and P were investigated as an estimation for the release of compounds that may increase the fouling rate of the nanofiltration membrane, used during the recycling of the spent extractant solution. The concentration of Na was

monitored to asses if relevant carbonation or precipitation of insoluble Na compounds occurred. The concentration of Sb could not be determined in the eluates from the treatment of the granulated materials obtained from Soil 1 (samples NE01, NE02, NE07, NE18, NE19 and NE20) due to the interference caused by the high quantity of Pb present, whose emission line (220.353 nm) covered the emission line at 217.581 nm used for Sb analysis by ICP -OES.

The first set of experiments was carried out by using the granules obtained from the treatment of Soil 1, as reported below.

7.4.2.3. Soil 1

Concentration of NaOH and residence time

The efficiency of the various heavy metals' extraction (**Table 7.15** and **Table 7.16**) varied significantly by changing the concentration of the NaOH solution used for both NE01 and NE02 samples. While the concentration of Be, Hg, Cd, Mg, and P in the extracting solution was always below the detection limit (2-6 µg/L), the removal of all the leached heavy metals increased almost linearly with NaOH concentration, in particular in the case of As, Pb, Tl and Sn. This effect, while still present, was much more contained for Co, Cu, Se, V, Zn, Ni, and Cr. In detail, the best results using NaOH 1M as extracting solution were observed for As (~16-19 %), Cr (~5-7 %), Cu (~6-7 %), Ni (~6-7 %), and Pb (~5-6 %), while only minor amounts of Zn (~1-2 %), V (~2 %), Tl (~3-4 %), Sn (~2-3 %), Se (~2 %), and Co (~1 %) were removed.

The higher release of Ni, Pb, Cu, As shown for sample NE02 with respect to sample NE01, can be attributed to both a reduced use of binder and to the absence of the additives (Mapeplast ECO1A/B) in the formulations used, leading to a less dense and more porous material. The release of Sn, Tl, Se and Co did not vary significantly between NE01 and NE02 samples, while the higher leaching of Zn, V and Cr detected for sample NE01, compared to that from sample NE02, can be attributed to the fact that these heavy metals were mainly present in the cement, whose percentage almost doubles between the two formulations (15% vs 26.7% for samples NE02 and NE01, respectively).

The leaching of heavy metals from both samples increased directly with the residence time (**Figure 7.2** and **Figure 7.3**) during the whole extraction in the case of As, Se, Zn, and Sn, while it tended to reach a plateau after around 72 hours for Cr, Ni, Pb, Tl, V, Cu and Co. Moreover, these trends were more pronounced when the concentration of the extracting solution increased (**Figure 7.4**).

Table 7.15. Removal % of As, Be, Cd, Co, Cr, Cu, Hg, Ni, Pb, Se, Sn, V, and Zn from sample NE01 using NaOH 0.1, 0.5 and 1 M as extracting solutions. (n.d.: not detected).

NE01	Time (h)	Removal (%)													
		As	Be	Cd	Co	Cr	Cu	Hg	Ni	Pb	Se	Sn	Tl	V	Zn
NaOH 1 M	2	0.97	n.d.	n.d.	0.33	1.79	0.76	n.d.	1.59	1.86	0.16	0.50	0.20	0.16	0.13
	4	1.42	n.d.	n.d.	0.38	2.27	1.02	n.d.	2.13	2.28	0.18	0.65	0.50	0.23	0.14
	8	2.00	n.d.	n.d.	0.47	2.87	1.37	n.d.	2.63	2.74	0.22	0.88	0.82	0.35	0.15
	24	3.62	n.d.	n.d.	0.57	3.83	2.27	n.d.	3.73	3.50	0.39	1.13	1.52	0.49	0.21
	48	4.90	n.d.	n.d.	0.60	4.34	2.61	n.d.	3.98	3.73	0.57	1.31	1.91	0.59	0.25
	72	6.55	n.d.	n.d.	0.65	4.74	3.16	n.d.	4.38	4.01	0.74	1.64	2.40	0.74	0.33
	96	8.87	n.d.	n.d.	0.74	5.55	3.99	n.d.	5.05	4.42	1.06	2.26	3.09	1.08	0.45
	168	15.7	n.d.	n.d.	0.84	6.84	5.84	n.d.	5.94	4.95	1.96	3.37	3.66	1.90	0.80
NaOH 0.5 M	2	0.34	n.d.	n.d.	0.27	1.40	0.55	n.d.	1.52	1.17	0.04	n.d.	n.d.	n.d.	0.07
	4	0.47	n.d.	n.d.	0.31	1.81	0.73	n.d.	1.93	1.44	0.06	n.d.	n.d.	0.15	0.07
	8	0.62	n.d.	n.d.	0.41	2.35	0.96	n.d.	2.45	1.70	0.12	n.d.	n.d.	0.18	0.08
	24	1.02	n.d.	n.d.	0.50	3.43	1.55	n.d.	3.48	1.92	0.23	n.d.	n.d.	0.28	0.13
	48	1.62	n.d.	n.d.	0.50	3.73	1.90	n.d.	3.83	2.04	0.35	0.67	n.d.	0.34	0.17
	72	2.29	n.d.	n.d.	0.58	4.16	2.31	n.d.	4.19	2.04	0.42	0.74	n.d.	0.44	0.23
	96	3.32	n.d.	n.d.	0.62	5.01	2.97	n.d.	4.93	2.07	0.57	0.83	n.d.	0.68	0.29
	168	6.27	n.d.	n.d.	0.75	6.27	4.23	n.d.	5.74	2.15	1.05	1.77	n.d.	1.15	0.42
NaOH 0.1 M	2	n.d.	n.d.	n.d.	0.23	0.82	0.30	n.d.	1.17	0.38	0.02	n.d.	n.d.	n.d.	0.03
	4	n.d.	n.d.	n.d.	0.29	1.02	0.39	n.d.	1.56	0.44	0.02	n.d.	n.d.	n.d.	0.03
	8	n.d.	n.d.	n.d.	0.34	1.27	0.50	n.d.	1.98	0.48	0.03	n.d.	n.d.	n.d.	0.04
	24	n.d.	n.d.	n.d.	0.37	1.82	0.74	n.d.	2.74	0.49	0.08	n.d.	n.d.	n.d.	0.05
	48	n.d.	n.d.	n.d.	0.43	2.38	1.01	n.d.	3.42	0.55	0.14	n.d.	n.d.	n.d.	0.05
	72	n.d.	n.d.	n.d.	0.46	2.53	1.22	n.d.	3.59	0.57	0.15	n.d.	n.d.	n.d.	0.07
	96	0.14	n.d.	n.d.	0.52	2.91	1.45	n.d.	3.89	0.65	0.17	n.d.	n.d.	0.16	0.09
	168	0.41	n.d.	n.d.	0.55	3.64	1.95	n.d.	4.53	0.70	0.31	n.d.	n.d.	0.43	0.16

Table 7.16. Removal % of As, Be, Cd, Co, Cr, Cu, Hg, Ni, Pb, Se, Sn, V, and Zn from sample NE02 using NaOH 0.1, 0.5 and 1 M as extracting solutions. (n.d.: not detected).

NE02	Time (h)	Removal (%)													
		As	**Be**	**Cd**	**Co**	**Cr**	**Cu**	**Hg**	**Ni**	**Pb**	**Se**	**Sn**	**Tl**	**V**	**Zn**
NaOH 1 M	2	1.53	n.d.	n.d.	0.35	1.71	1.09	n.d.	2.26	1.96	0.13	0.71	n.d	0.45	0.31
	4	2.22	n.d.	n.d.	0.38	2.22	1.51	n.d.	2.73	2.47	0.27	0.77	0.32	0.59	0.32
	8	3.07	n.d.	n.d.	0.42	2.79	2.06	n.d.	3.56	3.03	0.37	0.80	0.98	0.65	0.34
	24	6.03	n.d.	n.d.	0.57	3.89	3.49	n.d.	4.98	4.20	0.69	1.12	1.80	0.96	0.53
	48	8.6	n.d.	n.d.	0.71	4.46	4.58	n.d.	5.80	5.04	0.97	1.36	2.43	1.14	0.65
	72	10.8	n.d.	n.d.	0.73	4.69	5.17	n.d.	6.14	5.49	1.20	1.62	2.90	1.24	0.84
	96	13.9	n.d.	n.d.	0.74	4.84	5.91	n.d.	6.28	5.65	1.35	1.77	3.09	1.29	1.17
	168	18.9	n.d.	n.d.	0.78	5.18	6.81	n.d.	6.63	6.19	1.93	2.22	3.29	1.73	2.40
NaOH 0.5 M	2	0.40	n.d.	n.d.	0.28	1.31	0.76	n.d.	1.99	1.21	0.07	n.d.	n.d.	0.18	0.20
	4	0.56	n.d.	n.d.	0.35	1.74	1.02	n.d.	2.56	1.48	0.12	n.d.	n.d.	0.20	0.23
	8	0.77	n.d.	n.d.	0.37	2.22	1.35	n.d.	3.29	1.78	0.21	n.d.	n.d.	0.21	0.25
	24	1.12	n.d.	n.d.	0.49	3.21	2.15	n.d.	4.70	2.22	0.29	0.57	n.d.	0.31	0.36
	48	1.77	n.d.	n.d.	0.54	3.58	2.80	n.d.	5.29	2.32	0.53	0.62	n.d.	0.37	0.41
	72	2.33	n.d.	n.d.	0.61	3.86	3.21	n.d.	5.64	2.42	0.71	0.88	n.d.	0.46	0.49
	96	2.65	n.d.	n.d.	0.63	3.94	3.47	n.d.	5.68	2.47	0.88	1.12	n.d.	0.54	0.59
	168	4.86	n.d.	n.d.	0.68	4.47	4.49	n.d.	6.37	2.54	1.09	1.45	n.d.	0.79	0.96
NaOH 0.1 M	2	0.13	n.d.	n.d.	0.23	0.77	0.44	n.d.	1.53	0.30	0.04	n.d.	n.d.	n.d.	0.04
	4	0.14	n.d.	n.d.	0.28	1.00	0.57	n.d.	1.99	0.47	0.03	n.d.	n.d.	n.d.	0.05
	8	0.18	n.d.	n.d.	0.30	1.26	0.73	n.d.	2.57	0.52	0.06	n.d.	n.d.	n.d.	0.06
	24	0.26	n.d.	n.d.	0.39	1.80	1.05	n.d.	3.62	0.51	0.09	n.d.	n.d.	n.d.	0.08
	48	0.34	n.d.	n.d.	0.43	2.08	1.22	n.d.	4.31	0.58	0.15	n.d.	n.d.	0.13	0.10
	72	0.76	n.d.	n.d.	0.43	2.39	1.32	n.d.	4.81	0.65	0.27	n.d.	n.d.	0.18	0.13
	96	0.82	n.d.	n.d.	0.45	2.35	1.36	n.d.	4.76	0.63	0.37	n.d.	n.d.	0.19	0.15
	168	1.33	n.d.	n.d.	0.55	3.64	1.95	n.d.	4.53	0.70	0.31	n.d.	n.d.	0.43	0.16

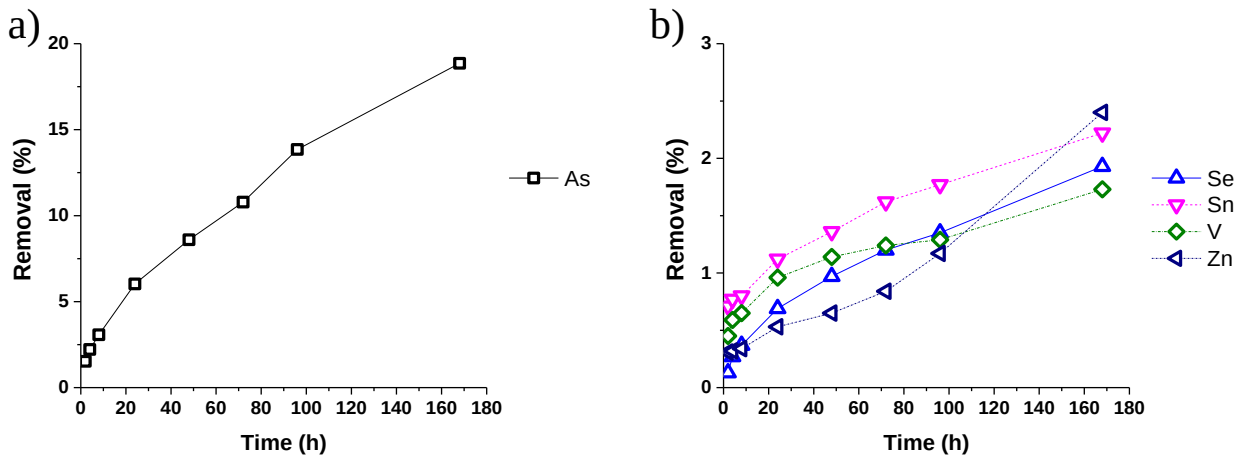

Figure 7.2. Removal % of (a) As and (b) Se, Sn, V and Zn from sample NE02 using NaOH 1 M

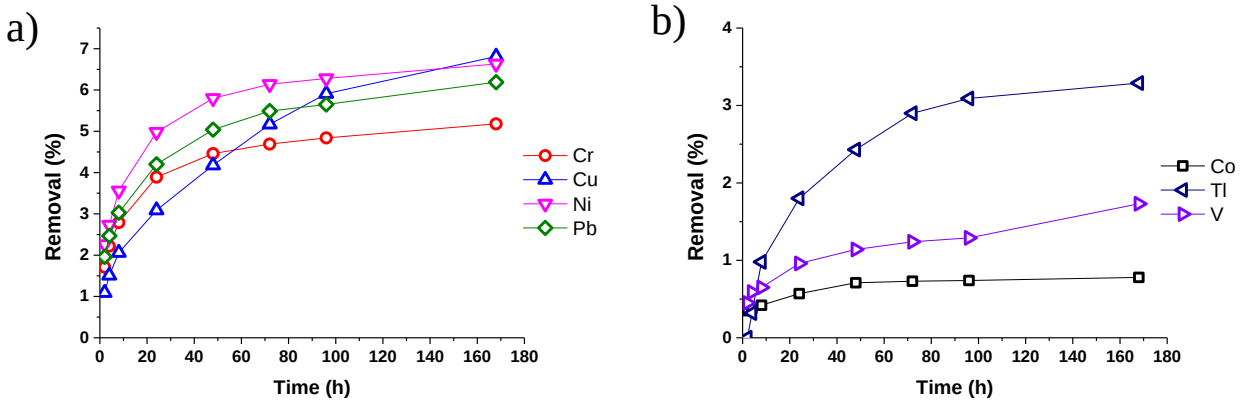

Figure 7.3. Removal % of (a) As and (b) Se, Sn, V and Zn from sample NE02 using NaOH 1 M

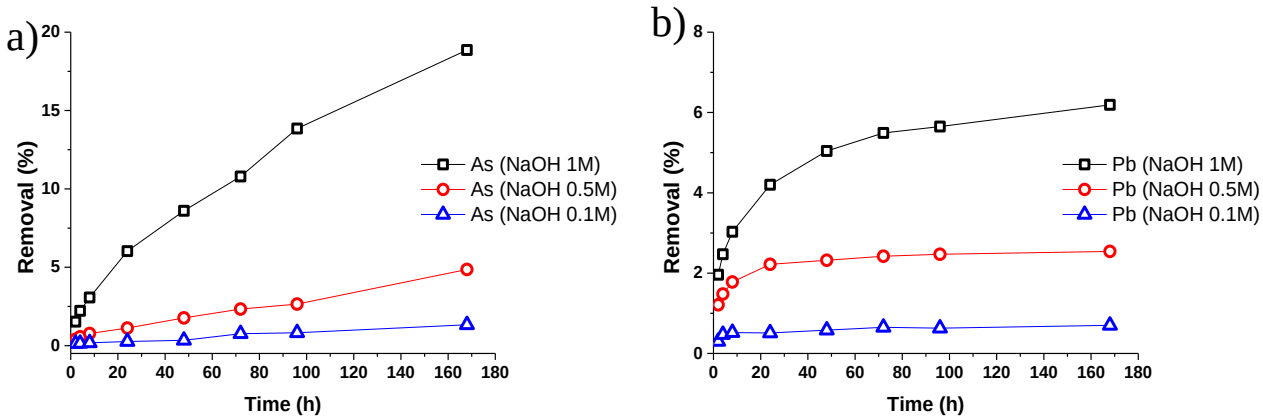

Figure 7.4. Removal of (a) As and (b) Pb from sample NE02 using NaOH 0.1, 0.5 and 1 M

Since the presence of both Ca and K in the eluate could lead to the formation of poorly soluble compounds that could increase the fouling of the NF membrane, the influence of both NaOH concentration and residence time on their concentration in the eluate were studied.

From the data reported in **Table 7.17** and **Figure 7.5** it is possible to observe how Ca started to dissolve immediately in the extracting solution and how its concentration began to decrease already after two hours, probably due to both its partial carbonation or to the gradual release of sulphates from the granular material (jarosite and anglesite) leading to the formation of insoluble calcium sulphates.

Table 7.17. Leaching of Ca and K from sample NE02 using NaOH 0.1, 0.5 and 1 M as the extracting solution.

NE01	Time	Ca	K	NE02	Time	Ca	K
	h	mg·L^{-1}			h	mg·L^{-1}	
	2	41.1	285		2	28.2	218
	4	39.1	315		4	25.0	268
	8	37.9	337		8	22.1	299
NaOH	24	33.1	350	**NaOH**	24	20.3	330
1 M	48	24.1	349	**1 M**	48	19.6	337
	72	13.3	350		72	18.4	339
	96	10.9	347		96	15.2	340
	168	6.0	347		168	13.2	341
	2	40.5	250		2	41.3	180
	4	38.2	286		4	39.4	215
	8	29.0	311		8	34.7	251
NaOH	24	19.8	326	**NaOH**	24	25.5	288
0.5 M	48	10.5	337	**0.5 M**	48	14.7	299
	72	6.8	340		72	13.8	306
	96	6.0	349		96	12.9	303
	168	5.0	348		168	9.2	313
	2	159	192		2	305	149
	4	143	223		4	256	174
	8	120	248		8	196	195
NaOH	24	102	285	**NaOH**	24	148	208
0.1 M	48	67.6	301	**0.1 M**	48	98.3	214
	72	39.3	302		72	54.5	218
	96	19.4	304		96	18.7	220
	168	12.9	308		168	7.9	215

Moreover, the concentration of Ca increased markedly with decreasing the concentration of the NaOH solution used, since the lower concentration of hydroxide ions reduced the displacement of the dissociation equilibrium of $Ca(OH)_2$ towards its undissociated form. On the other hand, the release of K clearly increased in the first 24 hours for all the samples, then reached a plateau due to the partial dissolution of potassium-rich mineralogical phases (i.e. jarosite and muscovite).

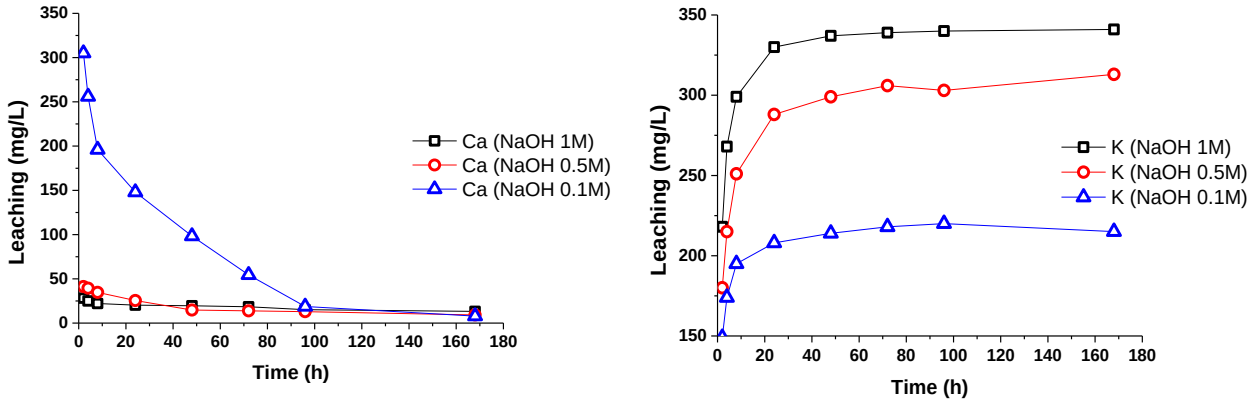

Figure 7.5. Leaching of Ca and K from sample NE02 using NaOH 0.1, 0.5 and 1 M as the extracting solution.

Binder

Based on the results already reported, it was decided to investigate the effects of the alkali-activated binders tested for the low-binder content formulation by using NaOH 1M as the extracting solution and maintaining a solid/liquid ratio of 5 and a maximum residence time of 7 days.

From the results reported in **Table 7.18**, **Table 7.19**, and **Figure 7.6**, it can be observed that changing the binder caused significant variations in the leaching of heavy metals, Ca, and K from the granules. As for the granules produced using CEM I 42.5 R as binder, no leaching of Be, Hg, Mg and P was detected, but the use of alkali-activated binders led to a significant removal of Cd (~4-6 %). Moreover, the granules made from these binders showed no significant leaching of Ni and V, and only minor leaching of Cr and Co (< 0.4 %). While CEM I 42.5 R provided the best results for the removal of As (~19 %), Cr (~5 %), and Ni (~7 %), showing also the removal of Cu (~7 %), its use led to the leaching only of quite low quantities of Sn ,V ,Zn, Se, Tl (~3 %), and Co(~0.5 %).

As far as alkali-activated binders are concerned, the granulate made by using GEO1 (Blast furnace slag and NaOH 4 M) as binder (sample NE19) gave the best results for the removal of Pb (~10 %), together with significant releases of As, Cd, Cu, Se, Tl, and Zn. The granulate made by using GEO2 (Blast furnace slag, sodium carbonate, lime and water) as binder (sample NE18) gave the best results in the removal of Cd (~7 %), Se (~3 %) and Cu (~8 %), alongside with a significant leaching of As, Pb, Sn, Tl and Zn. Using GEO 5 (Blast furnace slag, sodium carbonate, clinker and water) as binder (sample NE20) provided to be suitable for the removal of As, Cd, Cu, Pb, Se, Sn, Tl, and Zn, but with lower results compared to the other binders, save for GEO4 (Blast furnace slag, clinker and water), which gave the worst results for all the investigated heavy metals, showing only a limited removal of As, Cd, Cu, and Tl (~2-4 %).

Table 7.18. Removal % of As, Cd, Co, Cr, Cu, Ni, Pb, Se, Sn, Tl, V, and Zn from samples NE07, NE18, NE19 and NE20 (Soil 1, low binder content formulation) using NaOH 1 M as extracting solution. (n.d.: not detected).

Soil 1	Time (h)	Removal (%)													
		As	**Be**	**Cd**	**Co**	**Cr**	**Cu**	**Hg**	**Ni**	**Pb**	**Se**	**Sn**	**Tl**	**V**	**Zn**
	2	1.20	n.d.	n.d.	n.d.	n.d.	2.70	n.d.	n.d.	5.00	0.12	n.d.	n.d.	n.d.	0.31
	4	1.54	n.d.	n.d.	n.d.	n.d.	2.92	n.d.	n.d.	5.88	0.13	n.d.	n.d.	n.d.	0.36
	8	2.08	n.d.	1.31	n.d.	n.d.	3.56	n.d.	n.d.	6.84	0.18	n.d.	0.31	n.d.	0.49
NE18	24	4.52	n.d.	2.47	n.d.	n.d.	4.92	n.d.	n.d.	7.78	0.32	n.d.	0.81	n.d.	0.88
(GEO1)	48	6.58	n.d.	3.67	n.d.	n.d.	5.68	n.d.	n.d.	8.52	0.68	n.d.	1.71	n.d.	1.21
	72	8.56	n.d.	3.95	0.14	0.09	6.77	n.d.	n.d.	9.42	0.96	n.d.	2.38	n.d.	1.24
	96	9.57	n.d.	4.22	0.17	0.09	6.98	n.d.	n.d.	9.71	1.06	n.d.	3.37	n.d.	1.39
	168	12.9	n.d.	5.47	0.22	0.10	7.88	n.d.	n.d.	10.28	1.94	n.d.	4.11	n.d.	1.46
	2	1.83	n.d.	n.d.	n.d.	n.d.	0.62	n.d.	n.d.	4.74	0.46	n.d.	n.d.	n.d.	0.60
	4	2.63	n.d.	2.20	n.d.	n.d.	0.98	n.d.	n.d.	5.34	0.64	n.d.	0.52	n.d.	0.88
	8	4.13	n.d.	3.16	n.d.	n.d.	1.78	n.d.	n.d.	5.75	0.93	n.d.	1.43	n.d.	1.02
NE19	24	5.18	n.d.	5.19	0.14	n.d.	2.80	n.d.	n.d.	6.74	1.28	n.d.	2.03	n.d.	1.14
(GEO2)	48	7.17	n.d.	5.91	0.16	n.d.	4.16	n.d.	n.d.	7.38	1.58	0.57	2.23	n.d.	1.22
	72	9.00	n.d.	6.35	0.23	0.13	4.81	n.d.	n.d.	8.83	1.94	0.82	2.68	n.d.	1.35
	96	9.42	n.d.	6.85	0.26	0.13	6.28	n.d.	n.d.	9.06	2.05	1.00	3.05	n.d.	1.42
	168	11.1	n.d.	7.20	0.29	0.14	7.97	n.d.	n.d.	9.32	2.81	1.17	3.34	n.d.	1.47
	2	0.36	n.d.	n.d.	n.d.	n.d.	0.30	n.d.	n.d.	0.66	n.d.	n.d.	n.d.	n.d.	0.05
	4	0.50	n.d.	n.d.	n.d.	n.d.	0.45	n.d.	n.d.	0.92	0.13	n.d.	0.23	n.d.	0.05
	8	0.80	n.d.	n.d.	0.11	n.d.	0.66	n.d.	n.d.	1.34	0.15	n.d.	0.87	n.d.	0.09
NE07	24	1.49	n.d.	1.10	0.14	0.11	1.23	n.d.	n.d.	2.07	0.27	n.d.	1.93	n.d.	0.16
(GEO4)	48	2.14	n.d.	1.77	0.17	0.19	1.80	n.d.	n.d.	2.67	0.49	n.d.	2.40	n.d.	0.19
	72	2.49	n.d.	2.31	0.19	0.24	2.01	n.d.	n.d.	3.03	0.56	n.d.	2.87	n.d.	0.20
	96	3.18	n.d.	3.35	0.25	0.38	2.67	n.d.	n.d.	3.35	0.73	n.d.	3.48	n.d.	0.21
	168	4.15	n.d.	4.52	0.32	0.54	3.41	n.d.	n.d.	3.62	0.96	n.d.	4.71	n.d.	0.23

Table 7.19. Removal % of As, Cd, Co, Cr, Cu, Ni, Pb, Se, Sn, Tl, V, and Zn from samples NE07, NE18, NE19 and NE20 (Soil 1, low binder content formulation) using NaOH 1 M as extracting solution. (n.d.: not detected).

	Time (h)	Removal (%)													
		As	Be	Cd	Co	Cr	Cu	Hg	Ni	Pb	Se	Sn	Tl	V	Zn
NE20 (GEO5)	2	1.34	n.d.	1.26	0.13	0.09	0.57	n.d.	n.d.	3.67	0.57	n.d.	0.00	n.d.	0.46
	4	1.93	n.d.	1.45	0.13	0.14	0.89	n.d.	n.d.	4.18	0.62	n.d.	0.23	n.d.	0.69
	8	3.01	n.d.	2.37	0.14	0.21	1.63	n.d.	n.d.	4.74	0.96	n.d.	0.524	n.d.	0.81
	24	4.91	n.d.	3.18	0.17	0.24	2.73	n.d.	n.d.	5.31	1.22	0.56	1.03	n.d.	1.41
	48	7.11	n.d.	4.50	0.19	0.27	4.22	n.d.	n.d.	5.78	1.65	0.67	1.71	n.d.	1.74
	72	7.88	n.d.	4.53	0.22	0.30	4.83	n.d.	n.d.	6.17	1.78	1.00	2.05	n.d.	1.90
	96	8.38	n.d.	5.16	0.24	0.34	5.54	n.d.	n.d.	6.71	2.04	1.08	2.53	n.d.	1.92
	168	11.1	n.d.	6.21	0.28	0.36	7.32	n.d.	n.d.	7.28	2.76	1.30	3.91	n.d.	2.12

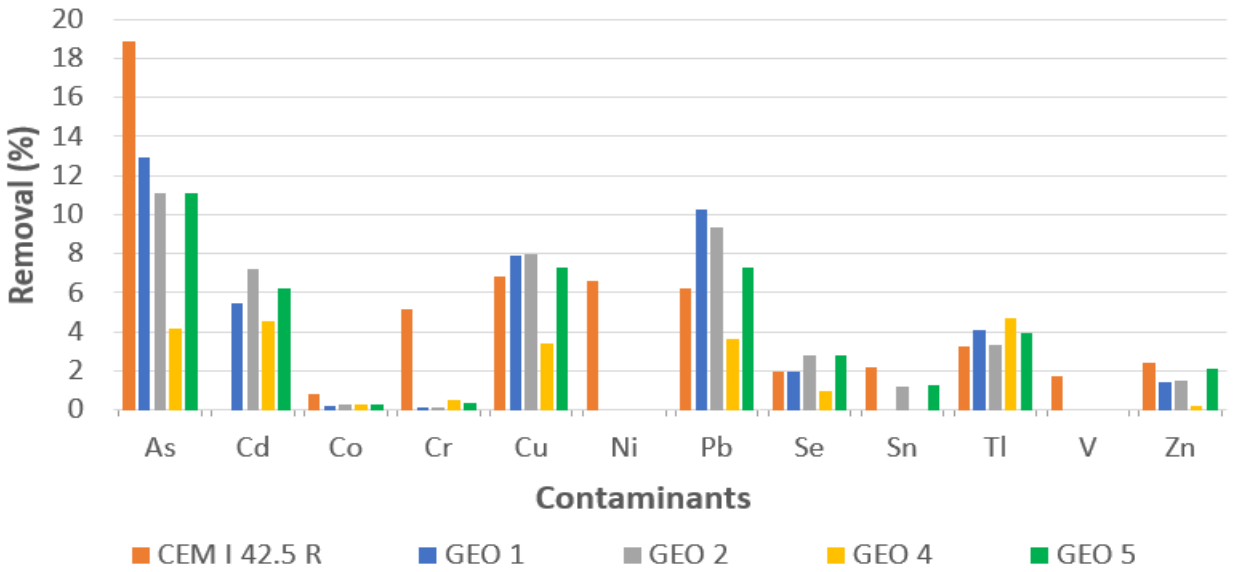

Figure 7.6. Removal % of As, Cd, Co, Cr, Cu, Ni, Pb, Se, Sn, Tl, V, and Zn from samples NE02, NE07, NE18, NE19 and NE20 (Soil 1, low binder content formulation) using NaOH 1 M as extracting solution.

The leaching of Ca and K from the granules containing Soil 1 with the different alkali-activated binders was also investigated, as reported in **Table 7.20** and **Figure 7.7**. The concentration of Ca showed the same trend reported for the other samples, starting from around 25 mg/L then decreasing up to around 10 mg/L after 7 days, while the leaching of K decreased of about 50% by using alkali-activated with respect to CEM I 42.5 R, but maintained the same trend, reaching a plateau after about 24 hours

Table 7.20. Leaching of Ca and K from samples NE02, NE07, NE18, NE19 and NE20 (Soil 1, low binder content formulation) using NaOH 1 M as extracting solution.

	Time	Ca	K		Time	Ca	K
	h	mg·L^{-1}			h	mg·L^{-1}	
	2	20.0	54		2	24.1	101
	4	18.4	68		4	23.8	101
	8	17.3	93		8	21.2	121
NE18	24	15.8	102	**NE19**	24	17.8	126
(GEO1)	48	14.4	111	**(GEO2)**	48	15.7	125
	72	12.9	114		72	13.4	139
	96	12.2	132		96	12.4	142
	168	11.9	144		168	11.2	169
	2	23.7	57		2	27.5	64
	4	21.3	85		4	25.4	80
	8	20.0	113		8	23.2	109
NE07	24	17.1	168	**NE20**	24	20.8	117
(GEO4)	48	12.9	203	**(GEO5)**	48	19.0	132
	72	7.9	200		72	15.7	128
	96	5.4	202		96	13.8	136
	168	3.6	205		168	11.8	157

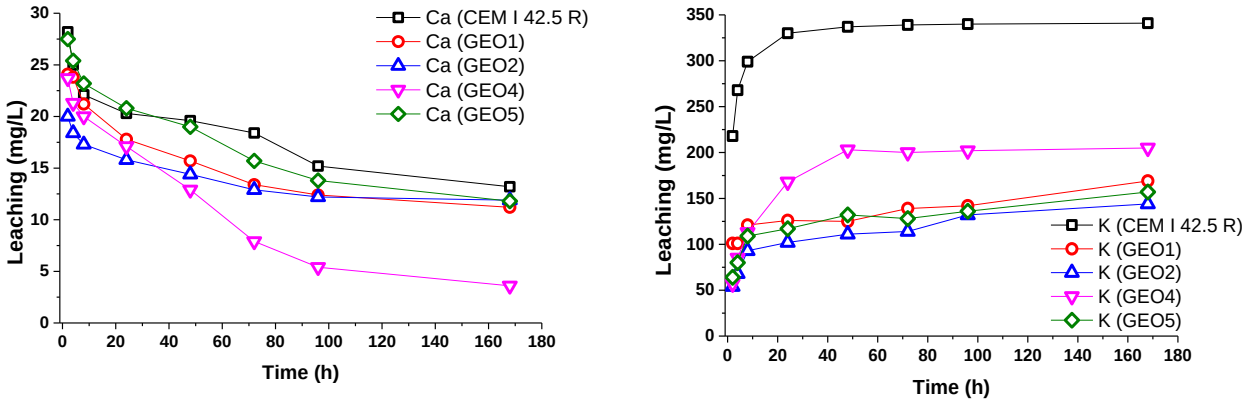

Figure 7.7. Leaching of Ca and K from samples NE02, NE07, NE18, NE19 and NE20 (Soil 1, low binder content formulation) using NaOH 1 M as extracting solution.

Use of chelating agents

Since sample NE02, produced with CEM I 42.5 R, gave the best results, it was used to investigate the effects of addition of several chelating agents to the NaOH 1 M solution used as extractant. While sodium oxalate was found to be poorly soluble in the NaOH solution used for the leaching tests and was not considered further, the results obtained for sodium citrate and sodium acetate are reported in **Table 7.22** and **Figure 7.8**, showing some changes for many heavy metals' leaching, compared to the extraction made using only NaOH. In particular, the use of both chelating agents led to the removal of around 8-10 % of the total Cd content of the sample, unlike the use of pure NaOH which caused no dissolution of this contaminant. The removal of Tl, Ni, and As increased respectively of about 95, 80, and 30 %, while the variations observed for Co, Cr, Cu, Pb, Se, Sn, and Zn were much more limited.

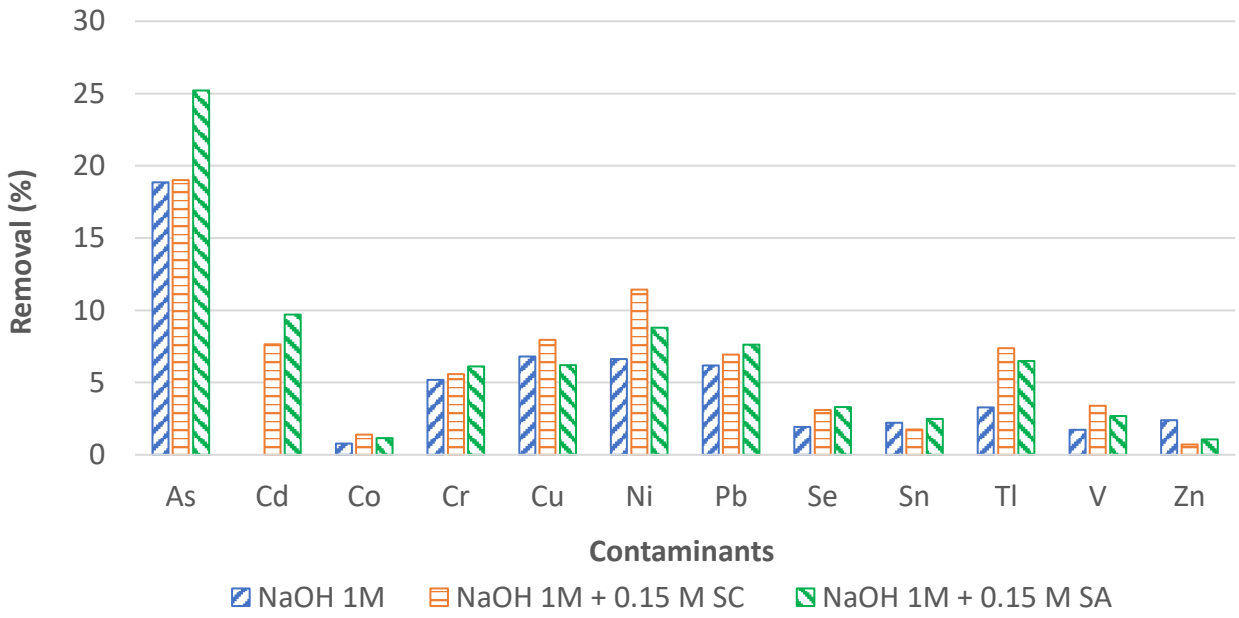

Figure 7.8. Removal % of As, Cd, Co, Cr, Cu, Ni, Pb, Se, Sn, Tl, V, and Zn from sample NE02 using NaOH 1 M, NaOH 1 M + SC 0.15 M and NaOH 1 M + SA 0.15 M as extracting solutions.

As can be seen from **Table 7.21** and **Figure 7.9**, the use of SA did not change the leaching of Ca compared to the pure NaOH solution, while the use of SC caused an increase of nearly two orders of magnitude, probably due to the formation of stable Ca-SC complexes [422].The leaching of K showed the same trend observed for the other samples, but the addition of the complexing agents caused its leaching to almost double

From these results it can be concluded that the addition of chelating agents led to significant improvements in the removal of some contaminants, but at generally longer extraction times. Furthermore, the increase of the solution ionic strength (+ 12.3 g/L for SA and + 38.4 g/L for SC, respectively) would lead to a clear decrease in the NF process efficiency, by decreasing the permeate's

flow and significantly lengthen the time required for this step, thus increasing the overall cost of the process. Moreover, the addition of other steps for recovering these reagents would only further increase the costs without significantly improve the removal of some pollutants. Furthermore, for many of the heavy metals studied, the leaching kinetics reveal that in the presence of these substances the time required for the leaching step was increased.

Based on these results, no chelating agents were used in the rest of the study.

Table 7.21. Leaching of Ca and K from sample NE02 using NaOH 1 M, NaOH 1 M + SC 0.15 M and NaOH 1 M + SA 0.15 M as extracting solutions.

NE02	Time	Ca	K		Time	Ca	K
	h	mg·L^{-1}			h	mg·L^{-1}	
	2	241	248		2	28.2	230
	4	285	321		4	27.4	297
	8	315	380		8	25.3	368
NaOH 1M + 0.15 M SC	24	351	486	**NaOH 1M + 0.15 M SA**	24	22.1	469
	48	346	525		48	26.1	532
	72	347	545		72	13.6	559
	96	353	546		96	10.3	572
	168	354	622		168	7.0	623

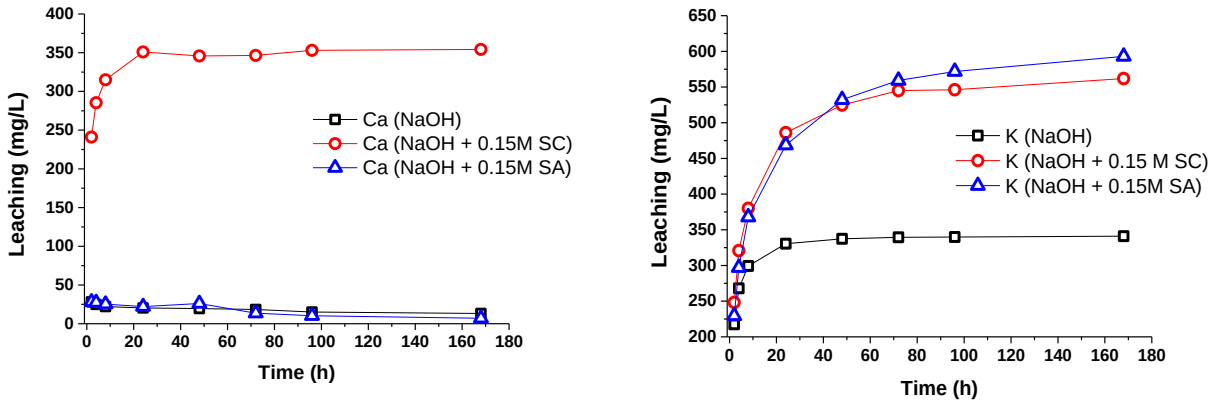

Figure 7.9. Leaching of Ca (a) and K (b) from sample NE02 using NaOH 1 M, NaOH 1 M + SC 0.15 M and NaOH 1 M + SA 0.15 M as extracting solutions.

Table 7.22. Removal % of As, Be, Cd, Co, Cr, Cu, Hg, Ni, Pb, Se, Sn, Tl, V, and Zn from sample NE02 using NaOH 1 M + SC 0.15 M and NaOH 1 M + SA 0.15 M as extracting solutions. (n.d.: not detected).

NE02	Time (h)	Removal (%)													
		As	**Be**	**Cd**	**Co**	**Cr**	**Cu**	**Hg**	**Ni**	**Pb**	**Se**	**Sn**	**Tl**	**V**	**Zn**
NaOH 1M + 0.15 M SC	2	1.89	n.d.	n.d.	n.d.	1.52	1.02	n.d.	1.90	1.68	0.50	0.73	2.39	0.41	0.19
	4	2.62	n.d.	n.d.	0.28	1.88	1.50	n.d.	2.77	2.46	0.53	0.95	2.82	0.63	0.25
	8	3.52	n.d.	n.d.	0.39	2.33	2.18	n.d.	3.72	3.22	0.56	1.37	3.65	0.97	0.35
	24	5.92	n.d.	2.05	0.73	3.35	3.66	n.d.	6.27	4.88	0.91	1.59	4.15	1.65	0.46
	48	8.43	n.d.	3.02	0.87	4.06	4.79	n.d.	7.76	5.85	1.24	1.60	5.66	2.18	0.56
	72	10.7	n.d.	4.33	1.03	4.42	5.40	n.d.	8.77	6.22	1.51	1.62	5.82	2.44	0.61
	96	12.4	n.d.	4.83	1.13	4.61	5.83	n.d.	9.15	6.42	1.84	1.66	6.51	2.60	0.64
	168	19.0	n.d.	7.64	1.39	5.59	7.96	n.d.	11.4	6.94	3.10	1.75	7.38	3.39	0.70
NaOH 1M + 0.15 M SA	2	1.39	n.d.	n.d.	n.d.	1.24	0.49	n.d.	0.92	1.61	0.36	n.d.	1.52	< 0.4	0.15
	4	1.94	n.d.	0.31	n.d.	1.64	0.74	n.d.	1.58	2.32	0.46	n.d.	2.01	< 0.4	0.19
	8	3.07	n.d.	0.56	0.23	2.19	1.20	n.d.	2.55	3.06	0.56	0.71	2.22	0.50	0.31
	24	6.52	n.d.	2.01	0.45	3.26	2.16	n.d.	4.45	4.98	0.92	0.98	3.29	0.91	0.42
	48	10.1	n.d.	4.15	0.63	4.23	3.18	n.d.	6.08	6.21	1.34	1.10	4.27	1.21	0.60
	72	13.1	n.d.	6.15	0.70	4.64	3.74	n.d.	6.78	6.79	1.66	1.29	4.49	1.42	0.64
	96	16.2	n.d.	7.24	0.95	5.04	4.39	n.d.	7.42	7.06	2.05	1.45	5.50	1.77	0.78
	168	25.2	n.d.	9.71	1.15	6.10	6.21	n.d.	8.80	7.62	3.31	2.48	6.49	2.68	1.06

Wet conditioning process

Since the effects of the wet conditioning (WC) process in improving both the mechanical characteristics of the pellets made using the standard HPSS® process and the retention of pollutants have been reported [238], its effects on the contaminant's removal have been investigated. Moreover, the possibility of using the extraction step of the HPSS-NanoExtra process as a substitute for this treatment was considered. An aliquot (1 kg) of sample NE01 was conditioned in water for 25 days, by using flowing tap water with a solid/liquid ratio of 1 kg/L and a flow of 1 L of water per day for each kilogram of pellets, while the system was stirred by insufflating compressed air from the bottom of the conditioning tank. Then, a sample of this granulate (NE01WC) was subjected to the decontamination step using a 1 M NaOH solution, with a S/L ratio of 1/5, for 72 hours. The results obtained are reported in **Table 7.24** and **Figure 7.10** showing, as in the case of sample NE01, no detectable leaching of Be, Hg and Cd, but also a clear reduction of the leaching of the other heavy metals. In particular, the leaching of Ni, Co and Cu showed the greatest decrease (~75-85 %), while the removal of Cr, Se, V, Zn and Tl was about 50% lower. The less affected heavy metals were As and Pb, whose leaching decreased of about 30%. To investigate the need for the WC process after the leaching step, the decontamination process (1 M NaOH, 72 hours) was applied four times to another aliquot (1kg) of sample NE01, which was then subjected to the UNI 12457-2:2004 leaching test. The results are reported in **Table 7.23**, showing values exceeding the Italian regulatory limits for the *"end of waste"* classification [114] for both pH and the leaching of Cr, Cu, Ni, Pb, and Se.

Table 7.23. Results of the leaching test UNI EN 12457-2:2004 of sample NE01 after 4 cycles (1M NaOH, 72 h) of the decontamination step. Parameters exceeding the regulatory limits are highlighted in bold.

Parameter	NE01 after decontamination	Regulatory Limit*
	$\mu g \cdot L^{-1}$	
As	3.19±0.51	50
Ba	172±6	1000
Be	< 0.1	10
Cd	0.12±0.02	5
Co	13.5±1.0	250
Cr	**72.9±2.9**	**50**
Cu	**286±13**	**50**
Hg	< 0.1	1
Ni	**216±6**	**10**
Pb	**5430±388**	**50**
Se	**55.9±3.6**	**10**
V	1.52±0.27	250
Zn	< 0.1	3000
pH	**12.75±0.10**	**5.5-12.0**

*Regulatory limit: Table 1 of Annex III of Ministerial Decree No 16 of 05th April 2006 [114].

Table 7.24. Removal % of As, Be, Cd, Co, Cr, Cu, Hg, Ni, Pb, Se, Sn, Tl, V, and Zn from sample NE01WC after 72 hours using NaOH 1 M as extracting solution.

NE01WC	Time (h)	Removal (%)													
		As	Be	Cd	Co	Cr	Cu	Hg	Ni	Pb	Se	Sn	Tl	V	Zn
NaOH 1 M	72	4.45	n.d.	n.d.	0.12	2.67	0.73	n.d.	0.64	2.71	0.39	1.03	1.20	0.35	0.17

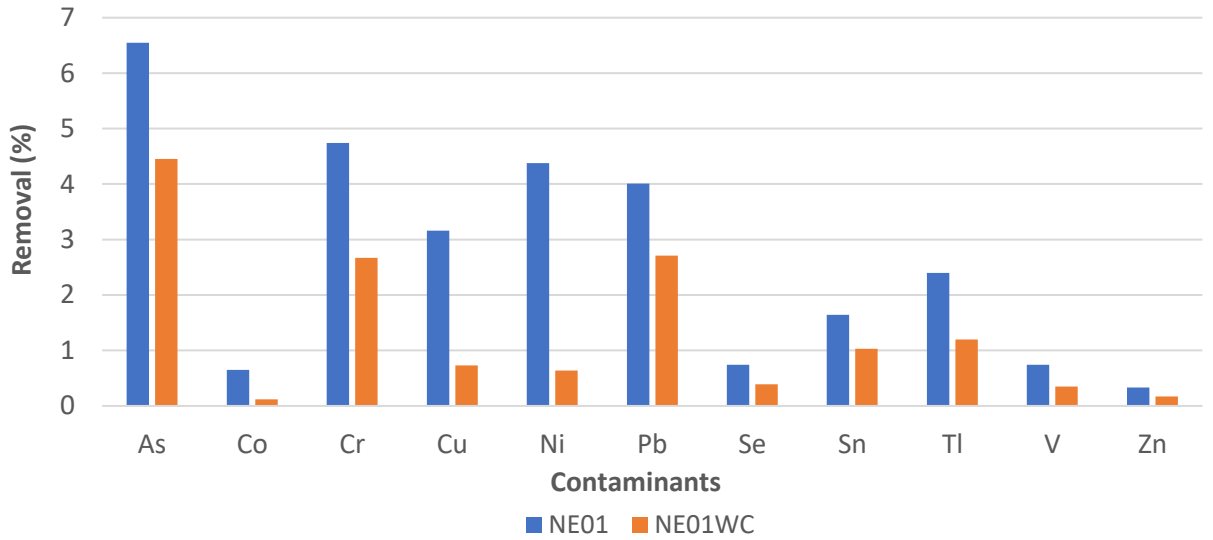

Figure 7.10. Removal % of As, Co, Cr, Cu, Ni, Pb, Se, Sn, Tl, V, and Zn from samples NE01 and NE01WC after 72 hours using NaOH 1 M as extracting solution.

An aliquot of 500 g d.w. of this granulate was subjected to a WC treatment (NE01WC2) for 14 days and then its leaching behaviour was investigated by following the UNI 12457-2:2004 standard. From the results, reported in **Table 7.25**, it can be seen that this granular material complied with all the Italian regulatory requirements for reuse.

Table 7.25. Results of the leaching test UNI EN 12457-2:2004 of sample NE01WC2.

Parameter	NE01WC2	Regulatory Limit*
	$\mu g \cdot L^{-1}$	
As	1.42±0.12	50
Ba	162±11	1000
Be	< 0.1	10
Cd	< 0.1	5
Co	1.79±0.20	250
Cr	25.8±5.8	50
Cu	17.4±1.3	50
Hg	< 0.1	1
Ni	5.99±0.36	10
Pb	< 0.1	50
Se	6.93±0.82	10
V	58.2±1.9	250
Zn	<0.1	3000
pH	11.6±0.1	5.5-12.0

*Regulatory limit: Table 1 of Annex III of Ministerial Decree No 186 of 05th April 2006 [114].

From these results it can be concluded that the decontamination step must be applied before the wet conditioning process, which is still necessary to obtain a decontaminated and stabilized cementitious granular material accomplishing all the Italian regulatory requirements for the "end of waste" classification [114].

Based on the results reported above, a second set of experiments was performed on the granules obtained from the treatment of the pre-treated fly ashes.

7.4.2.4. Fly ashes from MSW combustion

The second set of experiments was carried out on the granules obtained from the pelletisation of the pre-treated fly ashes from MSW combustion. Considering the previous results, these materials were extracted using NaOH 1 M for 7 days, without the use of chelating agents. Moreover, the lower concentration of Pb in the eluates obtained from the extraction of those granules compared to those observed in the eluates from the extraction of the pellets made from Soil 1, allowed also to analyse the concentration of Sb without any interference.

The pellets made by using the standard HPSS® formulation (sample NE04) were first tested showing, as reported in **Table 7.26**, no relevant leaching of Be, As, Cd, Cu, Co, Ni, Se, Tl, and Hg.

The removal of the other heavy metals (i.e. Cr, Sb, Sn, V, Zn) showed the same trends reported for the samples of granules made from Soil 1,but was also quite limited (~ 0.3-3 %), with only the leaching of Pb exceeding 3.5 % after 7 days.

Also in this case, the concentration of Ca increased for the first two hours and then decreased as the contact time increased, though the decrease was slightly less marked than for the samples obtained from Soil 1, probably due to the lower quantity of sulphates present. Similarly to the other samples, the release of K increased markedly in the first 24 hours and then reached a plateau in which the increase was much more contained. The final concentrations of both Ca and K reached at the end of the leaching tests were very similar to those reached by the samples of Soil 1 granulated with CEM I 42.5 R. The extraction of sample NE05, prepared by applying the low binder content formulation using CEM I 42.5 R (**Table 7.27**), showed similar results to sample NE04 for the removal of Be, As, Cd, Cu, Co, Ni, Se, Tl, Hg, Cr, Sb, Sn, V and Zn but a clear increase in the removal of Se (~5 %).

Since changing the binder used for the treatment of Soil 1 changed significantly the removal of several heavy metals that were not extracted from samples NE01 and NE02, the granules produced using alkali-activated binders form the pre-treated fly ashes were also tested. The results are reported in **Table 7.28**, **Table 7.29**, and **Figure 7.11**, showing that the use these binders increased the removal of As (~18 %), Se (~12 %) and V (~8 %) compared to the pellets made using CEM 42.5 R, in particular for GEO5 and GEO1. On the other hand, the leaching of Cu, Sb, Sn and Zn remained quite limited (< 2 %) for all binders investigated, while the leaching of Cr decreased compared to the granules made by using CEM I 42.5 R. The leaching of Ca was quite similar for all the granules made from the pre-treated fly ashes, but the leaching of K was about 30 % lower for the pellets made using alkali-activated binders with respect to those made using OPC.

Since the extraction was demonstrated to be effective only for the removal of As, Se, and V, whose amount in the granules was quite low (about 10, 15 and 50 mg/kg d.w., respectively) the pre-treated fly ashes were not further considered in this study.

Table 7.26. Removal % of As, Be, Cd, Co, Cr, Cu, Hg, Ni, Pb, Se, Sn, Tl, V, and Zn from sample NE04 using NaOH 1 M as extracting solution. Leaching of Ca and K from sample NE04 using NaOH 1 M as extracting solution. (n.d.: not detected).

Fly ashes	Time (h)	Removal (%)															Leaching (mg·L^{-1})	
		As	Be	Cd	Co	Cr	Cu	Hg	Ni	Pb	Se	Sb	Sn	Tl	V	Zn	Ca	K
NE04 (CEM I 42.5 R)	2	n.d.	n.d.	n.d.	n.d.	0.74	n.d.	n.d.	n.d.	1.55	n.d.	0.24	0.10	n.d.	n.d.	0.43	28.8	298
	4	n.d.	n.d.	n.d.	n.d.	0.95	n.d.	n.d.	n.d.	1.83	n.d.	0.25	0.11	n.d.	n.d.	0.51	28.1	323
	8	n.d.	n.d.	n.d.	n.d.	1.19	n.d.	n.d.	n.d.	2.05	n.d.	0.29	0.12	n.d.	0.11	0.58	26.8	336
	24	n.d.	n.d.	n.d.	n.d.	1.73	n.d.	n.d.	n.d.	2.50	n.d.	0.36	0.14	n.d.	0.28	0.73	22.2	341
	48	n.d.	n.d.	n.d.	n.d.	2.03	n.d.	n.d.	n.d.	2.67	n.d.	0.37	0.16	n.d.	0.47	0.81	18.9	340
	72	n.d.	n.d.	n.d.	n.d.	2.23	n.d.	n.d.	n.d.	2.75	n.d.	0.58	0.20	n.d.	0.48	1.00	14.6	342
	96	n.d.	n.d.	n.d.	n.d.	2.36	n.d.	n.d.	n.d.	3.03	n.d.	0.62	0.22	n.d.	0.59	1.26	13.6	344
	168	n.d.	n.d.	n.d.	n.d.	2.81	n.d.	n.d.	n.d.	3.64	n.d.	0.62	0.27	n.d.	0.96	1.52	10.2	348

Table 7.27. Removal % of As, Be, Cd, Co, Cr, Cu, Hg, Ni, Pb, Se, Sb, Sn, Tl, V, and Zn from sample NE05 using NaOH 1 M as extracting solution. Leaching of Ca and K from sample NE04 using NaOH 1 M as extracting solution. (n.d.: not detected).

Fly ashes	Time (h)	Removal (%)															Leaching (mg·L^{-1})	
		As	Be	Cd	Co	Cr	Cu	Hg	Ni	Pb	Se	Sb	Sn	Tl	V	Zn	Ca	K
NE05 (CEM I 42.5 R)	2	n.d.	n.d.	n.d.	n.d.	0.93	n.d.	n.d.	n.d.	2.62	n.d.	0.29	0.10	n.d.	n.d.	0.67	27.3	271
	4	n.d.	n.d.	n.d.	n.d.	1.13	n.d.	n.d.	n.d.	2.88	0.86	0.31	0.12	n.d.	n.d.	0.75	25.8	279
	8	n.d.	n.d.	n.d.	n.d.	1.34	n.d.	n.d.	n.d.	3.11	1.26	0.33	0.12	n.d.	0.12	0.82	24.1	289
	24	n.d.	n.d.	n.d.	n.d.	1.77	n.d.	n.d.	n.d.	3.60	3.32	0.42	0.14	n.d.	0.34	1.04	20.1	298
	48	n.d.	n.d.	n.d.	n.d.	1.94	n.d.	n.d.	n.d.	3.64	4.38	0.45	0.15	n.d.	0.61	1.14	18.0	305
	72	n.d.	n.d.	n.d.	n.d.	2.13	n.d.	n.d.	n.d.	3.74	5.08	0.47	0.16	n.d.	0.66	1.27	16.8	309
	96	n.d.	n.d.	n.d.	n.d.	2.32	n.d.	n.d.	n.d.	3.90	5.40	0.58	0.23	n.d.	0.91	1.46	14.9	310
	168	n.d.	n.d.	n.d.	n.d.	2.82	n.d.	n.d.	n.d.	4.11	5.35	0.76	0.30	n.d.	1.50	1.84	10.5	314

Table 7.28. Removal % of As, Be, Cd, Co, Cr, Cu, Hg, Ni, Pb, Se, Sb, Sn, Tl, V, and Zn from samples NE11, NE13 and NE09 using NaOH 1 M as extracting solution. Leaching of Ca and K from samples NE11, NE13 and NE09 using NaOH 1 M as extracting solution. (n.d.: not detected).

Fly ashes	Time (h)	Removal (%)															Leaching (mg·L^{-1})	
		As	Be	Cd	Co	Cr	Cu	Hg	Ni	Pb	Se	Sb	Sn	Tl	V	Zn	Ca	K
NE11 (GEO1)	2	3.34	n.d.	n.d.	n.d.	n.d.	n.d.	n.d.	n.d.	0.59	0.41	0.06	0.16	n.d.	0.65	0.26	18.0	85
	4	3.76	n.d.	n.d.	n.d.	n.d.	0.09	n.d.	n.d.	0.75	1.06	0.08	0.17	n.d.	0.90	0.35	14.8	107
	8	4.69	n.d.	n.d.	n.d.	n.d.	0.12	n.d.	n.d.	0.92	1.95	0.12	0.17	n.d.	1.18	0.46	11.1	138
	24	6.21	n.d.	n.d.	n.d.	0.12	0.19	n.d.	n.d.	1.25	4.83	0.20	0.23	n.d.	1.94	0.70	6.05	179
	48	11.1	n.d.	n.d.	n.d.	0.16	0.27	n.d.	n.d.	1.53	9.06	0.36	0.30	n.d.	2.97	0.93	3.97	223
	72	12.8	n.d.	n.d.	n.d.	0.18	0.29	n.d.	n.d.	1.55	11.8	0.42	0.42	n.d.	3.34	1.00	2.95	227
	96	14.5	n.d.	n.d.	n.d.	0.18	0.29	n.d.	n.d.	1.54	12.5	0.45	0.46	n.d.	3.47	0.96	2.36	236
	168	16.8	n.d.	n.d.	n.d.	0.19	0.31	n.d.	n.d.	1.56	13.0	0.47	0.62	n.d.	3.50	1.13	2.03	241
NE13 (GEO2)	2	1.50	n.d.	n.d.	n.d.	0.04	n.d.	n.d.	n.d.	1.83	n.d.	0.24	0.13	n.d.	0.21	0.55	34.3	101
	4	1.77	n.d.	n.d.	n.d.	0.06	n.d.	n.d.	n.d.	2.25	n.d.	0.31	0.14	n.d.	0.30	0.63	31.5	131
	8	2.09	n.d.	n.d.	n.d.	0.07	n.d.	n.d.	n.d.	2.73	n.d.	0.39	0.15	n.d.	0.37	0.73	27.4	164
	24	2.23	n.d.	n.d.	n.d.	0.11	n.d.	n.d.	n.d.	3.10	n.d.	0.48	0.18	n.d.	0.66	0.97	17.1	197
	48	2.61	n.d.	n.d.	n.d.	0.16	0.07	n.d.	n.d.	3.53	n.d.	0.76	0.30	n.d.	1.06	1.26	10.7	225
	72	2.81	n.d.	n.d.	n.d.	0.22	0.08	n.d.	n.d.	3.57	n.d.	0.88	0.36	n.d.	1.50	1.58	8.13	253
	96	4.61	n.d.	n.d.	n.d.	0.24	0.09	n.d.	n.d.	3.70	n.d.	0.94	0.44	n.d.	1.96	1.72	7.63	264
	168	7.00	n.d.	n.d.	n.d.	0.35	0.18	n.d.	n.d.	3.80	n.d.	0.99	0.56	n.d.	3.19	2.36	6.32	271
NE09 (GEO4)	2	1.50	n.d.	n.d.	n.d.	0.44	n.d.	n.d.	n.d.	2.28	n.d.	0.29	0.14	n.d.	0.30	0.54	29.9	189
	4	1.83	n.d.	n.d.	n.d.	0.56	n.d.	n.d.	n.d.	2.69	n.d.	0.33	0.15	n.d.	0.38	0.64	27.9	217
	8	2.25	n.d.	n.d.	n.d.	0.71	n.d.	n.d.	n.d.	3.08	n.d.	0.38	0.15	n.d.	0.49	0.74	24.6	236
	24	2.70	n.d.	n.d.	n.d.	0.98	n.d.	n.d.	n.d.	3.34	n.d.	0.45	0.17	n.d.	0.89	0.94	17.6	246
	48	3.10	n.d.	n.d.	n.d.	1.20	n.d.	n.d.	n.d.	3.95	n.d.	0.64	0.23	n.d.	1.23	1.19	13.5	251
	72	3.31	n.d.	n.d.	n.d.	1.33	n.d.	n.d.	n.d.	4.58	n.d.	0.67	0.23	n.d.	1.56	1.33	12.1	253
	96	4.13	n.d.	n.d.	n.d.	1.35	n.d.	n.d.	n.d.	4.69	n.d.	0.68	0.30	n.d.	1.88	1.42	10.4	255
	168	4.79	n.d.	n.d.	n.d.	1.57	n.d.	n.d.	n.d.	4.82	n.d.	0.69	0.36	n.d.	3.01	1.95	9.36	260

Table 7.29. Removal % of As, Be, Cd, Co, Cr, Cu, Hg, Ni, Pb, Se, Sb, Sn, Tl, V, and Zn from samples NE11, NE13 and NE09 using NaOH 1 M as extracting solution. Leaching of Ca and K from samples NE11, NE13 and NE09 using NaOH 1 M as extracting solution. (n.d.: not detected).

Fly ashes	Time (h)	Removal (%)															Leaching ($mg \cdot L^{-1}$)	
		As	Be	Cd	Co	Cr	Cu	Hg	Ni	Pb	Se	Sb	Sn	Tl	V	Zn	Ca	K
NE15 (GEO5)	2	4.79	n.d.	n.d.	n.d.	0.31	0.08	n.d.	n.d.	1.01	0.31	0.10	0.15	n.d.	1.20	0.36	21.4	146
	4	5.13	n.d.	n.d.	n.d.	0.45	0.13	n.d.	n.d.	1.50	1.03	0.28	0.25	n.d.	1.99	0.60	13.4	159
	8	5.70	n.d.	n.d.	n.d.	0.49	0.17	n.d.	n.d.	2.00	1.61	0.46	0.32	n.d.	2.91	0.91	9.75	178
	24	7.31	n.d.	n.d.	n.d.	0.58	0.22	n.d.	n.d.	2.60	3.51	0.70	0.43	n.d.	4.55	1.36	5.70	197
	48	13.31	n.d.	n.d.	n.d.	0.60	0.25	n.d.	n.d.	2.88	5.19	0.88	0.51	n.d.	6.17	1.65	3.10	226
	72	14.31	n.d.	n.d.	n.d.	0.64	0.26	n.d.	n.d.	2.94	7.45	0.96	0.59	n.d.	7.06	1.70	2.31	224
	96	16.69	n.d.	n.d.	n.d.	0.69	0.28	n.d.	n.d.	2.93	8.06	1.03	0.64	n.d.	7.65	1.76	1.56	227
	168	18.53	n.d.	n.d.	n.d.	0.73	0.30	n.d.	n.d.	3.07	8.48	1.11	0.67	n.d.	7.81	1.76	1.26	230

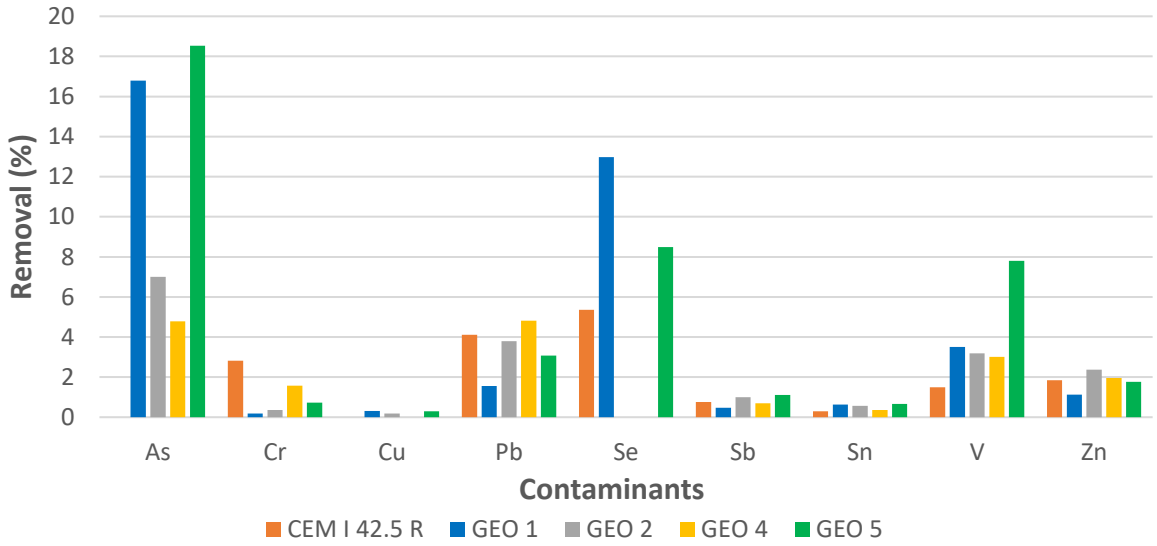

Figure 7.11. Removal % of As, Cr, Cu, Pb, Se, Sb, Sn, V, and Zn from samples NE05, NE09, NE11, NE13 and NE15 (Fly ashes, low binder content formulation) using NaOH 1 M as extracting solution.

7.5. WP5: Bench scale testing

Based on the results of the previous WPs, the following operating conditions were selected for the decontamination step:

- Extracting solution: 1 M NaOH
- Solid/liquid ratio: 1/5
- Time of residence: 72 hours

The results obtained were used to select the final design and operating conditions of the bench-scale plant. After assembling the whole prototype, the effectiveness of the nanofiltration step for NaOH recovery was investigated, followed by the optimization of the treatment to recover the heavy metals from the concentrated fraction. The entire process was tested on the granules produced from the treatment of Soil 1 with both HPSS® formulations (NE01 and NE02). The design of the bench scale prototype is reported in the following experimental section (**Figure 7.12 and Figure 7.13)**.

7.5.1. Experimental

7.5.1.1. Prototype design

The prototype was composed by the following installations:

- Leaching tank;
- Storage tank for eluate sedimentation;
- Sand filter and sleeve filter (5 μm mesh) for suspended solids removal;
- NF apparatus;
- Apparatus for the chemical-physical treatment of NF concentrated fraction for the removal of the heavy metals present;
- Apparatus for sludge removal and NaOH reintegrating for the recycling of the extracting solution.

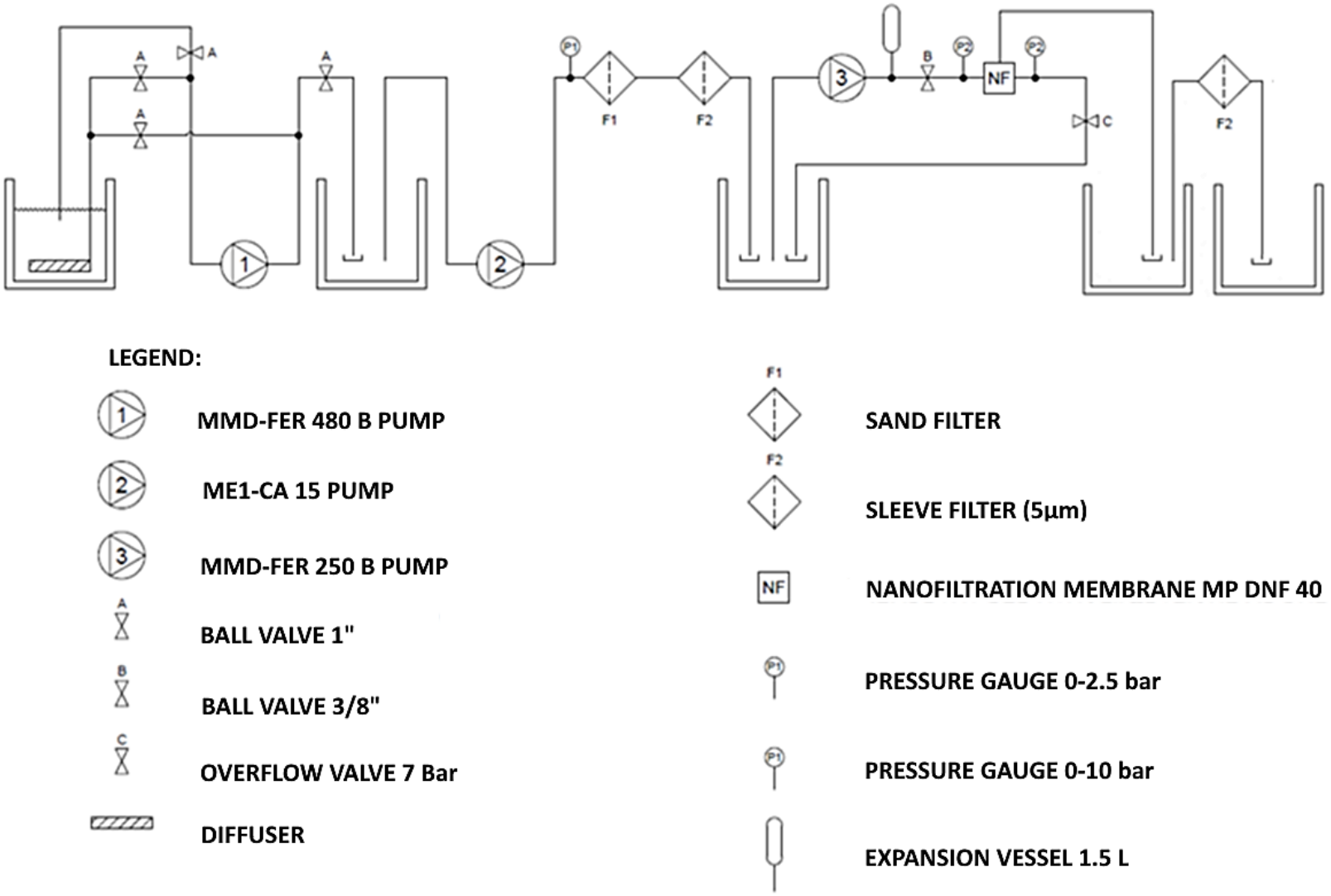

Figure 7.12. Bench scale prototype design.

Figure 7.13. Picture of the bench scale prototype

Leaching tank

In this tank the granulate (4 kg d.w.) was placed contact with a 1 M NaOH solution, prepared by diluting a commercial 30 % w/w solution with tap water, (20 L, solid/liquid ratio of 1/5) to remove the heavy metals present. A 45L PVC tank with a size of 59x39x30 cm was used for the leaching step. To better homogenize the extracting solution and ensure optimal contact with the granulate, the leachant was sucked from the surface of solution and re-injected through a system of pipes provided with special diffusers placed on the bottom of the tank under the granulate. For this purpose, a pump equipped with mechanical diaphragm and with spring return mechanism (MMD-FER 480 B) was used.

Storage tank for eluate sedimentation

Since the eluate obtained from the contaminants' extraction could contain a high concentration of suspended solid particles, an intermediate sedimentation step was necessary before the filtering on a sand filter in order to avoid the premature clogging of the filter itself. This operation took place in a PVC tank (30 L - 38x26.5x28.5 cm) in which the eluate was transferred using the same pump (MMD-FER 480 B) used for its homogenization.

Sand filter and sleeve filter (5 µm mesh) for suspended solids removal

The removal of the suspended solids left after sedimentation was carried out by filtering the eluate through a sand filter having a bed with a diameter of 2.5 cm, a height of 70 cm and a maximum flow and pressure of 12.5 L/h and 1.3 bar, respectively. The eluate after the sand filter was passed through a sleeve filter having a 5 µm mesh size. A constant analogical electromagnetic pump ME1-CA 15 was used to feed both filters.

Nanofiltration apparatus

The eluate, after suspended solids removal, was accumulated in a PVC tank (30 L - 38x26.5x28.5 cm) for the following NF process. NF was carried out by using a MP dNF 40 MEXFIL^{TM} membrane (NXFiltration, Enschede. The Netherlands). The membrane was fed by a pump equipped with a mechanical diaphragm and spring return mechanism (MMD-FER 250 B), to which a 1.5 L PVC pulsation damper and a pressure relief PVC valve were coupled. The concentrate was recycled into the feed accumulation tank until all NaOH was completely permeated, or until the permeate flow decreased significantly, indicating the clogging of the membrane. The permeate was discharged into another 30 L PVC tank. Pressure gauges were used to monitor the pressure of both the inflow and the outflow of the membrane feed. A safety valve was installed after the pulsation damper to prevent accidents due to over-pressure.

Apparatus for the chemical-physical treatment of NF concentrated fraction for the removal of the heavy metals present

The concentrate obtained after NF was stirred using a mechanical mixer (FALC AT-M 20) and subjected to a chemical-physical treatment to precipitate the heavy metals present. After treatment the solution was left to settle and manually filtered using a sleeve filter having a 5 μm mesh size to remove the sludge. To restore the extracting solution, the amount of NaOH that was not recovered with NF was reintegrated using a 10 M NaOH commercial solution.

7.5.1.2. Tests for the removal of suspended solids from the eluate

The performances of commercial quartz sand, Macrolite™ and VitroSphere Micro™ were tested to select the most efficient material to use as bed for the sand filter.
Aliquots (1 L) of spent extracting solution were filtered after sedimentation on each filter, evaluating its capability for the removal of suspended solid particles, heavy metals, K and Ca. To avoid cross contamination the entire system was flushed four times using 2 L of demineralized water between each test. The amount of suspended solids in each sample was determined by following the UNI EN 872:2005 standard [423].

7.5.1.3. Nanofiltration tests

Preliminary NF tests for the recovery of NaOH from the exhausted extracting solution were carried out on a 10 L aliquot of eluate after the removal of suspended solid particles. These tests were carried out on the eluate produced from the leaching of both sample NE01 and NE02.
As in the case of RO, the efficiency of the NF was studied as a function of the Volumetric Concentration Ratio (VCR).
Sampling (15 mL) was carried out at the following VCRs: 1.75, 2.5, 3.5, 4.5, 5.5, 6.5, 7.5, and 8.0.
The recovery of each analyte in the concentrated fraction was calculated with the following expression:

$$\%_{Recovey} = 100 - \left(\left[\frac{([A]_S \cdot V_S)}{([A]_P \cdot (w_P \cdot \rho_P))}\right] \cdot 100\right) \qquad \text{(Eq 7.5)}$$

The recovery of NaOH in the permeate was calculated with the following equation:

$$\%_{NaOH\ Recovey} = \left[([Na]_P \cdot (w_P \cdot \rho_P))/([Na]_S \cdot V_S))\right] \cdot 100 \qquad \text{(Eq 7.6)}$$

where:

A_S: starting concentration of the analyte in the sample subjected to NF

V_S: starting volume of the sample subjected to NF

A_P: concentration of the analyte in the permeated fraction

w_P: weight of the permeated fraction

ρ_P: density of the permeated fraction, as measured by a hydrometer

$[Na]_P$: concentration of Na in the permeated fraction

$[Na]_S$: starting concentration of Na in the sample subjected to NF

The pump used for NF was manually adjusted to obtain transmembrane pressure of about 6.5-7 bar, as a compromise between feed flow (~180 L/h) to minimize membrane fouling, permeate flow (1.10 L/h) and pump mechanical stress. A brief test was carried out using transmembrane pressure of 7.5-8.0 bar, but this caused a clear decrease of feed flow (~100 L/h) and the overheating of the pump after about 30 minutes of operation. The NF was backwashed every 3 hours using tap water treated with Na_2CO_3 to lessen its fouling and avoid clogging it.

7.5.1.4. Tests for heavy metals recovery

The treatment of the concentrate fraction obtained from NF was optimized testing different options for the preliminary acidification and coagulation steps:

- Preliminary acidification of the concentrate using H_3PO_4 (50 % w/w): acidification to pH 9.0 or to pH 7.0.
- Addition of the coagulating additive until sludge formation: use of $FeCl_3$ (40% w/w), $Fe_2(SO_4)_3$ (25% w/w) and polyaluminum chloride (18% w/w) solutions.

In detail, the treatment included the following steps:

- Preliminary acidification of the concentrate using H_3PO_4
- Addition of the coagulating additive until sludge formation
- Addition of $Ca(OH)_2$ up to reaching pH values between 11.8 and 12.0.
- Precipitation of residual Ca^{2+} ions with the addition of Na_2CO_3
- Addition of flocculating additive
- Sedimentation and filtration of the metal-rich sludge.

The optimization was performed using a 100 mL sample of concentrate for each test.

7.5.2. Results and discussions

7.5.2.1. Extraction tests

The results of the extraction tests, carried out on sample NE01 and NE02, showed very similar results to those obtained during the preliminary testing (**Table 7.30** and **Table 7.31**), but with a slight

increase in the leaching of As, Co, Cr, Cu, Mo, Ni, Pb, Se Tl and Zn. These results were probably due to the better homogenization guaranteed by the agitation system used which, unlike the Jar test apparatus used in the preliminary tests, was not limited to move the liquid over the pellets but pumped the leaching solution directly into the heap of granules. The concentration of Ca found in both eluates (NE01E and NE02E) was slightly higher than that found during the preliminary tests, probably because of the use of tap water for the preparation of the NaOH solution, while the leaching of K was essentially unchanged. In this case, the leaching of sulphates was also investigated, since these salts could contribute to the fouling of the NF membrane.

7.5.2.2. Tests for the removal of suspended solids from the eluate

The results of the tests reported in **Figure 7.14** showed that Macrolite™ and VitroSphere Micro™ had a slightly better performance than quartz sand for suspended solids removal, probably due to their more regular shape and lower diameter. All the materials caused no significant retention of NaOH or sulphates, and only a minor removal of most heavy metals, save for Macrolite™ which removed almost 70 % of V. The use quartz sand and VitroSphere Micro™ did not significantly change the amount of Ca, Mg and K in the eluate, while Macrolite™ stopped about 70% of Ca. For these reasons Macrolite™ was used as the sand filter's bed.

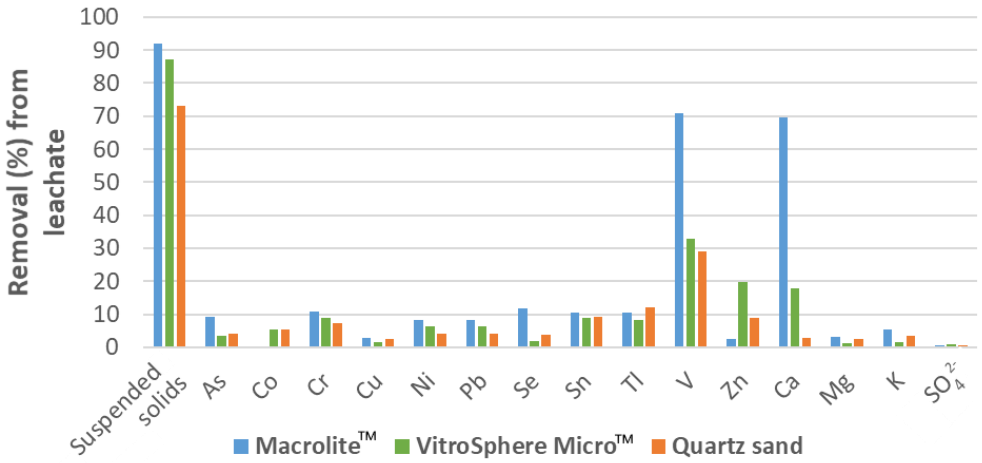

Figure 7.14. Removal (%) of suspended solids, As, CO, Cr, Co, Cr, Cu, Ni, Pb, Se, Sn, Tl, V, Zn, Ca, Mg, K and sulphates from the exhausted leaching solution using Macrolite™, VitroSphere Micro™ and quartz sand as the sand filter's bed.

Table 7.30. Removal % of As, Be, Cd, Co, Cr, Cu, Hg, Ni, Pb, Se, Sb, Sn, Tl, V, and Zn from sample NE01. using the bench scale prototype

Leaching of Ca, K and SO_4^{2-} from samples NE01. (n.d.: not detected).

NE01E	**Time (h)**	**Removal (%)**													**Leaching ($mg \cdot L^{-1}$)**		
		As	Be	Cd	Co	Cr	Cu	Hg	Ni	Pb	Se	Sn	Tl	V	Zn	Ca	K	SO_4^{2-}
NaOH 1 M	2	0.93	n.d.	n.d.	0.32	1.78	0.75	n.d.	1.61	1.88	0.16	0.52	n.d.	0.16	0.13	42.5	280	-
	4	1.50	n.d.	n.d.	0.38	2.18	0.97	n.d.	2.20	2.27	0.18	0.61	0.20	0.23	0.14	37.9	288	-
	8	1.94	n.d.	n.d.	0.48	2.86	1.39	n.d.	2.75	2.77	0.22	0.86	0.57	0.36	0.14	36.3	339	-
	24	3.70	n.d.	n.d.	0.59	3.95	2.16	n.d.	3.68	3.32	0.39	1.20	1.12	0.51	0.21	32.5	354	-
	48	5.06	n.d.	n.d.	0.60	4.51	2.54	n.d.	3.98	3.81	0.58	1.24	1.82	0.58	0.26	24.2	361	-
	72	6.51	n.d.	n.d.	0.62	4.81	3.31	n.d.	4.60	4.16	0.75	1.55	2.28	0.71	0.33	13.7	340	3030

Table 7.31. Removal % of As, Be, Cd, Co, Cr, Cu, Hg, Ni, Pb, Se, Sb, Sn, Tl, V, and Zn from sample NE02, using NaOH 1 M as extracting solution.

Leaching of Ca, K and SO_4^{2-} from samples NE02. (n.d.: not detected).

NE02E	**Time (h)**	**Removal (%)**													**Leaching ($mg \cdot L^{-1}$)**		
		As	Be	Cd	Co	Cr	Cu	Hg	Ni	Pb	Se	Sn	Tl	V	Zn	Ca	K	SO_4^{2-}
NaOH 1 M	2	1.26	n.d.	n.d.	0.24	2.00	0.87	n.d.	1.79	2.29	0.19	0.12	0.67	0.41	0.64	34.2	266	-
	4	1.98	n.d.	n.d.	0.28	2.36	1.18	n.d.	2.35	2.92	0.28	0.31	1.51	0.51	0.65	26.0	281	-
	8	3.40	n.d.	n.d.	0.39	3.24	1.87	n.d.	3.43	4.12	0.43	0.61	2.29	0.71	0.66	23.0	325	-
	24	7.70	n.d.	n.d.	0.60	4.70	3.60	n.d.	5.53	6.14	0.83	1.39	2.88	0.99	0.73	15.5	348	-
	48	11.3	n.d.	n.d.	0.79	5.47	5.02	n.d.	6.69	7.31	1.21	1.50	3.00	1.11	0.82	14.4	350	-
	72	13.5	n.d.	n.d.	0.82	5.88	5.80	n.d.	7.29	7.91	1.48	1.59	3.12	1.15	0.88	13.2	354	3015

7.5.2.3. Nanofiltration tests

Nanofiltration was first carried out on the eluate obtained from the decontamination of sample NE02 (NE02E), due to its higher concentration of contaminants compared to the eluate obtained from the treatment of sample NE01 (NE01E). As it can be seen from the data reported in **Table 7.32** and **Figure 7.15**, the NF allowed the recovery of approximately 90% of the NaOH solution reaching a VCR of 8.0. The recovery of all the heavy metals in the eluate decreased almost linearly increasing VCR, but a good recovery (>80%) was obtained for As, Cr, Co, Cu, Ni Tl and Se, while the process was slightly less effective for Pb and V (recovery of about 70 %). The worst results (recovery of about 50 %) were obtained for Sn and Zn. The membrane also retained about 70 % of the sulphates present in the solution.

When a VCR of 8.0 was reached, the flow of permeate decreased to about 50% of the starting flow, indicating either the fouling of the membrane or too high saline content of the feed, so it was decided to stop concentrating the eluate. As shown in **Table 7.33**, similar results were obtained from the nanofiltration of the eluate obtained from the decontamination of sample NE01 (NE01E). The remaining 10 litres of each eluate were manually filtered on the sleeve filter and subjected directly to NF up to a CVR of 8.0, without intermediate sampling. The two aliquots of permeate and concentrate obtained from each eluate were combined to obtain samples NE01C, NE02C (concentrates) NE01P and NE02P (permeates).

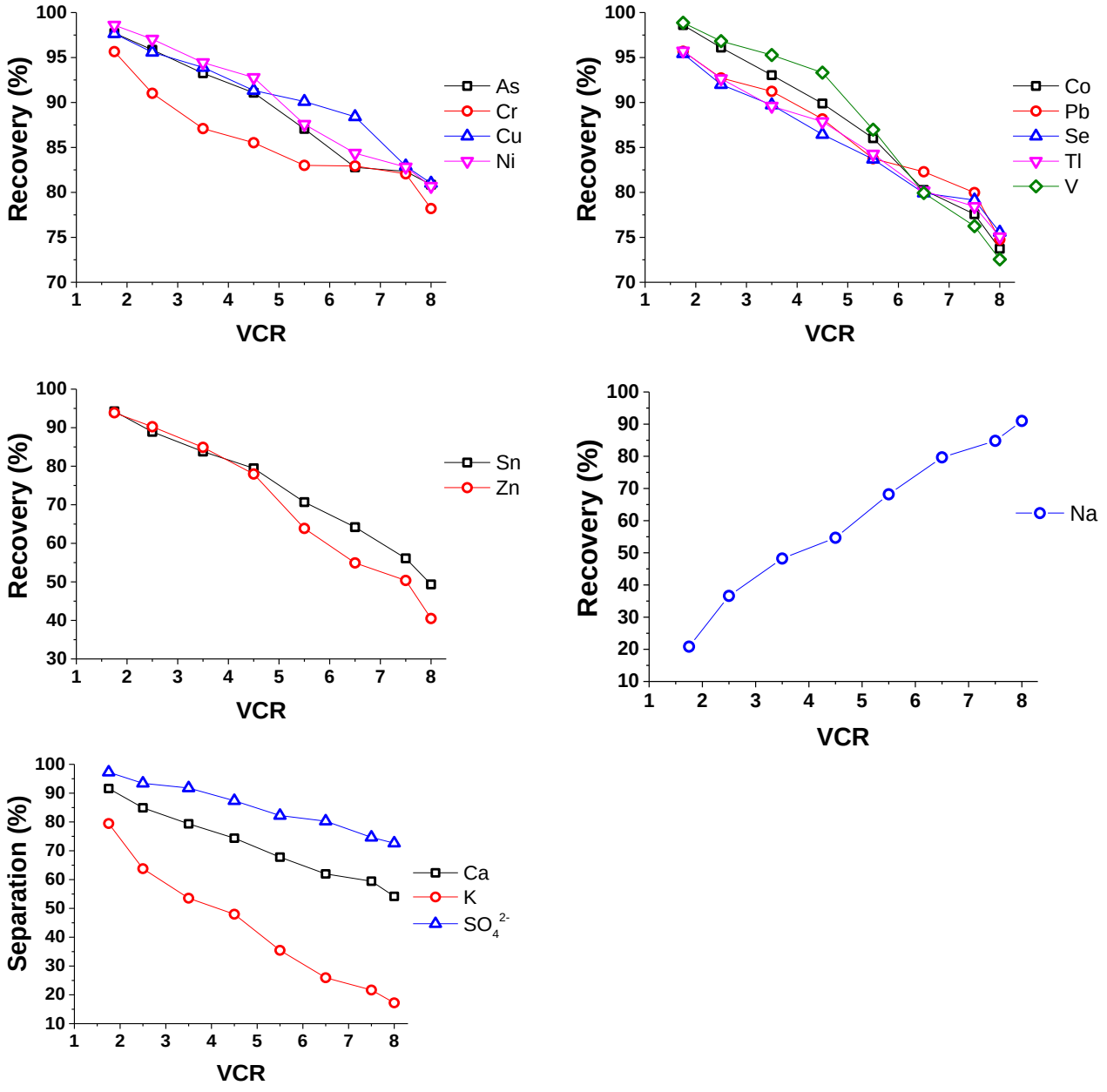

Figure 7.15. Recovery % of As, Co, Cr, Cu, Ni, Pb, Se, Sb, Sn, Tl, V, Zn, and Na from sample NE02E with nanofiltration, together with Ca, K, and SO_4^{2-} separation.

Table 7.32. Concentration of As, Be, Cd, Co, Cr, Cu, Hg, Ni, Pb, Se, Sb, Sn, Tl, V, Zn, Ca, K, Na, SO_4^{2-} in the eluate before NF, in the permeated and concentrated fractions at VCR of 8.00 for the treatment of sample NE02 using the bench scale prototype (n.d.: not detected).

NE02	As	Be	Cd	Co	Cr	Cu	Hg	Ni	Pb	Se	Sn	Tl	V	Zn	Ca	K	SO_4^{2-}	Na
	$\mu g \cdot L^{-1}$														$mg \cdot L^{-1}$			
NE02E	6403	n.d.	n.d.	41	268	2905	n.d.	381	562800	886	81	63	84	928	3.9	350	3015	18820
NE02P VCR 8.00	1454	n.d.	n.d.	12.3	66	643	n.d.	87	170100	245	48	18	27	629	2.5	344	930	19686
NE02C VCR 8.00	41050	n.d.	n.d.	246	1681	18740	n.d.	2440	3312240	5374	312	384	484	3026	13.6	395	17610	12750
	Recovery (%)																	
	As	Be	Cd	Co	Cr	Cu	Hg	Ni	Pb	Se	Sn	Tl	V	Zn	Ca	K	SO_4^{2-}	Na
VCR 1.75	98	-	-	98	96	98	-	99	96	96	94	96	99	94	90	79	97	22
VCR 2.50	96	-	-	96	91	96	-	97	93	92	88	93	97	90	81	64	94	38
VCR 3.50	93	-	-	91	87	94	-	95	91	89	84	90	95	85	75	53	92	49
VCR 4.50	91	-	-	89	85	92	-	93	88	87	79	88	93	77	68	47	88	57
VCR 5.50	87	-	-	86	83	90	-	87	84	83	70	84	87	64	60	35	82	69
VCR 6.50	83	-	-	79	82	88	-	85	81	80	62	80	80	55	53	25	81	80
VCR 7.50	81	-	-	77	81	83	-	83	79	78	55	78	77	49	50	20	75	86
VCR 8.00	80	-	-	74	78	81	-	80	74	76	48	76	72	41	43	14	73	92

Table 7.33. Concentration of As, Be, Cd, Co, Cr, Cu, Hg, Ni, Pb, Se, Sb, Sn, Tl, V, Zn, Ca, K, Na, SO_4^{2-} in the eluate before NF, in the permeated and concentrated fractions at VCR of 8.00 for the treatment of sample NE01 using the bench scale prototype (n.d.: not detected).

NE01	**As**	**Be**	**Cd**	**Co**	**Cr**	**Cu**	**Hg**	**Ni**	**Pb**	**Se**	**Sn**	**Tl**	**V**	**Zn**	**Ca**	**K**	**SO_4^{2-}**	**Na**
	$\mu g \cdot L^{-1}$														$mg \cdot L^{-1}$			
NE01E	2679	n.d.	n.d.	31	276	1492	n.d.	348	270384	389	68	41	76	288	10.2	333	2974	18956
NE01P VCR 8.00	586	n.d.	n.d.	9	69	324	n.d.	77	78048	109	40	12	24	196	5.3	315	930	19713
NE01C VCR 8.00	17331	n.d.	n.d.	181	1726	9668	n.d.	2248	1616732	2350	270	245	438	932	44	459	17284	13658
	Recovery (%)																	
	As	Be	Cd	Co	Cr	Cu	Hg	Ni	Pb	Se	Sn	Tl	V	Zn	Ca	K	SO_4^{2-}	Na
VCR 1.75	98	-	-	99	96	98	-	99	96	95	94	96	99	94	92	79	97	21
VCR 2.50	96	-	-	96	91	96	-	97	93	92	89	93	97	90	85	64	93	37
VCR 3.50	93	-	-	93	87	94	-	94	91	90	84	90	95	85	79	54	92	48
VCR 4.50	91	-	-	90	86	91	-	93	88	86	79	88	93	78	74	48	87	55
VCR 5.50	87	-	-	86	83	90	-	88	84	84	71	84	87	64	68	35	82	68
VCR 6.50	83	-	-	80	83	88	-	84	82	80	64	80	80	55	62	26	80	80
VCR 7.50	82	-	-	78	82	83	-	83	80	79	56	78	76	50	59	22	75	85
VCR 8.00	81	-	-	74	78	81	-	81	75	76	49	75	73	40	54	17	73	91

7.5.2.4. Tests for heavy metals recovery

The optimization of the heavy metals' recovery process was carried out on both the concentrated fractions obtained from the treatment of sample NE01 and NE02. The acidification of the concentrates required quite high dosages of phosphoric acid (~16 L/m^3), but the difference between the amounts needed to reach the two pH desired (9 and 7), was quite limited (~0.5 L/m^3). The dosages of $FeCl_3$ or $Fe_2(SO_4)_3$ needed to reach the coagulation were reduced of about 60% passing from the concentrates at pH 9 to the ones at pH 7, while this difference was reduced to the 20% when PAC is used instead of Fe-salts. The formation of sludge started upon reaching pH values of about 5 for Fe-salts, and 6 for PAC. The coagulant used for the treatment did not significantly influence the dosages of $Ca(OH)_2$ used to reach a pH of 12, but the effects of the pre-acidification were much more marked, causing an increase of nearly 50 % (**Table 7.34**).

Table 7.34. Dosages of H_3PO_4, $FeCl_3$, $Fe_2(SO_4)_3$, PAC and $Ca(OH)_2$ for the heavy metals' recovery.

	Pre-acidification	**NE01**		**NE02**	
	pH 9,01	15,65 $L \cdot m^{-3}$		15,81 $L \cdot m^{-3}$	
	pH 7,05	16,14 $L \cdot m^{-3}$		16,37 $L \cdot m^{-3}$	
	Coagulating additives	L/m^3	**pH of coagulation**	L/m^3	**pH of coagulation**
pH 9	$FeCl_3$	10.9	4.99	11.1	4.90
	$Fe_2(SO_4)_3$	10.1	5.02	10.0	5.17
	PAC	4.75	6.05	4.6	6.15
pH 7	$FeCl_3$	3.1	4.82	3.0	4.98
	$Fe_2(SO_4)_3$	4.2	5.11	4.0	5.41
	PAC	4.1	6.37	4.0	6.57
	$Ca(OH)_2$	kg/m^3	**Final pH**	kg/m^3	**Final pH**
pH 9	$FeCl_3$	6.49	11.99	6.29	11.94
	$Fe_2(SO4)_3$	6.21	11.90	6.17	11.98
	PAC	6.61	12.01	6.51	11.98
pH 7	$FeCl_3$	4.79	11.96	4.76	11.92
	$Fe_2(SO_4)_3$	4.81	11.93	4.61	11.90
	PAC	5.71	11.95	5.63	11.95

The outcomes of each test are reported in **Table 7.35**, showing that better performances could be obtained after pre-acidification to pH 7. The best results were obtained for the precipitation of Pb and sulphates (>99 %), together with good results for the removal of Cr, Cu, V and Zn (>95%). The removal of As, Co, and Sn ranged between 85 and 94 %, while only limited precipitation was obtained for Se and Tl (removal of about 60 % and 65 %, respectively). The use of $FeCl_3$ gave the best results for As, Co, Cr, Sn, Se, Tl, V, and Zn, while the best removal of Cu and Ni was obtained by using $Fe_2(SO_4)_3$ (**Figure 7.16**).

Table 7.35. Removal % of As, Co, Cr, Cu, Ni, Pb, Se, Sn, Tl, V and Zn from the concentrate obtained through NF of NE01 and NE02 eluates

NE01C	Coagulant	As	Co	Cr	Cu	Ni	Pb	Se	Sn	Tl	V	Zn
pH 9.0	$FeCl_3$	79.1	72.3	96.4	78.6	88.5	>99.9	56.4	40.6	47.7	71.1	99.1
	$Fe_2(SO_4)_3$	82.7	70.9	93.0	79.3	91.6	>99.9	55.4	43.5	42.2	84.9	91.7
	PAC	53.2	80.0	94.2	80.3	77.3	>99.9	50.8	30.6	41.2	72.3	98.1
pH 7.0	$FeCl_3$	92.1	82.7	99.4	83.5	93.7	>99.9	63.2	76.4	67.9	75.0	98.8
	$Fe_2(SO_4)_3$	91.0	76.7	99.2	88.4	88.2	>99.9	52.5	79.3	59.8	73.8	96.4
	PAC	77.9	83.2	89.4	83.0	78.5	>99.9	47.3	68.4	64.1	79.5	97.4

NE02C	Coagulant	As	Co	Cr	Cu	Ni	Pb	Se	Sn	Tl	V	Zn
pH 9.0	$FeCl_3$	80.1	75.4	96.4	78.7	92.5	>99.9	54.0	39.6	47.2	69.0	99.4
	$Fe_2(SO_4)_3$	77.5	72.3	95.1	76.7	89.5	>99.9	55.7	43.2	43.9	79.4	90.5
	PAC	49.2	78.2	92.0	80.3	81.0	>99.9	53.8	28.3	36.6	69.7	97.7
pH 7.0	$FeCl_3$	89.5	83.4	97.8	89.4	94.1	>99.9	57.1	77.9	66.1	78.4	99.2
	$Fe_2(SO_4)_3$	90.2	78.6	97.4	88.3	85.2	>99.9	52.9	82.8	58.9	75.2	95.7
	PAC	72.1	76.8	95.2	87.7	84.0	>99.9	51.8	65.0	62.9	75.0	98.1

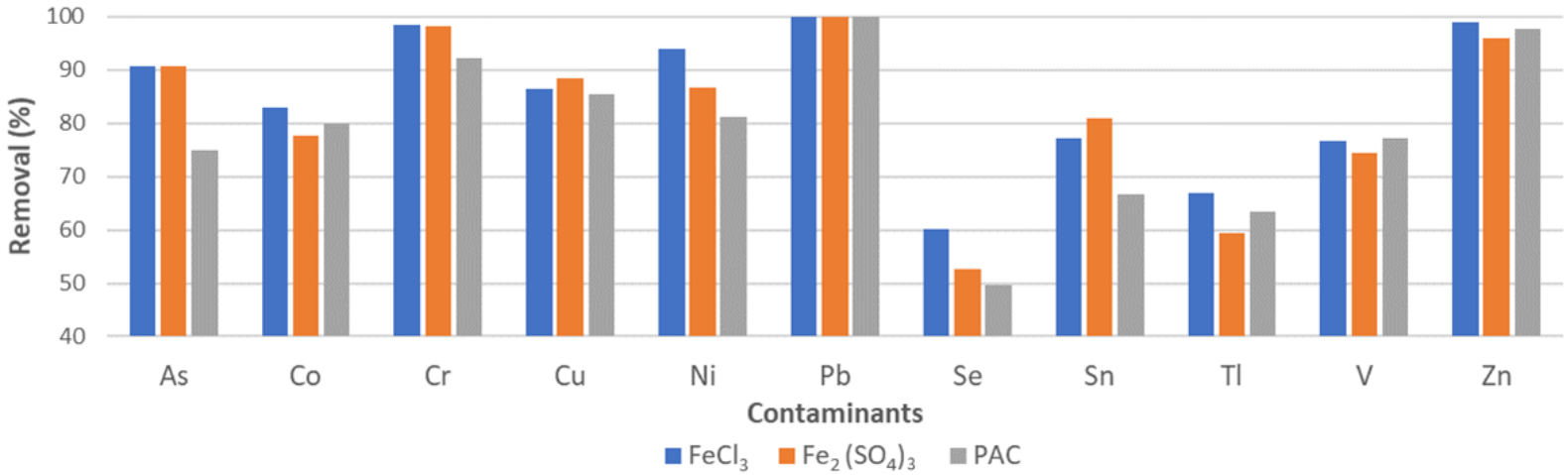

Figure 7.16. Removal % of As, Co, Cr, Cu, Ni, Pb, Se, Sn, Tl, V and Zn from sample NE02C after pre-acidification to pH 7.0.

From these results, we decided to decrease the pH of the concentrated fraction obtained after NF to 7, using a phosphoric acid commercial solution (75% w/w), and to use the $FeCl_3$ solution as coagulant. $Ca(OH)_2$ was added to reach a pH value of around12.0 and a flocculants was used (1 L/m^3) to aid flocs formation. The system was stirred for 20 minutes, then left to settle to be filtered using a 5 µm sleeve filter. The heavy metals' content of the sludges (NE01S and NE02S) produced from the treatment of the concentrates, using $FeCl_3$ and pre-acidification to pH of 7, is reported in **Table 7.36**, and it shows high concentrations of Pb, Cu and As, together with lower quantities of Ni, Cr and Se.

Table 7.36. Heavy metals content of the sludges (NE01S and NE02S) obtained from the treatment of the concentrates NE01C and NE02C, respectively.

Contaminants	NE01S	NE02S
	$mg \cdot kg^{-1}$ d.w.	
As	3184±248	7137±235
Be	< 0.5	< 0.5
Cd	< 0.5	< 0.5
Co	28.5±3.3	37.9±1.5
Cr	349±48	299±17
Cu	1507±215	3357±82
Hg	< 0.5	< 0.5
Ni	428±27	464±10
Pb	306780±4350	664401±17703
Se	285±19	583±20
Sn	41.3±3.8	46.2±4.5
Tl	34.1±2.5	50.9±2.6
V	64.8±6.1	68.4±1.0
Zn	192±11	553±36

7.5.2.5. Process testing

After optimizing each step of the process, samples NE01 and NE02 were both treated with the respective regenerated NaOH solutions. In the case of sample NE01, considering the overall results of the decontamination, especially in the case of As, Ni, Pb, Cr and Cu, it was decided to increase the number of decontamination cycles to four, thus removing about 20% of these heavy metals from the sample. At the end of the process, the granulate obtained was subjected to WC treatment and the UNI 12457/2:2004 leaching test was used to verify its conformity to the "end of waste" classification.
As far as the treatment of the NE02 sample is concerned, due the results obtained, the sample was treated until As concentration was within the limits set by the Italian regulation for the industrial use of soil and sediments [101]. To reach such concentration of As, six additional decontamination cycles were needed. The sand filter used for the suspended solids' removal performed at acceptable levels for all the reminder of the study, requiring backwashing only after filtering about 80 L of eluate.

The whole sample of each exhausted extracting solution was subjected to NF directly up to VCR of 8.0, without intermediate sampling. To avoid clogging, the membrane was regularly backwashed for 15 minutes, every 5 L of permeate produced, by using tap water treated with Na_2CO_3. The last washing, at the end of each NF step, lasted 2 hours to better clean the membrane.

Thanks to this, it was possible to recover about 90% of the spent NaOH for each treatment, with heavy metals' recoveries very similar to those already showed above.

The use of hydroxide precipitation, together with coagulation and flocculation led to the recovery of the heavy metals removed from the pellets, producing a metal-rich sludge that could be sold, leading to an amortization of the process' costs.

The heavy metals' content of NE02 sample after 1, 3, 5 and 7 cycles of decontamination is reported in **Table 7.37**, while **Figure 7.17** shows the overall metals removal.

Table 7.37. Heavy metals content of sample NE02 after 1, 3, 5 and 7 cycles of decontamination using regenerated 1 M NaOH solution as extractant.

Contaminants	NE02	NE02 after 1 cycle	NE02 after 3 cycles	NE02 after 5 cycles	NE02 after 7 cycles	Removal
	$mg \cdot kg^{-1}$ d.w.					%
As	261	225±15.8	163±11	101±7	38.2±2.7	85,3
Be	0.61	0.58±0.03	0.64±0.03	0.57±0.03	0.60±0.03	-
Cd	2.55	2.63±0.26	2.48±0.24	2.59±0.25	2.50±0.24	-
Co	25.2	24.9±1.8	24.6±1.9	24.3±2.0	24.0±1.9	4.5
Cr	25.6	24.1±1.7	21.4±1.6	18.7±1.43	16.1±1.2	37.6
Cu	258	243±8	217±10	191±8	165±6	35.9
Hg	6.69	6.81±0.62	6.72±0.84	6.5±0.71	6.73±0.64	-
Ni	29.1	27±2.1	23.5±1.8	20±1.5	16.4±1.2	43.6
Pb	40936	37698±2148	32646±1860	27594±1572	22541±1284	44.9
Sb	11.6	11.9±1.0	11.4±0.9	11.8±1.3	11.4±1.0	-
Se	340	335±13	327±11	318±14	310±12	8.8
Sn	28,6	28,2±1.2	27,6±0.9	27,1±1.0	26,6±0.8	7.1
Tl	11.4	11±0.8	10.5±0.7	9.92±0.73	9.31±0.68	18.3
V	51.2	50.6±3.1	49.7±3.0	48.8±5.2	47.9±2.5	6.3
Zn	512±7	508±8	500±5	493±6	485±6	5.2

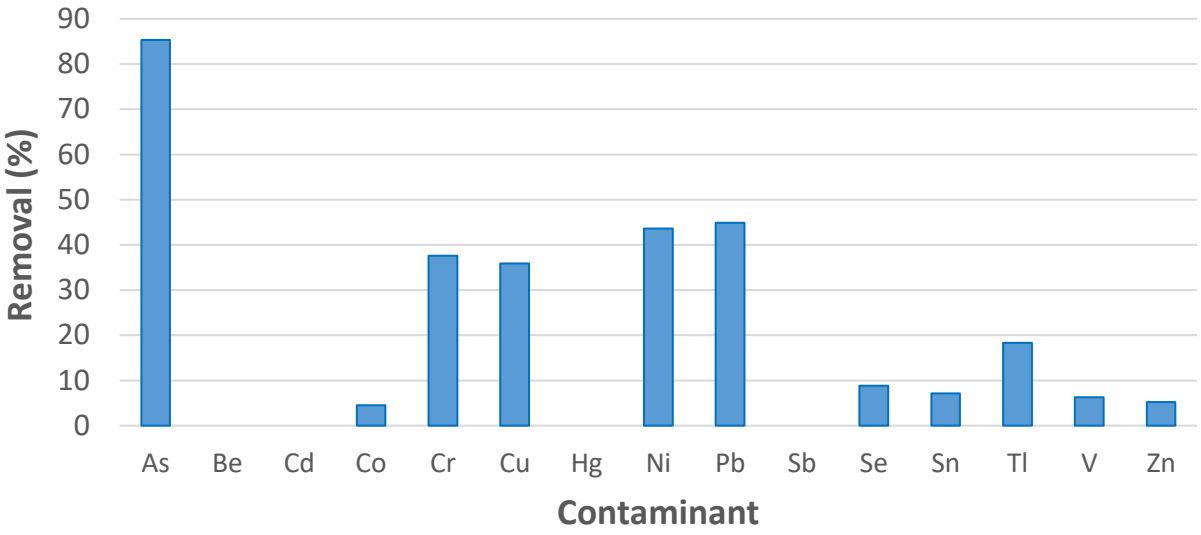

Figure 7.17. Heavy metals removal (%) from sample NE02 after 7 cycles of decontamination using regenerated 1 M NaOH solution as extractant.

As for sample NE02, the decontamination of granulate NE01 using the regenerated NaOH 1 M solution yielded results quite close to those already reported. The heavy metals' content of this sample after 2 and 4 cycles of decontamination is reported in **Table 7.38**, while the overall removal of each contaminant at the end of the treatment is reported in **Figure 7.18**.

Table 7.38. Heavy metals removal (%) from sample NE01 after 2 and 4 cycles of decontamination using regenerated 1 M NaOH solution as extractant.

Contaminants	NE01	NE01 after 2 cycles	NE01 after 4 cycles	Removal
	mg·kg^{-1} d.w.			%
As	225	167±12	114±8	49.4
Be	0.68	0.68±0.04	0.68±0.04	-
Cd	2.30	2.30±0.23	2.30±0.23	-
Co	24.2	23.9±1.9	23.6±1.9	2.7
Cr	31.2	27.7±1.9	24.4±1.7	21.7
Cu	231	206±3	183±3	20.9
Hg	5.75	5.75±0.61	5.75±0.61	-
Ni	40.4	35.0±2.7	30.1±2.3	25.4
Pb	35161	30209±1576	25870±1349	26.4
Sb	12.8	12.0±1.0	11.8±1.0	-
Se	292	284±11	277±11	5.2
Sn	25.2	24.6±1.7	24.1±1.7	4.3
Tl	9.80	9.22±0.46	8.7±0.72	10.7
V	68.9	67.5±3.1	66.3±4.0	3.7
Zn	455	447±7	441±5	3.0

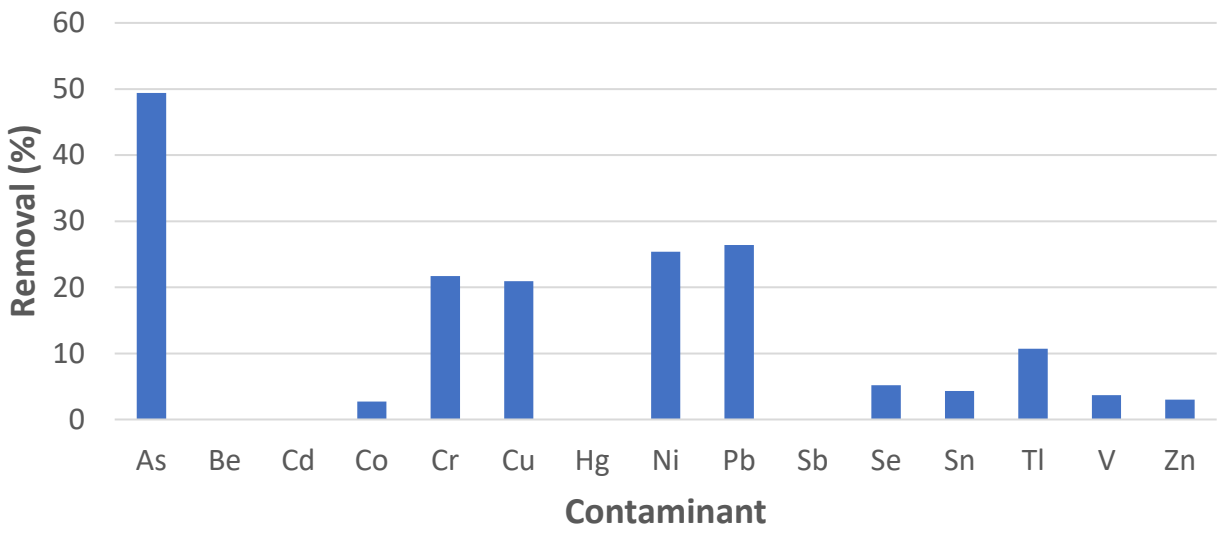

Figure 7.18. Heavy metals removal (%) from sample NE01 after 4 cycles of decontamination using regenerated 1 M NaOH solution as extractant.

The results of the UNI 12457-2:2004 leaching test (**Table 7.39**) performed on the sample of granulate NE01 after 4 cycles of decontamination and WC treatment (NE01WC3), , show that this material can be classified as reusable, according to the Italian regulation [114].

Table 7.39. Results of the leaching test UNI EN 12457-2:2004 for sample NE01WC3.

Parameter	NE01WC3	Regulatory limit*
	$\mu g \cdot L^{-1}$	
As	1.01±0.03	50
Ba	198±14	1000
Be	< 0.1	10
Cd	< 0.1	5
Co	0.98±0.11	250
Cr	20.3±3.8	50
Cu	18.4±1.9	50
Hg	< 0.1	1
Ni	7.52±0.41	10
Pb	< 0.1	50
Se	7.88±0.82	10
V	67.2±3.5	250
Zn	<0.1	3000
pH	11.7±0.1	5.5-12.0

*Regulatory limit: Table 1 of Annex III of Ministerial Decree n°186 of 05th April 2006 [114].

7.6. Cost estimate for the HPSS-NanoExtra process

The optimal conditions established for the HPSS-NanoExtra process were used to evaluate the economic feasibility of an industrial scale application, considering the production of 12.000 tonn/year of granular material. Since the process has been proven to be unsuitable for the decontamination of fly ashes, their pre-treatment has not been considered in this estimation.

The capital needed for the construction of the industrial scale plant has been quantified as follows:

- Initial investment: 400000 €;
- Annual amortization: 50000 €;
- Annual maintenance costs: 20000 €

Other management costs have been estimated separately for the use of both the tested formulations based on previous reclamation operations carried out by In.T.Ec. [222,223], as reported in **Table 7.40** and **Table 7.41**. As expected, the cost of the pellets obtained by applying the low-binder formulation is significantly lower than the cost of the pellets produced with the standard formulation due to the lower amount of cement needed and the absence of the additives. However, the process using low-binder formulation requires to treat a higher quantity of contaminated material each year (10200 tonn/year and 8800 tonn/year, respectively).

The application at the industrial scale of the HPSS-NanoExtra process can be considered cost effective if considering that the cost for landfill disposal of heavily contaminated and hazardous wastes in Italy can be estimated in about 140-160 €/tonn (excluding transport).

The sale of the metal-rich sludge obtained during the recycling of the extracting solution has not been considered in this evaluation since its heavy metals content, and therefore its value, is highly dependent on the treated matrix.

Table 7.40. Costs estimated for the production of 12000 tonn/year of decontaminated granular material using the standard HPSS® formulation.

Contaminated matrix treated (tonn/year)	8800

Cost item	**Unit cost**	**Annual cost**	**€/tonn $_{pellets}$**
Amortization	-	70000 €	5.83
Electricity	0.14 €/kWh	36000 €	3.00
CEM 42.5 R	85 €/tonn	275400 €	22.95
Mapeplast ECO 1A/1B	1100 €/tonn	72000 €	6.00
Sodium hydroxide	200 €/tonn	1000000 €	83.33
Manpower (3 workers)	6000 €/month	72000 €	6.00
Rental	2000 €/ month	24000 €	2.00
		Total	129.12 €/tonn

Table 7.41. Costs estimated for the production of 12000 tonn/year of decontaminated granular material using the low-binder HPSS® formulation.

Contaminated matrix treated (tonn/year)	10200

Cost item	Unit cost	Annual cost	€/tonn $_{pellets}$
Amortization	-	70000 €	5.83 €
Electricity	0.14 €/kWh	36000 €	3.00 €
CEM 42.5 R	85 €/tonn	153000 €	12.75 €
Sodium hydroxide	200 €/tonn	1000000 €	83.33 €
Manpower (3 workers)	6000 €/month	72000 €	6.00 €
Rental	2000 €/ month	24000 €	2.00 €
		Total	112.92 €

7.7. Conclusions

In this study the HPSS-NanoExtra process has been successfully developed and applied to remove As, Pb, Ni, Cr and Cu from a contaminated soil using both low-binder content and standard formulations, even though the process was not effective in removing Be, Cd, Hg, Co, V and Zn from the tested materials. Moreover, the decontaminated stabilized granular material obtained from the treatment of Soil 1 was compliant with all the regulatory limits required by the Italian legislation for the "*end of waste*" classification. Geopolymeric binders showed good performances for this application and were proved to be valid alternatives to ordinary Portland cement, in particular in the case of GEO1 (Blast furnace slag + NaOH 4M) and GEO5 (Blast furnace slag, clinker and $CaCO_3$) binders. This process offers a new and cost-effective way to further improve the environmental compatibility of the pellets produced from the HPSS® process by removing and recovering part of the heavy metals they contained, without compromising either the mechanical or leaching characteristics of the final product. In particular, the heavy metals extracted were partially recovered and the spent leaching solution could be recycled multiple times by combining nanofiltration and chemical precipitation method for its treatment.

8. Chapter 8
Conclusions

This thesis work on the inertization of materials contaminated by organic and inorganic pollutants (soils, sediments and ashes deriving from the combustion of municipal solid waste) through the use of cementitious and geopolymeric binders provided valuable insight into the mechanisms involved in the immobilization and release of these contaminants, and contributed to improve the performance of the materials obtained through the studied solidification/stabilization processes.

The thesis results have shown that by decreasing both the temperature and time of the thermal desorption treatment and including a wet conditioning step to the process, it was possible to markedly increase the performances of the stabilized granular materials obtained from the treatment of freshwater sediments contaminated by Hg and $C_{12\text{-}40}$ hydrocarbons. In particular, temperature and time reduction allowed to diminish the degradation of the cementitious phases of the granules, while the wet conditioning step allowed to improve the granules mechanical properties, as well as to further reduce the leaching of contaminants.

Regarding the use of other hydraulic binders as substitutes of OPC, the investigations carried out during the thesis proved that several the various hydration products obtained provided different immobilization mechanisms and performances. In particular, CAC gave better performances than OPC for most of the investigated metals, thus representing a good alternative to improve immobilizations treatments based on hydraulic binders. Furthermore, leaching tests together with XRD and SEM/EDX analysis, demonstrated the key role of ettringite in the retention of Cr, Pb, Ni, Co, Zn, and Tl, while the leaching of Se, Cu, Ba and V was observed to depend on both the pellets' mechanical performances (i.e. unilateral compressive strength and resistance to abrasion) and pH. These findings showed the importance of contaminants' physical encapsulation to obtain a successful immobilization. Finally, the use of NaOH-activated metakaolin led to a high retention of Pb, but further research is needed to overcome the lack of observed solidification.

Isotopic measurement tools, combined with the concentrations mapping of the contaminated site, have been successfully applied to ascertain that the polluted waste improperly disposed of inside a dismissed sulphuric acid production plant in Bagnolo Mella (Italy) does not account for the contamination of the surrounding area. The contamination detected in the topsoil samples taken

outside the industrial property was attributed to other anthropogenic sources, such as fuel combustion, emissions from the nearby smelters or other non-point sources.

As demonstrated by the results reported in this thesis for the HPSS-NanoExtra project (Veneto Region, POR FESR 2014-2020- ID 10052461), the High Performance Solidification/Stabilization process has been successfully integrated with chemical extraction and membrane separation processes to produce re-usable materials while also recovering heavy metals (As, Pb, Ni, Cr and Cu) to a significant extent.

References

[1] R. Stolz, "Nature over nation: Tanaka Shōzō's fundamental river law," *Japan Forum*, vol. 18, no. 3, pp. 417–437, 2006.

[2] M. L. Bell, D. L. Davis, and T. Fletcher, "A retrospective assessment of mortality from the london smog episode of 1952: The role of influenza and pollution," in *Urban Ecology: An International Perspective on the Interaction Between Humans and Nature*, Boston, MA: Springer US, 2008, pp. 263–268.

[3] A. Kabata-Pendias, *Trace elements in soils and plants*, 4th Ed. Boca Raton, FL: CRC Press, 2011.

[4] P. S. Hooda, *Trace Elements in Soils*. Wiley, 2010.

[5] A. Cachada, T. Rocha-Santos, and A. C. Duarte, "Soil and Pollution: An Introduction to the Main Issues," in *Soil Pollution*, Elsevier, 2018, pp. 1–28.

[6] A. Kabata-Pendias and A. B. Mukherjee, *Trace elements from soil to human*. Berlin: Springer, 2007.

[7] J. L. Tank, A. J. Reisinger, and E. J. Rosi, "Nutrient Limitation and Uptake," in *Methods in Stream Ecology*, 3rd Ed., vol. 2, Academic Press, 2017, pp. 147–171.

[8] C. H. Walker, R. M. Sibly, S. P. Hopkin, and D. B. Peakall, *Principles of ecotoxicology*. CRC Press, 2012.

[9] R. Alcock *et al.*, "Health Risks of Persistent Organic Pollutants From Long-Range," *Heal. San Fr.*, p. 274, 2003.

[10] J. Pacyna, "Environmental Emissions of Selected Persistent Organic Pollutants," in *Persistent Pollution – Past, Present and Future*, Berlin: Springer, 2011, pp. 49–56.

[11] V. S. Thomaidi, A. S. Stasinakis, V. L. Borova, and N. S. Thomaidis, "Assessing the risk associated with the presence of emerging organic contaminants in sludge-amended soil: A country-level analysis," *Sci. Total Environ.*, vol. 548–549, pp. 280–288, 2016.

[12] (US Environmental Protection Agency) US EPA, *FEDERAL WATER POLLUTION CONTROL ACT - (33 U.S.C. 1251 et seq.)*. U.S.A., 2002.

[13] R. M. Abhang, K. S. Wani, V. S. Patil, B. L. Pangarkar, and S. B. Parjane, "Nanofiltration for Recovery of Heavy Metal Ions from Waste Water - A Review," *Internaltional J. Res. Environ. Sci. Technol.*, vol. 3, no. 1, pp. 29–34, 2013.

[14] I. A. Mirsal and J. Agbenin, "Soil Pollution: Origin, Monitoring, Restoration," *Eur. J. Soil Sci.*, vol. 55, no. 3, pp. 634–635, 2004.

[15] Y. Zhao, L. Ye, and X.-X. Zhang, "Emerging Pollutants–Part I: Occurrence, Fate and Transport," *Water Environ. Res.*, vol. 90, no. 10, pp. 1301–1322, 2018.

[16] X. Ren *et al.*, "Sorption, transport and biodegradation – An insight into bioavailability of persistent organic pollutants in soil," *Sci. Total Environ.*, vol. 610–611, pp. 1154–1163, 2018.

[17] T. M. Young, D. A. Heeraman, G. Sirin, and L. L. Ashbaugh, "Resuspension of soil as a source of airborne lead near industrial facilities and highways," *Environ. Sci. Technol.*, vol. 36, no. 11, pp. 2484–2490, 2002.

[18] J. Schäfer, S. Norra, D. Klein, and G. Blanc, "Mobility of trace metals associated with urban particles exposed to natural waters of various salinities from the Gironde Estuary, France," *J. Soils Sediments*, vol. 9, no. 4, pp. 374–392, 2009.

[19] K. G. Taylor and P. N. Owens, "Sediments in urban river basins: A review of sediment-contaminant dynamics in an environmental system conditioned by human activities," *J. Soils Sediments*, vol. 9, no.

4, pp. 281–303, 2009.

[20] Y. Qian, F. J. Gallagher, H. Feng, and M. Wu, “A geochemical study of toxic metal translocation in an urban brownfield wetland,” *Environ. Pollut.*, vol. 166, pp. 23–30, 2012.

[21] D. Mackay and M. MacLeod, “Multimedia environmental models,” *Pract. Period. Hazardous, Toxic, Radioact. Waste Manag.*, vol. 6, no. 2, pp. 63–69, 2002.

[22] P. R. Anderson and T. H. Christensen, “Distribution coefficients of Cd, Co, Ni, and Zn in soils,” *J. Soil Sci.*, vol. 39, no. 1, pp. 15–22, 1988.

[23] S. Sauvé, S. Manna, M. C. Turmel, A. G. Roy, and F. Courchesne, “Solid-Solution Partitioning of Cd, Cu, Ni, Pb, and Zn in the Organic Horizons of a Forest Soil,” *Environ. Sci. Technol.*, vol. 37, no. 22, pp. 5191–5196, 2003.

[24] S. Sauvé, W. A. Norvell, M. McBride, and W. Hendershot, “Speciation and complexation of cadmium in extracted soil solutions,” *Environ. Sci. Technol.*, vol. 34, no. 2, pp. 291–296, 2000.

[25] V. Mohebbi, A. Naderifar, R. M. Behbahani, and M. Moshfeghian, “Determination of Henry’s law constant of light hydrocarbon gases at low temperatures,” *J. Chem. Thermodyn.*, vol. 51, pp. 8–11, 2012.

[26] R. P. Schwarzenbach, P. M. Gschwend, and D. M. Imboden, *Environmental Organic Chemistry*. John Wiley & Sons, Incorporated, 2016.

[27] L. J. Thibodeaux, *Environmental chemodynamics : movement of chemicals in air, water, and soil*, 2nd Ed. Wiley, 1996.

[28] D. Van de Meent, *SimpleBox: a generic multimedia fate evaluation model - RIVM Report 672720001/1993*. Bilthoven (The Netherlands), 1993.

[29] L. J. Brandes, H. den Hollander, and D. van de Meent, *SimpleBox 2.0: a nested multimedia fate model for evaluating the environmental fate of chemicals - RIVM Report 719101029/1996*. Bilthoven (The Netherlands), 1996.

[30] H. A. Den Hollander, J. C. H. Van Eijkeren, and D. Van de Meent, *SimpleBox 3.0: Multimedia mass balance model for evaluating the fate of chemical in the environment - RIVM Report 601200003/2004*. Bilthoven (The Netherlands), 2004.

[31] W. G. Whitman, “The two film theory of gas absorption,” *Int. J. Heat Mass Transf.*, vol. 5, no. 5, pp. 429–433, May 1962.

[32] S. N. Matsunaga, A. B. Guenther, Y. Izawa, C. Wiedinmyer, J. P. Greenberg, and K. Kawamura, “Importance of wet precipitation as a removal and transport process for atmospheric water soluble carbonyls,” *Atmos. Environ.*, vol. 41, no. 4, pp. 790–796, 2007.

[33] F. Sánchez-Bayo *et al.*, “Fate and Transport of Contaminants,” in *Ecological Impacts of Toxic Chemicals*, Bentham Science Publishers Ltd., 2011, pp. 13–42.

[34] H. Ghadiri, J. Hussein, and C. W. Rose, “A study of the interactions between salinity, soil erosion, and pollutant transport on three Queensland soils,” *Aust. J. Soil Res.*, vol. 45, no. 6, pp. 404–413, 2007.

[35] I. Shainberg, D. Warrington, and J. M. Laflen, “Soil Dispersibility, Rain Properties, and Slope Interaction in Rill Formation and Erosion,” *Soil Sci. Soc. Am. J.*, vol. 56, no. 1, p. 278, 2010.

[36] J. DePinto, R. McCulloch, T. Redder, J. Wolfe, and T. Dekker, “Deposition and Resuspension of Particles and the Associated Chemical Transport across the Sediment–Water Interface,” in *Handbook of Chemical Mass Transport in the Environment*, CRC Press, 2010, pp. 253–299.

[37] A. B. A. Boxall, “Transformation Products of Synthetic Chemicals in the Environment,” in *The Handbook of Environmental Chemistry*, vol. 2P, A. B. A. Boxall, Ed. Berlin: Springer, 2009.

[38] J. H. Montgomery and T. R. Crompton, *Environmental chemicals desk reference*. Boca Raton, FL:

CRC Press, 2017.

[39] S. Chen, D. Fan, and P. G. Tratnyek, “Novel Contaminant Transformation Pathways by Abiotic Reductants,” *Environ. Sci. Technol. Lett.*, vol. 1, no. 10, pp. 432–436, 2014.

[40] A. Neilson and A.-S. Allard, “Pathways and Mechanisms of Degradation and Transformation,” in *Organic Chemicals in the Environment*, 2nd Ed., London, UK: CRC Press, 2012, pp. 551–552.

[41] L. L. Van Eerd, R. E. Hoagland, R. M. Zablotowicz, and J. C. Hall, “Pesticide metabolism in plants and microorganisms,” *Weed Sci.*, vol. 51, no. 4, pp. 472–495, 2006.

[42] I. C. Nair and K. Jayachandran, “Enzymes for bioremediation and biocontrol,” in *Bioresources and Bioprocess in Biotechnology*, vol. 2, Singapore: Springer, 2017, pp. 75–97.

[43] W. B. Neely, *Environmental Exposure From Chemicals*. CRC Press, 2018.

[44] A. H. Neilson, *Organic chemicals in the aquatic environment: Distribution, persistence, and toxicity*. CRC Press, 2018.

[45] A. Violante, V. Cozzolino, L. Perelomov, A. G. Caporale, and M. Pigna, “Mobility and bioavailability of heavy metals and metalloids in soil environments,” *J. Soil Sci. Plant Nutr.*, vol. 10, no. 3, pp. 268–292, 2010.

[46] D. Hillel and J. L. Hatfield, “Factors of Soil Formation,” in *Encyclopedia of Soils in the Environment*, 1st Ed., Oxford: Academic Press, 2004, pp. 532–535.

[47] J. Gerrard, *Fundamentals of soils*, 1st Ed. London, UK: CRC Press, 2000.

[48] J. M. Brils, “The SedNet Strategy Paper: The opinion of SedNet on environmentally, socially and economically viable sediment management,” 2004.

[49] P. R. Owens and E. M. Rutledge, “Morphology,” *Encycl. Soils Environ.*, pp. 511–520, 2005.

[50] M. L. Brusseau, I. L. Pepper, and C. P. Gerba, *Environmental and Pollution Science*, 3rd Ed. Elsevier, 2019.

[51] J. M. Brils, *Contaminated SedimentS in european river Basins - EVK1-CT-2001-20002*. 2004.

[52] P. Krasilnikov, *A Handbook of Soil Terminology, Correlation and Classification*. Earthscan, 2014.

[53] A. D. Karathanasis, “SOIL MINERALOGY,” in *LAND USE, LAND COVER AND SOIL SCIENCES - Vol. VI*, Singapore: Eolss Publishers Co. Ltd., 2009, pp. 233–260.

[54] R. V. Gaines, H. C. W. Skinner, E. E. Foord, B. Mason, and Rosenzweig. A., *Dana’s New Mineralogy*, 8th Ed., no. 11. New York: Wiley/VCH, 1997.

[55] D. J. Vaughan, “MINERALS | Sulphides,” in *Encyclopedia of Geology*, Elsevier, 2005, pp. 574–586.

[56] U. Schwertmann and R. Fitzpatrick, “Iron minerals in surface environments,” *Catena Suppl.*, vol. 21, pp. 7–30, 1992.

[57] S. K. Haldar and J. Tišljar, “Basic Mineralogy,” in *Introduction to Mineralogy and Petrology*, Elsevier, 2013, pp. 39–79.

[58] C. Long, J. Xiaohong, W. Bo, L. Yuanshou, Z. Xuebin, and Z. Hong, “Effects of biological soil crusts on the characteristics of hygroscopic and condensate water deposition in alpine sandy lands,” *Acta Ecol. Sin.*, vol. 38, no. 14, 2018.

[59] P. S. Sha Valli Khan, G. V. Nagamallaiah, M. Dhanunjay Rao, K. Sergeant, and J. F. Hausman, “Abiotic Stress Tolerance in Plants: Insights from Proteomics,” in *Emerging Technologies and Management of Crop Stress Tolerance*, 1st Ed., Cambridge, MA, USA: Academic Press, 2014.

[60] B. D. Shaw *et al.*, “Analysis of Ion and Dissolved Organic Carbon Interference on Soil Solution Nitrate Concentration Measurements Using Ultraviolet Absorption Spectroscopy,” *Vadose Zo. J.*, vol. 13, no.

12, p. 0, 2016.

[61] D. E. Rolston, "AERATION," in *Encyclopedia of Soils in the Environment*, Elsevier, 2005, pp. 17–21.

[62] M. E. Hinkle, E. H. Denton, R. C. Bigelow, and R. L. Turner, "Helium in soil gases of the Roosevelt hot springs known geothermal resource area, Beaver county, Utah," *J Res US Geol Surv*, vol. 6, no. 5, pp. 563–569, 1978.

[63] H. G. Schlegel, "Production, modification, and consumption of atmospheric trace gases by microorganisms," *Tellus*, vol. 26, no. 1–2, pp. 11–20, 1974.

[64] R. Chester, *Marine Geochemistry*. Springer Netherlands, 1990.

[65] (University of Puerto Rico) UPRM, "Geological Oceanography Program - Biogenic Sediments," 2005. [Online]. Available: http://geology.uprm.edu/MorelockSite/morelockonline/8-biogenic.htm.

[66] W. H. Berger and G. Wefer, "Marine biogenic sediments," in *Encyclopedia of Earth Sciences Series*, Springer Netherlands, 2009.

[67] C. M. Robert, "Biogenic Sediments," in *Developments in Marine Geology*, vol. 3, 2008.

[68] G. M. Pierzynski, J. T. Sims, and G. F. Vance, *Soils and environmental quality*, 3rd Ed. Taylor & Francis, 2005.

[69] G. U. Chibuike and S. C. Obiora, "Heavy metal polluted soils: Effect on plants and bioremediation methods," *Appl. Environ. Soil Sci.*, vol. 2014, pp. 1–12, 2014.

[70] Z.-G. Shen, X.-D. Li, C.-C. Wang, H.-M. Chen, and H. Chua, "Lead phytoextraction from contaminated soil with high-biomass plant species," *J. Environ. Qual.*, vol. 31, no. 6, pp. 1893–1900, 2002.

[71] K. Vaxevanidou, N. Papassiopi, and I. Paspaliaris, "Removal of heavy metals and arsenic from contaminated soils using bioremediation and chelant extraction techniques," *Chemosphere*, vol. 70, no. 8, pp. 1329–1337, 2008.

[72] A. R. Wilson, *Environmental risk : identification and management*. CRC Press, 1991.

[73] A. C. Agnello, "Potential of alfalfa for use in chemically and biologically assisted phytoremediation of soil co-contaminated with petroleum hydrocarbons and metals," Université Paris-Est, 2014.

[74] US National Research Council, "Risk Assessment in the Federal Government," National Academies Press, Washington, D.C., 1983.

[75] J. Beard, "DDT and human health," *Sci. Total Environ.*, vol. 355, no. 1–3, pp. 78–89, 2006.

[76] J. Bone *et al.*, "From chemical risk assessment to environmental quality management: The challenge for soil protection," *Environ. Sci. Technol.*, vol. 45, no. 1, pp. 104–110, 2011.

[77] J. W. Doran and M. R. Zeiss, "Soil health and sustainability: managing the biotic component of soil quality," *Appl. Soil Ecol.*, vol. 15, no. 1, pp. 3–11, 2000.

[78] L. Poggio, B. Vrščaj, E. Hepperle, R. Schulin, and F. A. Marsan, "Introducing a method of human health risk evaluation for planning and soil quality management of heavy metal-polluted soils-An example from Grugliasco (Italy)," *Landsc. Urban Plan.*, vol. 88, no. 2–4, pp. 64–72, 2008.

[79] Z. Shen, D. Xu, L. Li, J. Wang, and X. Shi, "Ecological and health risks of heavy metal on farmland soils of mining areas around Tongling City, Anhui, China," *Environ. Sci. Pollut. Res.*, vol. 26, no. 15, pp. 15698–15709, May 2019.

[80] S. Chonokhuu, C. Batbold, B. Chuluunpurev, E. Battsengel, B. Dorjsuren, and B. Byambaa, "Contamination and Health Risk Assessment of Heavy Metals in the Soil of Major Cities in Mongolia," *Int. J. Environ. Res. Public Health*, vol. 16, no. 14, p. 2552, 2019.

[81] C. M. A. Iwegbue and B. S. Martincigh, "Ecological and human health risks arising from exposure to metals in urban soils under different land use in Nigeria," *Environ. Sci. Pollut. Res.*, vol. 25, no. 13, pp.

12373–12390, 2018.

[82] N. U. Kura *et al.*, “Assessment of groundwater vulnerability to anthropogenic pollution and seawater intrusion in a small tropical island using index-based methods,” *Environ. Sci. Pollut. Res.*, vol. 22, no. 2, pp. 1512–1533, 2014.

[83] A. Matzeu, R. Secci, and G. Uras, “Methodological approach to assessment of groundwater contamination risk in an agricultural area,” *Agric. Water Manag.*, vol. 184, pp. 46–58, 2017.

[84] F. A. Swartjes, *Dealing with Contaminated Sites*. Dordrecht: Springer, 2011.

[85] D. Vallero, “Air Pollutant Exposures,” in *Fundamentals of Air Pollution*, Academic Press, 2014, pp. 215–246.

[86] (International programme on chemical safety) IPCS, “IPCS Risk Assessment Terminology,” 2004.

[87] H. Lu, L. Axe, and T. A. Tyson, “Development and application of computer simulation tools for ecological risk assessment,” *Environ. Model. Assess.*, vol. 8, no. 4, pp. 311–322, 2003.

[88] W. Naito, M. Kamo, K. Tsushima, and Y. Iwasaki, “Exposure and risk assessment of zinc in Japanese surface waters,” *Sci. Total Environ.*, vol. 408, no. 20, pp. 4271–4284, 2010.

[89] P. Chanpiwat, B.-T. Lee, K.-W. Kim, and S. Sthiannopkao, “Human health risk assessment for ingestion exposure to groundwater contaminated by naturally occurring mixtures of toxic heavy metals in the Lao PDR,” *Environ. Monit. Assess.*, vol. 186, no. 8, pp. 4905–4923, 2014.

[90] T. N. Brown, J. M. Armitage, P. Egeghy, I. Kircanski, and J. A. Arnot, “Dermal permeation data and models for the prioritization and screening-level exposure assessment of organic chemicals,” *Environ. Int.*, vol. 94, pp. 424–435, 2016.

[91] Y. Shao, S. Ramachandran, S. Arnold, and G. Ramachandran, “Turbulent eddy diffusion models in exposure assessment - Determination of the eddy diffusion coefficient,” *J. Occup. Environ. Hyg.*, vol. 14, no. 3, pp. 195–206, 2017.

[92] T. E. Butt, M. Clark, F. Coulon, and K. O. K. Oduyemi, “A review of literature and computer models on exposure assessment,” *Environ. Technol.*, vol. 30, no. 14, pp. 1487–1501, 2009.

[93] C. C. P. Gerba, “Risk Assessment and Environmental Regulations,” in *Environmental Monitoring and Characterization*, Academic Press, 2004, pp. 377–392.

[94] Z. Wang *et al.*, “Critical review and probabilistic health hazard assessment of cleaning product ingredients in all-purpose cleaners, dish care products, and laundry care products,” *Environ. Int.*, vol. 125, pp. 399–417, 2019.

[95] D. Rouquié, C. Friry-Santini, F. Schorsch, H. Tinwell, and R. Bars, “Standard and molecular NOAELs for rat testicular toxicity induced by flutamide,” *Toxicol. Sci.*, vol. 109, no. 1, pp. 59–65, 2009.

[96] G. E. Dinse and D. M. Umbach, “Dose-response modeling,” in *Chemical Mixtures and Combined Chemical and Nonchemical Stressors: Exposure, Toxicity, Analysis, and Risk*, 2018, pp. 205–234.

[97] L. Edler and C. P. Kitsos, *Recent advances in quantitative methods in cancer and human health risk assessment*. J. Wiley, 2006.

[98] A. Valavanidis and T. Vlachogianni, “Ecotoxicity Test Methods and Ecological Risk Assessment . Aquatic and Terrestrial Ecotoxicology Tests under the Guidelines of International Organizations,” *Sci. Adv. Environ. Chem. Toxicol. Ecotoxicol. Issues*, no. September, p. 28, 2015.

[99] S. J. T. Pollard, M. Lythgo, and R. Duarte-Davidson, “The Extent of Contaminated Land Problems and the Scientific Response,” in *Assessment and Reclamation of Contaminated Land*, Cambridge: Royal Society of Chemistry, 2001, pp. 1–19.

[100] (Enviromental Ministry Decree) EMD, Ministerial Decree No 471 of 25th October 1999. in *Italian Official Gazzette n. 293 of 15th December 1999*; Enviromental Ministry, IT, 1999.

[101] (Enviromental Ministry Decree) EMD, Legislative Decree No 152 of 03rd April 2006. in *Italian Official Gazzette n. 88 of 14th April 2006*; Enviromental Ministry, IT, 2006.

[102] (American Society of Testing & Materials) ASTM, "ASTM E2205-02(2014) Standard Guide for Risk-Based Corrective Action for Protection of Ecological Resources." 2015.

[103] G. Cassar and A. Leonforte, "Contaminated land in Italy," *Pract. Law UK Artic.*, p. ID. 3-522-0477, 2015.

[104] (Italian Parliament) IP, Law n° 84 of 28th January 1994. in *Italian Official Gazzette n. 28 of 4th February 1994*; Italian Parliament, IT, 1994.

[105] (Enviromental Ministry Decree) EMD, Ministerial Decree No 172 of 15th July 2016. in *Italian Official Gazzette n.208 of 06th September 2016*; Enviromental Ministry, IT, 2016.

[106] (Enviromental Ministry Decree) EMD, Ministerial Decree of 7th November 2008. in *Italian Official Gazzette n. 284 of 04th December 2008*; Enviromental Ministry, IT, 2008.

[107] (Enviromental Ministry Decree) EMD, *Ministerial Decree No 173 of 15th July 2016*. in *Italian Official Gazzette n. 208 of 06th September 2016*; Enviromental Ministry, IT, 2016.

[108] (Italian Parliament) IP, Law n° 360 of 08th November 1991. in *Italian Official Gazzette n. 267 of 29th November 1991*; Italian Parliament, IT, 1991.

[109] (European Union) EU, Directive 2000/60/EC of the European Parliament and of the Council of 23 October 2000 establishing a framework for Community action in the field of water policy. in *Official Journal of the European Union (OJ L) No 327 of 22/12/2000*, pp. 1–73, 2000.

[110] (European Union) EU, Directive 2008/1/EC of the European Parliament and of the Council of 15 January 2008 concerning integrated pollution prevention and control. in *Official Journal of the European Union (OJ L) No 24 of 29/01/2008*, pp. 8–29, 2008.

[111] (European Union) EU, Directive 2013/39/EU of the European Parliament and of the Council of 12 August 2013 amending Directives 2000/60/EC and 2008/105/EC as regards priority substances in the field of water policy. in *Official Journal of the European Union (OJ L) No 226 of 24/08/2013*, pp. 1–17, 2013.

[112] (Enviromental Ministry Decree) EMD, Legislative Decree No 172 of 13rd October 2015. in *Italian Official Gazzette n. 250 of 27th December 2015*; Enviromental Ministry, IT, 2015.

[113] (Enviromental Ministry Decree) EMD, Ministerial Decree of 5th February 1998. in *Italian Official Gazzette n. 88 of 19th April 1998*; Enviromental Ministry, IT, 1998.

[114] (Enviromental Ministry Decree) EMD, Ministerial Decree No 186 of 05th April 2006. in *Italian Official Gazzette n.115 of 19th 2006*; Enviromental Ministry, IT, 2006.

[115] D. C. Adriano, "Trace elements in terrestrial environments : biogeochemistry, bioavailability, and risks of metals," vol. 32, no. 1, p. 374, 2001.

[116] T. A. Kirpichtchikova, A. Manceau, L. Spadini, F. Panfili, M. A. Marcus, and T. Jacquet, "Speciation and solubility of heavy metals in contaminated soil using X-ray microfluorescence, EXAFS spectroscopy, chemical extraction, and thermodynamic modeling," *Geochim. Cosmochim. Acta*, vol. 70, pp. 2163–2190, 2006.

[117] R. A. Wuana and F. E. Okieimen, "Heavy Metals in Contaminated Soils: A Review of Sources, Chemistry, Risks and Best Available Strategies for Remediation," *ISRN Ecol.*, vol. 2011, pp. 1–20, 2011.

[118] C. N. Mulligan, M. Fukue, and Y. Sato, *Sediments contamination and sustainable remediation*. IWA Pub, 2010.

[119] K. Valujeva, J. Burlakovs, I. Grinfelde, J. Pilecka, Y. Jani, and W. Hogland, "Phytoremediation as tool

for prevention of contaminant flow to hydrological systems," in *Research for Rural Development*, 2018, vol. 1, pp. 188–194.

[120] N. Gaurina-Medjimurec, *Handbook of research on advancements in environmental engineering*, 1st Ed. Hershey PA, USA: IGI Global, 2015.

[121] J. Burlakovs, "Contamination remediation with soil amendments by immobilization of heavy metals," University of Latvia, 2015.

[122] S. Khalid, M. Shahid, N. K. Niazi, B. Murtaza, I. Bibi, and C. Dumat, "A comparison of technologies for remediation of heavy metal contaminated soils," *J. Geochemical Explor.*, vol. 182, pp. 247–268, 2017.

[123] Z. Yao, J. Li, H. Xie, and C. Yu, "Review on Remediation Technologies of Soil Contaminated by Heavy Metals," *Procedia Environ. Sci.*, vol. 16, pp. 722–729, 2012.

[124] Y. Gong, D. Zhao, and Q. Wang, "An overview of field-scale studies on remediation of soil contaminated with heavy metals and metalloids: Technical progress over the last decade," *Water Res.*, vol. 147, pp. 440–460, 2018.

[125] Z. Derakhshan Nejad, M. C. Jung, and K.-H. Kim, "Remediation of soils contaminated with heavy metals with an emphasis on immobilization technology," *Environ. Geochem. Health*, vol. 40, no. 3, pp. 927–953, 2018.

[126] L. Zhu, W. Ding, L. juan Feng, Y. Kong, J. Xu, and X. yang Xu, "Isolation of aerobic denitrifiers and characterization for their potential application in the bioremediation of oligotrophic ecosystem," *Bioresour. Technol.*, vol. 108, pp. 1–7, 2012.

[127] C. Zheng and P. P. Wang, "A field demonstration of the simulation optimization approach for remediation system design," *Ground Water*, vol. 40, no. 3, pp. 258–65, 2002.

[128] J. Dawson, "Barrier containment technologies for environmental remediation applications," *J. Hazard. Mater.*, vol. 51, no. 1–3, p. 256, 1996.

[129] S. R. Mallampati, Y. Mitoma, T. Okuda, C. Simion, and B. K. Lee, "Dynamic immobilization of simulated radionuclide 133 Cs in soil by thermal treatment/vitrification with nanometallic Ca/CaO composites," *J. Environ. Radioact.*, vol. 139, pp. 118–124, 2015.

[130] P. Colombo, G. Brusatin, E. Bernardo, and G. Scarinci, "Inertization and reuse of waste materials by vitrification and fabrication of glass-based products," *Curr. Opin. Solid State Mater. Sci.*, vol. 7, no. 3, pp. 225–239, 2003.

[131] F. Dellisanti, P. L. Rossi, and G. Valdrè, "In-field remediation of tons of heavy metal-rich waste by Joule heating vitrification," *Int. J. Miner. Process.*, vol. 93, no. 3–4, pp. 239–245, 2009.

[132] J. L. Buelt and L. . Thompson, "In Situ Remediation Integrated Program: FY 1994 program summary," Richland, WA, 1995.

[133] A. Navarro, E. Cardellach, I. Cañadas, and J. Rodríguez, "Solar thermal vitrification of mining contaminated soils," *Int. J. Miner. Process.*, vol. 119, pp. 65–74, 2013.

[134] Y. Yang, Z. Shuzhen, H. Honglin, L. Lei, and W. Bei, "Arsenic accumulation and speciation in maize as affected by inoculation with arbuscular mycorrhizal fungus glomus mosseae," *J. Agric. Food Chem.*, vol. 57, no. 9, pp. 3695–3701, 2009.

[135] M. Vocciante, A. Caretta, L. Bua, R. Bagatin, and S. Ferro, "Enhancements in ElectroKinetic Remediation Technology: Environmental assessment in comparison with other configurations and consolidated solutions," *Chem. Eng. J.*, vol. 289, pp. 123–134, 2016.

[136] L. Yang, B. Huang, W. Hu, Y. Chen, M. Mao, and L. Yao, "The impact of greenhouse vegetable farming duration and soil types on phytoavailability of heavy metals and their health risk in eastern China," *Chemosphere*, vol. 103, pp. 121–130, 2014.

[137] X. Mao *et al.*, “Electro-kinetic remediation coupled with phytoremediation to remove lead, arsenic and cesium from contaminated paddy soil,” *Ecotoxicol. Environ. Saf.*, vol. 125, pp. 16–24, 2016.

[138] J. Virkutyte, M. Sillanpää, and P. Latostenmaa, “Electrokinetic soil remediation - Critical overview,” *Sci. Total Environ.*, vol. 289, no. 1–3, pp. 97–121, 2002.

[139] M. M. Page and C. L. Page, “Electroremediation of contaminated soils,” *J. Environ. Eng.*, vol. 128, no. 3, pp. 208–219, 2002.

[140] A. Careghini *et al.*, “Sequential solidification/stabilization and thermal process under vacuum for the treatment of mercury in sediments,” *J. Soils Sediments*, vol. 10, no. 8, pp. 1646–1656, 2010.

[141] USEPA, “Treatment Technologies for Mercury in Soil, Waste, and Water,” 2007.

[142] J. Wang, X. Feng, C. W. N. Anderson, H. Wang, L. Zheng, and T. Hu, “Implications of mercury speciation in thiosulfate treated plants,” *Environ. Sci. Technol.*, vol. 46, no. 10, pp. 5361–5368, 2012.

[143] J. Wang, X. Feng, C. W. N. Anderson, Y. Xing, and L. Shang, “Remediation of mercury contaminated sites - A review,” *J. Hazard. Mater.*, vol. 221–222, pp. 1–18, 2012.

[144] M. Sabir, E. A. Waraich, K. R. Hakeem, M. Öztürk, H. R. Ahmad, and M. Shahid, “Phytoremediation: Mechanisms and Adaptations. Mechanisms and Adaptations.,” in *Soil Remediation and Plants: Prospects and Challenges*, Academic Press, 2014, pp. 85–105.

[145] N. S. Bolan, J. H. Park, B. Robinson, R. Naidu, and K. Y. Huh, *Phytostabilization: A green approach to contaminant containment*, vol. 112. Academic Press, 2011.

[146] S. F. Cheng, C. Y. Huang, K. L. Chen, S. C. Lin, and Y. C. Lin, “Phytoattenuation of lead-contaminated agricultural land using Miscanthus floridulus—an in situ case study,” *Desalin. Water Treat.*, vol. 57, no. 17, pp. 7773–7779, 2016.

[147] K. R. Hakeem, M. Sabir, M. Öztürk, and A. R. Mermut, *Soil Remediation and Plants: Prospects and Challenges*. Elsevier, 2014.

[148] N. Rascio and F. Navari-Izzo, “Heavy metal hyperaccumulating plants: How and why do they do it? And what makes them so interesting?,” *Plant Sci.*, vol. 180, no. 2, pp. 169–181, 2011.

[149] V. Sheoran, A. S. Sheoran, and P. Poonia, “Factors Affecting Phytoextraction: A Review,” *Pedosphere*, vol. 26, no. 2, pp. 148–166, 2016.

[150] A. Mahar *et al.*, “Challenges and opportunities in the phytoremediation of heavy metals contaminated soils: A review,” *Ecotoxicol. Environ. Saf.*, vol. 126, pp. 111–121, 2016.

[151] A. Bhargava, F. F. Carmona, M. Bhargava, and S. Srivastava, “Approaches for enhanced phytoextraction of heavy metals,” *J. Environ. Manage.*, vol. 105, pp. 103–120, 2012.

[152] M. Shahid, C. Dumat, M. Aslama, and E. Pinelli, “Assessment of lead speciation by organic ligands using speciation models,” *Chem. Speciat. Bioavailab.*, vol. 24, no. 4, pp. 248–252, 2012.

[153] A. P. G. C. Marques, A. O. S. S. Rangel, and P. M. L. Castro, “Remediation of heavy metal contaminated soils: Phytoremediation as a potentially promising clean-Up technology,” *Crit. Rev. Environ. Sci. Technol.*, vol. 39, no. 8, pp. 622–654, 2009.

[154] N. Verbruggen, C. Hermans, and H. Schat, “Molecular Mechanisms of Metal Hyperaccumulation in Plants Authors (s): Nathalie Verbruggen , Christian Hermans and Henk Schat Source : The New Phytologist , Vol . 181 , No . 4 (Mar ., 2009), pp . 759-776 Published by : Wiley on behalf of the New Phyto,” *New Phytol.*, vol. 181, no. 4, pp. 759–776, 2016.

[155] G. Wu, H. Kang, X. Zhang, H. Shao, L. Chu, and C. Ruan, “A critical review on the bio-removal of hazardous heavy metals from contaminated soils: Issues, progress, eco-environmental concerns and opportunities,” *J. Hazard. Mater.*, vol. 174, no. 1–3, pp. 1–8, 2010.

[156] L. C. Tan, Y. V. Nancharaiah, E. D. van Hullebusch, and P. N. L. Lens, “Selenium: environmental

significance, pollution, and biological treatment technologies," *Biotechnol. Adv.*, vol. 34, no. 5, pp. 886–907, 2016.

[157] S. K. Porter, K. G. Scheckel, C. A. Impellitteri, and J. A. Ryan, "Toxic metals in the environment: Thermodynamic considerations for possible immobilization strategies for Pb, Cd, As, and Hg," *Crit. Rev. Environ. Sci. Technol.*, vol. 34, no. 6, pp. 495–604, 2004.

[158] M. Shahid *et al.*, "Influence of plant species and phosphorus amendments on metal speciation and bioavailability in a smelter impacted soil: A case study of food-chain contamination," *J. Soils Sediments*, vol. 14, no. 4, pp. 655–665, 2014.

[159] A. Austruy *et al.*, "Mechanisms of metal-phosphates formation in the rhizosphere soils of pea and tomato: Environmental and sanitary consequences," *J. Soils Sediments*, vol. 14, no. 4, pp. 666–678, 2014.

[160] Y. Sun, Y. Xu, Y. Xu, L. Wang, X. Liang, and Y. Li, "Reliability and stability of immobilization remediation of Cd polluted soils using sepiolite under pot and field trials," *Environ. Pollut.*, vol. 208, pp. 739–746, 2016.

[161] A. Ashraf *et al.*, "Chromium(VI) sorption efficiency of acid-activated banana peel over organo-montmorillonite in aqueous solutions," *Int. J. Phytoremediation*, vol. 19, no. 7, pp. 605–613, 2017.

[162] M. A. R. Soares, M. J. Quina, and R. M. Quinta-Ferreira, "Immobilisation of lead and zinc in contaminated soil using compost derived from industrial eggshell," *J. Environ. Manage.*, vol. 164, pp. 137–145, 2015.

[163] I. Smičiklas, S. Smiljanić, A. Perić-Grujić, M. Šljivić-Ivanović, M. Mitrić, and D. Antonović, "Effect of acid treatment on red mud properties with implications on Ni(II) sorption and stability," *Chem. Eng. J.*, vol. 242, pp. 27–35, 2014.

[164] X. Liang, J. Han, Y. Xu, Y. Sun, L. Wang, and X. Tan, "In situ field-scale remediation of Cd polluted paddy soil using sepiolite and palygorskite," *Geoderma*, vol. 235–236, pp. 9–18, 2014.

[165] Y. Sun, Y. Li, Y. Xu, X. Liang, and L. Wang, "In situ stabilization remediation of cadmium (Cd) and lead (Pb) co-contaminated paddy soil using bentonite," *Appl. Clay Sci.*, vol. 105–106, pp. 200–206, 2015.

[166] N. S. Bolan, D. C. Adriano, P. Duraisamy, A. Mani, and K. Arulmozhiselvan, "Immobilization and phytoavailability of cadmium in variable charge soils. I. Effect of phosphate addition," *Plant Soil*, vol. 250, no. 1, pp. 83–94, 2003.

[167] G. W. Ware *et al.*, "Role of Phosphorus in (Im)mobilization and Bioavailability of Heavy Metals in the Soil-Plant System," *Rev. Environ. Contam. Toxicol.*, vol. 177, pp. 1–44, 2003.

[168] J. E. Lim *et al.*, "Effects of lime-based waste materials on immobilization and phytoavailability of cadmium and lead in contaminated soil," *Clean - Soil, Air, Water*, vol. 41, no. 12, pp. 1235–1241, 2013.

[169] H. He, N. F. Y. Tam, A. Yao, R. Qiu, W. C. Li, and Z. Ye, "Effects of alkaline and bioorganic amendments on cadmium, lead, zinc, and nutrient accumulation in brown rice and grain yield in acidic paddy fields contaminated with a mixture of heavy metals," *Environ. Sci. Pollut. Res.*, vol. 23, no. 23, pp. 23551–23560, 2016.

[170] M. S. Ko, J. Y. Kim, H. S. Park, and K. W. Kim, "Field assessment of arsenic immobilization in soil amended with iron rich acid mine drainage sludge," *J. Clean. Prod.*, vol. 108, pp. 1073–1080, 2015.

[171] G. Okkenhaug *et al.*, "Antimony (Sb) and lead (Pb) in contaminated shooting range soils: Sb and Pb mobility and immobilization by iron based sorbents, a field study," *J. Hazard. Mater.*, vol. 307, pp. 336–343, 2016.

[172] N. K. Niazi *et al.*, "Removal and Recovery of Metals by Biosorbents and Biochars Derived From Biowastes," in *Environmental Materials and Waste: Resource Recovery and Pollution Prevention*,

Academic Press, 2016, pp. 149–177.

[173] M. Shahid, M. Sabir, M. A. Ali, and A. Ghafoor, “Effect of organic amendments on phytoavailability of nickel and growth of berseem (Trifolium alexandrinum) under nickel contaminated soil conditions,” *Chem. Speciat. Bioavailab.*, vol. 26, no. 1, pp. 37–42, 2014.

[174] D. J. Walker, R. Clemente, and M. P. Bernal, “Contrasting effects of manure and compost on soil pH, heavy metal availability and growth of Chenopodium album L. in a soil contaminated by pyritic mine waste,” *Chemosphere*, vol. 57, no. 3, pp. 215–224, 2004.

[175] L. Beesley *et al.*, “Assessing the influence of compost and biochar amendments on the mobility and toxicity of metals and arsenic in a naturally contaminated mine soil,” *Environ. Pollut.*, vol. 186, pp. 195–202, 2014.

[176] Y. A. Almaroai, A. R. A. Usman, M. Ahmad, K. R. Kim, M. Vithanage, and Y. Sikok, “Role of chelating agents on release kinetics of metals and their uptake by maize from chromated copper arsenate-contaminated soil,” *Environ. Technol.*, vol. 34, no. 6, pp. 747–755, 2013.

[177] A. Moutsatsou, M. Gregou, D. Matsas, and V. Protonotarios, “Washing as a remediation technology applicable in soils heavily polluted by mining–metallurgical activities,” *Chemosphere*, vol. 63, no. 10, pp. 1632–1640, 2006.

[178] K. K. Fedje, L. Yillin, and A. M. Strömvall, “Remediation of metal polluted hotspot areas through enhanced soil washing - Evaluation of leaching methods,” *J. Environ. Manage.*, vol. 128, pp. 489–496, 2013.

[179] G. Zhu *et al.*, “Washing out heavy metals from contaminated soils from an iron and steel smelting site,” *Front. Environ. Sci. Eng.*, vol. 9, no. 4, pp. 634–641, 2015.

[180] S. I. Alghanmi, A. F. Al Sulami, T. A. El-Zayat, B. G. Alhogbi, and M. Abdel Salam, “Acid leaching of heavy metals from contaminated soil collected from Jeddah, Saudi Arabia: kinetic and thermodynamics studies,” *Int. Soil Water Conserv. Res.*, vol. 3, no. 3, pp. 196–208, 2015.

[181] M. Bilgin and S. Tulun, “Removal of heavy metals (Cu, Cd and Zn) from contaminated soils using EDTA and FeCl3,” *Glob. Nest J.*, vol. 18, no. 1, pp. 98–107, 2016.

[182] Z. H. Yang, C. Di Dong, C. W. Chen, Y. T. Sheu, and C. M. Kao, “Using poly-glutamic acid as soil-washing agent to remediate heavy metal-contaminated soils,” *Environ. Sci. Pollut. Res.*, vol. 25, no. 6, pp. 5231–5242, 2018.

[183] D. Kulikowska, Z. M. Gusiatin, K. Bułkowska, and B. Klik, “Feasibility of using humic substances from compost to remove heavy metals (Cd, Cu, Ni, Pb, Zn) from contaminated soil aged for different periods of time,” *J. Hazard. Mater.*, vol. 300, pp. 882–891, 2015.

[184] B. Park and Y. Son, “Ultrasonic and mechanical soil washing processes for the removal of heavy metals from soils,” *Ultrason. Sonochem.*, vol. 35, pp. 640–645, 2017.

[185] X. Guo, Z. Wei, Q. Wu, C. Li, T. Qian, and W. Zheng, “Effect of soil washing with only chelators or combining with ferric chloride on soil heavy metal removal and phytoavailability: Field experiments,” *Chemosphere*, vol. 147, pp. 412–419, 2016.

[186] M. Shahid, B. Pourrut, C. Dumat, M. Nadeem, M. Aslam, and E. Pinelli, “Heavy-metal-induced reactive oxygen species: Phytotoxicity and physicochemical changes in plants,” *Rev. Environ. Contam. Toxicol.*, vol. 232, pp. 1–44, 2014.

[187] A. Ferraro, E. D. van Hullebusch, D. Huguenot, M. Fabbricino, and G. Esposito, “Application of an electrochemical treatment for EDDS soil washing solution regeneration and reuse in a multi-step soil washing process: Case of a Cu contaminated soil,” *J. Environ. Manage.*, vol. 163, pp. 62–69, 2015.

[188] P. Hu *et al.*, “Assessment of EDTA heap leaching of an agricultural soil highly contaminated with heavy metals,” *Chemosphere*, vol. 117, no. 1, pp. 532–537, 2014.

[189] G. Wang *et al.*, "Effect of soil washing with biodegradable chelators on the toxicity of residual metals and soil biological properties," *Sci. Total Environ.*, vol. 625, pp. 1021–1029, 2018.

[190] C. R. Evanko and D. A. Dzombak, "Remediation of Metals-contaminated Soils and Groundwater, Technology Evaluation Report, TE-97–01," in *Ground-Water Remediation Technologies Analysis Center*, 1997, no. 412, pp. 373–1973.

[191] J. R. Conner and S. L. Hoeffner, "A critical review of stabilization/solidification technology," *Crit. Rev. Environ. Sci. Technol.*, vol. 28, no. 4, pp. 397–462, 1998.

[192] D. S. S. Raj, C. Aparna, P. Rekha, V. H. Bindhu, and Y. Anjaneyulu, "Stabilisation and solidification technologies for the remediation of contaminated soils and sediments: An overview," *L. Contam. Reclam.*, vol. 13, no. 1, pp. 23–48, 2005.

[193] M. E. Tittlebaum, R. K. Seals, F. K. Cartledge, and S. Engels, "State of the art on stabilization of hazardous organic liquid wastes and sludges," *Crit. Rev. Environ. Control*, vol. 15, no. 2, pp. 179–211, 1995.

[194] J. R. Conner, *Chemical fixation and solidification of hazardous wastes*. London: Van Nostrand Reinhold, 1990.

[195] R. D. Spence and S. Caijun, *Stabilization and Solidification of Hazardous, Radioactive,and Mixed Wastes*. Washington, D.C: CRC PRESS, 2005.

[196] F. Wang, H. Wang, and A. Al-Tabbaa, "Leachability and heavy metal speciation of 17-year old stabilised/solidified contaminated site soils," *J. Hazard. Mater.*, vol. 278, pp. 144–151, 2014.

[197] M. I. Ojovan, W. E. Lee, and S. N. Kalmykov, "Immobilisation of Radioactive Waste in Bitumen," *An Introd. to Nucl. Waste Immobil.*, pp. 305–318, 2019.

[198] N. Bougharraf, D. Louati, M. Mosbahi, M. J. Rouis, and H. Rigane, "Comparison of the effectiveness of different binders in solidification/stabilization of a contaminated soil," *Arab. J. Geosci.*, vol. 11, no. 13, p. 348, 2018.

[199] G. E. Voglar and D. Leštan, "Efficiency modeling of solidification/stabilization of multi-metal contaminated industrial soil using cement and additives," *J. Hazard. Mater.*, vol. 192, no. 2, pp. 753–762, 2011.

[200] M. U. Okoronkwo, M. Balonis, L. Katz, M. Juenger, and G. Sant, "A thermodynamics-based approach for examining the suitability of cementitious formulations for solidifying and stabilizing coal-combustion wastes," *J. Environ. Manage.*, vol. 217, pp. 278–287, 2018.

[201] J. Bizzozero, "Hydration and dimensional stability of calcium aluminate cement based systems," École Polytechnique Fédérale De Lausanne, 2014.

[202] I. Navarro-Blasco, A. Duran, R. Sirera, J. M. Fernández, and J. I. Alvarez, "Solidification/stabilization of toxic metals in calcium aluminate cement matrices," *J. Hazard. Mater.*, vol. 260, pp. 89–103, 2013.

[203] A. K. Prodjosantoso, Septiani, M. P. Utomo, and K. S. Budiasih, "Hydration of strontium-doped monocalcium aluminate," *Orient. J. Chem.*, vol. 34, no. 1, pp. 444–449, 2018.

[204] H. F. W. Taylor, "Cement chemistry," *Cem. Concr. Compos.*, vol. 20, no. 4, p. 335, 2003.

[205] A. D. Guerrero-Flores, A. Uribe-Salas, G. I. Dávila-Pulido, and J. M. Flores-Álvarez, "Simultaneous removal of calcium and sulfate ions from flotation water of complex sulfides," *Miner. Eng.*, vol. 123, pp. 28–34, 2018.

[206] Q. Y. Y. Chen, M. Tyrer, C. D. D. Hills, X. M. M. Yang, and P. Carey, "Immobilisation of heavy metal in cement-based solidification/stabilisation: A review," *Waste Manag.*, vol. 29, no. 1, pp. 390–403, 2009.

[207] B. Batchelor, "Overview of waste stabilization with cement," *Waste Manag.*, vol. 26, no. 7, pp. 689–

698, 2006.

[208] C. D. Hills, C. J. Sollars, and R. Perry, "A calorimetric and microstructural study of solidified toxic wastes -Part 2: A model for poisoning of OPC hydration," *Waste Manag.*, vol. 14, no. 7, pp. 601–612, 1994.

[209] B. Wu, X. Li, B. Ma, and M. Zhang, "Solidification of Heavy Metals in Ettringite and Its Stability Research," in *Second International Conference on Microstructural-related Durability of Cementitious Composites*, 2012, no. April, pp. 1–9.

[210] B. Guo, K. Sasaki, and T. Hirajima, "Characterization of the intermediate in formation of selenate-substituted ettringite," *Cem. Concr. Res.*, vol. 99, pp. 30–37, 2017.

[211] W. Wang, Y. Shao, H. Hou, and M. Zhou, "Synthesis and thermodynamic properties of arsenate and sulfate-arsenate ettringite structure phases," *PLoS One*, vol. 12, no. 7, p. e0182160, 2017.

[212] A. Vollpracht and W. Brameshuber, "Binding and leaching of trace elements in Portland cement pastes," *Cem. Concr. Res.*, vol. 79, pp. 76–92, 2016.

[213] X. Zhou *et al.*, "Reductive solidification/stabilization of chromate in municipal solid waste incineration fly ash by ascorbic acid and blast furnace slag," *Chemosphere*, vol. 182, pp. 76–84, 2017.

[214] J. D. Ortego, Y. Barroeta, F. K. Cartledge, and H. Akhter, "Leaching Effects on Silicate Polymerization. An FTIR and 29Si NMR Study of Lead and Zinc in Portland Cement," *Environ. Sci. Technol.*, vol. 25, no. 6, pp. 1171–1174, 1991.

[215] P. Purnell, O. J. Francis, and C. L. Page, "Formation of thaumasite in synthetic cement mineral slurries," in *Cement and Concrete Composites*, 2003, vol. 25, no. 8, pp. 857–860.

[216] H. F. W. Taylor, C. Famy, and K. L. Scrivener, "Delayed ettringite formation," *Cement and Concrete Research*, vol. 31, no. 5. pp. 683–693, -2001.

[217] Q. Chen, "Examination of Hydrated and Accelerated Carbonated Cement-Heavy Metal Mixtures," University of Greenwich, 2003.

[218] B. Johannesson and P. Utgenannt, "Microstructural changes caused by carbonation of cement mortar," *Cem. Concr. Res.*, vol. 31, no. 6, pp. 925–931, 2001.

[219] A. C. Garrabrants, F. Sanchez, and D. S. Kosson, "Changes in constituent equilibrium leaching and pore water characteristics of a Portland cement mortar as a result of carbonation," *Waste Manag.*, vol. 24, no. 1, pp. 19–36, 2004.

[220] T. Van Gerven *et al.*, "Effects of progressive carbonation on heavy metal leaching from cement-bound waste," *AIChE J.*, vol. 52, no. 2, pp. 826–837, 2006.

[221] G. Ferrari and R. Pellay, "Lithoidal granular materials," EP1858821, 2007.

[222] P. Scanferla, G. Ferrari, R. Pellay, A. Volpi Ghirardini, G. Zanetto, and G. Libralato, "An innovative stabilization/solidification treatment for contaminated soil remediation: Demonstration project results," *J. Soils Sediments*, vol. 9, no. 3, pp. 229–236, 2009.

[223] P. Scanferla *et al.*, "Remediation of a heavy metals contaminated site with a botanical garden: Monitoring results of the application of an advanced S/S technique," *Chem. Eng. Trans.*, vol. 28, no. February 2012, pp. 235–240, 2012.

[224] G. Ferrari, A. Bravo, T. Cerulli, R. Pellay, and D. Zavan, "Method for treatment of contaminated soils and sediment," EP1914017A3, 2008.

[225] (British Standards Institution) BSI, "UNI EN 1008:2002 - Mixing water for concrete. Specification for sampling, testing and assessing the suitability of water, including water recovered from processes in the concrete industry, as mixing water for concrete." British Standards Institution, London, UK, 2002.

[226] C. Bettiol, L. Stievano, M. Bertelle, F. Delfino, and E. Argese, "Evaluation of microwave-assisted acid

extraction procedures for the determination of metal content and potential bioavailability in sediments," *Appl Geochem*, vol. 23, pp. 1140–1151, 2008.

[227] IRSA-APAT-CNR, "Metodo 3020 -"Determinazione di elementi chimici mediante spettroscopia di emissione con sorgente al plasma (ICP-OES)" [Method 3020 - 'Determination of chemical elements by emission spectroscopy with plasma source (ICP-OES)']," in *Manuali e Linee Guida 29/2003: Metodi analitici per le acque - Volume Primo [Manuals and Guidelines 29/2003: Analytical methods for water - Vol. I]*, 2003.

[228] (British Standards Institution) BSI, "UNI EN 12457-2:2004 - Characterization of waste - Leaching - Compliance test for leaching of granular waste materials and sludges - Part 2: One stage batch test at a liquid to solid ratio of 10 l/kg for materials with particle size below 4 mm." British Standards Institution, London, UK, 2004.

[229] (British Standards Institution) BSI, "UNI EN 12457-4:2004 - Characterization of waste - Leaching - Compliance test for leaching of granular waste materials and sludges - Part 4: One stage batch test at a liquid to solid ratio of 10l/kg for materials with particle size below 10 mm." British Standards Institution, London, UK, 2004.

[230] (British Standards Institution) BSI, "UNI EN 14429:2015 - Characterization of waste - Leaching behaviour test - Influence of pH on leaching with initial acid/base addition." British Standards Institution, London, UK, 2015.

[231] IRSA-APAT-CNR, "Metodo 2060 - 'pH,'" in *Manuali e Linee Guida 29/2003: Metodi analitici per le acque - Volume Primo [Manuals and Guidelines 29/2003: Analytical methods for water - Vol. I]*, 2003.

[232] IRSA-APAT-CNR, "Metodo 5130 - 'Richiesta chimica di ossigeno (COD)' [Method 5130 - 'Chemical Oxygen Demand (COD)']," in *Manuali e Linee Guida 29/2003: Metodi analitici per le acque - Volume Primo [Manuals and Guidelines 29/2003: Analytical methods for water - Vol. I]*, 2003.

[233] (American Society of Testing & Materials) ASTM, "ASTM D7012 - 14 Standard Test Methods for Compressive Strength and Elastic Moduli of Intact Rock Core Specimens under Varying States of Stress and Temperatures." American Society of Testing & Materials, 2014.

[234] (British Standards Institution) BSI, "UNI EN 1097-2:2010 - Tests for mechanical and physical properties of aggregates - Part 2: Methods for the determination of resistance to fragmentation." British Standards Institution, London, UK, 2010.

[235] L. Bonomo *et al.*, "Feasibility studies for the treatment and reuse of contaminated marine sediments," *Environ. Technol.*, vol. 30, no. 8, pp. 817–823, 2009.

[236] G. Ferrari, G. Artioli, and M. Parisatto, "From HPC to HPSS: The use of superplasticizers for the improvement of S/S technology," *S/S Tech - International Solidification/Stabilization Forum*. Cape Breton University, Sydney, Nova Scotia, pp. 193–203, 2010.

[237] B. Nematollahi and J. Sanjayan, "Efficacy of available superplasticizers on geopolymers," *Res. J. Appl. Sci. Eng. Technol.*, vol. 7, no. 7, pp. 1278–1282, 2014.

[238] L. Calgaro *et al.*, "Consecutive thermal and wet conditioning treatments of sedimentary stabilized cementitious materials from HPSS® technology: Effects on leaching and microstructure," *J. Environ. Manage.*, vol. 250, p. 109503, 2019.

[239] (Enviromental Ministry Decree) EMD, *Legislative Decree No 179 of 31st July 2002*. in Italian Official Gazzette n. 189 of 13th August 2002; Enviromental Ministry, IT, 2002.

[240] ICRAM, "Piano di caratterizzazione ambientale dell'area lacuale del sito di bonifica di interesse nazionale 'Laghi di Mantova e polo chimico' [Environmental characterization plan of the lake area of the remediation site of national interest of "Mantova lakes and ," 2007.

[241] ISPRA, "CII-LO-Laghi di Mantova e Polo Chimico-Relazione-01.07 [CII-LO-Mantova Lakes and Chemical Pole - Report-01.07]." 2009.

[242] Q. Zhou and F. P. Glasser, “Thermal stability and decomposition mechanisms of ettringite at <120°C,” *Cem. Concr. Res.*, vol. 31, no. 9, pp. 1333–1339, 2001.

[243] A. E. Lewis, “Review of metal sulphide precipitation,” *Hydrometallurgy*, vol. 104, no. 2, pp. 222–234, 2010.

[244] C. J. Engelsen, H. A. Van Der Sloot, G. Wibetoe, H. Justnes, W. Lund, and E. Stoltenberg-Hansson, “Leaching characterisation and geochemical modelling of minor and trace elements released from recycled concrete aggregates,” *Cem. Concr. Res.*, vol. 40, no. 12, pp. 1639–1649, 2010.

[245] C. J. Engelsen, H. A. van der Sloot, and G. Petkovic, “Long-term leaching from recycled concrete aggregates applied as sub-base material in road construction,” *Sci. Total Environ.*, vol. 587–588, no. 2017, pp. 94–101, 2017.

[246] W. Kurdowski, *Cement and concrete chemistry*, vol. 9789400779. Dordrecht: Springer Netherlands, 2014.

[247] M. L. D. L. D. D. Gougar, B. E. E. Scheetz, and D. M. M. Roy, *Ettringite and C-S-H portland cement phases for waste ion immobilization: A review*, vol. 16, no. 4. 1996, pp. 295–303.

[248] H. He and H. Suito, “Immobilization of Hexavalent Chromium in Aqueous Solution through the Formation of 3CaO (Al,Fe)2O3 Ca(OH)2 xH2O Phase, Ettringite and C-S-H Gel.,” *ISIJ Int.*, vol. 42, no. 2, pp. 139–145, 2008.

[249] Y. Li, X. Min, Y. Ke, J. Fei, D. Liu, and C. Tang, “Immobilization potential and immobilization mechanism of arsenic in cemented paste backfill,” *Miner. Eng.*, vol. 138, pp. 101–107, 2019.

[250] Y. S. Wang, J. G. Dai, L. Wang, D. C. W. Tsang, and C. S. Poon, “Influence of lead on stabilization/solidification by ordinary Portland cement and magnesium phosphate cement,” *Chemosphere*, vol. 190, pp. 90–96, 2018.

[251] L. Wang *et al.*, “Green remediation of As and Pb contaminated soil using cement-free clay-based stabilization/solidification,” *Environ. Int.*, vol. 126, pp. 336–345, 2019.

[252] N. Bakhshi, A. Sarrafi, and A. A. Ramezanianpour, “Immobilization of hexavalent chromium in cement mortar: leaching properties and microstructures,” *Environ. Sci. Pollut. Res.*, vol. 26, no. 20, pp. 20829–20838, 2019.

[253] Y. Su, J. Yang, D. Liu, S. Zhen, N. Lin, and Y. Zhou, “Solidification/stabilization of simulated cadmium-contaminated wastes with magnesium potassium phosphate cement,” *Environ. Eng. Res.*, vol. 21, no. 1, pp. 15–21, 2016.

[254] X. Li, C. He, Y. Bai, B. Ma, G. Wang, and H. Tan, “Stabilization/solidification on chromium (III) wastes by C3A and C3A hydrated matrix,” *J. Hazard. Mater.*, vol. 268, pp. 61–67, 2014.

[255] L. Wang *et al.*, “Low-carbon and low-alkalinity stabilization/solidification of high-Pb contaminated soil,” *Chem. Eng. J.*, vol. 351, pp. 418–427, 2018.

[256] B. Guo, B. Liu, J. Yang, and S. Zhang, *The mechanisms of heavy metal immobilization by cementitious material treatments and thermal treatments: A review*, vol. 193. Academic Press, 2017, pp. 410–422.

[257] Y. Lv, X. Li, G. De Schutter, and B. Ma, “Stabilization of Cr(III) wastes by C3S and C3S hydrated matrix: comparison of two incorporation methods,” *Mater. Struct. Constr.*, vol. 49, no. 8, pp. 3109–3118, 2016.

[258] M. Zhang *et al.*, “Immobilization of Cr(VI) by hydrated Portland cement pastes with and without calcium sulfate,” *J. Hazard. Mater.*, vol. 342, pp. 242–251, 2018.

[259] M. Niu, G. Li, Y. Wang, Q. Li, L. Han, and Z. Song, “Comparative study of immobilization and mechanical properties of sulfoaluminate cement and ordinary Portland cement with different heavy metals,” *Constr. Build. Mater.*, vol. 193, pp. 332–343, 2018.

[260] L. Lu, Y. He, C. Xiang, F. Wang, and S. Hu, “Distribution of heavy metal elements in chromium (III), lead-doped cement pastes,” *Adv. Cem. Res.*, vol. 31, no. 6, pp. 270–278, 2019.

[261] T. H. Ahn, K. B. Shim, K. H. So, and J. S. Ryou, “Influence of lead and chromium ions as toxic heavy metals between AFt and AFm phases based on C3A and C4A3S,” *J. Ceram. Process. Res.*, vol. 15, no. 6, pp. 539–544, 2014.

[262] British Standards Institution, “Tests for geometrical properties of aggregates Part 1: Determination of Particle Size Distribution - Sieving Method,” *Bs En 933-11997*, vol. 3, no. 1, pp. 1–7, 2005.

[263] J. M. Bigham and D. K. Nordstrom, “Iron and Aluminum Hydroxysulfates from Acid Sulfate Waters,” *Rev. Mineral. Geochemistry*, vol. 40, no. 1, pp. 351–403, 2011.

[264] A. Akcil and S. Koldas, “Acid Mine Drainage (AMD): causes, treatment and case studies,” *J. Clean. Prod.*, vol. 14, no. 12-13 SPEC. ISS., pp. 1139–1145, 2006.

[265] R. E. Stoffregen, C. N. Alpers, and J. L. Jambor, “Alunite-Jarosite Crystallography, Thermodynamics, and Geochronology,” *Rev. Mineral. Geochemistry*, vol. 40, no. 1, pp. 453–479, 2011.

[266] J. Aguilar-Carrillo, L. Herrera, E. J. Gutiérrez, and I. A. Reyes-Domínguez, “Solid-phase distribution and mobility of thallium in mining-metallurgical residues: Environmental hazard implications,” *Environ. Pollut.*, vol. 243, pp. 1833–1845, 2018.

[267] C. Yang, Y. Chen, P. Peng, C. Li, X. Chang, and Y. Wu, “Trace element transformations and partitioning during the roasting of pyrite ores in the sulfuric acid industry,” *J. Hazard. Mater.*, vol. 167, no. 1–3, pp. 835–845, 2009.

[268] P. M. Dove and C. A. Czank, “Crystal chemical controls on the dissolution kinetics of the isostructural sulfates: Celestite, anglesite, and barite,” *Geochim. Cosmochim. Acta*, vol. 59, no. 10, pp. 1907–1915, 1995.

[269] F. M. Lea, *Lea’s Chemistry of Cement and Concrete*, Fourth Edi., vol. 58, no. 10. Elsevier, 2004.

[270] K. B. Krauskopf, “Dissolution and precipitation of silica at low temperatures,” *Geochim. Cosmochim. Acta*, vol. 10, no. 1–2, pp. 1–26, 1956.

[271] T. H. Ahna, K. B. Shima, and K. H. Shob, “Influence of lead, chromium and zinc ions as toxic heavy metals between C-S-H phases based on C3S,” *J. Ceram. Process. Res.*, vol. 16, no. 6, pp. s40–s44, 2015.

[272] D. Zhang, Z. Cao, T. Zhang, and X. Su, “Effect of carbonation on leaching behavior, engineering properties and microstructure of cement-stabilized lead-contaminated soils,” *Environ. Earth Sci.*, vol. 76, no. 21, p. 724, 2017.

[273] B. Pandey, S. D. Kinrade, and L. J. J. Catalan, “Effects of carbonation on the leachability and compressive strength of cement-solidified and geopolymer-solidified synthetic metal wastes,” *J. Environ. Manage.*, vol. 101, pp. 59–67, 2012.

[274] F. Liu, X. Qiao, L. Zhou, and J. Zhang, “Migration and Fate of Acid Mine Drainage Pollutants in Calcareous Soil,” *Int. J. Environ. Res. Public Health*, vol. 15, no. 8, p. 1759, 2018.

[275] Y. Dong, F. Liu, X. Qiao, L. Zhou, and W. Bi, “Effects of Acid Mine Drainage on Calcareous Soil Characteristics and Lolium perenne L. Germination,” *Int. J. Environ. Res. Public Health*, vol. 15, no. 12, p. 2742, 2018.

[276] K. K. Kefeni, T. A. M. Msagati, and B. B. Mamba, “Acid mine drainage: Prevention, treatment options, and resource recovery: A review,” *Journal of Cleaner Production*, vol. 151. pp. 475–493, -2017.

[277] V. Thiéry, V. Trincal, and C. A. Davy, “The elusive ettringite under the high-vacuum SEM – a reflection based on natural samples, the use of Monte Carlo modelling of EDS analyses and an extension to the ettringite group minerals,” *J. Microsc.*, vol. 268, no. 1, pp. 84–93, 2017.

[278] A. Duran, R. Sirera, M. Pérez-Nicolás, I. Navarro-Blasco, J. M. Fernández, and J. I. Alvarez, "Study of the early hydration of calcium aluminates in the presence of different metallic salts," *Cem. Concr. Res.*, vol. 81, pp. 1–15, 2016.

[279] J. M. Fernández, I. Navarro-Blasco, A. Duran, R. Sirera, and J. I. Alvarez, "Treatment of toxic metal aqueous solutions: Encapsulation in a phosphate-calcium aluminate matrix," *J. Environ. Manage.*, vol. 140, pp. 1–13, 2014.

[280] G. E. Voglar and D. Leštan, "Equilibrium leaching of toxic elements from cement stabilized soil," *J. Hazard. Mater.*, vol. 246–247, pp. 18–25, 2013.

[281] C. Shi, G. Zhang, T. He, and Y. Li, "Effects of superplasticizers on the stability and morphology of ettringite," *Constr. Build. Mater.*, vol. 112, pp. 261–266, 2016.

[282] Z. Wang, C. Guo, Y. Song, B. Wang, and H. Xu, "Stability of thaumasite and ettringite," *Kuei Suan Jen Hsueh Pao/Journal Chinese Ceram. Soc.*, vol. 44, no. 2, pp. 292–298, 2016.

[283] M. Balonis, "Thermodynamic modelling of temperature effects on the mineralogy of Portland cement systems containing chloride," *Cem. Concr. Res.*, vol. 120, pp. 66–76, 2019.

[284] J. Plank, M. Zhang-Preße, N. P. Ivleva, and R. Niessner, "Stability of single phase C3A hydrates against pressurized CO2," *Constr. Build. Mater.*, vol. 122, pp. 426–434, 2016.

[285] K. Wieczorek-Ciurowa, K. Fela, and A. J. Kozak, "Chromium(III)-ettringite formation and its thermal stability," in *Journal of Thermal Analysis and Calorimetry*, 2001, vol. 65, no. 2, pp. 655–660.

[286] M. Palou, J. Majling, M. Drábik, and A. Ayadi, "Ettringite & its chromate analogue, structure and thermal stability," in *Solid State Phenomena*, 2003, vol. 90–91, pp. 395–400.

[287] P. Lopez-Arce and E. Doehne, "Kinetics of sodium sulfate efflorescence as observed by humidity cycling with ESEM," in *Heritage, Weathering & Conservation Conference*, 2006.

[288] L. Valentini, "Modeling Dissolution–Precipitation Kinetics of Alkali-Activated Metakaolin," *ACS Omega*, vol. 3, no. 12, pp. 18100–18108, 2018.

[289] P. Wang, Q. Xue, J. S. Li, and T. T. Zhang, "Effects of pH on leaching behavior of compacted cement solidified/stabilized lead contaminated soil," *Environ. Prog. Sustain. Energy*, vol. 35, no. 1, pp. 149–155, 2016.

[290] Soil Science Division Staff., "Soil Chemical Properties," in *Soil survey manual, United States Department of Agriculture (USDA) Handbook 18.*, C. Ditzler, K. Scheffe, and H. C. Monger, Eds. Washington, D.C.: Government Printing Office, 2017.

[291] S. Contessi *et al.*, "Stabilization of lead contaminated soil with traditional and alternative binders," *J. Hazard. Mater.*, vol. 382, p. 120990, 2020.

[292] L. K. Davidson, T. Demirel, and R. L. Handy, "Soil Pulverization and Lime Migration Soil-Lime Stabilization," *Highw. Res. Board*, vol. 92, no. 92, pp. 103–126, 1965.

[293] N. Ukrainczyk, N. Vrbos, and J. Sipusic, "Influence of metal chloride salts on calcium aluminate cement hydration," *Adv. Cem. Res.*, vol. 24, no. 5, pp. 249–262, 2012.

[294] G. Salihoglu, "Immobilization of antimony waste slag by applying geopolymerization and stabilization/solidification technologies," *J. Air Waste Manag. Assoc.*, vol. 64, no. 11, pp. 1288–1298, 2014.

[295] K. M. Patel and C. P. Devatha, "Investigation on leaching behaviour of toxic metals from biomedical ash and its controlling mechanism," *Environ. Sci. Pollut. Res.*, vol. 26, no. 6, pp. 6191–6198, 2019.

[296] M. Chrysochoou and D. Dermatas, "Evaluation of ettringite and hydrocalumite formation for heavy metal immobilization: Literature review and experimental study," *J. Hazard. Mater.*, vol. 136, no. 1 SPEC. ISS., pp. 20–33, 2006.

[297] K. Moussaceb, A. Ait-Mokhtar, and D. Merabet, “Influence of leaching conditions on the release kinetics of lead, chromium and nickel from solidified/stabilized cementitious materials,” *Environ. Technol. (United Kingdom)*, vol. 33, no. 24, pp. 2681–2690, 2012.

[298] M. Leist, R. J. Casey, and D. Caridi, “The fixation and leaching of cement stabilized arsenic,” *Waste Manag.*, vol. 23, no. 4, pp. 353–359, 2003.

[299] J. A. Connor and T. E. McHugh, *Impact of risk-based corrective action (RBCA) on state LUST corrective action programs*, vol. 8, no. 3. 2002, pp. 573–589.

[300] (American Society of Testing & Materials) ASTM, “ASTM E2081-00(2015), Standard Guide for Risk-Based Corrective Action.” American Society of Testing & Materials, 2015.

[301] M. M. (Mustafa M. . Aral, *Environmental modeling and health risk analysis (ACTS/RISK)*. Springer, 2010.

[302] H. Cheng and Y. Hu, *Lead (Pb) isotopic fingerprinting and its applications in lead pollution studies in China: A review*, vol. 158, no. 5. Elsevier Ltd, 2010, pp. 1134–1146.

[303] N. Nanos and J. A. Rodríguez Martín, “Multiscale analysis of heavy metal contents in soils: Spatial variability in the Duero river basin (Spain),” *Geoderma*, vol. 189–190, pp. 554–562, 2012.

[304] A. Khalil, L. Hanich, R. Hakkou, and M. Lepage, “GIS-based environmental database for assessing the mine pollution: A case study of an abandoned mine site in Morocco,” *J. Geochemical Explor.*, vol. 144, pp. 468–477, 2014.

[305] I. Guagliardi, D. Cicchella, R. De Rosa, and G. Buttafuoco, “Assessment of lead pollution in topsoils of a southern Italy area: Analysis of urban and peri-urban environment,” *J. Environ. Sci.*, vol. 33, pp. 179–187, 2015.

[306] C. Micó, L. Recatalá, M. Peris, and J. Sánchez, “Assessing heavy metal sources in agricultural soils of an European Mediterranean area by multivariate analysis,” *Chemosphere*, vol. 65, no. 5, pp. 863–872, 2006.

[307] J. Martínez, J. F. Llamas, E. de Miguel, J. Rey, and M. C. Hidalgo, “Soil contamination from urban and industrial activity: example of the mining district of Linares (southern Spain),” *Environ. Geol.*, vol. 54, no. 4, pp. 669–677, . 2008.

[308] A. Franco-Uría, C. López-Mateo, E. Roca, and M. L. Fernández-Marcos, “Source identification of heavy metals in pastureland by multivariate analysis in NW Spain,” *J. Hazard. Mater.*, vol. 165, no. 1–3, pp. 1008–1015, 2009.

[309] N. Walraven *et al.*, “The lead (Pb) isotope signature, behaviour and fate of traffic-related lead pollution in roadside soils in The Netherlands,” *Sci. Total Environ.*, vol. 472, pp. 888–900, 2014.

[310] M. Kayhanian, “Trend and concentrations of legacy lead (Pb) in highway runoff,” *Environ. Pollut.*, vol. 160, no. 1, pp. 169–177, 2012.

[311] J. Sun, R. Yu, G. Hu, G. Su, and Y. Zhang, “Tracing of heavy metal sources and mobility in a soil depth profile via isotopic variation of Pb and Sr,” *Catena*, vol. 171, no. July, pp. 440–449, 2018.

[312] H. Kong, Y. Teng, L. Song, J. Wang, and L. Zhang, “Lead and strontium isotopes as tracers to investigate the potential sources of lead in soil and groundwater: A case study of the Hun River alluvial fan,” *Appl. Geochemistry*, vol. 97, no. October 2017, pp. 291–300, 2018.

[313] J. Longman, D. Veres, V. Ersek, D. L. Phillips, C. Chauvel, and C. G. Tamas, “Quantitative assessment of Pb sources in isotopic mixtures using a Bayesian mixing model,” *Sci. Rep.*, vol. 8, no. 1, pp. 1–16, 2018.

[314] P. Álvarez-Iglesias, B. Rubio, and J. Millos, “Isotopic identification of natural vs. anthropogenic lead sources in marine sediments from the inner Ría de Vigo (NW Spain),” *Sci. Total Environ.*, vol. 437, pp. 22–35, 2012.

[315] F. Trifirò, “Il contributo della chimica contro la fame nel mondo -Innovazioni nel gas di sintesi e nei fertilizzanti azotati.,” *La chimica e l’industria*, 2007.

[316] C. Gallon, A. Tessier, C. Gobeil, and L. Beaudin, “Sources and chronology of atmospheric lead deposition to a Canadian Shield lake: Inferences from Pb isotopes and PAH profiles,” *Geochim. Cosmochim. Acta*, 2005.

[317] T. Hosono, K. Alvarez, and M. Kuwae, “Lead isotope ratios in six lake sediment cores from Japan Archipelago: Historical record of trans-boundary pollution sources,” *Sci. Total Environ.*, 2016.

[318] K. J. R. Rosman and P. D. P. Taylor, “Isotopic compositions of the elements 1997 (Technical Report),” *Pure Appl. Chem.*, vol. 70, no. 1, pp. 217–235, 1998.

[319] Y. M. Alyazichi, B. G. Jones, and E. McLean, *Lead isotope fingerprinting used as a tracer of lead pollution in marine sediments from Botany Bay and Port Hacking estuaries, southern Sydney, Australia*, vol. 7. 2016, pp. 136–141.

[320] M. Barbaste *et al.*, “Evaluation of the accuracy of the determination of lead isotope ratios in wine by ICP MS using quadrupole, multicollector magnetic sector and time-of-flight analyzers,” *Talanta*, vol. 54, no. 2, pp. 307–317, 2001.

[321] G. Naidu, S. Ryu, R. Thiruvenkatachari, Y. Choi, S. Jeong, and S. Vigneswaran, “A critical review on remediation, reuse, and resource recovery from acid mine drainage,” *Environmental Pollution*, vol. 247. pp. 1110–1124, -2019.

[322] T. Valente *et al.*, “Characterization of water reservoirs affected by acid mine drainage: geochemical, mineralogical, and biological (diatoms) properties of the water,” *Environ. Sci. Pollut. Res.*, vol. 23, no. 7, pp. 6002–6011, 2016.

[323] S. W. Yun *et al.*, “Analysis of metal(loid)s contamination and their continuous input in soils around a zinc smelter: Development of methodology and a case study in South Korea,” *Environ. Pollut.*, vol. 238, pp. 140–149, 2018.

[324] A. Eichler, G. Gramlich, T. Kellerhals, L. Tobler, and M. Schwikowski, “Pb pollution from leaded gasoline in South America in the context of a 2000-year metallurgical history,” *Sci. Adv.*, vol. 1, no. 2, p. e1400196, 2015.

[325] F. J. Peryea and T. L. Creger, “Vertical distribution of lead and arsenic in soils contaminated with lead arsenate pesticide residues,” *Water, Air, Soil Pollut.*, vol. 78, no. 3–4, pp. 297–306, 1994.

[326] S. Goix *et al.*, “Field isotopic study of lead fate and compartmentalization in earthworm–soil–metal particle systems for highly polluted soil near Pb recycling factory,” *Chemosphere*, vol. 138, pp. 10–17, 2015.

[327] G. Tóth, T. Hermann, G. Szatmári, and L. Pásztor, “Maps of heavy metals in the soils of the European Union and proposed priority areas for detailed assessment,” *Sci. Total Environ.*, vol. 565, pp. 1054–1062, 2016.

[328] Z. He *et al.*, “Electrochemically created roughened lead plate for electrochemical reduction of aqueous CO2,” *Catal. Commun.*, vol. 72, pp. 38–42, 2015.

[329] L. Palumbo, “Sediment Management of Nations in Europe,” *Sustain. Manag. Sediment Resour.*, vol. 2, pp. 11–58, 2007.

[330] J. Herin, “Eawag: Swiss Federal Institute of Aquatic Science and Technology - Annual Report 2008,” 2008.

[331] M. J. Rogoff and F. Screve, *Waste-to-Energy: Technologies and Project Implementation*. William Andrew, 2012.

[332] G. Dermont, M. Bergeron, G. Mercier, and M. Richer-Laflèche, *Soil washing for metal removal: A review of physical/chemical technologies and field applications*, vol. 152, no. 1. 2008, pp. 1–31.

[333] I. K. (Iskandar K. Iskandar, *Environmental Restoration of Metals-Contaminated Soils*. Lewis Publishers, 2010.

[334] A. Tessier, P. G. C. C. Campbell, and M. Bisson, "Sequential Extraction Procedure for the Speciation of Particulate Trace Metals," *Anal. Chem.*, vol. 51, no. 7, pp. 844–851, 1973.

[335] X. D. Li *et al.*, *Heavy metal speciation and leaching behaviors in cement based solidified/stabilized waste materials*. 2001.

[336] R. W. Peters, *Chelant extraction of heavy metals from contaminated soils*, vol. 66, no. 1–2. 1999, pp. 151–210.

[337] H. A. Elliott and N. L. Shastri, "Extractive decontamination of metal polluted soils using oxalate," *Water, Air, Soil Pollut.*, vol. 110, pp. 335–346, 1999.

[338] S. A. Wasay, W. J. Parker, and P. J. Van Geel, "Contamination of a calcareous soil by battery industry wastes. II. Treatment," *Can. J. Civ. Eng.*, vol. 28, pp. 349–354, 2001.

[339] R. S. Tejowulan and W. H. Hendershot, "Removal of trace metals from contaminated soils using EDTA-incorporating resin trapping techniques," *Environ. Pollut.*, vol. 103, no. 1, pp. 135–142, 1998.

[340] S. Tampouris, N. Papassiopi, and I. Paspaliaris, "Removal of contaminant metals from fine grained soils, using agglomeration, chloride solutions and pile leaching techniques," *J. Hazard. Mater.*, vol. 84, pp. 297–319, 2001.

[341] T. K. Gupta, C. K.; Mukherjee, *Hydrometallurgy in Extraction Processes, Volume I*. Boca Raton, FL: CRC Press, 1990.

[342] S. Kuo, M. S. Lai, and C. W. Lin, "Influence of solution acidity and CaCl2 concentration on the removal of heavy metals from metal-contaminated rice soils," *Environ. Pollut.*, vol. 144, pp. 918–925, 2006.

[343] M. Isoyama and S. I. Wada, "Remediation of Pb-contaminated soils bywashing with hydrochloric acid and subsequent immobilization with calcite and allophanic soil," *J. Hazard. Mater.*, vol. 143, pp. 636–642, 2007.

[344] I. Ko, Y. Y. Chang, C. H. Lee, and K. W. Kim, "Assessment of pilot-scale acid washing of soil contaminated with As, Zn and Ni using theBCRthree-step sequential extraction," *J. Hazard. Mater.*, vol. 127, pp. 1–13, 2005.

[345] N. Reynier, J. F. Blais, G. Mercier, and S. Besner, "Treatment of arsenic-,chromium-, copper-and pentachlorophenol-polluted soil using flotation," *Water, Air, Soil Pollut.*, vol. 224, pp. 1–12, 2013.

[346] K. Elgh-Dalgren *et al.*, "Laboratory and pilot scale soilwashing of PAH and arsenic from a wood preservation site: changes in concentration and toxicity," *J. Hazard. Mater.*, vol. 172, pp. 1033–1040, 2009.

[347] M. Jang, J. S. Hwang, and S. Il Choi, "Sequential soil washing techniques using hydrochloric acid and sodium hydroxide for remediating arsenic-contaminated soils in abandoned iron-ore mines," *Chemosphere*, vol. 66, no. 1, pp. 8–17, 2007.

[348] C. N. Neale, R. Bricka, and A. C. Chao, "Evaluating acids and chelating agents forremoving heavy metals from contaminated soils," *Environ. Prog.*, vol. 16, pp. 274–280, 1997.

[349] S. McGrath and J. Cegarra, "Chemical extractability of heavy metals during andafter long-term applications of sewage sludge to soil," *J. Soil Sci.*, vol. 43, pp. 313–321, 1992.

[350] R. J. Abumaizar and E. H. Smith, "Heavy metal contaminants removal by soil washing," *J. Hazard. Mater.*, no. B70, pp. 71–86, 1999.

[351] L. Di Palma and R. Mecozzi, "Heavy metals mobilization from harbour sediments using EDTA and citric acid as chelating agents," *J. Hazard. Mater.*, vol. 147, no. 3, pp. 768–775, 2007.

[352] T. T. Lim, P. C. Chui, and K. H. Goh, "Process evaluation for optimization of EDTA use and recovery

for heavy metal removal from a contaminated soil," *Chemosphere*, vol. 58, pp. 1031–1040, 2005.

[353] T. Nedwed and D. A. Clifford, "Feasibility of extracting lead from lead battery recycling site soil using high-concentration chloride solutions," *Environ. Prog.*, vol. 19, pp. 197–206, 2000.

[354] N. Meunier, P. Drogui, C. Montane, R. Hausler, J. F. Blais, and G. Mercier, "Heavy metals removal from acidic and saline soil leachate using either electrochemical coagulation or chemical precipitation," *J. Environ. Eng.*, vol. 132, pp. 545–554, 2006.

[355] A. G. Fane, R. Wang, and Y. Jia, "Membrane Technology: Past, Present and Future," in *Membrane and Desalination Technologies*, Totowa, NJ: Humana Press, 2010, pp. 1–45.

[356] H. K. Lonsdale, "The growth of membrane technology," *Journal of Membrane Science*, vol. 10, no. 2–3. pp. 81–181, -1982.

[357] W. S. Winston Ho and K. K. Sirkar, *Membrane Handbook Volume I*. New York: Van Nostrand Reinhold, 2001.

[358] P. Meares, "Membrane science and technology. Edited by Y. Osada and T. Nakagawa'. Marcel Dekker Inc., New York, 1992. pp. vii + 467, price US$ 165.00. ISBN 0-8247-8694-7," *Polym. Int.*, vol. 33, no. 4, pp. 440–440, 1994.

[359] H. Strathmann, *Ion-Exchange Membrane Separation Processes*, no. 1. Elsevier, 2004.

[360] H. Strathmann, "Introduction to Membrane Technology," in *An Introduction to Membrane and Science Technology*, Institute on Membrane Technology, Ed. CNR - Consigli Nazionale delle Ricerche, 2012, pp. 3–13.

[361] A. G. Fane and C. J. D. Fell, "A review of fouling and fouling control in ultrafiltration," *Desalin.*, vol. 62, pp. 117–136, 1987.

[362] X. Wei, R. Wang, and A. G. Fane, "Development of a novel electrophoresis-UV grafting method to modify PES UF membranes used for NOM removal," *J. Memb. Sci.*, vol. 273, pp. 47–57, 2006.

[363] J. Ren and R. Wang, "Preparation of Polymeric Membranes," in *Membrane and Desalination Technologies*, Totowa, NJ: Humana Press, 2011, pp. 47–100.

[364] W. J. Conlon, "Pilot field test data for prototype ultra low pressure reverse osmosis elements," *Desalination*, vol. 56, pp. 203–226, 1985.

[365] M. Kurihara, T. Uemura, Y. Nakagawa, and T. Tonomura, "The thin-film composite low-pressure reverse osmosis membranes," *Desalination*, vol. 54, pp. 75–88, 1985.

[366] R. Rautenbach and A. Gröschl, "Separation potential of nanofiltration membranes," *Desalination*, vol. 77, no. C, pp. 73–84, 1990.

[367] E. J. Son, E. K. Choe, and J. W. Kim, "Nanofiltration membrane technology for caustic soda recovery," *Text. Chem. Color. Am. Dyest. Report.*, vol. 32, no. 3, pp. 46–52, 2000.

[368] Y. Zhang, S. Shao, W. Yu, F. Yang, and X. Xu, "Study on Recycling Alkali from the Wastewater of Textile Mercerization Process by Nanofiltration," *IERI Procedia*, vol. 9, pp. 71–76, 2014.

[369] A. Arkell, H. Krawczyk, J. Thuvander, and A.-S. S. Jönsson, "Evaluation of membrane performance and cost estimates during recovery of sodium hydroxide in a hemicellulose extraction process by nanofiltration," *Sep. Purif. Technol.*, vol. 118, pp. 387–393, 2013.

[370] E. K. Choe, E. J. Son, B. S. Lee, S. H. Jeong, H. C. Shin, and J. S. Choi, "NF process for the recovery of caustic soda and concentration of disodium terephthalate from alkaline wastewater from polyester fabrics," *Desalination*, vol. 186, no. 1–3, pp. 29–37, 2005.

[371] L. Zhao and W. Xia, "Stainless steel membrane UF coupled with NF process for the recovery of sodium hydroxide from alkaline wastewater in chitin processing," *Desalination*, vol. 249, no. 2, pp. 774–780, 2009.

[372] S. Novalic, A. Dabrowski, and K. D. Kulbe, “Nanofiltration of caustic and acidic cleaning solutions with high COD part 1. Recycling of sodium hydroxide,” *J. Food Eng.*, vol. 38, no. 2, pp. 125–132, 1998.

[373] M. Mulder, *Basic Principles of Membrane Technology*. Dordrecht: Springer Netherlands, 1996.

[374] L. M. Ortega, R. Lebrun, J.-F. F. Blais, R. Hausler, and P. Drogui, “Effectiveness of soil washing, nanofiltration and electrochemical treatment for the recovery of metal ions coming from a contaminated soil,” *Water Res.*, vol. 42, no. 8–9, pp. 1943–1952, 2008.

[375] L. M. Ortega, R. Lebrun, J. F. Blais, and R. Hausler, “Treatment of an acidic leachate containing metal ions by nanofiltration membranes,” *Sep. Purif. Technol.*, vol. 54, no. 3, pp. 306–314, 2007.

[376] K. Volchek, D. Velicogna, A. Obenauf, A. Somers, B. Wong, and A. Y. Tremblay, “Novel applications of membrane processes in soil cleanup operations,” *Desalination*, vol. 147, no. 1–3, pp. 123–126, Sep. 2002.

[377] J. López, M. Reig, O. Gibert, and J. L. Cortina, “Recovery of sulphuric acid and added value metals (Zn, Cu and rare earths) from acidic mine waters using nanofiltration membranes,” *Sep. Purif. Technol.*, vol. 212, pp. 180–190, . 2019.

[378] Y. Ku and I. L. Jung, “Photocatalytic reduction of Cr(VI) in aqueous solutions by UV irradiation with the presence of titanium dioxide,” *Water Res.*, vol. 35, pp. 135–142, 2001.

[379] J. L. Huisman, G. Schouten, and C. Schultz, “Biologically produced sulphide for purification of process streams, effluent treatment and recovery of metals in the metal and mining industry,” *Hydrometallurgy*, vol. 83, pp. 106–113, 2006.

[380] K. A. Baltpurvins, R. C. Burns, G. A. Lawrance, and A. D. Stuart, “Effect of electrolyte composition on zinc hydroxide precipitation by lime,” *Water Res.*, vol. 31, pp. 973–980, 1997.

[381] L. Charerntanyarak, “Heavy metals removal by chemical coagulation and precipitation,” *Wat. Sci. Technol.*, vol. 39, pp. 135–138, 1999.

[382] M. M. Matlock, K. R. Henke, and D. A. Atwood, “Effectiveness of commercial reagents for heavy metal removal from water with new insights for future chelate designs,” *J. Hazard. Mater.*, vol. 92, no. 2, pp. 129–142, 2002.

[383] N. Kongsricharoern and C. Polprasert, “Electrochemical precipitation of chromium (Cr6+) from an electroplating wastewater,” *Wat. Sci. Technol.*, vol. 31, pp. 109–117, 1995.

[384] F. Fu and Q. Wang, *Removal of heavy metal ions from wastewaters: A review*, vol. 92, no. 3. Elsevier Ltd, 2011, pp. 407–418.

[385] D. Bhattacharyya, A. B. Jumawan, and R. B. Grieves, “Separation of Toxic Heavy Metals by Sulfide Precipitation,” *Sep. Sci. Technol.*, vol. 14, no. 5, pp. 441–452, 1979.

[386] A. Özverdi and M. Erdem, “Cu2+, Cd2+ and Pb2+ adsorption from aqueous solutions by pyrite and synthetic iron sulphide,” *J. Hazard. Mater.*, vol. 137, pp. 626–632, 2006.

[387] P. Ghosh, A. N. Samanta, and S. Ray, “Reduction of COD and removal of Zn2þ from rayon industry wastewater by combined electro-Fenton treatment and chemical precipitation,” *Desalination*, vol. 266, no. 1–3, pp. 213–217, 2011.

[388] A. Papadopoulos, D. Fatta, K. Parperis, A. Mentzis, K. J. Haralambous, and M. Loizidou, “Nickel uptake from a wastewater stream produced in a metal finishing industry by combination of ion-exchange and precipitation methods,” *Sep. Purif. Technol.*, vol. 39, pp. 181–188, 2004.

[389] L. K. Wang, *Handbook of Advanced Industrial and Hazardous Wastes Management*. CRC Press, 2017.

[390] M. J. González-Muñoz, M. A. Rodríguez, S. Luque, J. R. Álvarez, S. Luquea, and J. R. Álvareza, “Recovery of heavy metals from metal industry waste waters by chemical precipitation and

nanofiltration," *Desalination*, vol. 200, no. 1–3, pp. 742–744, 2006.

[391] M. M. Matlock, B. S. Howerton, and D. A. Atwood, "Chemical precipitation of heavy metals from acid mine drainage," *Water Res.*, vol. 36, pp. 4757–4764, 2002.

[392] F. L. Fu, R. M. Chen, and Y. Xiong, "Application of a novel strategydcoordination polymerization precipitation to the treatment of Cu2+-containing wastewaters," *Sep. Purif. Technol.*, vol. 52, pp. 388–393, 2006.

[393] F. L. Fu, H. Y. Zeng, Q. H. Cai, R. L. Qiu, J. Yu, and Y. Xiong, "Effective removal of coordinated copper from wastewater using a new dithiocarbamate-type supramolecular heavy metal precipitant," *Chemosphere*, vol. 69, pp. 1783–1789, 2007.

[394] Y. K. Chang, J. E. Chang, T. T. Lin, and Y. M. Hsu, "Integrated copper-containing wastewater treatment using xanthate process," *J. Hazard. Mater.*, vol. 94, pp. 89–99, 2002.

[395] Q. Chang, M. Zhang, and J. X. Wang, "Removal of Cu2+ and turbidity from wastewater by mercaptoacetyl chitosan," *J. Hazard. Mater.*, vol. 169, pp. 621–625, 2009.

[396] Q. Yang, Z. Li, X. Lu, Q. Duan, L. Huang, and J. Bi, *A review of soil heavy metal pollution from industrial and agricultural regions in China: Pollution and risk assessment*, vol. 642. Elsevier B.V., 2018, pp. 690–700.

[397] S. Y. Bratskaya, A. V. Pestov, Y. G. Yatluk, and V. A. Avramenko, "Heavy metals removal by flocculation/precipitation using N-(2-carboxyethyl)chitosans," *Colloids Surfaces A Physicochem. Eng. Asp.*, vol. 339, no. 1–3, pp. 140–144, 2009.

[398] Q. Chang and G. Wang, "Study on the macromolecular coagulant PEX which traps heavy metals," *Chem. Eng. Sci.*, vol. 62, pp. 4636–4643, 2007.

[399] T. A. Kurniawan, G. Y. S. Chan, W. H. Lo, and S. Babel, "Physicoechemical treatment techniques for wastewater laden with heavy metals," *Chem. Eng. J.*, vol. 118, pp. 83–98, 2006.

[400] H. Mikulčić, J. J. Klemeš, M. Vujanović, K. Urbaniec, and N. Duić, "Reducing greenhouse gasses emissions by fostering the deployment of alternative raw materials and energy sources in the cleaner cement manufacturing process," *J. Clean. Prod.*, vol. 136, pp. 119–132, 2016.

[401] A. M. M. Al Bakri, O. A. Abdulkareem, A. R. Rafiza, Y. Zarina, M. N. Norazian, and H. Kamarudin, "Review on Processing of Low Calcium Fly Ash Geopolymer ," *Concrete*, vol. 7, pp. 342–349, 2013.

[402] J. Davidovits, *Geopolymer Chemistry and Applications*, 4th ed. Saint-Quentin, France: Institut Géopolymère, 2015.

[403] J. L. Provis and J. S. J. van Deventer, *Geopolymers - Structures, Processing, Properties and Industrial Applications*, 1st Editio. Cambridge - UK: Woodhead Publishing, 2009.

[404] J. Davidovits, *Geopolymer chemistry and sustainable development*. 2005.

[405] B. Nematollahi, J. Sanjayan, and F. U. A. Shaikh, "Synthesis of heat and ambient cured one-part geopolymer mixes with different grades of sodium silicate," *Ceram. Int.*, vol. 41, no. 4, pp. 5696–5704, 2015.

[406] T. Luukkonen, Z. Abdollahnejad, J. Yliniemi, P. Kinnunen, and M. Illikainen, "One-part alkali-activated materials: A review," *Cement and Concrete Research*, vol. 103. pp. 21–34, Jan-2018.

[407] D. Koloušek, J. Brus, M. Urbanova, J. Andertova, V. Hulinsky, and J. Vorel, "Preparation, structure and hydrothermal stability of alternative (sodium silicate-free) geopolymers," *J. Mater. Sci.*, vol. 42, no. 22, pp. 9267–9275, 2007.

[408] K.-H. K.-H. Yang, J.-K. J.-K. Song, A. F. Ashour, and E.-T. E.-T. Lee, "Properties of cementless mortars activated by sodium silicate," *Constr. Build. Mater.*, vol. 22, no. 9, pp. 1981–1989, 2008.

[409] J. G. S. G. S. Van Jaarsveld, J. S. J. S. J. van Deventer, and L. Lorenzen, "Potential use of geopolymeric

materials to immobilize toxic metals: Part I. Theory and applications," *Miner. Eng.*, vol. 10, no. 7, pp. 659–669, 1997.

[410] C. Shi and A. Fernández-Jiménez, "Stabilization/solidification of hazardous and radioactive wastes with alkali-activated cements," *J. Hazard. Mater.*, vol. 137, pp. 1656–1663, 2006.

[411] J. W. Phair, J. S. J. Van Deventer, and J. D. Smith, " Effect of Al source and alkali activation on Pb and Cu immobilization in fly-ash based 'geopolymer,'" *Appl. Geochemistry*, vol. 19, pp. 423–434, 2004.

[412] T. Hanzlíček and M. Steinerová-Vondráková, "Immobilization of toxic metals insolidified systems of siloxo-sial networks," *J. Am. Ceram. Soc.*, vol. 89, pp. 968–970, 2006.

[413] L. Di Palma and P. Ferrantelli, "Copper leaching from a sandy soil: mechanism and parameters affecting EDTA extraction," *J. Hazard. Mater.*, vol. B122, pp. 85–90, 2005.

[414] B. Sun, F. J. Zhao, E. Lombi, and S. P. Mcgrath, *Leaching of heavy metals from contaminated soils using EDTA*, vol. 113. 2001, pp. 111–120.

[415] T. Spanos, A. Ene, and I. B. Karadjova, "Assessment of toxic elements Cu, Cr, Ni, Pb, Cd, Hg, Zn, As and hexavalent chromium in sewage sludge from municipal wastewater treatment plants by combined spectroscopic techniques," *Rom. J. Phys.*, vol. 60, no. 1–2, pp. 237–245, 2015.

[416] K. K. Shamuyarira and J. R. Gumbo, "Assessment of heavy metals in municipal sewage sludge: A case study of Limpopo Province, South Africa," *Int. J. Environ. Res. Public Health*, vol. 11, no. 3, pp. 2569–2579, 2014.

[417] G. Rossini and A. M. Bernardes, "Galvanic sludge metals recovery by pyrometallurgical and hydrometallurgical treatment," *J. Hazard. Mater.*, vol. 131, no. 1–3, pp. 210–216, 2006.

[418] S. K. Verma, S. S. Bhadauria, and S. Akhtar, "Evaluating effect of chloride attack and concrete cover on the probability of corrosion ," *Front. Struct. Civ. Eng.*, vol. 7, p. 379, 2013.

[419] S. Setoodeh Jahromy, C. Jordan, M. Azam, A. Werner, M. Harasek, and F. Winter, "Fly Ash from Municipal Solid Waste Incineration as a Potential Thermochemical Energy Storage Material," *Energy and Fuels*, vol. 33, no. 7, pp. 5810–5819, 2019.

[420] A. Asadzadeh, M. K. Maleki-Kaklar, N. Soiltanalinejad, and F. Shabani, "Central Composite Design Optimization of Zinc Removal from Contaminated Soil, Using Citric Acid as Biodegradable Chelant," *Sci. Rep.*, vol. 8, p. 2633, 2018.

[421] M. J. Quina *et al.*, "Technologies for the management of MSW incineration ashes from gas cleaning: New perspectives on recovery of secondary raw materials and circular economy," *Science of the Total Environment*, vol. 635. pp. 526–542, Sep-2018.

[422] R. P. Singh, Y. D. Yeboah, E. R. Pambid, and P. Debayle, "Stability Constant of the Calcium-Citrate(3-) Ion Pair Complex," *J. Chem. Eng. Data*, vol. 36, no. 1, pp. 52–54, 1991.

[423] (British Standards Institution) BSI, "UNI EN 872:2005 - Water quality - Determination of suspended solids - Method by filtration through glass fibre filters." British Standards Institution, London, UK, 2005.

Estratto per riassunto della tesi di dottorato

L'estratto deve essere redatto sia in lingua italiana che in lingua inglese e nella lingua straniera eventualmente indicata dal Collegio dei docenti.
L'estratto va firmato e rilegato come ultimo foglio della tesi.

Studente: CALGARO LORIS matricola: 834759

Dottorato: SCIENZE AMBIENTALI

Ciclo: 32°

Titolo della tesi[1] **:** Stabilized materials from contaminated waste recycling: characterization, immobilization, and leaching of contaminants

Abstract:

The contamination of soils, sediments, and industrial wastes from both heavy metals and organic pollutants is recognised as a very important environmental problem, highlighting the need to improve or develop effective remediation techniques to support sustainable management strategies.

This Ph.D. thesis focuses on the characterization of several stabilized granular materials obtained from the application of the "High Performance Solidification/Stabilization" process by means of Inductively Coupled Plasma Mass and Optical Emission Spectrometry (ICP-MS and ICP-OES), Ultraviolet–Visible spectroscopy (UV-Vis), Gas Chromatography (GC), X-Ray Diffraction (XRD), and Scanning Electron Microscopy (SEM).

The results obtained were helpful to elucidate the mechanisms, mineralogical phases, and key parameters regulating the performances of the different binders used in the treatment of different contaminated matrixes. A new integrated process for heavy metals' recovery from stabilized matrixes through alkaline soil washing, nanofiltration and heavy metals' chemical precipitation was developed and tested.

The overall experimental activity led to the draft of four manuscripts that are discussed in detail in this thesis.

La contaminazione di suoli, sedimenti e rifiuti industriali da metalli pesanti ed inquinanti organici è riconosciuta come un problema ambientale molto importante, evidenziando la necessità di migliorare o sviluppare tecniche di bonifica efficaci per supportare delle strategie di gestione sostenibili.

Questa tesi di dottorato si concentra sulla caratterizzazione di numerosi materiali granulari stabilizzati ottenuti dall'applicazione del processo "High Performance Solidification/Stabilization" mediante spettrometria, ottica e di massa, al plasma accoppiato induttivamente (ICP-MS e ICP-OES), spettroscopia

---

[1] Il titolo deve essere quello definitivo, uguale a quello che risulta stampato sulla copertina dell'elaborato consegnato.

ultravioletta-visibile (UV- Vis), gascromatografia (GC), diffrazione ai raggi X (XRD) e microscopia elettronica a scansione (SEM). I risultati ottenuti sono stati utili per chiarire i meccanismi, le fasi mineralogiche e i parametri chiave che regolano le prestazioni dei diversi leganti utilizzati nel trattamento di diverse matrici contaminate. È stato sviluppato e testato un nuovo processo integrato per il recupero dei metalli pesanti da matrici stabilizzate mediante lavaggio alcalino, nanofiltrazione e precipitazione chimica dei metalli pesanti.

L'attività sperimentale complessiva ha portato alla stesura di quattro manoscritti discussi in dettaglio in questa tesi.

Firma dello studente

Sofia Calgaro